Topological Order in Superconductors and Quantum Hall Liquids

by

Guang Yang

B.Eng. and B.M.S., Tianjin University; Tianjin, China, 2006

M.Sc., Auburn University; Auburn, AL, 2008

A dissertation submitted in partial fulfillment of the
requirements for the degree of Doctor of Philosophy
in the Department of Physics at Brown University

PROVIDENCE, RHODE ISLAND

May 2014

This dissertation by Guang Yang is accepted in its present form
by the Department of Physics as satisfying the
dissertation requirement for the degree of Doctor of Philosophy.

Date_____ _____

Prof. Dmitri E. Feldman, Ph.D., Advisor

Recommended to the Graduate Council

Date_____ _____

Prof. John M. Kosterlitz, Ph.D., Reader

Date_____ _____

Prof. Vesna F. Mitrovic, Ph.D., Reader

Approved by the Graduate Council

Date_____ _____

Peter M. Weber, Dean of the Graduate School

Curriculum Vitae

Personal Information

- Name: Guang Yang
- Place of Birth: Renqiu, Hebei, China

Education

- **Brown University, Providence, RI**

  Ph.D. in Physics, Department of Physics (May 2014)

- **Auburn University, Auburn, AL**

  M.Sc. in Physics, Department of Physics (May 2008)

- **Tianjin University, Tianjin, China**

  B.Eng. in Electrical Engineering, College of Precision Instrument and Opto-electronics Engineering (June 2006)

  B.M.S. in Project Management, College of Management and Economics (June 2006)

Publications

1. Guang Yang and D. E. Feldman, Experimental constraints and a possible quantum Hall state at $\nu = 5/2$, in preparation.

2. Guang Yang and D. E. Feldman, Exact zero modes and decoherence in systems of interacting Majorana fermions, Phys. Rev. B **89**, 035136 (2014).

3. Guang Yang and D. E. Feldman, Influence of device geometry on tunneling in the ν=5/2 quantum Hall liquid, Phys. Rev. B **88**, 085317 (2013).

4. Guang Yang and Yu Zhou, New Development of Research in Carbon Nanotube Technology, Materials Review (in Chinese), **20**(**z2**), 94 (2006).

Acknowledgements

Eight years ago, I was fascinated by the beauty of physics and jumped into this whole new world. It is the best decision I have made so far in my life. Now I am about to finish my education and start my career. I wish to thank all the people who have helped me along the way.

First of all, I want to thank my advisor Professor Dima Feldman, for making my days at Brown a quality training process. I thank him for helping me transform from an amateur physics lover into a serious researcher who cares about the real physical world and does not take things for granted. I am extremely grateful for his incredible patience during my first year of research when I was not able to concentrate on my own project. I admire Dima's ability to formulate unfamiliar problems and dig straight and deep into them without much pre-knowledge, although he is among the most knowledgeable people I have ever met. To me, this is the definition of intelligence.

I wish to sincerely thank Professor An-Ban Chen, who offered me the first opportunity to receive education in physics. I thank him for his patience, consideration and help when I struggled with my first physics course. I thank him for his continuous encouragement and honest criticism after I left Auburn. I wish one day I could be as good as he expected.

I would like to thank Professor Michael Kosterlitz and Professor Vesna Mitrovic

for being the readers of my dissertation. I appreciate very much your time and help. I also thank Professor Rashid Zia for being part of my preliminary exam committee and all other physics professors for their teaching and helpful discussions in seminars and journal clubs.

I want to thank all my fellow graduate students. It was nice spending five years with you taking classes, discussing physics and hanging out. In particular, I thank Chenjie Wang for his kind help on research and everything else. I thank all my friends at Brown, in Boston and at Auburn, especially my buddies in the Brown Dragon team, who I have been playing soccer with during the past five years. It was such a joyful moment winning the intramural championship with you.

I thank the National Science Foundation for supporting my Ph.D. research through Grant No. DMR-1205715.

Finally, I take this chance to thank my parents and my brother. They have always been there to support me no matter what I choose to do. Thank you and I love you.

Abstract of "Topological Order in Superconductors and Quantum Hall Liquids" by Guang Yang, Ph.D., Brown University, May 2014

Fractional quantum Hall (FQH) liquids are interesting two-dimensional electron systems that possess quasiparticle excitations with fractional charges, obeying quantum statistics different from those of bosons and fermions. In particular, the FQH liquid at filling factor $\frac{5}{2}$ was proposed to host Majorana bound state (MBS) with exotic non-Abelian statistics. A collection of MBSs can span a topological Hilbert space, in which each many-particle state is topologically distinct, depending on the historical trajectories of all the MBSs in the system. Logic operations in quantum computation can be encoded in the linear transformations in topological Hilbert space and in principle be protected against local defects and perturbations, which are topologically trivial and cannot induce transitions between different many-particle states.

Despite such intriguing theoretical picture, experiments probing the nature of the $\frac{5}{2}$ FQH liquid are controversial. In this dissertation, we provide an explanation of two seemingly contradicting experiments in the $\frac{5}{2}$ FQH liquid, by exploring the role of electrostatic interaction closely related to the geometries of the devices. We also construct several new $\frac{5}{2}$ FQH states, by making use of the particle-hole symmetry in FQH systems, to account for a recent experiment observing upstream neutral edge transport in the $\frac{5}{2}$ FQH liquid, which ruled out most of the existing theories. In addition to the new particle-hole states, we propose another topological description of the $\frac{5}{2}$ FQH liquid which reconciles all existing transport experiments. Later, we turn our attention to the MBSs in superconductor systems. We study the approaches to minimizing the decoherence of a Majorana-fermion-based qbit due to its interaction with environment, based on a full classification of the fermionic zero modes in a system of interacting Majorana fermions.

Contents

List of Tables

List of Figures

Chapter One

Introduction

The quantum Hall effect [1] is an important macroscopic quantum phenomenon discovered [2, 3] in the early 1980s. It features the almost vanishing longitudinal resistance $R_{xx} \approx 0$ and the quantized transverse (Hall) resistance $R_{xy} = \frac{1}{\nu}\frac{h}{e^2}$ in two-dimensional magnetotransport. The quantity ν that can be determined through mesoscopic measurement is in nature quantum mechanical. It is the ratio of the number of electrons to the number of quantum states per degeneracy in the system, called the filling factor. Experimentally observed ν can be either an integer or a rational fraction, with which the system is referred to as exhibiting integer quantum Hall (IQH) effect or fractional quantum Hall (FQH) effect. The quantum mechanical nature of ν is evidenced by the remarkably precise quantization of the Hall resistance, which has been measured to the accuracy of nearly one part in a billion [4].

The quantum Hall effect occurs when a two-dimensional electron gas (2DEG) is subject to strong perpendicular magnetic field, in the limit that the energy scale set by the external magnetic field is much larger than the energy scales set by the in-sample disorder potential, the inter-electron Coulomb potential and the thermal energy. In such a case, electrons are frozen in quantized Landau levels. The remanent (yet rich) physical properties of the 2DEG then depend on the interplay between the disorder potential and the intra-Landau-level electron-electron interaction. In the case that the disorder potential is much stronger than the electron-electron interaction, IQH effect is observed. On the contrary, if the electron-electron interaction dominates over the disorder potential, one arrives at the regime of FQH effect.

The physics of IQH effect is better understood than that of FQH effect. To a good approximation, one may ignore the electron-electron interaction within the Landau level and view the IQH system as a collection of non-interaction electrons. The observed non-dissipative transport and the quantization of Hall resistance can be explained under the framework of single particle quantum mechanics, taking into

account the existence of localized electron states due to disorders and impurities.

FQH systems, on the other hand, contain much richer physics. To understand the physics of FQH effect, one must not neglect the intra-Landau-level Coulomb interaction among electrons. From theoretical point of view, FQH liquids possess internal structures, called "topological orders" [5], that involve strong correlation and collective motion of all degrees of freedom in the system, as a result of the simultaneous presence of strong magnetic field and electron-electron interaction. The nontrivial topological orders distinguish FQH liquids from IQH liquids, which are essentially free electron systems having trivial topological order.

Due to their nontrivial topological orders, FQH liquids possess quasiparticle excitations with fractional charges, obeying quantum statistics different from those of bosons and fermions [6]. The new quantum statistics can be either Abelian or non-Abelian. When two Abelian quasiparticles are exchanged, the many-particle wave function acquires a phase factor that is different from ± 1. This phase factor defines the topological property of the Abelian quasiparticles. What is more interesting are the non-Abelian quasiparticles. A collection of non-Abelian quasiparticles can span a topological Hilbert space, in which each many-particle state is topologically distinct, depending on the historical trajectories of all the non-Abelian quasiparticles. Local defects and perturbations are topologically trivial and cannot induce transitions among different many-particle states. On the other hand, braidings of non-Abelian quasiparticles give rise to unitary transformations in the topological Hilbert space, which can be used to encode logic operations in quantum computation. As such, the non-Abelian FQH quasiparticles are potential building blocks for topological quantum computer [7, 8], whose operation is in principle topologically protected against various decoherence processes due to defects and perturbations.

The FQH liquid at filling factor $\nu = 5/2$ [9] was expected to host one simple kind of non-Abelian quasiparticle, the Majorana bound state (MBS). Such quasiparticles were predicted in a theory proposed by Moore and Read [10] to explain the even denominator of the filling factor. The Moore-Read theory, however, is not the only candidate for the $\nu = 5/2$ FQH state. Competing theories [11, 12] exist to predict the quantum liquid an Abelian system. Unfortunately, experiments [13–24] probing the topological nature of the $\nu = 5/2$ FQH liquid are controversial. A large part of this dissertation is devoted to understanding experiments in the $\nu = 5/2$ FQH liquid, as well as constructing new candidate theories for the $\nu = 5/2$ FQH state. The application of MBSs to topological quantum computation is also an interesting subject [8, 25]. In the later part of the dissertation, I study the approaches to optimizing the reliability of topological quantum computation with MBSs.

Before jumping into the details of my dissertation work, I first give an introduction to the experimental and theoretical aspects of the quantum Hall effect. The introduction is by no means comprehensive. It is primarily a review of the basics that will prepare the reader the necessary background and motivation to understand the later chapters of the dissertation. In Section 1.1, I discuss experiments and show the incapability of classical theory in explaining the quantum Hall effect. In Section 1.2, I introduce the successful theory of IQH effect, which is based on single particle quantum mechanics. The theory of FQH effect is surveyed in Section 1.3, including discussions of the wave function approach, the effective field theory, and quasiparticle tunneling between FQH edges which links the theory to experiments. In Section 1.4, I give a special discussion of the FQH liquid at filling factor $\nu = 5/2$, where MBSs may exist. The idea of topological quantum computation using MBSs is also explained. Section 1.5 is an outline of the following chapters.

1.1 Experimental aspects of quantum Hall effect

To observe the quantum Hall effect, one needs to construct a 2DEG. Experimentally, a 2DEG is realized by freezing the degrees of freedom of electrons in the third spatial dimension. This can be done, for example, in a heterostructure of two different semiconducting alloys whose band structure mismatch creates a "quantum well" for the electron motion in one of the spatial directions. The energy level spacing in the quantum well can be of order 10^3K, much larger than the temperature at which quantum Hall experiments are performed. Hence, the kinetic energies of electrons in the third spatial direction are quenched in the lowest energy level in the quantum well and the electron system becomes effectively a 2DEG.

Fig. 1.1 shows the measured transport data [26] in the quantum Hall effect. As we can see, the Hall resistance scales linearly with the perpendicular magnetic field. At certain magnetic field, plateaus appear where the Hall resistance becomes universal constants,

$$R_{xy} = \frac{1}{\nu}\frac{h}{e^2}, \tag{1.1}$$

where ν is an integer or a rational fraction. Along with the Hall resistance plateaus, the longitudinal resistance drops to almost zero and the transport becomes dissipationless. These phenomena cannot be explained by the classical theory of magneto-transport in two dimensions, as we now show.

In classical Hall effect, electrons move under an electric field $\mathbf{E}$ and a perpendicular magnetic field $\mathbf{B}$. The electric field has a component perpendicular to both the magnetic field and the direction of current flow which balances the Lorentz force by the magnetic field, and a component in the direction of current flow to provide drift

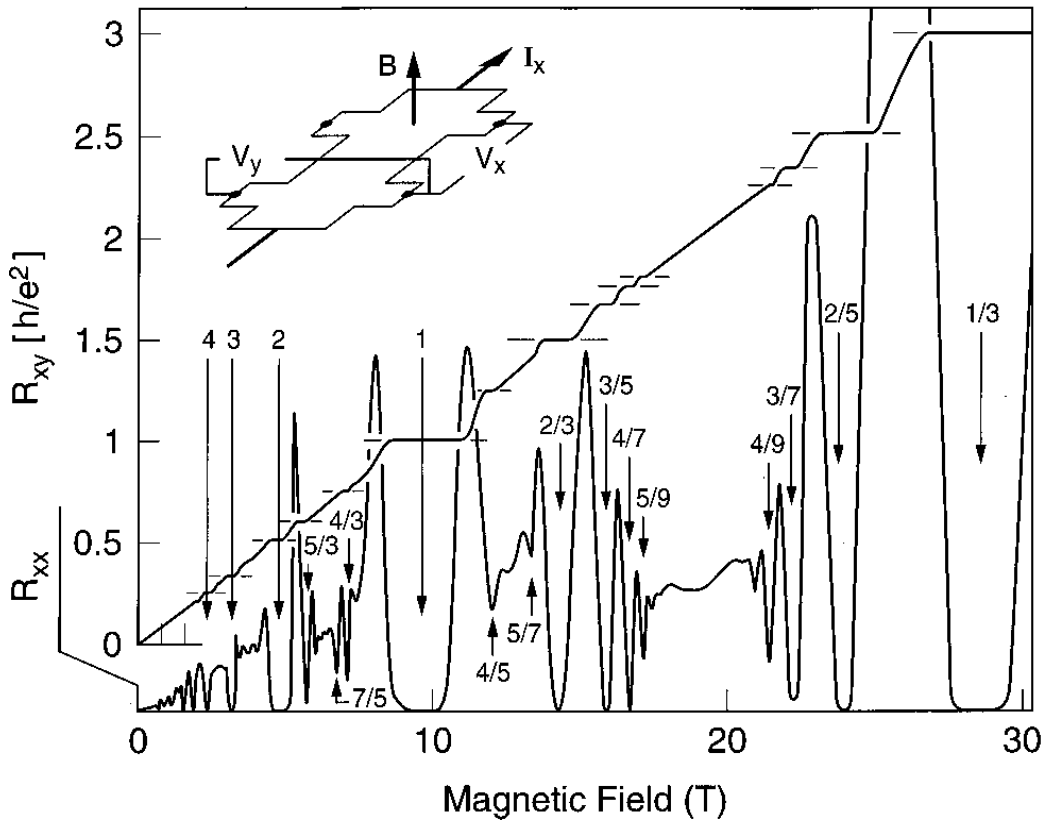

Figure 1.1: Transport in the quantum Hall regime. The numbers indicate the filling factors at which plateaus of Hall resistance R_{xy} appear, associated with the vanishing of longitudinal resistance R_{xx}. Adopted from Ref. [26].

velocity $\mathbf{v}$ of electrons. The transport can be described by Drude theory [27],

$$m\frac{d\mathbf{v}}{dt} = -(e\mathbf{E} + \frac{e}{c}\mathbf{v}\times\mathbf{B}) - m\frac{\mathbf{v}}{\tau}, \tag{1.2}$$

where m is the effective electron mass, $-e$ is the electron charge and τ is the relaxation time set by various scattering mechanisms in the 2DEG, e.g., due to phonons (in the quantum Hall regime, phonon excitations are almost completely suppressed) and impurities. At equilibrium, $\frac{d\mathbf{v}}{dt} = 0$. Solving Eq. (1.2) at equilibrium with $\mathbf{v} = v\hat{x}, \mathbf{B} = -B\hat{z}, \mathbf{E}\cdot\hat{z} = 0$ gives

$$\begin{pmatrix} E_x \\ E_y \\ 0 \end{pmatrix} = \begin{pmatrix} \frac{m}{ne^2\tau} \\ \frac{B}{nec} \\ 0 \end{pmatrix} j \tag{1.3}$$

where $\mathbf{j} = -ne\mathbf{v}$ is the conducting current density. From Eq. (1.3), we obtain the longitudinal and Hall resistances

$$R_{xx} = \frac{E_x}{j} = \frac{m}{ne^2\tau} \quad \text{and} \quad R_{xy} = \frac{E_y}{j} = \frac{B}{nec}. \tag{1.4}$$

We see that in classical Hall effect, the longitudinal resistance is nonzero, reflecting the dissipation in transport due to scattering mechanisms, and the Hall resistance is a linear function of the perpendicular magnetic field. From the $\hat{y}$ component of Eq. (1.3), we also find that the electron drift velocity $v = cE_y/B$.

Drude theory gives qualitatively correct explanation of the transport data when the system is outside the quantum Hall regime. However, it does not explain the appearance of Hall resistance plateaus and the associated vanishing longitudinal resistance in Fig. 1. These puzzles can only be understood after one admits quantum mechanical treatment.

Another important observation in the quantum Hall systems is that the 2DEG turns into an incompressible liquid state when the Hall resistance plateaus appear. This implies a gapped excitation spectrum in the bulk of the system which is fundamentally quantum mechanical. To see this connection, recall the definition of compressibility κ,

$$\kappa^{-1} = -V\frac{\partial P}{\partial V} = V\frac{\partial^2 E}{\partial V^2} \tag{1.5}$$

where V, E are the volume and the internal energy of the system, respectively, and P is the pressure applied to the system. For the 2DEG, it is convenient to rewrite the above definition in terms of quantities defined per electron per unit area. Let N, A be the electron number and the area of the system, respectively. Using $E = N\epsilon(n)$, $n = N/A$ and the definition of chemical potential $\mu = \partial E/\partial N$, we find

$$\kappa^{-1} = n^2\frac{d\mu}{dn}. \tag{1.6}$$

where n is the electron density and $\epsilon(n)$ is the internal energy density as a function of n. Hence, the incompressibility condition $\kappa = 0$ is equivalent to a discontinuity in the chemical potential $\mu(n)$ as a function of n, which then means a gapped excitation spectrum.

In the following sections, we discuss the physical origins and consequences of incompressibility in IQH effect (Section 1.2) and in FQH effect (Subsection 1.3.1). The case of IQH effect is immediately clear after one solves the quantum mechanical problem of free electrons under strong magnetic field. The case of FQH effect, however, requires a closer look at the Coulomb interaction among electrons.

1.2 Quantum Hall effect at integer filling factors

To understand the physics of IQH effect, we first study the quantum dynamics of an electron moving under strong perpendicular magnetic field $\mathbf{B} = B\hat{z}$.

We choose Landau gauge for the vector potential $\mathbf{A} = xB\hat{y}$. The Hamiltonian of the problem then reads

$$H = \frac{1}{2m}[p_x^2 + (p_y + \frac{eB}{c}x)^2], \tag{1.7}$$

where m is the effective mass of electrons in the sample. In Eq. (1.7), we have ignored the kinetic energy from the electron motion in $\hat{z}$ direction, which as we mentioned before is simply the lowest possible energy in a one-dimensional quantum well. After a bit of algebra, the Hamiltonian can be written as that of a simple harmonic oscillator. It is then straightforward to obtain the energy eigenfunctions and eigenvalues,

$$\begin{aligned} \psi_{nk}(\mathbf{r}) &= \frac{1}{\sqrt{L}} e^{iky} H_n(x + kl_B^2) e^{-\frac{1}{2l_B^2}(x+kl_B^2)^2} \\ \epsilon_{nk} &= (n + \frac{1}{2})\hbar\omega_c \end{aligned} \tag{1.8}$$

where H_n is the nth Hermite polynomial, L is the system size in $\hat{y}$ direction, $\hbar k$ is the quantized linear momentum in $\hat{y}$ direction, $l_B = \sqrt{\frac{\hbar c}{eB}}$ is the magnetic length and $\omega_c = \frac{eB}{mc}$ is the cyclotron frequency. We see that the kinetic energies of electrons are quenched in quantized energy levels, call Landau levels, labeled by integers n.

The degree of degeneracy in each Landau level is obtained as follows. First we note that the energy in each Landau level is independent of the wave number k in $\hat{y}$ direction. Hence, we much sum over all possible values of k in order to count the

number of states in each Landau level. For given k, the eigenfunction in $\hat{x}$ direction is a harmonic oscillator located at $x = -kl_B^2$. Suppose the sizes of the 2DEG in $\hat{x}$ and $\hat{y}$ directions are L' and L, respectively. The range of allowed wave vectors is then $[0, L'/l_B^2]$. The number N_0 of states in each Landau level is

$$N_0 = \frac{L}{2\pi}\int_0^{L'/l_B^2} dk = \frac{LL'}{2\pi l_B^2} = \frac{LL'B}{\Phi_0} = N_\Phi \tag{1.9}$$

where $\Phi_0 = \frac{hc}{e}$ is the magnetic flux quantum and $N_\Phi = N_0$ is the number of flux quanta penetrating through the area of the 2DEG.

The filling factor ν is defined as the ratio of the number of electrons to the degree of degeneracy in each Landau level (or the number of flux quanta penetrating through the area of the 2DEG),

$$\nu = \frac{N}{N_0} = \frac{N}{N_\Phi}. \tag{1.10}$$

IQH effect corresponds to the situations where ν takes integer values.

To study transport in an IQH system, consider an electric field $\mathbf{E}$ applied to the 2DEG, in addition to the magnetic field. Let $\mathbf{E} = E\hat{x}$. This amounts to adding a potential energy $V(\mathbf{r}) = eEx$ to the Hamiltonian in Eq. (1.7). By completing the square in x in the Hamiltonian, the problem is simply a quantum harmonic oscillator shifted by $-\frac{eE}{m\omega_c^2}$ in $\hat{x}$ direction. The new eigenfunctions are now located at $x_k = -kl_B^2 - \frac{eE}{m\omega_c^2}$ with eigenvalues depending on k,

$$\epsilon_{nk} = (n + \frac{1}{2})h\omega_c + eEx_k + \frac{1}{2}mv^2, \tag{1.11}$$

where $v = cE/B$. The group velocity of electrons in the nth Landau level is

$$\mathbf{v_{nk}} = \frac{1}{\hbar}\nabla_{\mathbf{k}}\epsilon_{nk} = -\frac{cE}{B}\hat{y} = -v\hat{y}. \tag{1.12}$$

Hence, upon applying an electric field, electrons in all the Landau levels drift at the same velocity v, in the direction perpendicular to both the electric field and the magnetic field. The drift velocity we find by solving the quantum mechanical problem agrees with the drift velocity in classical Hall effect, obtained after Eq. (1.3).

In a realistic quantum Hall system, an electrical potential is created (e.g., by metallic gates or by chemical etching) to confine the 2DEG to the area of interest. Near the edge of the 2DEG, an electric field exists as the gradient of the confining potential. This electric field, however, is screened out in the bulk. Hence, transport only happens on the edge of the quantum Hall system.

Fig. 1.2 shows the energy levels in an IQH system. Deep in the bulk of the 2DEG, the electric field due to the confining potential is completely screened out such that the excitation spectrum is given by Eq. (1.8), gapped by the Landau level spacing $\hbar\omega_c$. Near the edge of the system, gapless excitations appear as extended electron states, as a result of the nonzero electric field. These extended states form edge channels of the IQH system, in which conducting current flows.

IQH effect occurs when the chemical potential lies in between two Landau levels. In such a case, the lower Landau levels are completely filled, while the upper Landau levels are empty. An edge channel in a quantum Hall system is defined as consisting of all the extended states in a Landau level. Such edge channels have finite widths, unlike those in quantum wires. We now show that in an IQH system, the Hall conductance in each edge channel is quantized as $\frac{e^2}{h}$. Let L be the size of the system

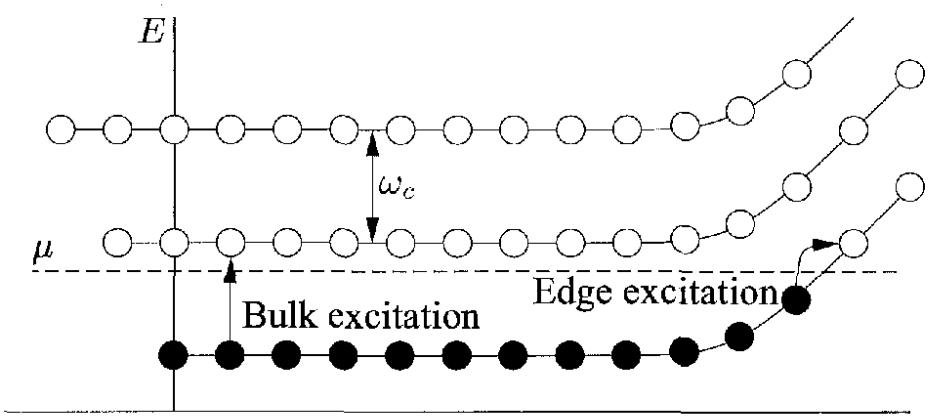

Figure 1.2: Energy levels in an IQH system. μ is the chemical potential, below which the electron states are occupied. Excitations in the bulk are gapped by Landau level spacing ω_c (setting $\hbar = 1$). Gapless excitations exist on the edge where there is a nonzero electric field produced by the confining potential. Adopted from Ref. [5].

in the longitudinal direction of an edge channel. The number of extended states per wave number is then $\frac{L}{2\pi}$. All the extended states in the edge channel are occupied by conducting electrons, with group velocities $\frac{1}{\hbar}\nabla_{\mathbf{k}}\epsilon_{nk}$. To a good approximation, we use Fermi function at zero temperature for the quantum Hall system. The current in the nth edge channel is

$$\begin{aligned} I &= -\frac{e}{L}\int dk \frac{L}{2\pi}\frac{1}{\hbar}\nabla_{\mathbf{k}}\epsilon_{nk} \\ &= -\frac{e}{h}\int_0^{\mu} d\epsilon \\ &= -\frac{e^2}{h}V \end{aligned} \tag{1.13}$$

where $\mu = eV$ is the chemical potential in the edge channel and in the second line we have used the fact that the integrand in the first line is a perfect derivative. Hence, the Hall conductance $\sigma_{xy} = \frac{e^2}{h}$ in each edge channel. For realistic transport experiments, let μ_S, μ_D be the chemical potentials in the source and in the drain. The net current $I = -\nu\frac{e}{h}(\mu_S - \mu_D) = -\nu\frac{e^2}{h}V_{SD}$, where V_{SD} is the voltage difference between the source and the drain, and ν is the number of edge channels contributing

to transport.

We can now explain the transport data in IQH effect. The number N_0 of states in each Landau level is related to the magnetic field B via Eq. (1.9). At certain magnetic field, N_0 reaches a value such that the number N of electrons in the 2DEG is an integer multiple ν of N_0. By Eq. (1.10), there are ν completely occupied Landau levels below the chemical potential. The edge channel of each Landau level contributes $\frac{e^2}{h}$ to the Hall conductance. Altogether, we have a Hall conductance $\sigma_{xy} = \nu\frac{e^2}{h}$. In a quantum Hall system, electrons flow in the direction perpendicular to both the electric field and the magnetic field. No current flow can be measured along the direction of the electric field. Hence, the longitudinal conductance $\sigma_{xx} = 0$. The resistance matrix $\overline{\mathbf{R}}$ is the inverse of the conductance matrix $\overline{\sigma}$,

$$\overline{\mathbf{R}} = \overline{\sigma}^{-1} = \begin{pmatrix} 0 & -\nu\frac{e^2}{h} \\ \nu\frac{e^2}{h} & 0 \end{pmatrix}^{-1} = \begin{pmatrix} 0 & \frac{1}{\nu}\frac{h}{e^2} \\ -\frac{1}{\nu}\frac{h}{e^2} & 0 \end{pmatrix}, \tag{1.14}$$

from which we find the longitudinal resistance $R_{xx} = 0$ and the Hall resistance $R_{xy} = \frac{1}{\nu}\frac{h}{e^2}$.

The vanishing of the longitudinal resistance R_{xx} is a result of the excitation gap $\hbar\omega_c$ between the filled νth Landau level and the empty $(\nu + 1)$th Landau level. The gap prevents electrons from being excited between different Landau levels and ensures that all ν lower Landau levels remain completely filled. In such a case, electron scatterings are greatly suppressed because of the lack of unoccupied states in any of the ν Landau levels to accommodate the scattered electrons. The transport is hence dissipationless, reflected by the nearly vanishing longitudinal resistance. The excitation gap also explains the incompressibility of the 2DEG in IQH effect.

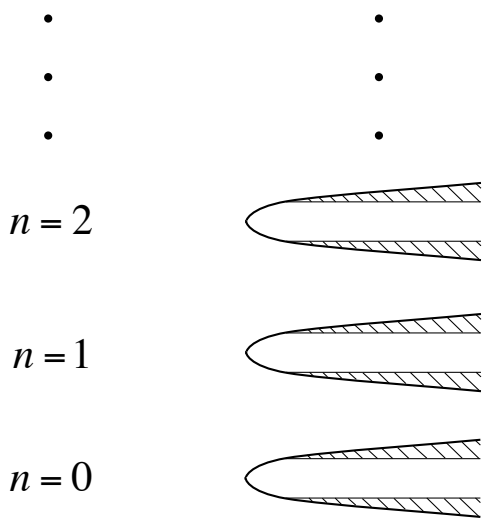

Figure 1.3: Broadening of Landau levels by localized electron states (shaded areas) near disorders. n labels Landau levels. Electron states in the white strips between neighboring shaded areas are non-localized and can contribute to transport in the presence of an electric field. A Hall resistance plateau appears when the chemical potential lies between two white-strip regions.

To understand the Hall resistance plateaus, we need to take into account the role of disorders. As mentioned in the beginning of this chapter, IQH effect occurs when the disorder potential is much stronger than the electron-electron interaction. The disorders turn some of the degenerate states in each Landau level into localized electron states with different energies. As shown in Fig. 1.3, this effectively broadens the Landau levels. As the chemical potential of the system moves (e.g., due to the change of magnetic field B, Eqs. (1.9)(1.10)) in the reservoir of localized energy levels, all the Landau levels below the chemical potential remain fully occupied such that the Hall resistance is still quantized. The Hall resistance plateaus then appear.

1.3 Theory of quantum Hall effect at fractional filling factors

In Section 1.2, we see that IQH effect is well explained using single particle quantum mechanics. However, similar arguments do not apply to FQH effect. FQH effect occurs when the uppermost Landau level is partially filled. Naively, the availability of unoccupied states in the uppermost Landau level should allow electron scattering which gives rise to nonzero longitudinal resistance. But this is not what has been observed. In fact, FQH liquids are in nature strongly-correlated electron systems [1, 5, 28, 29] with rich internal structures. The Coulomb repulsion between electrons within the Landau level plays an important role in the formation of FQH liquids.

Before discussing the theory of FQH effect, I first use a two-body problem to answer a basic question about FQH liquids: Why are FQH liquids incompressible? Incompressibility is the starting point of all theoretical attempts to FQH effect.

1.3.1 A two-body problem: Understanding incompressibility

Let us study the quantum mechanical problem of two interacting electrons under strong magnetic field $\mathbf{B}$. The energy scale set by Coulomb interaction between the electrons is much smaller than the Landau level spacing. Hence, we can solve the problem using perturbation theory, by treating Coulomb interaction as a perturbation and using the eigenfunctions of the free electron Hamiltonian, Eq. (1.7), as zeroth order basis functions. Here, it is more convenient to use the symmetric gauge

$\mathbf{A} = -\frac{1}{2}(y\hat{x} - x\hat{y})B$. The zeroth order basis functions are found to be

$$\psi_m = \frac{1}{\sqrt{2\pi l_B^{2m+2} 2^m m!}} z^m e^{-\frac{1}{4l_B^2}|z|^2}, \tag{1.15}$$

where $z = x + iy$ is the complex coordinate of the electron and $m \in \mathbb{Z}$ is the quantum number labeling the degeneracy in the Landau level, $m \geq 0$. The physical meaning of m is the conserved angular momentum of ψ_m.

Now consider two electrons in the eigenstates $\psi_{m_1}(z_1)$ and $\psi_{m_2}(z_2)$. Their Coulomb interaction $V(|z_1 - z_2|) = \frac{e^2}{\varepsilon|z_1 - z_2|}$, where ε is the dielectric constant in the sample, typically of order 10. We solve the problem by switching to the center-of-mass coordinate $Z = z_1 + z_2$ (ignoring the factor 1/2) and the relative coordinate $z = z_1 - z_2$. Correspondingly, we define the center-of-mass angular momentum M and relative angular momentum m. The zeroth order wave function of the two-electron system

$$\Psi_{m_1,m_2}(z_1, z_2) = \psi_{m_1}(z_1)\psi_{m_2}(z_2) = \Psi_{M,m}(Z, z) \approx Z^M z^m e^{-\frac{1}{8}(|Z|^2 + |z|^2)}, \tag{1.16}$$

where after "$\approx$" we have ignored the normalization factor. The Coulomb potential $V(|z_1 - z_2|) = V(|z|) = \frac{e^2}{\varepsilon|z|}$. The first-order corrections to the energy eigenvalues

$$V_m = \frac{\langle \Psi_{M,m}|V|\Psi_{M,m}\rangle}{\langle \Psi_{M,m}|\Psi_{M,m}\rangle} = \frac{e^2}{\varepsilon l_B} \frac{\Gamma(m + \frac{1}{2})}{2 \cdot m!}, \tag{1.17}$$

are independent of the center-of-mass angular momenta M and are referred to as Haldane pseudopotentials [30]. Fig. 1.4 shows Haldane pseudopotential V_m versus the relative angular momentum m (or equivalently, versus the distance $r_m \propto m l_B$) between two electrons. We see that the potential energy of the system is quantized in unit of $\frac{e^2}{\varepsilon l_B}$, due to the simultaneous presence of Coulomb repulsion between electrons and the strong external magnetic field. Electrons can no longer approach each other

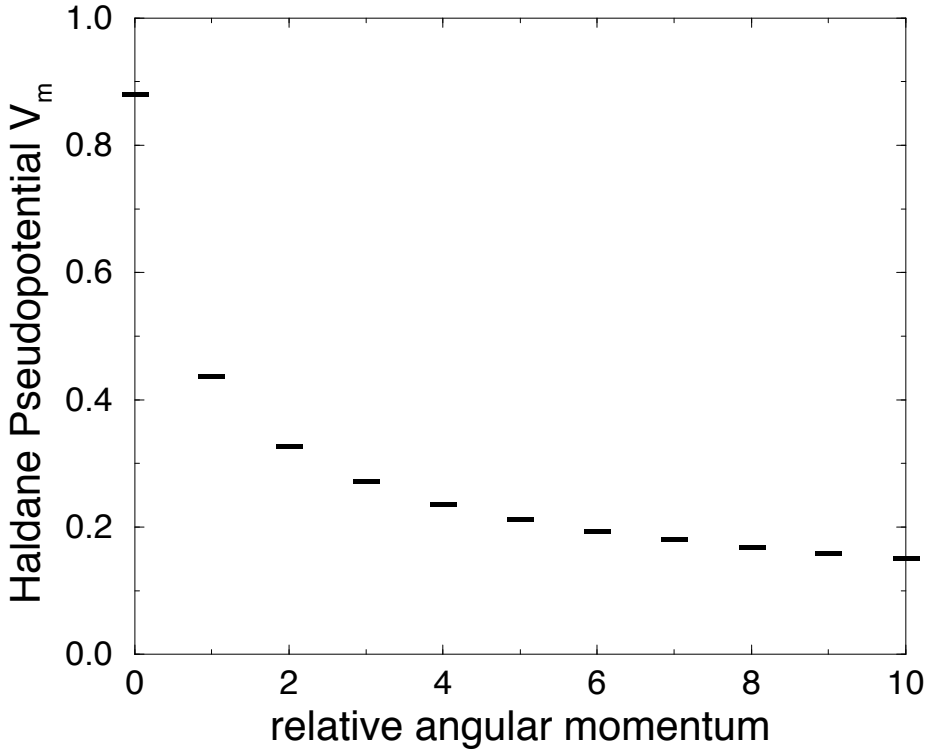

Figure 1.4: Haldane pseudopotential V_m (in unit of $e^2/\varepsilon l_B$) versus the relative angular momentum m between two electrons. Adopted from Ref. [29].

in a continuous way. Instead, they must take quantized steps r_m and overcome a gap $\sim \frac{e^2}{\varepsilon l_B}$ during each step.

The above results for the two-electron system can be qualitatively extended to a system of many electrons, for example, to a FQH system which is essentially an interacting 2DEG under strong magnetic field. We can infer a gapped spectrum in a FQH liquid, despite that the uppermost Landau level is not completely occupied by electrons. The gap $\sim \frac{e^2}{\varepsilon l_B}$ preserves the uniform structure of the ground state and turns the 2DEG into an incompressible liquid. Transport in FQH liquids consists of the collective motion of all the electrons while the system remains in its ground state. Electron scattering in FQH liquids is considerably suppressed, because of the difficulty of moving an electron towards the other electrons. As a result, transport in FQH liquids is non-dissipative with an almost vanishing longitudinal resistance.

1.3.2 Wave function approach

We now discuss the wave function approach to FQH effect, first introduced by R. B. Laughlin [31].

The many-particle wave function Laughlin wrote down for the ground state of the FQH liquid at filling factor $\nu = 1/m$ is

$$\Psi^m([z_i]) = \prod_{i<j}(z_i - z_j)^m e^{-\frac{1}{4l_B^2}\sum_i |z_i|^2}, \tag{1.18}$$

where m must be an odd integer to ensure fermionic statistics between electrons and $[z_i]$ denotes the set of complex coordinates z_i labeling the positions of electrons. This wave function vanishes quickly when two electrons approach each other. Hence, in such a state, electrons tend to stay away from one another and the total Coulomb energy of the system is minimized.

Expanding $\Psi^m([z_i])$ into a polynomial in z_i, we see that it is a superposition of several many-particle states. In all such constituent states, electrons are well dispersed so that the relative angular momentum of any pair of electrons is equal to or greater than m. This fact guarantees that $\Psi^m([z_i])$ is the exact ground state of a FQH system with short-ranged electron-electron interaction. To see this, approximate the total Coulomb energy in the FQH system as the sum of Haldane pseudopotentials between all pairs of electrons and ignore the total kinetic energy which is a constant independent of the electron index. The Hamiltonian is then

$$H = \sum_{m'=0}^{\infty} \sum_{i<j} V_{m'} P_{m'}^{ij}, \tag{1.19}$$

where $P_{m'}^{ij}$ is a projection operator operating on a many-particle wave function Ψ.

$P^{ij}_{m'}\Psi = \Psi$ if the relative angular momentum of z_i, z_j electrons in Ψ equals m, and $P^{ij}_{m'}\Psi = 0$ if otherwise. Hence, we have

$$H\Psi^m([z_i]) = \sum_{m'=m}^{\infty} \sum_{i<j} V_{m'} P^{ij}_{m'} \Psi^m([z_i]). \tag{1.20}$$

If we artificially truncate the range of the Haldane pseudopotential such that $V_{m'} = 0, m' \geq m$, i.e. $V_{m'}$ becomes a "hard-core potential", $\Psi^m([z_i])$ is explicitly the exact ground state of the Hamiltonian. The excited states are obtained by squeezing pairs of electrons such that their relative angular momenta become smaller than m. As illustrated in the previous subsection, this must overcome an energy gap $\sim \frac{e^2}{\varepsilon l_B} \sim V_1$.

The filling factor ν of the FQH state described by $\Psi^m([z_i])$ is obtained through the plasma analogue [5,31], which treats the square of $\Psi^m([z_i])$, describing the probability density of finding an electron in the realistic FQH system, as the Boltzmann weight function in a classical system describing the probability distribution of classical particles. Writing $|\Psi^m([z_i])|^2 = e^{-\beta F}$ with $\beta = 2/m$, we obtain a classical energy function

$$F = -m^2 \sum_{i<j} \ln|z_i - z_j| + \frac{m}{4l_B^2} \sum_i |z_i|^2, \tag{1.21}$$

which describes a two-dimensional plasma system. In the plasma system, each particle z_i carries a "plasma charge" m and sees a potential $\frac{m}{4l_B^2}|z|^2$ produced by the background "charge" density $n_0 = \frac{1}{2\pi l_B^2}$. To keep the system "charge" neutral, the total "charge" density of the plasma particles must equal the background charge density. Hence, we demand $mn = n_0$, where n is the number density of plasma particles. Switching back to reality, each plasma particle corresponds to an electron in the FQH system. Hence, n is also the number density of physical electrons. Besides, the background "charge" density n_0 in the plasma system coincides with the density of states (or the density of flux quanta) in the FQH system. Hence, we find

$\nu = n/n_0 = 1/m$.

Laughlin also suggested the many-particle wave functions for localized excitations in a FQH system. The excitations can be positively charged, called "quasiholes", or negatively charged, called "quasielectrons". A fundamental quasihole located at ξ in the $\nu = 1/m$ Laughlin state is described by the wave function

$$\Psi^{qh}([z_i], \xi) = \prod_i (z_i - \xi)\Psi^m([z_i]), \tag{1.22}$$

where we have ignored the normalization factor. A fundamental quasielectron located at ξ has the wave function

$$\Psi^{qp}([z_i], \xi) = \prod_i (2\partial_{z_i} - \xi^*)\Psi^m([z_i]), \tag{1.23}$$

where ξ^* is the complex conjugate of ξ. Interestingly, quasiholes and quasielectrons in a FQH system may carry fractional charges and obeying quantum statistics which are different from those of bosons and fermions.

The charges and statistics of quasiholes and quasielectrons can be extracted from the plasma analogue. We take quasiholes for example.

In the presence of a quasihole located at ξ, the classical energy function

$$F^{qh} = F - m\sum_i \ln|z_i - \xi| \tag{1.24}$$

in the plasma analogue. The last term in F^{qh} means that there is an impurity particle in the system, with "plasma charge" 1. All the rest of the particles have "plasma charge" m. The impurity repels $1/m$ number of "charge" m particles out of its neighborhood so as to keep the system "charge" neutral everywhere. Switching

back to the realistic FQH system, this means the absence of $1/m$ number of electrons near ξ, which forms a quasihole with e/m electric charge.

Consider now the two-quasihole wave function

$$\Psi^{2qh}([z_i],\xi_1,\xi_2)=\frac{1}{\sqrt{C(\xi_1,\xi_1^*,\xi_2,\xi_2^*)}}\prod_i(z_i-\xi_1)\prod_i(z_i-\xi_2)\Psi^m([z_i]), \tag{1.25}$$

where C is the normalization factor depending on $\xi_1,\xi_1^*,\xi_2,\xi_2^*$. Using plasma analogue, we can find C. The two quasiholes can be viewed as two "charge" 1 impurities in the plasma system. Taking into account the mutual interaction between the impurities and the interaction between the impurities and the background charge, the classical energy function

$$\begin{aligned}F^{2qh}=&F-m\sum_i\ln|z_i-\xi_1|-m\sum_i\ln|z_i-\xi_2|-\ln|\xi_1-\xi_2|\\&+\frac{1}{4l_B^2}(|\xi_1|^2+|\xi_2|^2)\end{aligned} \tag{1.26}$$

Using $|\tilde{\Psi}^{2qh}|^2=e^{-\beta F^{2qh}}$ where $\beta=2/m$, we can define an unnormalized wave function

$$\tilde{\Psi}^{2qh}=|\xi_1-\xi_2|^{\frac{1}{m}}e^{-\frac{1}{4ml_B^2}(|\xi_1|^2+|\xi_2|^2)}\prod_i(z_i-\xi_1)\prod_i(z_i-\xi_2)\Psi^m([z_i]), \tag{1.27}$$

which differs from the normalized wave function Ψ^{2qh} only by a constant that does not depend on ξ_1,ξ_2. Comparing Eq. (1.27) with Eq. (1.25), we find

$$C(\xi_1,\xi_1^*,\xi_2,\xi_2^*)\propto|\xi_1-\xi_2|^{-\frac{2}{m}}e^{\frac{1}{2ml_B^2}(|\xi_1|^2+|\xi_2|^2)}, \tag{1.28}$$

up to a constant that does not depend on ξ_1,ξ_2.

For the statistical property of quasiholes, we adiabatically move one quasihole ξ_1 around another ξ_2. The Berry phase acquired by the many-particle wave function Ψ^{2qh} contains the statistical phase between two quasiholes. During the motion of the quasihole, the coordinate ξ_1 is the only parameter in the Hamiltonian that change in time, $\xi_1 = \xi_1(t)$. Consider a small time slice δt of the process, the Berry phase is

$$\begin{aligned} & e^{i(a_{\xi_1}\dot{\xi_1}+a_{\xi_1^*}\dot{\xi_1^*})\delta t} \\ & = \langle \Psi^{2qh}([z_i],[z_i^*],\xi_1(t+\delta t),\xi_1^*(t+\delta t),\xi_2,\xi_2^*)|\Psi^{2qh}([z_i],[z_i^*],\xi_1(t),\xi_1^*(t),\xi_2,\xi_2^*)\rangle, \end{aligned} \tag{1.29}$$

where a_{ξ_1} is the effective gauge potential as seen by quasihole ξ_1, written in complex coordinate ξ_1, and $a_{\xi_1}^*$ is the complex conjugate of a_{ξ_1}. We can take the continuous limit of this difference equation by letting $\delta t \to 0$ to obtain

$$\begin{aligned} & a_{\xi_1}\dot{\xi_1} + a_{\xi_1^*}\dot{\xi_1^*} \\ & = i\langle \Psi^{2qh}([z_i],[z_i^*],\xi_1(t),\xi_1^*(t),\xi_2,\xi_2^*)|\frac{d}{dt}|\Psi^{2qh}([z_i],[z_i^*],\xi_1(t),\xi_1^*(t),\xi_2,\xi_2^*)\rangle \end{aligned} \tag{1.30}$$

Using $\frac{d}{dt} = \dot{\xi_1}\partial_{\xi_1} + \dot{\xi_1^*}\partial_{\xi_1^*}$, we have

$$\begin{aligned} a_{\xi_1} =& i\langle \Psi^{2qh}([z_i],[z_i^*],\xi_1,\xi_1^*,\xi_2,\xi_2^*)|\partial_{\xi_1}|\Psi^{2qh}([z_i],[z_i^*],\xi_1,\xi_1^*,\xi_2,\xi_2^*)\rangle \\ &= -i\sqrt{C}\partial_{\xi_1}\frac{1}{\sqrt{C}} \\ &= \frac{i}{2}\partial_{\xi_1}\ln C. \end{aligned} \tag{1.31}$$

The dependence of C on quasihole coordinates is given in Eq. (1.28). Hence, we find

$$a_{\xi_1} = \frac{i}{2}(\frac{1}{2ml_B^2}\xi_1^* - \frac{1}{m}\frac{1}{\xi_1-\xi_2}). \tag{1.32}$$

The first term in a_{ξ_1} corresponds to the Aharonov-Bohm phase due to the external

magnetic field. The Aharonov-Bohm phase depends on the area enclosed by the trajectory of quasihole ξ_1 and is non-topological. The second term however is topological. It contributes a phase $\frac{2\pi}{m}$ to the many-particle wave function after quasihole ξ_1 winds around quasihole ξ_2. This gives the statistical phase $\frac{\pi}{m}$ upon exchanging the two quasiholes.

Before ending this subsection, we briefly discuss the idea of hierarchical FQH states [30, 32–34], invented to explain the FQH effect at filling factors other than $\nu = 1/m$. A hierarchical FQH state is constructed by condensing the quasiholes (quasielectrons) of a parental FQH state into a FQH state of quasiholes (quasielectrons). For example, starting from the $\nu_0 = 1/p$ Laughlin state, we can condense the fundamental quasiholes with charge e/p into a $\nu_1 = 1/q$ Laughlin state. The wave function of this quasihole hierarchical state is

$$\int \prod_i d^2\xi_i \prod_{i<j}(z_i - z_j)^p \prod_{i,j}(\xi_i - z_j) \prod_{i<j}(\xi_i^* - \xi_j^*)^q e^{-\frac{1}{4l_B^2}\sum_i |z_i|^2} e^{-\frac{1}{4pl_B^2}\sum_i |\xi_i|^2}. \quad (1.33)$$

The filling factor of above FQH state is obtained as follows. Let N_0, N_1, N_2 be the number of available states (per Landau level), electrons, quasiholes in the system, respectively. By definition,we have $N_2/N_1 = 1/q$. Each quasihole is e/p charged and is equivalent to the absence of $1/p$ of an electron. Hence, the total N_2 quasiholes is equivalent to the absence of $N_1/(pq)$ electrons. Imagine these missing electrons were present in the system. Then, adding them to the physically existing N_1 electrons makes the FQH state a Laughlin state at filling factor $1/p$. Hence, we have

$$\frac{N_1 + \frac{1}{pq}N_1}{N_0} = \frac{1}{p}, \quad (1.34)$$

from which we obtain the realistic filling factor

$$\nu = \frac{N_1}{N_0} = \frac{1}{p + \frac{1}{q}} \tag{1.35}$$

of the FQH state in Eq. (1.33).

We can also construct quasielectron hierarchical states. This time we condense the fundamental quasielectrons in a $\nu_0 = 1/p$ Laughlin state into a $\nu_1 = 1/q$ Laughlin state. The hierarchical wave function is

$$\int \prod_i d^2\xi_i \prod_{i<j} (z_i - z_j)^p \prod_{i,j} (\xi_i^* - 2\partial_{z_j}) \prod_{i<j} (\xi_i - \xi_j)^q e^{-\frac{1}{4l_B^2}\sum_i |z_i|^2} e^{-\frac{1}{4pl_B^2}\sum_i |\xi_i|^2}. \tag{1.36}$$

The filling factor is found by a similar argument to that in the quasihole hierarchical state. Each quasielectron is $-e/p$ charged and is equivalent to the presence of $1/p$ of an electron. This gives

$$\nu = \frac{N_1}{N_0} = \frac{1}{p - \frac{1}{q}}. \tag{1.37}$$

Eqs. (1.33)(1.36) only constructed one level of hierarchy. In general, one can construct infinite levels of hierarchies. This produces a series of filling factors to explain almost all observed FQH states.

The above picture of forming hierarchical FQH states was proposed by Haldane and Halperin [30, 32] and is referred to as "Haldane-Halperin hierarchy". There is yet another picture of understanding the FQH states at filling factors other than $\nu = 1/m$, called "composite fermion" [35–38]. The two pictures are equivalent [39] in the sense that they both generate FQH states at all odd-denominator filling factors and predict identical fractional charges and statistical properties for quasiparticle excitations.

1.3.3 Effective field theory

We now discuss the low-energy effective theories [5, 12] of FQH liquids. In this subsection, we use using Einstein summation convention: Repeated indices are implicitly summed.

We start by showing how the effective theory is constructed for the $\nu = 1/m$ Laughlin state, whose ground wave function is given in Eq. (1.18). In the presence of magnetic field $\mathbf{B}$, electrons in the 2DEG couple to the electromagnetic gauge potential A_μ through a term $eA_\mu j^\mu$ in the Lagrangian density, where $j^\mu = (j^0, \mathbf{j})$ is the four-vector form of the electron number density j^0 and the electron number current density $\mathbf{j}$. Here and below, we set $\hbar = c = 1$. The coupling constant e is called the unit electric charge. Incompressibility in the FQH liquid requires that j^0 is linked to the magnetic field $\mathbf{B}$ through the filling factor, $\nu = \frac{1}{m} = \frac{j^0}{B/\Phi_0} = \frac{2\pi j^0}{eB}$, where $\Phi_0 = 2\pi/e$ is the magnetic flux quantum. Hence, the response δj^0 in the electron density to a change δB in the magnetic field is $\delta j^0 = \frac{e}{2\pi m}\delta B$. We can introduce another gauge field a_μ to describe the conserved electron density, $j^\mu = \frac{1}{2\pi}\varepsilon^{\mu\nu\lambda}\partial_\nu a_\lambda$, where $\varepsilon^{\mu\nu\lambda}$ is the Levi-Civita symbol. Then we write the response equation in terms of a_μ, in 4-vector form,

$$\varepsilon^{\mu\nu\lambda}\partial_\nu \delta a_\lambda = \frac{e}{m}\varepsilon^{\mu\nu\lambda}\partial_\nu \delta A_\lambda. \tag{1.38}$$

The Lagrangian density that reproduces this response equation is

$$\mathcal{L} = -\frac{1}{4\pi}[m\varepsilon^{\mu\nu\lambda}a_\mu\partial_\nu a_\lambda - 2e\varepsilon^{\mu\nu\lambda}A_\mu\partial_\nu a_\lambda], \tag{1.39}$$

which is an Abelian Chern-Simons theory with $U(1)$ gauge group. This is the effective theory for the Laughlin state at filling factor $\nu = 1/m$.

Quasiparticle excitations are considered as the particle density $\tilde{j}^\mu$ coupled to the gauge field a_μ. Hence, we add a source term $la_\mu\tilde{j}^\mu$ to Eq. (1.39) to include quasiparticle excitations. The coupling constant l is the "charge" associated with the gauge field a_μ. It must be quantized to an integer in order to ensure the single-valuedness of the many-particle wave function of the Laughlin state. The full effective theory for the $\nu = 1/m$ Laughlin state is

$$\mathcal{L} = -\frac{1}{4\pi}[m\varepsilon^{\mu\nu\lambda}a_\mu\partial_\nu a_\lambda - 2e\varepsilon^{\mu\nu\lambda}A_\mu\partial_\nu a_\lambda] + la_\mu\tilde{j}^\mu. \tag{1.40}$$

For a quasiparticle located at $\mathbf{r}_0$, the density $\tilde{j}^0(\mathbf{r}) = \delta(\mathbf{r}-\mathbf{r}_0)$. The Euler-Lagrangian equation of the gauge field a_μ can be easily obtained, whose 0th component is

$$\frac{1}{2\pi}\varepsilon^{0\nu\lambda}\partial_\nu a_\lambda = j^0 = \frac{e}{2\pi m}B + \frac{l}{m}\delta(\mathbf{r}-\mathbf{r}_0). \tag{1.41}$$

On the right side of the equation, the first term reflects the filling factor $\nu = 1/m$, while the second term means there is an extra l/m number of electrons at $\mathbf{r}_0$, due to the presence of the quasiparticle. Hence, the quasiparticle has an electric charge $-le/m$. The e/m-charged fundamental quasihole (wave function given in Eq. (1.22)) corresponds to an excitation with $l = -1$ and the $-e/m$-charged fundamental quasi-electron (wave function given in Eq. (1.23)) corresponds to an excitation with $l = 1$.

The exchange statistical phase of two quasiparticles with $l = l_1$ and $l = l_2$ can also be obtained. We first replace the source $l\tilde{j}^\mu$ in Eq. (1.40) with $(l_1\tilde{j}_1^\mu + l_2\tilde{j}_2^\mu)$, where $\tilde{j}_1^\mu(\mathbf{r}_1) = (\delta(\mathbf{r}-\mathbf{r}_1), \dot{\mathbf{r}}_1\delta(\mathbf{r}-\mathbf{r}_1))$ and $\tilde{j}_2^\mu(\mathbf{r}_2) = (\delta(\mathbf{r}-\mathbf{r}_2), \dot{\mathbf{r}}_2\delta(\mathbf{r}-\mathbf{r}_2))$. Then, we integrate out the gauge field a_μ to obtain an effective theory for only the quasiparticles $\tilde{j}_1^\mu$ and $\tilde{j}_2^\mu$, in which there is a term

$$\mathcal{L}_{12} = \tilde{j}_1^\mu \frac{l_1 l_2}{\frac{m}{2\pi}\partial_\lambda\varepsilon^{\mu\lambda\nu}}\tilde{j}_2^\nu. \tag{1.42}$$

We can treat this term as the way $\tilde{j}_1^\mu$ (or $\tilde{j}_2^\mu$) couples to an extra gauge field $(\delta A)_\mu$, in addition to the electromagnetic gauge field A_μ, where $(\delta A)_\mu$ satisfies $\frac{m}{2\pi l_1 l_2}\varepsilon^{\mu\nu\lambda}\partial_\nu(\delta A)_\lambda = \tilde{j}_2^\mu$ (or $\frac{m}{2\pi l_1 l_2}\varepsilon^{\mu\nu\lambda}\partial_\nu(\delta A)_\lambda = \tilde{j}_1^\mu$). By moving one of the quasiparticles to the origin and keeping it still, $\mathbf{r}_2 = \dot{\mathbf{r}}_2 = 0$, we find that $(\delta A)_\mu$ is simply the gauge field that appeared as the second term (multiplied by $l_1 l_2$) in Eq. (1.32), which produces an exchange statistical phase $\pi l_1 l_2/m$.

In general, a FQH state can be a hierarchical state of multiple levels in which the densities of quasiparticles are described by several gauge fields $a_{I\mu}$, $I = 1, 2, \cdots$. The effective theory of such a general FQH state is

$$\mathcal{L} = -\frac{1}{4\pi}K_{IJ}\varepsilon^{\mu\nu\lambda}a_{I\mu}\partial_\nu a_{J\lambda} + \frac{e}{2\pi}t_I\varepsilon^{\mu\nu\lambda}A_\mu\partial_\nu a_{I\lambda}, \tag{1.43}$$

where A_μ is the electromagnetic gauge field, K_{IJ} is an integer-valued matrix called "K matrix" and t_I is called "charge vector". t_I determines how the quasiparticle densities $j_I^\mu = \frac{1}{2\pi}\varepsilon^{\mu\nu\lambda}\partial_\nu a_{I\lambda}$ couple to the electromagnetic gauge field. $t_I = 1$ if I labels a physical electron layer at the bottom level of the hierarchy. $t_I = 0$ if I labels a quasiparticle condensate layer at a higher level of the hierarchy. In the case when I labels a physical layer of $2e$-charged Cooper-pairs, $t_I = 2$. The K matrix and the charge vector together characterize the topological order of the FQH state. The number of "1" entries in the charge vector equals the number of layers of physical electrons at the bottom level of the hierarchical state. The filling factor of this hierarchical state is given by

$$\nu = t_I(K^{-1})_{IJ}t_J. \tag{1.44}$$

A generic quasiparticle excitation is created by the source term $l_I a_{I\mu} j^\mu$, where $j^\mu(\mathbf{r}) = (\delta(\mathbf{r}-\mathbf{r}), \dot{\mathbf{r}}\delta(\mathbf{r}-\mathbf{r}))$. The integers l_I define the properties of the quasiparticle. By the same argument as for the Laughlin state, the electric charge e^* of the quasiparticle

is given by

$$e^*/e = l_I (K^{-1})_{IJ} t_J. \tag{1.45}$$

The exchange statistical phase θ of two quasiparticles labeled by the integers $(l_1)_I$ and $(l_2)_I$ is given by

$$\theta/\pi = (l_1)_I (K^{-1})_{IJ} (l_2)_J. \tag{1.46}$$

1.3.4 Example: Connection between wave function approach and effective field theory

In this subsection, we illustrate the connection between the wave function approach (Subsection 1.3.2, Refs. [30, 32–34]) and the effective field theory (Subsection 1.3.3, Refs. [5, 12]). The two formalisms are equivalent in describing the phenomenological properties of a FQH system, such as the filling factor and the quasiparticle charge and statistics. We verify such equivalence for a generic 3 by 3 K matrix

$$K_{3\times 3} = \begin{pmatrix} m_1 & n & p_1 \\ n & m_2 & p_2 \\ p_1 & p_2 & -m_3 \end{pmatrix} \tag{1.47}$$

with charge vector $\mathbf{t}^T_{1\times 3} = (1, 1, 0)$ and a generic 4 by 4 K matrix

$$K_{4\times 4} = \begin{pmatrix} m_1 & n & p_1 & p_3 \\ n & m_2 & p_2 & p_4 \\ p_1 & p_2 & -m_3 & -l \\ p_3 & p_4 & -l & -m_4 \end{pmatrix} \tag{1.48}$$

with charge vector $\mathbf{t}^T_{1\times 4} = (1, 1, 0, 0)$. The material presented here is a straightforward exercise based on the method in Ref. [34].

We first write down the wave function of the parental FQH state,

$$\Psi_0([z_i], [w_i]) = \prod_{i<j}(z_i - z_j)^{m_1} \prod_{i<j}(w_i - w_j)^{m_2} \prod_{i,j}(z_i - w_j)^n e^{-\frac{1}{4l_B^2}(\sum_i |z_i|^2 + \sum_i |w_i|^2)}. \quad (1.49)$$

This is a bi-layer state. Electrons in the first and the second layer are labeled by the sets of coordinates $[z_i]$ and $[w_i]$, respectively. The corresponding K matrix is

$$K_{2\times 2} = \begin{pmatrix} m_1 & n \\ n & m_2 \end{pmatrix} \quad (1.50)$$

with the charge vector $\mathbf{t}^T_{1\times 2} = (1, 1)$.

3 by 3 K matrix

Consider a quasihole in the parental FQH state, described by the wave function

$$\Psi_1([z_i], [w_i], \xi) = \prod_i (z_i - \xi)^{p_1} \prod_i (w_i - \xi)^{p_2} \Psi_0([z_i], [w_i]). \quad (1.51)$$

In K-matrix formalism, such quasiholes are characterized by a two-component vector $\mathbf{p} = (p_1, p_2)$, defined with respect to the K matrix $K_{2\times 2}$. In K-matrix formalism (Subsection 1.3.3), the electric charge of the quasihole is

$$(\mathbf{p}^T K^{-1}_{2\times 2} \mathbf{t}_{1\times 2}) e = \frac{(m_2 - n)p_1 + (m_1 - n)p_2}{m_1 m_2 - n^2} e \quad (1.52)$$

and the statistical phase between two such quasiholes is

$$(\mathbf{p}^T K_{2\times 2}^{-1}\mathbf{p})\pi = \frac{m_2 p_1^2 + m_1 p_2^2 - 2np_1p_2}{m_1 m_2 - n^2}\pi. \tag{1.53}$$

In the following, we show that the charge and statistics of the quasihole can also be obtained in the wave function approach, through the plasma analogue.

In the plasma analogue, the bi-layer parental FQH state corresponds to a system of two kinds of plasma particles. Each particle carries two types of plasma "charges" . Writing $|\Psi_1|^2 = e^{-\beta F_1}$, where $\beta = 2$, we find the classical energy function

$$\begin{aligned} F_1([z_i],[w_i],\xi) = &- m_1 \sum_{i<j} \ln|z_i - z_j| - m_2 \sum_{i<j} \ln|w_i - w_j| - n \sum_{i,j} \ln|z_i - w_j| \\ &- p_1 \sum_i \ln|z_i - \xi| - p_2 \sum_i \ln|w_i - \xi| \\ &+ \frac{1}{4l_B^2}(\sum_i |z_i|^2 + \sum_i |w_i|^2) \end{aligned} \tag{1.54}$$

of the plasma system, where z_i labels one kind of particles and w_i labels the other kind. The coupling constants among plasma particles are: m_2 between two z_i particles, m_2 between two w_i particles, and n between a z_i particle and a w_i particle. We can imagine that each z_i particle carries $\sqrt{m_1}$ amount of type-one "charge" and $\frac{n}{\sqrt{m_2}}$ amount of type-two "charge", whereas each w_i particle carries $\frac{n}{\sqrt{m_1}}$ amount of type-one "charge" and $\sqrt{m_2}$ amount of type-two "charge". Moreover, z_i particles only see and interact with type-one "charge", whereas w_i particles only see and interact with type-two "charge". Hence, we have the coupling constants in F_1. In addition to the z_i, w_i particles, there is an impurity particle located at ξ. We can deduce its "charges" from the fact that it couples to z_i and w_i particles through coupling constants p_1 and p_2, respectively. The impurity has $\frac{p_1}{\sqrt{m_1}}$ amount of type-one "charge" and $\frac{p_2}{\sqrt{m_2}}$ amount of type-two "charge". To keep "charge" neutrality of the

system everywhere, there must be a number x_1 of z_i particles and a number x_2 of w_i particles missing near the impurity. The total "charges" of the missing plasma particles equal the "charges" of the impurity particle. Hence, we have

$$\begin{aligned} \sqrt{m_1}x_1 + \tfrac{n}{\sqrt{m_1}}x_2 &= \tfrac{p_1}{\sqrt{m_1}} \qquad \text{(type-one plasma "charge")} \\ \tfrac{n}{\sqrt{m_2}}x_2 + \sqrt{m_2}x_1 &= \tfrac{p_2}{\sqrt{m_2}} \qquad \text{(type-two plasma "charge")}, \end{aligned} \tag{1.55}$$

or in matrix format,

$$\begin{pmatrix} m_1 & n \\ n & m_2 \end{pmatrix} \begin{pmatrix} x_1 \\ x_2 \end{pmatrix} = \begin{pmatrix} p_1 \\ p_2 \end{pmatrix}. \tag{1.56}$$

This gives $x_1 = \frac{m_2 p_1 - n p_2}{m_1 m_2 - n^2}$ and $x_2 = \frac{m_1 p_2 - n p_1}{m_1 m_2 - n^2}$. Switching to the realistic FQH system, this means the quasihole at ξ is composed of x_1 number of z_i holes (absence of electrons) and x_2 number of w_i holes. Both z_i holes and w_i holes have positive electric charge e. Hence, the electric charge of the quasihole at ξ is qe, where

$$q = x_1 + x_2 = \frac{(m_2 - n)p_1 + (m_1 - n)p_2}{m_1 m_2 - n^2}, \tag{1.57}$$

which agrees with the result (Eq. (1.52)) in K-matrix formalism.

We now obtain the statistics of quasiholes. In the plasma analogue, we consider the case when many impurity particles are present in the system. We label the impurities by ξ_i. We complete the expression $\tilde{F}_1$ of classical energy function by adding the mutual interaction between impurities and the interaction of impurities

with the background charge,

$$\begin{aligned}\tilde{F}_1([z_i],[w_i],[\xi_i]) =& -m_1\sum_{i<j}\ln|z_i-z_j| - m_2\sum_{i<j}\ln|w_i-w_j| - n\sum_{i,j}\ln|z_i-w_j| \\ & - p_1\sum_{i,j}\ln|z_i-\xi_j| - p_2\sum_{i,j}\ln|w_i-\xi_j| - r\sum_{i<j}\ln|\xi_i-\xi_j| \\ & + \frac{1}{4l_B^2}(\sum_i|z_i|^2+\sum_i|w_i|^2) + \frac{q}{4l_B^2}\sum_i|\xi_i|^2, \end{aligned} \tag{1.58}$$

where the coupling constant

$$\begin{aligned} r =& (\sqrt{m_1}x_1)^2 + (\sqrt{m_2}x_2)^2 + (\sqrt{m_1}x_1)(\frac{n}{\sqrt{m_1}}x_2) + (\frac{n}{\sqrt{m_2}}x_1)(\sqrt{m_2}x_2) \\ =& \frac{m_2p_1^2+m_1p_2^2-2np_1p_2}{m_1m_2-n^2}. \end{aligned} \tag{1.59}$$

Using $|\tilde{\Psi}_1|^2 = e^{-\beta\tilde{F}_1}$, where $\beta = 2$, we find the normalized many-quasihole wave function

$$\tilde{\Psi}_1([z_i],[w_i],[\xi_i]) = \prod_{i,j}(z_i-\xi_j)^{p_1}\prod_{i,j}(w_i-\xi_j)^{p_2}\prod_{i<j}|\xi_i-\xi_j|^r e^{-\frac{q}{4l_B^2}\sum_i|\xi_i|^2}\Psi_0([z_i],[w_i]), \tag{1.60}$$

up to a constant that does not depend on quasihole coordinates ξ_i, ξ_i^*. Hence, the normalization factor

$$C([\xi_i],[\xi_i^*]) = \prod_{i<j}|\xi_i-\xi_j|^{-2r}e^{\frac{q}{2l_B^2}\sum_i|\xi_i|^2}, \tag{1.61}$$

up to a constant that does not depend on ξ_i, ξ_i^*.

The statistical phase of quasiholes is contained in the Berry phase when a quasihole moves around another quasihole. Following Subsection 1.3.2, we can calculate the effective gauge potential a_{ξ_k} seen by a quasihole located at ξ_k, produced by the

rest degrees of freedom in the FQH system,

$$\begin{aligned} a_{\xi_k} =& i\langle\tilde{\Psi}_1|\partial_{\xi_k}|\tilde{\Psi}_1\rangle = \frac{i}{2}\frac{\partial}{\partial\xi_k}\ln C \\ =& \frac{i}{2}\big(\frac{q}{2l_B^2}\xi_k^* - \sum_{j\neq k}\frac{r}{\xi_k-\xi_j}\big). \end{aligned} \tag{1.62}$$

The first term in a_{ξ_k} is due to the external magnetic field and the second term gives the statistical phase $r\pi$ when two quasiholes are exchanged. The statistical phase obtained here agrees with that (Eq. (1.53)) obtained in K-matrix formalism.

We now study the hierarchical states formed by the above quasiholes, with electric charge qe and statistical phase $r\pi$. First of all, let us find the ground state wave function of a $\nu = 1/m_3$ FQH state made of the quasiholes. The effective Hamiltonian that describes the dynamics of quasiholes is

$$H_{\text{eff}} = \frac{1}{2m^*}\sum_i(\mathbf{p}_i - \mathbf{a}_i)^2 + \sum_{i<j}V(\mathbf{r}_i - \mathbf{r}_j), \tag{1.63}$$

where i is the quasihole index, m^* is the quasihole effective mass and $\mathbf{a}_i$ is the effective gauge potential given in Eq. (1.62), which produces correct quasihole statistics. In writing the Hamiltonian, we have set $\hbar = c = 1$. $V(\mathbf{r}_i - \mathbf{r}_j)$ is the electrostatic potential between quasiholes. We let it be short-ranged in the quasihole FQH state, for example, $V(\mathbf{r}) = \partial_{\mathbf{r}}^2\delta(\mathbf{r})$.

We want to find the ground state wave function of H_{eff}. This involves three steps. First, we drop the second term in the gauge potential $\mathbf{a}_i$ and set the interaction potential $V = 0$. The problem becomes that of a free quasihole in a magnetic field. Solving Schrodinger equation, the eigenfunctions in the lowest energy level take the form $f(\xi^*)e^{-\frac{q}{4l_B^2}|\xi|^2}$, where $f(\xi^*)$ is an arbitrary anti-holomorphic function of ξ. The anti-holomorphicity reflects the fact that quasiholes are positively

charged. If we let $f(\xi^*) = (\xi^*)^m$, the eigenfunctions have definite angular momenta m. Second, we turn on the interaction potential V. We then are dealing with a strongly-correlated system. According to Subsection (1.3.2), Laughlin state is the ground state of such a system, provided that V is sufficiently short-ranged, which we will use as an assumption. At filling factor $\nu = 1/m_3$, the quasihole Laughlin wave function is $\prod_{i<j}(\xi_i^* - \xi_j^*)^{m_3} e^{-\frac{q}{4l_B^2}\sum_i |\xi_i|^2}$. Using integration by part, we can verify that it is indeed the ground state of $V(\mathbf{r}) = \partial_{\mathbf{r}}^2 \delta(\mathbf{r}) = \partial_\xi \partial_{\xi^*} \delta(\mathbf{r})$. At this point, note that $\prod_{i<j}(\xi_i^* - \xi_j^*)^{m_3} e^{-\frac{q}{4l_B^2}\sum_i |\xi_i|^2}$ describes a collection of quasiholes with trivial statistics. In the last step, we recover the mutual statistics of quasiholes by restoring the second term in the gauge potential $\mathbf{a}_i$, when writing H_{eff}. Correspondingly, we add to the quasihole Laughlin wave function a normalization factor $\prod_{i<j} |\xi_i - \xi_j|^r$, which can be obtained through the plasma analogue. The resulting wave function

$$\Phi_1 = \prod_{i<j} |\xi_i - \xi_j|^r (\xi_i^* - \xi_j^*)^{m_3} e^{-\frac{q}{4l_B^2}\sum_i |\xi_i|^2} \tag{1.64}$$

is the ground state of the many-quasihole system H_{eff}.

The complete wave function of the hierarchical state is

$$\begin{aligned} \int \prod_i d^2\xi_i \tilde{\Psi}_1 \Phi_1 = \int \prod_i d^2\xi_i \prod_{i<j} (z_i - z_j)^{m_1} \prod_{i<j} (w_i - w_j)^{m_2} \prod_{i,j} (z_i - w_j)^n \\ \times \prod_{i,j} (z_i - \xi_j)^{p_1} \prod_{i,j} (w_i - \xi_j)^{p_2} \prod_{i<j} |\xi_i - \xi_j|^{2r} (\xi_i^* - \xi_j^*)^{m_3} \\ \times e^{-\frac{q}{2l_B^2}\sum_i |\xi_i|^2 - \frac{1}{4l_B^2}(\sum_i |z_i|^2 + \sum_i |w_i|^2)}. \end{aligned} \tag{1.65}$$

The filling factor of this hierarchical state can be found by again the plasma analogue. This time we have a system of three kinds of plasma particles. Each particle carries three types "charge". Let n_1, n_2 be the densities of electrons in the first, second layer, respectively. Let n_q be the density of quasiholes. Let $n_0 = \frac{1}{2\pi l_B^2}$ be the density

of states in a Landau level. "Charge" neutrality of the plasma system requires,

$$\begin{aligned}
\sqrt{m_1}n_1 + \tfrac{n}{\sqrt{m_1}}n_2 + \tfrac{p_1}{\sqrt{m_1}}n_q &= \tfrac{n_0}{\sqrt{m_1}} \\
\tfrac{n}{\sqrt{m_2}}n_1 + \sqrt{m_2}n_2 + \tfrac{p_2}{\sqrt{m_2}}n_q &= \tfrac{n_0}{\sqrt{m_2}} \\
\tfrac{p_1}{\sqrt{m_3+2r}}n_1 + \tfrac{p_2}{\sqrt{m_3+2r}}n_2 + \sqrt{m_3+2r}n_q &= \tfrac{2qn_0}{\sqrt{m_3+2r}},
\end{aligned} \tag{1.66}$$

or in matrix format,

$$\begin{pmatrix} m_1 & n & p_1 \\ n & m_2 & p_2 \\ p_1 & p_2 & m_3+2r \end{pmatrix} \begin{pmatrix} n_1 \\ n_2 \\ n_q \end{pmatrix} = \begin{pmatrix} n_0 \\ n_0 \\ 2qn_0 \end{pmatrix}, \tag{1.67}$$

where $q = \frac{(m_2-n)p_1+(m_1-n)p_2}{m_1m_2-n^2}$ and $r = \frac{m_2p_1^2+m_1p_2^2-2np_1p_2}{m_1m_2-n^2}$ were obtained before. Solving Eq. (1.66) or Eq. (1.67) for n_1, n_2 and n_q, we find the filling factor

$$\nu = \frac{n_1+n_2}{n_0} = \frac{m_1m_3+m_2m_3-2m_3n+p_1^2-2p_1p_2+p_2^2}{m_1m_2m_3-m_3n^2+m_2p_1^2-2np_1p_2+m_1p_2^2}. \tag{1.68}$$

As one can check, this agrees with the result

$$\nu = \mathbf{t}_{1\times3}^T K_{3\times3}^{-1} \mathbf{t}_{1\times3} \tag{1.69}$$

in K-matrix formalism.

4 by 4 K matrix

In this case, we consider two types of quasiholes. In the most general case, let ξ_i label the first type of quasiholes which couple to the z_i, w_i electrons through integers p_1, p_2, and let η_i label the second type of quasiholes which couple to the z_i, w_i electrons

through integers p_3, p_4. The wave function for a quasihole of the first type is

$$\Psi_1^{qh1}([z_i],[w_i],\xi) = \prod_i (z_i-\xi)^{p_1} \prod_i (w_i-\xi)^{p_2} \Psi_0([z_i],[w_i]). \tag{1.70}$$

The wave function for a quasihole of the second type is

$$\Psi_1^{qh2}([z_i],[w_i],\eta) = \prod_i (z_i-\eta)^{p_3} \prod_i (w_i-\eta)^{p_4} \Psi_0([z_i],[w_i]). \tag{1.71}$$

We can apply the plasma analogue as before to find the electric charges $q_1 e$ and $q_2 e$ of the first type and the second type of quasiholes, respectively. We have $q_1 = \frac{(m_2-n)p_1+(m_1-n)p_2}{m_1 m_2-n^2}$ and $q_2 = \frac{(m_2-n)p_3+(m_1-n)p_4}{m_1 m_2-n^2}$. Hence, a quasihole of the first type is composed of $x_1 = \frac{m_2 p_1 - n p_2}{m_1 m_2 - n^2}$ amount of z_i holes and $x_2 = \frac{m_1 p_2 - n p_1}{m_1 m_2 - n^2}$ amount of w_i holes. A quasihole of the second type is composed of $x_3 = \frac{m_2 p_3 - n p_4}{m_1 m_2 - n^2}$ amount of z_i holes and $x_4 = \frac{m_1 p_4 - n p_3}{m_1 m_2 - n^2}$ amount of w_i holes.

In the presence of many quasiholes, the coupling constants between different types of quasiholes are: $r_1 = m_1 x_1^2 + m_2 x_2^2 + 2n x_1 x_2$ between two quasiholes of the first type, $r_2 = m_1 x_3^2 + m_2 x_4^2 + 2n x_3 x_4$ between two quasiholes of the second type, and $r_3 = m_1 x_1 x_3 + m_2 x_2 x_4 + n(x_1 x_4 + x_2 x_3)$ between a quasihole of the first type and a quasihole of the second type. Using $|\tilde{\Psi}_1|^2 = e^{-\beta \tilde{F}_1}$, where $\beta = 2$ and $\tilde{F}_1$ is the complete classical energy function including mutual interaction between quasiholes and the interaction of quasiholes with the background, we find the normalized wave function of many quasiholes

$$\begin{aligned}\tilde{\Psi}_1([z_i],[w_i],[\xi_i],[\eta_i]) = & \prod_{i,j}(z_i-\xi_j)^{p_1} \prod_{i,j}(w_i-\xi_j)^{p_2} \prod_{i,j}(z_i-\eta_j)^{p_3} \prod_{i,j}(w_i-\eta_j)^{p_4} \\ & \times \prod_{i<j} |\xi_i-\xi_j|^{r_1} \prod_{i<j} |\eta_i-\eta_j|^{r_2} \prod_{i<j} |\xi_i-\eta_j|^{r_3} \\ & \times e^{-\frac{q_1}{4l_B^2}\sum_i |\xi_i|^2 - \frac{q_2}{4l_B^2}\sum_i |\eta_i|^2} \Psi_0([z_i],[w_i]),\end{aligned} \tag{1.72}$$

up to a constant that does not depend on the quasihole coordinates. Hence, the normalization factor

$$C([\xi_i],[\xi_i^*],[\eta_i],[\eta_i^*]) = \prod_{i<j}|\xi_i-\xi_j|^{-2r_1}\prod_{i<j}|\eta_i-\eta_j|^{-2r_2}\prod_{i<j}|\xi_i-\eta_j|^{-2r_3}e^{\frac{q_1}{2l_B^2}\sum_i|\xi_i|^2+\frac{q_2}{2l_B^2}\sum_i|\eta_i|^2}, \tag{1.73}$$

up to a constant. Substituting C into Eq. (1.31), we find the effective gauge potentials on quasiholes which produce the same statistics as one would obtain in K-matrix formalism.

Consider now the hierarchical states formed by quasiholes. Suppose the quasiholes form a bi-layer FQH state characterized by three integers: m_3, m_4, l. The complete wave function of the hierarchical state can be written down as

$$\begin{aligned}
&\int\prod_i d^2\xi_i\prod_i d^2\eta_i\prod_{i<j}(z_i-z_j)^{m_1}\prod_{i<j}(w_i-w_j)^{m_2}\prod_{i,j}(z_i-w_j)^n\\
&\times\prod_{i,j}(z_i-\xi_j)^{p_1}\prod_{i,j}(w_i-\xi_j)^{p_2}\prod_{i,j}(z_i-\eta_j)^{p_3}\prod_{i,j}(w_i-\eta_j)^{p_4}\\
&\times\prod_{i<j}|\xi_i-\xi_j|^{2r_1}\prod_{i<j}|\eta_i-\eta_j|^{2r_2}\prod_{i<j}|\xi_i-\eta_j|^{2r_3}\\
&\times\prod_{i<j}(\xi_i^*-\xi_j^*)^{m_3}\prod_{i<j}(\eta_i^*-\eta_j^*)^{m_4}\prod_{i,j}(\xi_i^*-\eta_j^*)^l\\
&\times e^{-\frac{q_1}{2l_B^2}\sum_i|\xi_i|^2-\frac{q_2}{2l_B^2}\sum_i|\eta_i|^2-\frac{1}{4l_B^2}(\sum_i|z_i|^2+\sum_i|w_i|^2)},
\end{aligned} \tag{1.74}$$

following the argument that leads to Eq. (1.65). The filling factor of the hierarchical state is obtained by solving the matrix equation

$$\begin{pmatrix} m_1 & n & p_1 & p_3\\ n & m_2 & p_2 & p_4\\ p_1 & p_2 & (m_3+2r_1) & (l+2r_3)\\ p_3 & p_4 & (l+2r_3) & (m_4+2r_2)\end{pmatrix}\begin{pmatrix} n_1\\ n_2\\ n_{q1}\\ n_{q2}\end{pmatrix} = \begin{pmatrix} n_0\\ n_0\\ 2q_1n_0\\ 2q_2n_0\end{pmatrix} \tag{1.75}$$

in the plasma analogue, where n_1, n_2 are the densities of z_i, w_i electrons and n_{q_1} and n_{q_2} are the densities of ξ_i, η_i quasiholes. The result $\nu = \frac{n_1+n_2}{n_0}$ agrees with the filling factor

$$\nu = \mathbf{t}_{1\times 4}^T K_{4\times 4}^{-1} \mathbf{t}_{1\times 4} \tag{1.76}$$

in K-matrix formalism.

1.3.5 Edge dynamics: Consequence of incompressibility

We now discuss the edge dynamics of a FQH liquid. In Subsection 1.3.1, we have seen that a FQH liquid is incompressible in the bulk, i.e. there exists an energy gap which prevents the bulk from being squeezed. As a result, at low energy, gapless excitations only exist on the one-dimensional edge of the FQH liquid, in the form of area-preserving shape distortion [29] of the 2DEG. It turns out [5, 40] that the edge physics of a FQH liquid is described by a Luttinger liquid theory [41].

Below, we provide a scenario on how the incompressibility condition turns an one-dimensional free electron system, which describes the edge of a 2DEG which partially fills a Landau level, into a Luttinger liquid, which describes the edge of a FQH liquid.

From Sections 1.1 and 1.2, we know that an electron drifts at a velocity $v = cE/B$, under mutually perpendicular electric field $\mathbf{E}$ and magnetic field $\mathbf{B}$. This is true both from classical and quantum mechanical points of view. Consider a 2DEG which fills the Landau level partially but does not form a FQH state. In such a case, we view the electrons as non-interacting particles. Consider the edge of the 2DEG, parameterized in x coordinate, as shown in Fig. 1.5, left panel. We assume a constant gradient of

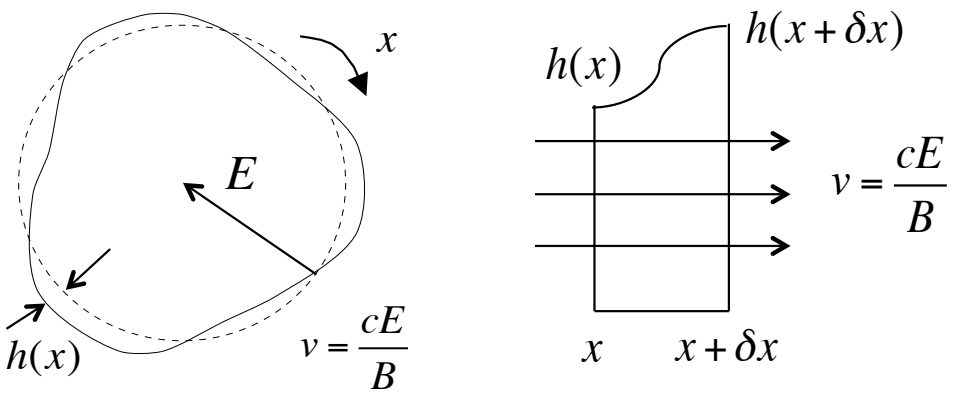

Figure 1.5: Edge dynamics of a FQH liquid. The edge is parameterized in x coordinate. The confining potential of 2DEG provides a radial electric field E. Electrons drift at the velocity $v = cE/B$. Local height of the FQH edge is defined with respect to the equilibrium radius (dashed circle) of the 2DEG and is denoted by $h(x)$.

the confining potential such that all the electrons feel the same electric field and drift at the same velocity v. On the edge, the fluctuation of local electron density gives rise to the variation of the local height of the edge. We can take a slice of the edge (Fig. 1.5, right panel) and write down its continuity equation,

$$\frac{d(\rho(x)\delta x)}{dt} = j(x)(h(x) - h(x+\delta x)) \approx -j(x)\frac{d(h(x))}{dx}\delta x \tag{1.77}$$

where $\rho(x)$, $j(x)$ and $h(x)$ are the local electron density, the local electron current density and the local height of the edge defined with respect to the equilibrium radius of 2DEG (Fig. 1.5), respectively. We now apply the incompressibility condition. This means a uniform area density n of electrons throughout the 2DEG. In particular, electrons are dispersed evenly along the radial direction of the 2DEG. Accordingly, we demand $\rho(x)\delta x = nh(x)\delta x$ and $j(x) = nv$ in the slice. The continuity equation then becomes

$$\frac{d\rho(x)}{dt} = -v\frac{d\rho(x)}{dx}, \tag{1.78}$$

which is simply the equation of motion of a (right-moving) chiral density wave $\rho(x)$, on the edge of the FQH liquid.

The edge wave obtained here is analogous to the gravity wave in shallow water where the density of the constituent particles is uniform and all the particles feel the same gravitational force. Here, the gravitational force is replaced by the electrostatic force produced by the confining potential.

By a similar logic, we can obtain the Hamiltonian of the chiral edge wave in Eq. (1.78). We start from a non-interacting 2DEG under magnetic field. By Eq. (1.11), the kinetic energy of an electron in the lowest Landau level is $\frac{1}{2}\hbar\omega_c + \frac{1}{2}m_0v^2$, where m_0 is the effective mass of electron. The potential energy of an electron due to the constant-gradient confining potential is eEz, where z is the radial coordinate defined with respect to the equilibrium radius of the 2DEG. The Hamiltonian of the non-interacting 2DEG is hence

$$H_0 = \int dx \int dz[\frac{1}{2}\hbar\omega_c + \frac{1}{2}m_0v^2 + eEz]\rho(x,z) \tag{1.79}$$

where x still parameterizes the azimuthal direction along the edge. $\rho(x,z)$ is the local area density of electrons. Next, we turn on the electron-electron interaction which converts the 2DEG into an incompressible liquid with uniform area density n of electrons. The incompressibility condition suggests the replacement

$$\delta x \int dz\rho(x,z) \to \delta x n(h(x) + r_0) = \delta x(\rho(x) + nr_0), \tag{1.80}$$

in Eq. (1.79), where $\rho(x) = nh(x)$ and r_0 is the equilibrium radius of the 2DEG,

such that

$$\begin{aligned} H_0 \to H &= \int dx[\frac{1}{2}\hbar\omega_c + \frac{1}{2}m_0v^2 + eE\frac{h(x)}{2}][\rho(x) + nr_0] \\ &= \int dx[(\frac{1}{2}\hbar\omega_c + \frac{1}{2}m_0v^2 + \frac{1}{2}eEr_0)\rho(x) + \pi\frac{v}{\nu}\rho^2(x)] \\ &\to \int dx\pi\frac{v}{\nu}\rho^2(x). \end{aligned} \tag{1.81}$$

In the first line, $eE\frac{h(x)}{2}$ is the averaged potential energy per electron in a local "tower" of evenly-spaced electrons with height $h(x)$: An electron at the bottom of the "tower" has zero potential energy while an electron at the top of the "tower" has a potential energy $eEh(x)$. In the second line, we have defined the filling factor $\nu = n/n_\Phi$ as the ratio of the density n of electrons to the density $n_\Phi = B/\Phi_0$ of magnetic flux quanta in a Landau level, where $\Phi_0 = 2\pi/e$. In the third line, we have shifted the reference with respect to which we define the electron density operator $\rho(x)$,

$$\rho \to \rho - \frac{\nu}{4\pi v}(\hbar\omega_c + m_0v^2 + eEr_0). \tag{1.82}$$

As we see, upon applying the incompressibility condition, the non-interaction one-dimensional electron system H_0 becomes a chiral Luttinger liquid H.

One can proceed to quantize the density mode ρ in the edge theory H of the FQH liquid at filling factor $\nu = 1/m$. For this end, it is convenient to bosonize [42,43] the density mode using $\rho(x) = \frac{1}{2\pi}\partial_x\phi(x)$. The commutation relation of the field operator ϕ is

$$[\phi(x), \phi(x')] = i\frac{\pi}{m}\mathrm{sgn}(x - x'), \tag{1.83}$$

where $\mathrm{sgn}(x)$ is the signum function. The electron operator Ψ_e on the edge of the

FQH liquid is obtained by the fact that it annihilates a localized electric charge e,

$$[\rho(x), \Psi_e^\dagger(x')] = \delta(x - x')\Psi_e^\dagger(x'), \tag{1.84}$$

which gives

$$\Psi_e(x) \propto e^{im\phi(x)} \tag{1.85}$$

by Eq. (1.83). We hence have

$$\Psi_e(x)\Psi_e(x') = (-)^m \Psi_e(x')\Psi_e(x), \tag{1.86}$$

such that the electrons obey fermionic statistics. Similarly, the fundamental quasiparticle operator Ψ_{qp} annihilates a localized electric charge e/m,

$$[\rho(x), \Psi_{qp}^\dagger(x')] = \frac{1}{m}\delta(x - x')\Psi_{qp}^\dagger(x'), \tag{1.87}$$

which gives,

$$\Psi_{qp}(x) \propto e^{i\phi(x)}. \tag{1.88}$$

We have

$$\Psi_{qp}(x)\Psi_{qp}(x') = (-)^{\frac{1}{m}} \Psi_{qp}(x')\Psi_{qp}(x), \tag{1.89}$$

such that the fundamental quasiparticles obey fractional statistics with exchange statistical phase π/m, in agreement with Eqs. (1.32)(1.42).

The correlation functions of the electron operator Ψ_e and the fundamental quasiparticle operator Ψ_{qp} are obtained as follows. First, we combine the equation of motion (Eq. (1.78)), the Hamiltonian (Eq. (1.81)) and the bosonization identity

$\rho = \frac{1}{2\pi}\partial_x\phi$ to write down the Lagrangian density of the $\nu = 1/m$ FQH liquid,

$$\mathcal{L} = -\frac{m}{4\pi}[\partial_t\phi\partial_x\phi + v(\partial_x\phi)^2]. \tag{1.90}$$

Then, we can compute the correlation function of ϕ field,

$$\langle\phi(x,t)\phi(0,0)\rangle = -\frac{1}{m}\ln[\sigma i(t+x)+a] + \text{constant} \tag{1.91}$$

where $a \to 0$ is the infinitesimal regulator and $\sigma = \text{sgn}(t)$ is the sign of time t. The correlation functions of $\Psi_e(x) \propto e^{im\phi(x)}$ and $\Psi_{qp}(x) \propto e^{i\phi(x)}$ then follow easily,

$$\langle\Psi_e(x,t)\Psi_e(0,0)\rangle \propto [\frac{1}{i(t+x)+\sigma a}]^m \tag{1.92}$$

and

$$\langle\Psi_{qp}(x,t)\Psi_{qp}(0,0)\rangle \propto [\frac{1}{i(t+x)+\sigma a}]^{\frac{1}{m}}. \tag{1.93}$$

In general, the edge of a FQH liquid may support multiple density modes ϕ_I, where $I = 1, 2, 3, \cdots$. These density modes may propagate in the same direction or in opposite directions. The Lagrangian density for a general FQH edge is [5]

$$\mathcal{L} = -\frac{1}{4\pi}\sum_{I,J}[K_{IJ}\partial_t\phi_I\partial_x\phi_J + V_{IJ}\partial_x\phi_I\partial_x\phi_J], \tag{1.94}$$

where K_{IJ} is the K matrix that appears in the bulk effective theory of the FQH liquid and V_{IJ} is the potential matrix which must be positive-definite to ensure the stability of the FQH edge. The connection between the edge effective theory and the bulk effective theory of a FQH liquid is termed as "edge-bulk correspondence". It is this correspondence that allows experimentalists to detect the bulk topological order of a FQH liquid through quasiparticle tunneling [23, 24] on the edge. In fact,

it can be shown [5] that the edge effective theory (Eq. (1.94)) contains the necessary degrees of freedom one should put on the boundary of the 2DEG in order to keep the total system (edge + bulk effective theory) invariant under gauge transformation. Upon quantization, the density modes in Eq. (1.94) have the commutation relations

$$[\phi_I(x), \phi_J(x')] = i\pi(K^{-1})_{IJ}\mathrm{sgn}(x - x'). \tag{1.95}$$

A generic quasiparticle operator on the FQH edge described by Eq. (1.94) is

$$\Psi_{\mathbf{l}} \propto e^{i\sum_I l_I\phi_I}, \tag{1.96}$$

where $\mathbf{l}$ is an integer-valued vector, $(\mathbf{l})_I = l_I$. Using the same argument around Eqs. (1.84)(1.87), the electric charge of $\Psi_{\mathbf{l}}$ can be found to be $\mathbf{l}K^{-1}\mathbf{t}e$, where $\mathbf{t}$ is the charge vector. Given two quasiparticles $\Psi_{\mathbf{l}_1}$ and $\Psi_{\mathbf{l}_2}$, the exchange statistical phase is $\mathbf{l}_1K^{-1}\mathbf{l}_2\pi$. These formulas agree with the formulas in Subsection 1.3.3 for quasiparticles in the bulk of a FQH liquid.

Eq. (1.94) does not exhaust all possible FQH edge physics. For example, in certain FQH states [10, 44, 45], Majorana fermion modes exist. A (right-moving) Majorana mode ψ on the edge of a FQH liquid has the Lagrangian density

$$\mathcal{L} = i\psi(x)(\partial_t + v\partial_x)\psi(x). \tag{1.97}$$

Unlike the density modes which are bosonic and obey commutation relations, Majorana fermions obey anti-commutation relations.

1.3.6 Quasiparticle tunneling on the quantum Hall edge

In this subsection, we discuss quasiparticle tunneling between two FQH edges, within a FQH liquid. The material presented here is the theoretical basis of the quasiparticle tunneling experiments [23, 24] discussed in Chapter 2.

As explained in Subsections 1.3.1 and 1.3.5, the low energy physics of a FQH liquid is on the edge, i.e. as the area-preserving shape distortion of the incompressible bulk. In the absence of edge reconstruction [46], the edge dynamics is described by a Luttinger liquid theory which captures the topological property of the bulk. Quasiparticles as collective excitations of electrons exist and propagate on the edge. Assuming translational invariance on the edge, the linear momenta of edge modes are well defined. The presence of gauge field requires edge modes with different linear momenta to be spatially separated, and vice versa. Hence, a mismatch in linear momentum exists between the upper and the lower FQH edges, which serves as a barrier for the tunneling of quasiparticles. The mismatch is gauge invariant and is proportional to the distance between opposite edges. In the vicinity of a quantum point contact (QPC), the two opposite edges are brought close so that the momentum mismatch is greatly reduced. On the other hand, quasiparticles on the QPC have large uncertainties in momenta due to small cross-sectional dimension of the QPC. Tunneling of quasiparticles is justified when the momentum mismatch between opposite edges is accomodated by the uncertainties in momenta of quasiparticles, and is more likely to happen when quasiparticles circumvent impurities in their ways of propagation. If the QPC is narrow, unscreened Coulomb interaction couples charged edge modes across the QPC. The interaction modifies the scaling behaviors of charged modes and as a result, changes the tunneling exponent.

The Hamiltonian for the tunneling of quasiparticles between an upper and a lower

FQH edges has the general expression

$$H = H_0 + \sum_n (\Gamma_n O_n + \text{H.c.}), \tag{1.98}$$

where H_0 is the Luttinger liquid theory describing dynamics on both FQH edges in the absence of tunnelings. Terms in H_0 include self interactions within the same edge modes, mutual interactions among different edge modes and unscreened Coulomb interaction across any narrow QPC involved, all in the form of density-density interaction. In the context of a vector space spanned by different species of edge modes, H_0 can be viewed as a symmetric bilinear form, called the potential matrix, which is positive-definite [5] in order for the FQH edge it describes to be stable. O_n is an operator describing the tunneling of a quasiparticle on the QPC. Γ_n is a complex parameter characterizing the strength of O_n, the tunneling amplitude. In a tunneling event, a quasiparticle is removed from the upper edge and becomes another quasiparticle added to the lower edge, or vice versa. The removed and the added quasiparticle operators do not have to be identical as long as the electric and topological charges are conserved during the process. A tunneling operator O_n has the form $\Psi_n^u \Psi_n^{d\dagger}$, where Ψ_n^u and Ψ_n^d are the quasiparticle operators from the upper and the lower edges, respectively, participating in the tunneling event described by O_n. For tunnelings at low temperature, it suffices to consider only the most relevant quasiparticle operators in the given FQH state. Accordingly, the sum $\sum_n$ in the Hamiltonian includes only the most relevant tunneling operators.

The Hamiltonian can be cast in a bosonized [42,43] form in which edge modes are described by boson fields. Let ϕ_I^μ be the bosonized I^{th} mode on edge μ, where $\mu = u, d$ labels the upper or the lower edge, respectively, and both edges are parameterized in x. H_0 is written in boson fields after the identity, $\rho_I^\mu(x) = \frac{1}{2\pi}((-)^{\gamma_I}\partial_x \phi_I^\mu(x) + k_{F,I}^\mu)$, where $\rho_I^\mu(x)$ is the local electron number density at x and $k_{F,I}^\mu$ is the Fermi momen-

tum, of edge mode ϕ_I^μ. $\gamma_I = 0$ or 1 depending on whether ϕ_I^μ is right-moving or left-moving. Tunneling operators are bosonized following the bosonization of quasiparticle operators, the latter having a general expression $\Psi_n^\mu(x) = e^{i\sum_I l_{n,I}^\mu(\phi_I^\mu(x)+(-)^{\gamma_I}k_{F,I}^\mu x)}$, or $\Psi_n^\mu(x) = \psi^\mu(x)e^{i\sum_I l_{n,I}^\mu(\phi_I^\mu(x)+(-)^{\gamma_I}k_{F,I}^\mu x)}$ if Majorana fermions ψ^μ exist on the edges. The constants $l_{n,I}^\mu$ denote the linear combination in ϕ_I^μ in order to bosonize Ψ_n^μ. For convenience, we let the tunneling happen at an impurity located at $x = 0$ such that Fermi momenta disappear in the bosonized quasiparticle operators and hence in the tunneling operators.

The tunneling current operator I is the time evolution of total electron number operator N^u on the upper edge (or $-N^d$ on the lower edge), $I = -ie[N^u, H] = ie[N^d, H]$. Upon bosonization, $N^u = \frac{1}{2\pi}\sum_I(\int dx(-)^{\gamma_I}\partial_x\phi_I^u + k_{F,I}^u L)$, where L is the length of the upper edge and ϕ_I^u are the charged modes. In the absence of tunneling, N^u is a good quantum number and its commutator with H_0 vanishes, $[N^u, H_0] = 0$. Hence,

$$I = -ie[N^u, \sum_n(\Gamma_n O_n(x=0) + \text{H.c.})]. \tag{1.99}$$

The commutator is evaluated using commutation relations of ϕ_I^u, which gives

$$I = -ie^*\sum_n(\Gamma_n O_n(x=0) - \text{H.c.}), \tag{1.100}$$

where e^* is the quasiparticle charge.

Quasiparticle tunneling is a nonequilibrium process. One can use Keldysh formalism [47] to compute the tunneling current, as the expectation of the tunneling current operator. We start from an equilibrium system described by H_0 in the remote past $t = -\infty$. Then, we adiabatically turn on the tunneling term in the Hamiltonian and evolve the system to the moment when tunneling happens. After the interac-

tion, we rewind time back to $t = -\infty$ and return to the initial system. The closed path of time evolution is the Keldysh contour, with the components before and after tunneling the + and − branches of the contour. The expectation is conveniently evaluated in interaction picture. Let V be the voltage bias between the upper and the lower edges across which tunneling of quasiparticles happens. The chemical potential difference between the two edges contributes a time dependent factor $e^{-i\omega t}$ to quasiparticle tunneling operators written in interaction picture, where $\omega = e^*V$. In interaction picture, the tunneling current operator is explicitly time dependent and the tunneling current is

$$\langle I(t)\rangle = \frac{1}{Z}\mathrm{Tr}\{e^{-\beta H_0}S_{K^-}(-\infty,t)I(t)S_{K^+}(t,-\infty)\} \tag{1.101}$$

at finite temperature $\beta = 1/T$, where

$$S_{K^\pm}(t_1,t_2) = \mathcal{T}\exp\Big(-i\int_{t_2}^{t_1}dt(\sum_n \Gamma_n O_n(t) + \mathrm{H.c.})\Big) \tag{1.102}$$

are the interaction picture time-evolution operators on the + and − branches of Keldysh contour, where $\mathcal{T}$ is the time-ordering operator. Z is the partition function of the initial equilibrium system in the remote past. The trace $\mathrm{Tr}\{\cdots\}$ is taken over energy eigenstates of the initial system. Here and for the rest of the paper, we suppress the spatial coordinate of tunneling operators and keep in mind they are valued at $x = 0$. For weak tunneling, we expand $S_{K^\pm}$ to obtain the tunneling current to lowest nonvanishing order in Γ_n,

$$\langle I\rangle = e^*\sum_n |\Gamma_n|^2\int_{-\infty}^{+\infty}dt(e^{i\omega t} - e^{-i\omega t})\langle O_n^\dagger(t)O_n(0)\rangle, \tag{1.103}$$

where the bracket $\langle\cdots\rangle$ is understood to be the finite temperature average in Eq. (1.101). At finite temperature, the equal-space correlation functions are $\langle O_n^\dagger(t)O_n(0)\rangle$ =

$(\frac{\pi T}{\sin \pi T(\epsilon+it)})^{2g}$ with g identified as the scaling dimension of the most relevant tunneling operators O_n and ϵ the infinitesimal regulator. Evaluating [48] the integral,

$$\langle I\rangle \sim T^{2g-1}B(g+i\frac{\omega}{2\pi T}, g-i\frac{\omega}{2\pi T})\sinh(\frac{\omega}{2T}), \tag{1.104}$$

where $B(x,y)$ is the Euler Beta function. The exponent g in the expression of tunneling current is defined as the tunneling exponent. As we see, the tunneling exponent comes directly from the scaling dimension in the correlation function. Hence, computing the tunneling exponent in a given FQH state is equivalent to finding the scaling dimension of the most relevant tunneling operators in the state. The value of the tunneling exponent is determined by the topological order of the FQH state.

The differential tunneling conductance is the derivative of tunneling current with respect to the voltage bias V,

$$\begin{aligned}\frac{d\langle I\rangle}{dV} &\sim T^{2g-2}B(g+i\frac{\omega}{2\pi T}, g-i\frac{\omega}{2\pi T}) \\ &\times(\pi\cosh(\frac{\omega}{2T}) - 2\sinh(\frac{\omega}{2T})\ \mathrm{Im}\{\Upsilon(g+i\frac{\omega}{2\pi T})\}),\end{aligned} \tag{1.105}$$

where $\Upsilon(x) = \Gamma'(x)/\Gamma(x)$ is the digamma function with $\Gamma(x)$ the gamma function. Eq. (1.105) is used to fit the data in the quasiparticle tunneling experiments [23, 24].

1.4 The quantum Hall effect at filling factor $\nu = \frac{5}{2}$

Shortly after the first discovery of FQH effect [3], a FQH state at filling factor $\nu = 5/2$ was observed [9]. This interesting FQH state cannot be incorporated into

the standard hierarchical construction (Subsections 1.3.2 and 1.3.3) of FQH states, where the filing factors are rational fractions $\nu = p/q$ with q an odd integer. The Hall resistance plateau at $\nu = 5/2$ is rather robust, with a measured energy gap ~ 500mK.

The even denominator in the filling factor $\nu = 5/2$ can be interpreted as due to a pairing mechanism. Along this line, various models [10–12, 44, 45, 49–55] were proposed to explain the $\nu = 5/2$ FQH state. In all these proposals, it is assumed that the physics of the $\nu = 5/2$ FQH liquid is completely captured by the $\nu = 1/2$ FQH state in the second Landau level, whereas the completely filled first Landau level is treated as an inert background. Such an assumption becomes exact at very high magnetic field B where Landau level mixing, proportional to $B^{-1/2}$, is negligible.

Among the proposed $\nu = 5/2$ FQH states, the Pfaffian state invented by Moore and Read [10] is interesting. It predicts quasiparticle excitations with non-Abelian statistics, which can be used for topological quantum computation [7,8]. The Pfaffian state has a ground state wave function

$$\Psi([z_i]) = \prod_{i<j}(z_i - z_j)^2 e^{-\frac{1}{4l_B^2}\sum_i |z_i|^2} \mathrm{Pf}\{\frac{1}{z_i - z_j}\}, \tag{1.106}$$

where $\mathrm{Pf}\{\cdots\}$ is the square root of the determinant of an anti-symmetric matrix, called the the Pfaffian. The Pfaffian state is fully spin-polarized. A fundamental quasiparticle excitation located at ξ is described by the wave function [56]

$$\Psi^{qp}([z_i], \xi) = \prod_i (z_i - \xi)^{\frac{1}{2}} \prod_{i<j}(z_i - z_j)^2 e^{-\frac{1}{4l_B^2}\sum_i |z_i|^2} \mathrm{Pf}\{\frac{1}{z_i - z_j}\}, \tag{1.107}$$

which is the FQH analogue to a vortex in a BCS superfluid like Helium-3. In the

presence of two fundamental quasiparticles, the wave function [57] is

$$\Psi^{2qp}([z_i],\xi_1,\xi_2)=\prod_{i<j}(z_i-z_j)^2 e^{-\frac{1}{4l_B^2}\sum_i|z_i|^2}\mathrm{Pf}\{\frac{(z_i-\xi_1)(z_j-\xi_2)+(z_i-\xi_2)(z_j-\xi_1)}{z_i-z_j}\}. \tag{1.108}$$

Exchange of quasiparticles ξ_1,ξ_2 gives rise to a statistical phase $\exp(i\pi/4)$. When there are four fundamental quasiparticles in the system, interesting things happen. For such a system, there are two linearly independent wave functions [57]

$$\begin{aligned}\Psi^{4qp}_{13,24}([z_i],\xi_1,\xi_2,\xi_3,\xi_4)&=\prod_{i<j}(z_i-z_j)^2 e^{-\frac{1}{4l_B^2}\sum_i|z_i|^2}\\ &\times\mathrm{Pf}\{\frac{(z_i-\xi_1)(z_i-\xi_3)(z_j-\xi_2)(z_j-\xi_4)+(z_i-\xi_2)(z_i-\xi_4)(z_j-\xi_1)(z_j-\xi_3)}{z_i-z_j}\}\\ \Psi^{4qp}_{14,23}([z_i],\xi_1,\xi_2,\xi_3,\xi_4)&=\prod_{i<j}(z_i-z_j)^2 e^{-\frac{1}{4l_B^2}\sum_i|z_i|^2}\\ &\times\mathrm{Pf}\{\frac{(z_i-\xi_1)(z_i-\xi_4)(z_j-\xi_2)(z_j-\xi_3)+(z_i-\xi_2)(z_i-\xi_3)(z_j-\xi_1)(z_j-\xi_4)}{z_i-z_j}\},\end{aligned} \tag{1.109}$$

or in a more convenient basis

$$\begin{aligned}\Psi_1&=\frac{(\xi_{13}\xi_{24})^{\frac{1}{4}}}{(1+\sqrt{1-x})^{\frac{1}{2}}}(\Psi^{4qp}_{13,24}+\sqrt{1-x}\Psi^{4qp}_{14,23})\\ \Psi_2&=\frac{(\xi_{13}\xi_{24})^{\frac{1}{4}}}{(1-\sqrt{1-x})^{\frac{1}{2}}}(\Psi^{4qp}_{13,24}-\sqrt{1-x}\Psi^{4qp}_{14,23}),\end{aligned} \tag{1.110}$$

where $\xi_{ij}=\xi_i-\xi_j$ is the relative coordinates between quasiparticles and $x=\frac{\xi_{12}\xi_{34}}{\xi_{13}\xi_{24}}$. By Eq. (1.110), exchange of quasiparticles ξ_1,ξ_3 or quasiparticles ξ_2,ξ_4 gives a statistical phase $\exp(i\pi/4)$ but does not change the many-particle state. However, exchange of quasiparticles ξ_2,ξ_3 results in a nontrivial rotation in the two-dimensional Hilbert space spanned by Ψ_1 and Ψ_2, which can be used to encode logic operations in quantum computation.

The fusion and statistical properties of the fundamental quasiparticles in the Pfaffian state agree with those of the MBSs. In addition to FQH systems, MBSs are predicted in many other condensed matter systems, such as p-wave superconductors [25, 59] and heterostructures [60] of superconductors and topological insulators. The benefit from using MBSs for quantum computation is that braidings of MBSs are topological. The linear transformations generated by braiding MBSs are independent of the trajectories along with the MBSs travel. Hence, deformation of braiding paths during quantum computation due to local defects and perturbations does not affect the stored information. Quantum computation with MBSs is an example of topological quantum computation [7, 8].

Despite the fascinating picture of topological quantum computation provided by the Pfaffian state, the Pfaffian state is not the only candidate for the FQH state at filling factor $\nu = 5/2$. Abelian models [11, 12] such as the Halperin 331 state also exist. The 331 state comes in two versions with different spin polarizations. The spin-polarized 331 state has the ground state wave function

$$\int \prod_i d^2\xi_i \prod_{i<j}(z_i - z_j)^3 \prod_{i,j}(\xi_i^* - 2\partial_{z_j})^2 \prod_{i<j}(\xi_i - \xi_j)^4 e^{-\frac{1}{4l_B^2}\sum_i |z_i|^2} e^{-\frac{1}{6l_B^2}\sum_i |\xi_i|^2}, \quad (1.111)$$

while the spin-unpolarized 331 state has the ground state wave function

$$\prod_{i<j}(z_i - z_j)^3 \prod_{i<j}(w_i - w_j)^3 \prod_{i,j}(z_i - w_j) e^{-\frac{1}{4l_B^2}(\sum_i |z_i|^2 + \sum_i |w_i|^2)}. \quad (1.112)$$

The fact that the Pfaffian state is fully spin-polarized whereas the 331 state can be spin-unpolarized suggests distinguishing the two states by measuring the spin polarization of the $\nu = 5/2$ FQH liquid. Such attempts, unfortunately, are controversial [17–20]. There is support for both 0 and 100% polarization.

A more complete list of the theoretical proposals for the $\nu = 5/2$ FQH state can be found in Section 2.2, with an emphasis on the edge theories.

1.5 Outline of dissertation

I end this chapter with a brief outline of the upcoming chapters, which are based on my past research projects with Prof. Dima Feldman.

In Chapter 2, we consider two experiments [23, 24] measuring the temperature and voltage dependence of quasiparticle tunneling through a QPC in the $\nu = 5/2$ FQH liquid. The results of those experiments led to conflicting conclusions about the nature of the quantum Hall state. We show that the conflict can be resolved by recognizing different geometries of the devices in the experiments. We argue that in some of those geometries there is significant unscreened electrostatic interaction between the segments of the quantum Hall edge on the opposite sides of the point contact. Coulomb interaction affects the tunneling current. We compare experimental results with theoretical predictions for the Pfaffian [10], $SU(2)_2$ [49], 331 [11] and $K = 8$ [12] states and their particle-hole conjugates (some of the particle-hole conjugate states are constructed in Chapter 3, for the first time). We find that, after Coulomb corrections are taken into account, measurements in all geometries agree with the spin-polarized and spin-unpolarized Halperin 331 states.

Two appendices supplement Chapter 2. Appendix A proves a condition which is crucial for obtaining the results in Chapter 2. Appendix B verifies the conclusion of Chapter 2 by an explicit numerical study of the 331 state.

The work in Chapter 3 is motivated by the observation [16] of upstream neutral

edge modes in the $\nu = 5/2$ FQH liquid. In that chapter, we discuss particle-hole symmetry in FQH systems and apply the symmetry to construct new FQH states at filling factor $\nu = 5/2$. We show that some of the constructed states indeed support upstream neutral modes with universal edge physics. Quasiparticle tunneling in these new $\nu = 5/2$ states is discussed in Chapter 2.

In Chapter 4, we propose a new topological order at filling factor $\nu = 5/2$, based on a scenario of the separation of charged and neutral degrees of freedom on the edge of the FQH liquid. The proposed model reconciles all existing data from transport experiments and can be distinguished from other competing models using an electronic Mach-Zehnder interferometer [61].

Topological quantum computation is an interesting topic. Understanding its limit and seeking ways of improving its reliability are important. In Chapter 5, we consider two realistic problems while applying Majorana fermions to topological quantum computation: (1) Majorana fermions often coexist and interact with nearby low-energy fermionic excitations [62,63]; and (2) Decoherence in qbit happens when the Majorana fermion system can interact with the outside environment [64–78]. For problem (1), topological quantum computation requires the use of fermionic zero modes of the many-body system, in place of the original Majorana fermions. In Chapter 5, we classify all fermionic zero modes in a system of interacting Majorana fermions and show how one can maximize the lifetime of a qbit by selecting the zero mode of best quality. This addresses problem (2). We find that in a typical interacting system, the maximal lifetime of a qbit is within one order of magnitude from the life time of a qbit based on the local part of the fermion parity operator.

Chapter 5 focuses on explaining the physical picture and summarizing the obtained results. We include all related technical details in Appendix C.

Chapter Two

The Quasiparticle Tunneling Experiments

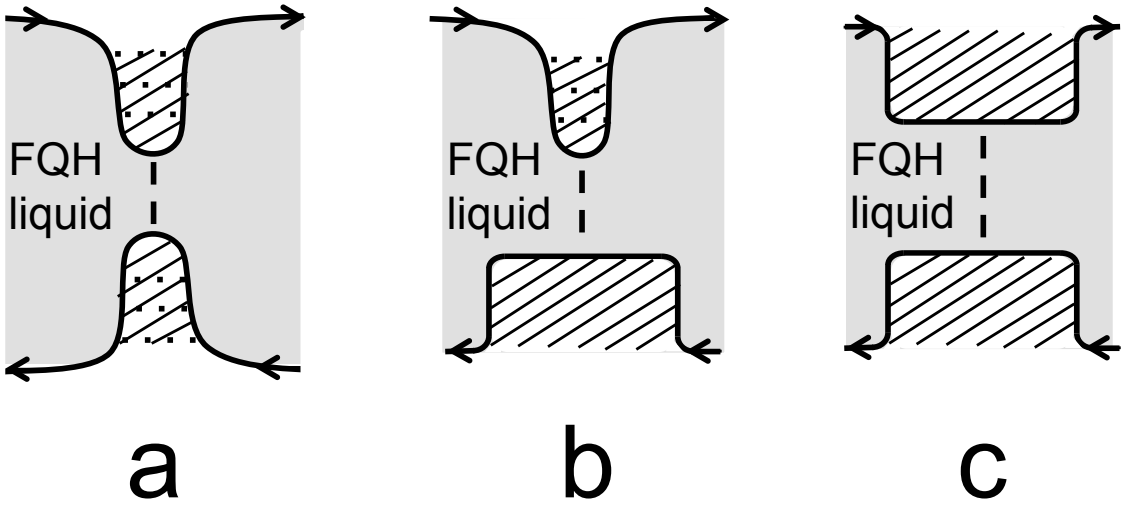

Figure 2.1: The three QPC geometries in the experiments. The arrows follow the current propagation direction on the edge. Dashed lines denote quasiparticle tunneling. Dotted lines across narrow gates in the geometries 2.1a and 2.1b represent the electrostatic interaction.

2.1 Introduction

Among numerous phases of two-dimensional electron gases (2DEG), the even-denominator quantum Hall states with the filling factors [9] 5/2 and 7/2 are particularly interesting. In contrast to odd-denominator fractional quantum Hall (FQH) liquids, they cannot be explained by a straightforward generalization of the Laughlin variational wave function. An early attempt to understand their nature led to the beautiful idea of non-Abelian states of matter [10]. In non-Abelian systems, the types and positions of quasiparticles do not uniquely determine the quantum state. This results in unusual physics and may open a road to topological quantum computation [7, 8]. However, the existence of non-Abelian quasiparticles has not been proven and the nature of the 5/2 state remains a puzzle.

Both Abelian and non-Abelian candidate states were proposed as possible theoretical explanations of the 5/2 FQH effect [10–12, 44, 45, 49–55]. A number of methods [53–55, 79–91] were invented and several experiments [13–24] were performed in

an attempt to determine the right ground state. One approach [23, 24] consists in the measurement of the tunneling current through a quantum point contact (QPC) between the edges of a 5/2 FQH liquid. The low-temperature conductance exhibits a power-law behavior $G \sim T^{2g-2}$, where the exponent g depends on the topological order in the bulk [5]. The exponent g was measured in two recent experiments [23, 24]. The results of the earlier experiment [23] were interpreted as supporting the non-Abelian anti-Pfaffian or $SU(2)_2$ states. The best fit for the second experiment [24] comes from the Abelian 331 state.

We argue that the discrepancy between those results can be explained by different geometries of point contacts in Refs. [23] and [24]. The geometry of the device from Ref. [23] is shown schematically in Fig. 2.1a. Figs. 2.1b and 2.1c illustrate the two geometries from Ref. [24]. In all cases, transport is supported by FQH edge channels defined by top gates. In Fig. 2.1a and for the upper gate in Fig. 2.1b, the gate widths are comparable to their distances from 2DEG. The gates are considerably wider in Fig. 2.1c. Thus, the distance between the edge points, connected by the dotted lines in Figs. 2.1a and 2.1b, is shorter than the screening length due to the metallic gates. In other words, the repulsive Coulomb interaction between the FQH edge segments on the opposite sides of QPC is not fully screened by the gates in the geometries of Figs. 2.1a,b but is screened completely in the geometry of Fig. 2.1c.

It is well known that repulsive interaction suppresses tunneling in quantum wires [92]. Similar physics has been addressed in the context of edge transport in Laughlin FQH states in Refs. [93, 94]. We find that in our case the Coulomb interaction drives the tunneling exponents g_A and g_B in the geometries 2.1a and 2.1b above the exponent g_C in the geometry 2.1c. Only the latter assumes a universal value while the former depend on the strength of the interaction across the gates. Hence, information about the nature of the 5/2 state can be extracted from

a comparison of the experimental g_C (Ref. [24]) but not g_A and g_B with universal theoretical predictions in various proposed phases. Such predictions are available for the Abelian $K = 8$ and spin-polarized and unpolarized 331 states [11, 12, 52], the non-Abelian $SU(2)_2$ and Pfaffian states [10, 49, 52] and the particle-hole conjugate of the Pfaffian state, the anti-Pfaffian state [44, 45]. Since Ref. [16] provides support for the existence of contra-propagating edge channels in the 5/2 FQH liquid, it is particularly interesting to consider candidate states with upstream edge modes. In the above list, only the anti-Pfaffian state has such property. The particle-hole conjugates of the other proposed states also exhibit upstream edge transport and we compute g_C in them below. The comparison with the experiment shows that the Halperin 331 state agrees best with the tunneling data [24].

This chapter is organized as follows. We review theoretically proposed $\nu = 5/2$ FQH states in Section 2.2, including the anti-331 state, the anti-$SU(2)_2$ state and the anti-$K = 8$ state, which we have studied for the first time. We refer to Chapter 3 the detailed constructions of these new 5/2 states. In Section 2.3, we discuss qualitatively the effects of Coulomb interaction across the gate. Detailed calculations are given in Section 2.4 and Appendix A. In Section 2.5 we compare our results and the experimental findings [23, 24] with the information obtained from other types of experiments.

Some of the results presented in this chapter are abstract. In Appendix B, we give a concrete example using the 331 state to verify those results. We show analytically and numerically how the Coulomb interaction across a narrow metallic gate affect the quasiparticle tunneling in the 331 state.

2.2 Candidate $\nu = \frac{5}{2}$ quantum Hall states

Here we review several simplest topological orders, proposed for the 5/2 state, and address their edge properties which we will need in the subsequent sections.

In all candidate states, the lowest quasiparticle charge is $e/4$, where e is the electron charge. This is rather different from the odd denominator states, where we usually expect that the lowest quasiparticle charge of the p/q state is e/q. The $e/4$ charge follows a general rule [95] for even denominator states: The ratio of the quantized Hall conductance to the lowest possible charge must be $2ne/h$, where n is an integer. The $e/4$ value of the charge agrees with the experiments [13, 14, 24] on the 5/2 FQH liquids. The best fits for the quasiparticle charge in the tunneling experiments [23, 24] are $0.17e$ in the geometry 2.1a, $0.25e$ in the geometry 2.1b and $0.22e$ in the geometry 2.1c. In all cases the nearest possible excitation charge is $e/4$. Thus, we conclude that in all geometries the tunneling current is carried by $e/4$-quasiparticles.

We start our overview with the simplest Abelian topological orders. To simplify our notation we set $\hbar$ to 1.

We first consider the $K = 8$ state [12]. We assume that electrons form pairs in the second Landau level and single-electron excitations are gapped. In particular, no single-electron tunneling into the FQH edge channel of a 5/2 system is possible at low energies. The filling factor for bosonic electron pairs is 1/8. Thus, we use the edge theory of a Laughlin state of bosons at that filling factor. The Lagrangian density [52]

$$\mathcal{L} = -\frac{1}{4\pi}[8\partial_t\phi\partial_x\phi + 8v(\partial_x\phi)^2] + \mathcal{L}_2 + \mathcal{L}_{\rm int}, \tag{2.1}$$

where

$$\mathcal{L}_2 = -\frac{1}{4\pi}[\sum_{i=1,2} \partial_t \phi_i^0 \partial_x \phi_i^0 + \sum_{ij} U_{ij} \partial_x \phi_i^0 \partial_x \phi_j^0] \tag{2.2}$$

describes two integer edge modes, $\mathcal{L}_{\text{int}}$ contains information about the interaction of the integer and fractional modes, the charge density on the FQH edge is $\rho(x) = e\partial_x\phi/\pi$ and the charge density on the integer edges is $\rho_2 = e(\phi_1^0 + \phi_2^0)/2\pi$. The operator $\Psi(x) = \exp(i\phi(x))$ annihilates a charge-$e/4$ anyon. The pair annihilation operator on the fractional edge is $\Psi_{2e}(x) = \exp(i8\phi(x))$.

We do not make assumptions about the spin of the electron pairs in the $K = 8$ state. The same edge theory describes spin-polarized and unpolarized FQH liquids. Certainly, the particle-hole conjugate system has the filling factor 5/2 only for the spin-polarized $K = 8$ liquid.

Next, we consider the 331 state [11, 52]. This state comes in two shapes with identical signatures in the tunneling experiment but different spin polarizations [52].

The spin-unpolarized version can be understood as a Halperin bilayer state with spin-up and -down electrons playing the role of two layers. The Lagrangian density on the edge

$$\mathcal{L} = -\frac{1}{4\pi} \sum_{I,J=1,2} [K_{IJ} \partial_t \phi_I \partial_x \phi_J + V_{IJ} \partial_x \phi_I \partial_x \phi_J] + \mathcal{L}_2 + \mathcal{L}_{\text{int}}, \tag{2.3}$$

where the K-matrix [5]

$$K = K_{\text{unpolarized}} = \begin{pmatrix} 3 & 1 \\ 1 & 3 \end{pmatrix} \tag{2.4}$$

and $\mathcal{L}_2$ and $\mathcal{L}_{\text{int}}$ are defined in the same way as in the previous subsection. The

charge density on the fractional edge is $e(\partial_x\phi_1 + \partial_x\phi_2)/2\pi$ and the most relevant operators that annihilate quasiparticles with charge $e/4$ are $\exp(i\phi_{1,2})$. There are two independent electron operators: $\Psi_1(x) = \exp(i[3\phi_1 + \phi_2])$ and $\Psi_2(x) = \exp(i[3\phi_2 + \phi_1])$. The spin-unpolarized 331 state is not an eigenstate of the total spin and is related [96] to the physics of superfluid He-3.

The spin-polarized version of the 331 state emerges from the condensation of the charge-$2e/3$ quasiparticles on top of the Laughlin state with the filling factor 1/3. The K-matrix

$$K = K_{\text{polarized}} = \begin{pmatrix} 3 & -2 \\ -2 & 4 \end{pmatrix} \tag{2.5}$$

can be expressed as $K_{\text{polarized}} = W^{\mathrm{T}} K_{\text{unpolarized}} W$ with

$$W = \begin{pmatrix} 0 & 1 \\ 1 & -1 \end{pmatrix} \tag{2.6}$$

and hence describes the same topological order as the matrix (2.4). Note that the particle-hole conjugate of the 331 state has the filling factor 5/2 only for its spin-polarized version.

The third candidate is the non-Abelian Pfaffian state [8, 10]. The Pfaffian state can be seen as a p-wave superconductor with the wave function

$$\mathrm{Pf}[\frac{1}{z_i - z_j}]\Pi_{i<j}(z_i - z_j)^2 \exp(-\frac{1}{4}\sum |z_i|^2), \tag{2.7}$$

where $z_k = x_k + iy_k$ is the position of the kth electron, Pf stays for the Pfaffian of a matrix and we ignore the two filled Landau levels for a moment. The edge theory is

described by the following Lagrangian density

$$\mathcal{L} = -\frac{2}{4\pi}[\partial_t\phi_1\partial_x\phi_1 + v_1(\partial_x\phi_1)^2] + i\psi(\partial_t + v_\psi\partial_x)\psi + \mathcal{L}_2 + \mathcal{L}_{\rm int}, \tag{2.8}$$

where the charge density on the fractional edge is $e\partial_x\phi_1/2\pi$, ψ is a neutral Majorana fermion, v_1 and v_ψ are the velocities of the charged and neutral modes and the meaning of $\mathcal{L}_2$ and $\mathcal{L}_{\rm int}$ is the same as in the preceding subsections. The charge $e/4$-quasiparticle annihilation operator $\Psi(x) = \sigma(x)\exp(i\phi_1(x)/2)$, where the operator σ changes the boundary conditions for the Majorana fermion from periodic to antiperiodic and has the scaling dimension 1/16. The Pfaffian state is spin-polarized.

The fourth candidate is the $SU(2)_2$ state [49]. This is another spin-polarized non-Abelian state. Its wave function can be derived from the parton construction [49]. We split an electron into a fermion $\psi_{1/2}$ of charge $e/2$ and two fermions $\psi_{1/4a,}$, $\psi_{1/4,b}$ of charge $e/4$:

$$\Psi_e = \psi_{1/2}\psi_{1/4,a}\psi_{1/4,b}. \tag{2.9}$$

The filling factor for the $e/2$-partons is 1. For each of the two sorts of $e/4$-partons the filling factor is 2. For decoupled partons the wave function would simply be a product of three integer quantum Hall (IQH) wave functions. Taking into account that the three types of partons occupy exactly the same positions, we find the ground state wave function of the form [52]

$$\Psi(\{z_k\}) = [\chi_2(z_k)]^2\Pi_{k<l}(z_k - z_l)\exp(-\frac{1}{4}\sum|z_k|^2), \tag{2.10}$$

where χ_2 is the polynomial factor in the wave function of two filled Landau levels.

The decomposition (2.9) exhibits $U(1)\times SU(2)$ gauge symmetry (the factor $SU(2)$ acts on $\psi_{1/4,a}$ and $\psi_{1/4,b}$; $U(1)$ describes the freedom to choose the phase of $\psi_{1/2}$).

For decoupled partons, the edge theory would contain 5 IQH edge channels. The theory of the FQH edge is obtained by keeping only gauge invariant states and is described by the Lagrangian density [52]

$$\begin{aligned}\mathcal{L} = &-\frac{1}{4\pi}[2\partial_t\phi_\rho\partial_x\phi_\rho + \partial_t\phi_n\partial_x\phi_n + 2v_\rho(\partial_x\phi_\rho)^2 + v_n(\partial_x\phi_n)^2] \\ &+ i\psi(\partial_t + v_\psi\partial_x)\psi, \end{aligned} \tag{2.11}$$

where ϕ_ρ is a bosonic mode carrying electric charge, ϕ_n is an electrically neutral bosonic mode and ψ is a neutral Majorana fermion. The charge density is $e\partial_x\phi_\rho/2\pi$. The neutral mode ϕ_n describes "pseudo-polarization", i.e., the difference in the occupation of the two Landau levels for $e/4$-partons. The two integer edge modes should be included in the same way as in Eqs. (2.1,2.3,2.8). The $e/4$-quasiparticle annihilation operators are $\sigma(x)\exp(\pm i\phi_n(x)/2)\exp(i\phi_\rho(x)/2)$, where σ twists the boundary conditions for the Majorana fermion and has the scaling dimension 1/16. Three operators annihilate an electron on the fractional edge: $\psi(x)\exp(2i\phi_\rho(x))$ and $\exp(\pm i\phi_n(x))\exp(2i\phi_\rho(x))$.

In the presence of disorder the "pseudo-polarization" does not conserve and the action can contain tunneling operators of the form $\xi_\pm(x)\psi(x)\exp(\pm i\phi_n(x))$, where $\xi_\pm(x)$ are random functions of the coordinate. Their effect is the same as the effect of similar operators in the anti-Pfaffian state [44, 45] and the anti-331 and anti-$SU(2)_2$ states (Subsections 3.2.1 and 3.2.2). The theory acquires an emergent $SO(3)$ symmetry. The neutral modes should be described as three Majorana fermions with equal velocities. In contrast to Subsections 3.2.1 and 3.2.2, however, this does not affect the scaling dimension of the most relevant quasiparticle operators.

We now turn to the particle-hole conjugates of the above four states. In Subsection 3.2.3 we argue that the particle-hole conjugate of the $K = 8$ state does not

exhibit universal behavior in the tunneling experiment with a broad range of possible values for the tunneling exponent g. Moreover, we do not expect the quantized conductance $5e^2/2h$ in that state at sufficiently low temperatures and voltages. Its physics is thus quite different from the physics of the other seven states considered in this chapter.

The particle-hole conjugate of the 331 state, called the anti-331 state, is more interesting. The edge theory of the anti-331 state can be constructed by reversing the direction of the two FQH edge modes and adding another integer edge channel in the opposite direction to the reversed fractional channels. The presence of impurities ensures electron tunneling between the fractional edge and the additional integer edge. At weak interaction this tunneling turns out to be irrelevant and the physics become nonuniversal just like in the anti-$K = 8$ state. In contrast to the anti-$K = 8$ case, the anti-331 state exhibits universal conductance and tunneling exponents at stronger interactions. This is the situation addressed in Subsection 3.2.1. The FQH edge theory possesses the $SO(4)$ symmetry and contains a bosonic charge mode and four upstream Majorana fermions with identical velocities. The Lagrangian density

$$\begin{aligned}\mathcal{L} = &-\frac{2}{4\pi}[\partial_t\phi_\rho\partial_x\phi_\rho + v_\rho(\partial_x\phi_\rho)^2] + i\sum_{k=1}^{4}\tilde{\psi}_k(\partial_t - \bar{v}_n\partial_x)\tilde{\psi}_k \\ &+ \frac{\pi}{6}v_{n_1n_2}\sum_{ijkl}\varepsilon_{ijkl}\tilde{\psi}_i\tilde{\psi}_j\tilde{\psi}_k\tilde{\psi}_l + \mathcal{L}_2 + \mathcal{L}_{\rm int},\end{aligned} \tag{2.12}$$

where $\tilde{\psi}_k$ are four Majoranas, the charge density on the FQH edge is $e\partial_x\phi_\rho/2\pi$ and the contributions $\mathcal{L}_2$ and $\mathcal{L}_{\rm int}$ describe two integer channels as above.

The most relevant quasiparticles carry the electric charge $e/2$. There are four most relevant $e/4$-particle annihilation operators of the structure $\sigma_\alpha(x)\exp(i\phi_\rho/2)$ ($\alpha = 1, \ldots, 4$), where σ_α changes the boundary conditions from periodic to antiperi-

odic for all four Majorana fermions (see Subsection 3.2.1 for an explicit expression) and has the scaling dimension 1/4.

The particle-hole conjugate of the Pfaffian state, called the anti-Pfaffian state [44, 45], is obtained from the Pfaffian state in exactly the same way as the anti-331 state can be obtained from the 331 state. The edge theory is very similar to (2.12) and exhibits the $SO(3)$ symmetry. The edge Lagrangian density is

$$\mathcal{L} = -\frac{2}{4\pi}[\partial_t\phi_\rho\partial_x\phi_\rho + v_\rho(\partial_x\phi_\rho)^2] + \sum_{k=1}^{3} i\psi_k(\partial_t - \bar{v}_n\partial_x)\psi_k + \mathcal{L}_2 + \mathcal{L}_{\text{int}}. \tag{2.13}$$

The two most relevant $e/4$-quasiparticle operators express as $\sigma_\alpha \exp(i\phi_\rho/2)$ ($\alpha = 1, 2$), where σ_α changes the boundary conditions from periodic to antiperiodic for all Majorana fermions and has the scaling dimension 3/16.

Lastly, we consider the particle-hole conjugate of the $SU(2)_2$ state, the anti-$SU(2)_2$ state. Its edge theory is similar to the anti-Pfaffian and anti-331 cases. Its derivation is given in Subsection 3.2.2. There are 5 Majorana fermions on the edge. This corresponds to the emergent $SO(5)$ symmetry. The edge Lagrangian density

$$\mathcal{L} = -\frac{2}{4\pi}[\partial_t\phi_\rho\partial_x\phi_\rho + v_\rho(\partial_x\phi_\rho)^2] + \sum_{k=1}^{5} i\psi_k(\partial_t - \bar{v}_n\partial_x)\psi_k + \mathcal{L}_2 + \mathcal{L}_{\text{int}} \tag{2.14}$$

differs from Eq. (2.13) only by the number of upstream neutral modes. The four most relevant $e/4$-anyon operators can be written as $\sigma_\alpha \exp(i\phi_\rho/2)$ ($\alpha = 1, \ldots, 4$), where σ_α changes the boundary conditions from periodic to antiperiodic for all Majorana fermions and has the scaling dimension 5/16.

2.3 Qualitative picture

In Luttinger liquid systems with position-independent interaction constants, such as the edge theories discussed in Section 2.2, the low-energy tunneling density of states scales as $\rho(E) \sim E^{g-1}$, where g depends on the details of the system [97]. We argue below that g assumes different values in different geometries. The tunneling conductance is proportional to the product of the tunneling densities of states ρ_u and ρ_l on the upper and lower edges at $E \sim k_B T$ (Ref. [97]). In general, the edges are described by two different exponents g_u and g_l. At low temperatures, the linear conductance for the tunneling current $G \sim T^{g_u+g_l-2}$. Hence, the experimentally measured $g = (g_u + g_l)/2$.

As we discussed in Section 2.2, in all three geometries the tunneling current is carried by quasiparticles with charge $e/4$. The best fits [23, 24, 98] for the tunneling exponent at this quasiparticle charge are $g_A = 0.45$, $g_B = 0.42$ and $g_C = 0.38$. We want to connect these numbers with the nature of the topological order.

Since the electric current is carried by the edges, the exponent g depends on the edge physics near the QPC. The size of the relevant region near the point contact is set by the distance a charge can travel during the tunneling event: $L = vt$, where v is the velocity of the edge excitation and t is the duration of the tunneling event. The latter can be estimated from the uncertainty relations, $t \sim \hbar/E$, where $E \sim \max(k_B T, eV)$ is the uncertainty of the quasiparticle energy. Assuming that $v \sim 10^7$ cm/s, we find $L \sim 10$ μm at relevant values of the temperature and voltage bias.

Let us look at the geometry of the edges within 10 μm from the QPC. The edges are defined by gates at the distance of 200 nm from 2DEG. The widths of both gates

in the geometry 2.1a and the upper gate in the geometry 2.1b have the same order of magnitude of hundreds nanometers [98]. The width is 2200 nm for the lower gate in the geometry 2.1b and both gates in the geometry 2.1c. The distance between the edge channel segments on the opposite sides of a gate differs from its width. In our case there are several edge channels that can run at different locations. It is not easy to determine those locations. In particular, the annealing procedure used in Refs. [23, 24] changes the device electrostatics but it is unclear what its effect on the geometry is. A crude estimate of the edge channel positions can be obtained from Ref. [99]. We find that the edge channels run within the distance of hundreds nanometers from the gates. This agrees with the upper bound one can derive from the gate geometry in Fig. 2.1b. The tip of the upper gate is at 600 nm from the lower gate. The distance between the outermost edge channel and the gate is thus expected to be below 600/2 nm = 300 nm. We conclude that the gate width, the gate distance from 2DEG and the distance between the edge modes on the opposite sides of the gate all have the same order of magnitude for both gates in the geometry 2.1a and the upper gate in the geometry 2.1b. This means that there is a significant unscreened Coulomb interaction between the segments of the edge on the opposite sides of the gates. On the other hand, in the geometry 2.1c and for the lower gate in the geometry 2.1b, the width of the gates is close to the distance between the edge channels on their opposite sides and much greater than the gate distance from the 2DEG plane. Thus, we expect that the Coulomb interaction across the gates is almost completely screened in the latter geometries. One can also neglect the electrostatic interaction between the edge channels defined by two different gates in all geometries. Indeed, an edge point at the distance $\sim L \sim 10$ μm from the tip of the gate is much further from the edge on the other side of the QPC than from the gate.

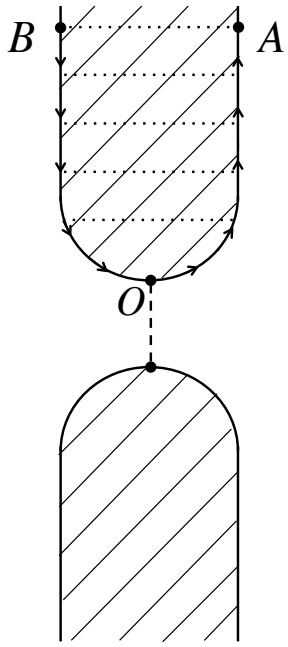

Figure 2.2: Charge tunnels to point O and travels along the edge to point A. Dotted lines show Coulomb repulsion. Arrows show the transport direction on the chiral edge.

What is the effect of the electrostatic interaction across the gate on the tunneling current? It is easy to see that repulsive Coulomb interaction suppresses tunneling. Indeed, after a tunneling event, the tunneling charge must move away from the QPC. Due to the chiral transport on the quantum Hall edge, it moves along segment OA in Fig. 2.2. When the excess charge arrives at point A, it pushes charge from point B due to their repulsive electrostatic interaction. Because of chirality the charge from point B can only move towards the tip O of the gate. Thus, excess charge accumulates in point O. This means lower tunneling density of states than for a noninteracting system where charge rapidly distributes over a large region. Hence, one expects higher values of the tunneling exponent g in the geometries 2.1a and 2.1b than in the geometry 2.1c. This is exactly what has been observed.

The lower edge has the same geometry in Figs. 2.1b and 2.1c and its tunneling density of states is described by the same exponent g_l. The same exponent also describes the upper edge in Fig. 2.1c. Thus, $g_C = g_l$. The upper edge in the

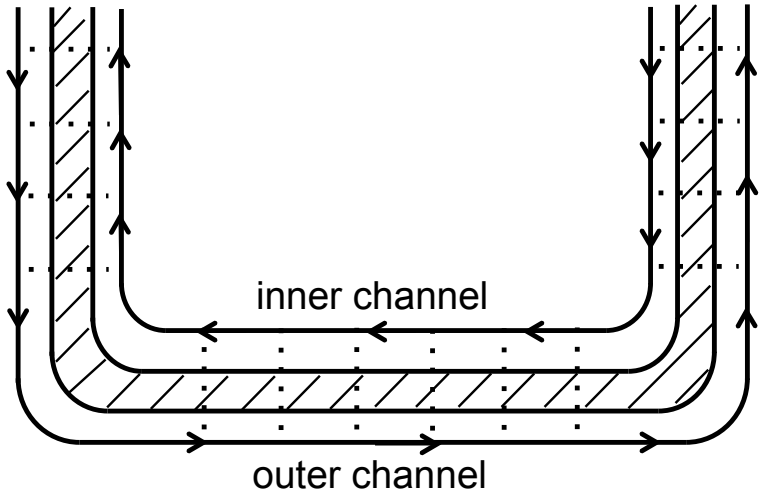

Figure 2.3: The Π-shaped gate defines an inner and outer quantum Hall channels. Dotted lines illustrate Coulomb interaction across the gate.

geometry 2.1b is described by a different exponent g_u. Hence, $g_B = (g_l + g_u)/2$. If two identical gates of the same geometry as the upper gate in Fig. 2.1b were used in Fig. 2.1a then one would obtain $g_A = g_u$. In such situation g_A, g_B and g_C form an arithmetic series. Interestingly, this agrees with experiment. At the same time, device 2.1a was made in a different sample and its geometry details are different from the upper gate in Fig. 2.1b. Besides, the gate width changes linearly [98] with the distance x from the QPC at the distances $x \sim L$ in the geometry 2.1a. This means that the effective interaction strength depends on the temperature since it depends on the gate width at the distance $x \sim \hbar v/k_B T$. Hence, there are corrections to the power law for the tunneling density of states in the geometry 2.1a. This may be a reason for a poor fit for the quasiparticle charge $e/4$ from the data in that geometry.

The above discussion has focused on the geometry 2.1a and the upper gate in Fig. 2.1b. We now briefly discuss some features of the lower gate in the geometry 2.1b and both gates in the geometry 2.1c. Those gates are Π-shaped, as shown in Fig. 2.3, with the width of the metal strips on the order of 200nm. Thus, each gate gives rise to two FQH edge channels inside and outside the gate. We are interested in

state	$K=8$	331	Pfaffian	$SU(2)_2$	anti-331	anti-Pfaffian	anti-$SU(2)_2$
g	1/8	3/8	1/4	1/2	5/8	1/2	3/4

Table 2.1: Exponent g in the tunneling density of states $\rho(E) \sim E^{g-1}$ for a straight edge in various 5/2 states.

the tunneling in the outer channel. Its Coulomb interaction with the inner channel affects the tunneling exponent g. We investigate that effect in Subsection 2.4.4 below and show that it can be neglected, provided that the interaction across the gate is such that the system is not close to the interaction-driven instability.

Our main conclusion is that only g_C is unaffected by the electrostatic interaction between different edge segments. Thus, the information about the topological order at the filling factor 5/2 can be obtained from the comparison of $g_C = 0.38$ with theoretical predictions for the models from Section 2.2. Table I shows the predictions for g. We find that the 331 state gives the best fit with an excellent agreement between the theoretical $g = 3/8$ and the experimental value 0.38. As discussed in Subsection 2.4.4, for a system on the verge of instability, all three exponents g_A, g_B and g_C considerably exceed the universal value in the absence of interactions across the gates. In this unlikely scenario, the data [24] do not exclude the Pfaffian state.

2.4 Edge physics and tunneling current

In this section we compute the tunneling exponents g for various models of the 5/2 state in the presence of unscreened Coulomb interaction across the gate. This will allow us to estimate the strength of the electrostatic interaction across the gate. Even though the difference of the tunneling exponents is rather small in the geometries 2.1b

and 2.1c, we find that the electrostatic interaction is strong: the interaction between the nearest points of the edge segments on the opposite sides of the upper gate in Fig. 2.1b turns out comparable with the interaction between the charges, placed in those points in the absence of a gate. This agrees with what one expects from the geometry of the gates.

2.4.1 Lagrangian

The general structure of the action of a straight edge is

$$L_0 = \int dxdt\mathcal{L} = -\frac{1}{4\pi}\int_{-\infty}^{+\infty} dxdt \sum_{ij}[K_{ij}\partial_t\phi_i\partial_x\phi_j + V_{ij}\partial_x\phi_i\partial_x\phi_j] + L_\psi, \qquad (2.15)$$

where ϕ_i denote various edge Bose-modes and L_ψ is the action of the Majorana fermion degrees of freedom in the Pfaffian, $SU(2)_2$, anti-$SU(2)_2$, anti-331 and anti-Pfaffian states. Modes ϕ_i include two fields describing integer quantum Hall channels. Stability requires that the symmetric matrix V_{ij} is positive definite. As seen from Section 2.2, there are no relevant or marginal interactions between the Bose and Majorana degrees of freedom.

Consider now the geometry of the edge, defined by a narrow gate, Fig. 2.4. We can still extend integration in Eq. (2.15) from minus to plus infinity, assuming that x is measured along the edge, i.e., x is negative on the edge segment above the gate and positive below the gate, Fig. 2.4. However, Eq. (2.15) is no longer the only contribution to the action. We must also include the electrostatic interaction across the gate. In the presence of the gate the interaction is short range and hence can be described by local operators coupling fields at the points x and $-x$. Since we consider low temperature physics, we are interested in relevant and marginal operators only.

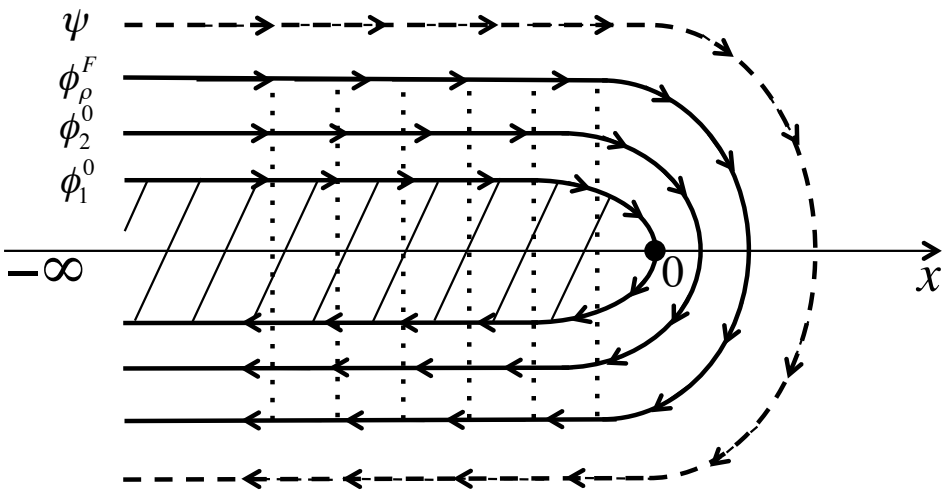

Figure 2.4: Two integer modes ϕ_1^0 and ϕ_2^0, the charged FQH mode ϕ_ρ^F and the neutral mode ψ travel around the shaded gate. Electrostatic interaction across the gate is illustrated by dotted lines.

In the following discussion we will assume that the list of such operators remains the same as in the limit of the weak Coulomb interaction. This will allow us to use the same scaling dimensions as in the absence of the electrostatic force across the gate.

The most obvious interaction contribution to the action is

$$-\frac{1}{4\pi}\int dt \int_{-\infty}^{0} dx \sum_{ij} U_{ij}\partial_x\phi_i(x)\partial_x\phi_j(-x). \tag{2.16}$$

All other contributions made of derivatives of Bose fields are irrelevant. What about contributions with operators of the form $\exp(i\sum_n a_n\phi_n)$ which shift charge between different edge channels on each side of the gate (certainly, no charge tunneling across the gate is allowed)? One might think that some such operators must be included. Indeed, consider the operator $O_1 = \exp(i[\phi_1^0(x) + \phi_1^0(-x) - \phi_2^0(x) - \phi_2^0(-x)])$ which moves one electron between the two integer modes on each side of the gate. It appears to be marginal. However, there is inevitable disorder in our system. Disorder can be described by adding contributions of the form $\sum_k \zeta_k(x)\partial_x\phi_k(x)$ with random $\zeta_k(x)$ to the Lagrangian density. We omitted all such contributions in Eq. (2.15)

since one can gauge out disorder by redefining $\phi_k \to \phi_k + 2\pi \sum_k (V^{-1})_{ki} \int \zeta_i dx$. We expect that disorder contains a contribution with no correlation between the opposite sides of the gate. Then our redefinition of the fields introduces randomness in the operator O_1 and makes it irrelevant. A similar argument excludes operators, containing $\exp(\pm i\phi_n)$ in the $SU(2)_2$ state. What about other neutral-mode contributions such as operators with Majorana fermions? The list of possible operators is restricted by the requirement that the topological charge conserves on each side of the gate: Indeed, topological charge cannot travel under the gate where there is no FQH liquid. One might still construct some marginal operators that conserve topological charge on both sides in some of the states from Section 2.2. For example, the operator $O_2 = \tilde{\psi}_1(x)\tilde{\psi}_2(x)\tilde{\psi}_3(-x)\tilde{\psi}_4(-x)$ is marginal in the anti-331 state. However, all such operators are prohibited by symmetry. Indeed, as discussed in Subsection 3.2.1, disorder gives rise to the emergent $SO(4)$ symmetry in the anti-331 state. The electrostatic coupling between the sides of the gate has the same form as for an infinitely long gate. In the latter case, the system is invariant with respect to two independent $SO(4)$ symmetry groups acting on the two electrostatically coupled edges. The combined $SO(4) \times SO(4)$ symmetry excludes the operator O_2. A similar argument applies in the anti-Pfaffian and anti-$SU(2)_2$ states. We conclude that the action can be chosen in the form

$$L = L_0 - \frac{1}{4\pi} \int dt \int_{-\infty}^{0} dx \sum_{ij} U_{ij} \partial_x \phi_i(x) \partial_x \phi_j(-x). \tag{2.17}$$

2.4.2 Tunneling exponent g

The tunneling at the QPC at $x = 0$ is described by the contribution to the action

$$L_T = \sum_{\alpha,\beta} \int dt \Gamma_{\alpha\beta} \Psi^\dagger_{u,\alpha}(x=0) \Psi_{l,\beta}(x=0) + \text{H.c.}, \tag{2.18}$$

where $\Psi_{u,\alpha}$ and $\Psi_{l,\beta}$ are quasiparticle operators on the upper and lower edges, α and β distinguish different quasiparticle operators, $\Gamma_{\alpha\beta} = \Gamma_{\alpha\beta}(E_c)$ are the tunneling amplitudes and E_c is the ultraviolet cut-off energy. Certainly, every allowed tunneling process conserves the electric and topological charges. In order to find the low-temperature conductance, it is convenient to perform the renormalization group procedure. We integrate out fast degrees of freedom and rescale $\Gamma_{\alpha\beta}$. Only the terms with the most relevant $e/4$-excitation operators $\Psi^\dagger_{u,\alpha}$ and $\Psi_{l,\beta}$ with the scaling dimensions Δ_u and Δ_l must be kept. We stop at the energy scale $E \sim k_B T$. At that scale $\Gamma_{\alpha\beta}(E = k_B T) \sim (k_B T/E_c)^{\Delta_u + \Delta_l - 1} \Gamma_{\alpha\beta}(E_c)$. The linear conductance $G \sim T^{2g-2} = T^{g_u + g_l - 2}$ can now be found from the perturbation theory: $G \sim |\Gamma(k_B T)|^2$. We conclude that $g_u = 2\Delta_u$, $g_l = 2\Delta_l$ and $g = \Delta_u + \Delta_l$.

Thus, to find g we need to compute the scaling dimensions of quasiparticle operators of a general structure $\Psi_{e/4} = \sigma(x=0) \exp(i \sum a_k \phi_k(x=0))$, where the operator σ acts on the Majorana sector (and is just an identity operator in some models) and a_k are constants (see Section 2.2). Since the Majorana sector is decoupled from the Bose modes, the scaling dimension of the operator σ is not affected by the interaction across the gate and can be taken from Section 2.2. We thus focus on the exponential factor in $\Psi_{e/4}$.

In all models of Section 2.2, the symmetric K-matrix K_{ij} is positive definite. In the rest of this subsection we also assume that U_{ij}, Eq. (2.17), is symmetric. This

is automatically satisfied, if the gate configuration has a symmetry plane such that reflections in the plane transform the segments of the edge above and below the gate into each other. The gate configuration [23], Fig. 2.1a, has such a symmetry plane. The configuration of the upper gate, Fig. 2.1b, used in Ref. [24], does not have a symmetry plane but is approximately symmetric beyond about 10 μm from the QPC. Note that U_{ij} can be symmetric even in the absence of a symmetry plane. This happens if one can neglect all interactions across the gate except the interaction of the charged modes. Then U_{ij} becomes a 1×1 matrix. This is the case in the model of the next subsection. Thus, in Subsection 2.4.3, we can rely on Subsection 2.4.2 even without assuming the existence of a symmetry plane. Certainly, our qualitative discussion in Section 2.3 is also free from that assumption. Calculations are similar but more cumbersome without the symmetry. We focus on the symmetric situation because it allows a proof of two general theorems: 1) in Appendix A we demonstrate that U_{ij} is positive definite; 2) we show that the positive definite U_{ij} drives the tunneling exponent above the universal value without interaction across the gate. The physical origin of the latter claim has been addressed in Section 2.3.

At this point it is convenient to change notation. We define $\bar{\phi}_i(x) = (\phi_i(x) + \phi_i(-x))/\sqrt{2}$ and $\theta_i = (\phi_i(x) - \phi_i(-x))/\sqrt{2}$, $x < 0$. The Bose-mode contribution to the action now reads

$$L_B = -\frac{1}{4\pi}\int dt \int_{-\infty}^{0} dx \sum_{ij} \{2K_{ij}\partial_t\bar{\phi}_i\partial_x\theta_j + [V_{ij} + \frac{U_{ij}}{2}]\partial_x\theta_i\partial_x\theta_j + [V_{ij} - \frac{U_{ij}}{2}]\partial_x\bar{\phi}_i\partial_x\bar{\phi}_j\}. \tag{2.19}$$

The quasiparticle operator becomes $\Psi_{e/4} = \sigma \exp(i\sum a_k\bar{\phi}_k(0)/\sqrt{2})$. Stability implies that $V \pm U/2$ are positive definite matrices. We next diagonalize the bilinear form $K_{ij}\partial_t\bar{\phi}_i\partial_x\theta_j$ with the transformation $\bar{\phi}_i = \sum_k S_{ik}\tilde{\phi}_k; \theta_i = \sum_k S_{ik}\tilde{\theta}_k$, where the matrix

S is such that $S^T K S = E$. The Bose contribution to the action becomes

$$L_B = -\frac{1}{4\pi}\int dt \int_{-\infty}^{0} dx \sum_{ij} \{2\delta_{ij}\partial_t \tilde{\phi}_i \partial_x \tilde{\theta}_j + [\tilde{V}_{ij} + \tilde{\Lambda}_{ij}]\partial_x \tilde{\theta}_i \partial_x \tilde{\theta}_j + [\tilde{V}_{ij} - \tilde{\Lambda}_{ij}]\partial_x \tilde{\phi}_i \partial_x \tilde{\phi}_j\}, \tag{2.20}$$

where $\tilde{V} = S^T V S$ and $\tilde{\Lambda} = S^T U S/2$ are positive definite symmetric matrices. Integrating out the fields $\tilde{\theta}_i$ one gets

$$L_B = \frac{1}{4\pi}\int dt \int_{-\infty}^{0} dx \sum_{ij} \{(\tilde{V} + \tilde{\Lambda})^{-1}_{ij} \partial_t \tilde{\phi}_i \partial_t \tilde{\phi}_j - (\tilde{V} - \tilde{\Lambda})_{ij} \partial_x \tilde{\phi}_i \partial_x \tilde{\phi}_j\}. \tag{2.21}$$

The quasiparticle operator assumes the form $\Psi_{e/4} = \sigma \exp(i \sum_{kj} a_k S_{kj} \tilde{\phi}_j(0)/\sqrt{2})$.

We introduce another piece of notation now. Consider a symmetric positive definite matrix A. We define $\sqrt{A}$ in the following way. We first find such orthogonal matrix O that $A = O^T \bar{A} O$, where $\bar{A}$ is a diagonal matrix with positive diagonal entries. Next, we define $\sqrt{\bar{A}}$ as a diagonal matrix with positive diagonal entries such that $(\sqrt{\bar{A}})^2 = \bar{A}$. Finally, we set $\sqrt{A} = O^T \sqrt{\bar{A}} O$. Obviously, $\sqrt{A}$ is a symmetric positive definite matrix whose square is A; $(\sqrt{A})^{-1} = \sqrt{A^{-1}}$. We make the following change of variables

$$\tilde{\phi}_i = \sum_j \left(\sqrt{\tilde{V} + \tilde{\Lambda}} \left[\sqrt[4]{\sqrt{\tilde{V} + \tilde{\Lambda}}(\tilde{V} - \tilde{\Lambda})\sqrt{\tilde{V} + \tilde{\Lambda}}} \right]^{-1} \right)_{ij} \hat{\phi}_j. \tag{2.22}$$

The action becomes

$$L_B = \frac{1}{4\pi}\int dt \int_{-\infty}^{0} dx \sum_{ij} \left\{ P^{-1}_{ij} \partial_t \hat{\phi}_i \partial_t \hat{\phi}_j - P_{ij} \partial_x \hat{\phi}_i \partial_x \hat{\phi}_j, \right\} \tag{2.23}$$

where

$$P = \sqrt{\sqrt{\tilde{V} + \tilde{\Lambda}}(\tilde{V} - \tilde{\Lambda})\sqrt{\tilde{V} + \tilde{\Lambda}}}. \tag{2.24}$$

At this point we trace back the steps that led us to Eq. (2.21) with Eq. (2.23) as the starting point. We introduce auxiliary fields $\hat{\theta}_i$ and rewrite the action in the form, similar to Eq. (2.20):

$$L_B = -\frac{1}{4\pi}\int dt \int_{-\infty}^{0} dx \sum_{ij} \{2\delta_{ij}\partial_t\hat{\phi}_i\partial_x\hat{\theta}_j + P_{ij}\partial_x\hat{\theta}_i\partial_x\hat{\theta}_j + P_{ij}\partial_x\hat{\phi}_i\partial_x\hat{\phi}_j\}. \qquad (2.25)$$

Next, we define new fields Φ_i according to $\hat{\phi}_i(x) = (\Phi_i(x) + \Phi_i(-x))/\sqrt{2}$ and $\hat{\theta}_i(x) = (\Phi_i(x) - \Phi_i(-x))/\sqrt{2}$, $x < 0$, and end up with the action

$$L_B = -\frac{1}{4\pi}\int_{-\infty}^{+\infty} dtdx \sum_{ij} \left[\delta_{ij}\partial_t\Phi_i\partial_x\Phi_j + P_{ij}\partial_x\Phi_i\partial_x\Phi_j\right], \qquad (2.26)$$

In Eq. (2.26) we return to our initial definition of the coordinate $-\infty < x < +\infty$ and the points x and $-x$ no longer interact. The quasiparticle operator $\Psi_{e/4} = \sigma \exp\left[i\sum_{kj} a_k \left(S\sqrt{\tilde{V}+\tilde{\Lambda}}\sqrt{P^{-1}}\right)_{kj}\Phi_j(0)\right]$. It is now easy to write down the scaling dimension Δ of $\Psi_{e/4}$ and $g = 2\Delta$:

$$g = 2\Delta_\sigma + \sum_{ij}\left(S\sqrt{\tilde{V}+\tilde{\Lambda}}P^{-1}\sqrt{\tilde{V}+\tilde{\Lambda}}S^T\right)_{ij} a_i a_j, \qquad (2.27)$$

where Δ_σ is the scaling dimension of the operator σ.

We now prove that for any choice of a_i, i.e., for any quasiparticle operator, g in Eq. (2.27) exceeds the value one would obtain without Coulomb interaction between the edge segments on the opposite sides of the gate. In the above expression the electrostatic interaction across the gate enters only through the symmetric positive definite matrix $\tilde{\Lambda}$. We thus wish to prove that g, Eq. (2.27), is greater at $\tilde{\Lambda} \neq 0$ than at $\tilde{\Lambda} = 0$.

Δ_σ does not depend on $\tilde{\Lambda}$. The symmetric positive definite matrix

$$N = \sqrt{\tilde{V} + \tilde{\Lambda}} P^{-1} \sqrt{\tilde{V} + \tilde{\Lambda}} \tag{2.28}$$

that enters (2.27) reduces to the identity matrix at $\tilde{\Lambda} = 0$. Hence, it is enough to prove that all eigenvalues n_i of N are greater than 1. For this end, we notice that

$$N^{-1}(\tilde{V} + \tilde{\Lambda})N^{-1} = (\tilde{V} - \tilde{\Lambda}). \tag{2.29}$$

Let us work in the eigenbasis of N and look at the diagonal elements of the above Eq. (2.29). We find

$$\frac{1}{n_i^2}\left(\tilde{V}_{ii} + \tilde{\Lambda}_{ii}\right) = \left(\tilde{V}_{ii} - \tilde{\Lambda}_{ii}\right) \tag{2.30}$$

and hence $n_i = +1/\sqrt{1 - \frac{2\tilde{\Lambda}_{ii}}{\tilde{V}_{ii}+\tilde{\Lambda}_{ii}}}$. Since both matrices $\tilde{\Lambda}$ and $(\tilde{V} + \tilde{\Lambda})$ are positive definite, their diagonal matrix elements are positive. Hence, $n_i > 1$ and g (2.27) increases indeed at nonzero $\tilde{\Lambda}$ compared to the case of $\tilde{\Lambda} = 0$. This agrees with the relation between the exponents g_A, g_B and g_C in Refs. [23, 24].

2.4.3 Estimates of the electrostatic force

In this subsection we address an apparent paradox: The geometry suggests a rather strong interaction across the upper gate in geometry 2.1b; why is then the tunneling exponent g_B close to g_C?

The expression (2.27) depends on several unknown parameters. They cannot be extracted from a single observable g. In particular, one cannot compute the strength of the interaction across the gate. We can only estimate its order of magnitude from g_C and g_B. Our estimates show that despite a small difference $g_B - g_C$, the

interaction is not weak. Interestingly, our estimates do not depend on the nature of the bulk topological order.

The estimates will be based on two simple models. In the first model we will assume that the interaction contribution U to the action reduces to the product of the charged modes on the opposite sides of the gate,

$$U = -\frac{2}{4\pi}\int dt \int_{-\infty}^{0} dx \frac{2}{5}\lambda_1 \partial_x \Phi_\rho(x)\partial_x \Phi_\rho(-x), \tag{2.31}$$

where $e\partial_x\Phi_\rho/2\pi$ stays for the linear charge density. Such model is legitimate, if all edge channels on each side of the gate run much closer to each other than to the gate. In our second model the across-the-gate interaction includes only the charge density in the FQH channel:

$$U = -\frac{2}{4\pi}\int dt \int_{-\infty}^{0} dx 2\lambda_2 \partial_x \Phi_\rho^F(x)\partial_x \Phi_\rho^F(-x), \tag{2.32}$$

where $e\partial_x\Phi_\rho^F/2\pi$ is the linear charge density on the edge channel, separating the $\nu = 2$ and $\nu = 5/2$ regions. Model 2 is legitimate, if the gate is close to 2DEG and all integer channels run under the gate while fractional channels are sufficiently far from the gate.

It is unlikely that either of the above two sets of assumptions accurately describes the experimental system. At the same time, our estimates of λ in Eqs. (2.31) and (2.32) will give an idea of the range of possible interaction strength.

For simplicity we will assume that the mode Φ_ρ in model 1 and the mode Φ_ρ^F in model 2 do not interact with any other edge modes on the same side of the gate. The application of Eq. (2.27) then becomes very easy.

Consider first model 1. We can always make a linear change of the variables ϕ_i such that one of the new variables is Φ_ρ and all other new variables commute with Φ_ρ. Then the dynamics of the charged mode is completely independent from all other modes. The form of the charged mode action is dictated [5] by the quantum Hall conductance $\frac{5e^2}{2h}$:

$$L_\rho = -\frac{1}{4\pi}\int dt \int_{-\infty}^{+\infty} dx \left[\frac{2}{5}\partial_t\Phi_\rho\partial_x\Phi_\rho + \frac{2}{5}v_\rho\partial_x\Phi_\rho\partial_x\Phi_\rho\right], \tag{2.33}$$

where v_ρ is the velocity of the mode. Since the quasiparticle charge is $e/4$, the field Φ_ρ must enter the quasiparticle operator as $\exp(i\Phi_\rho/[4\times\frac{5}{2}]) = \exp(i\Phi_\rho/10)$. Finally, from Eq. (2.27) one finds:

$$g_B - g_C = \frac{1}{80}\left[\sqrt{\frac{v_\rho+\lambda_1}{v_\rho-\lambda_1}} - 1\right]. \tag{2.34}$$

In model 2 we similarly assume that the charged mode of the FQH edge is decoupled from all other modes. It is controlled by the action

$$L_\rho = -\frac{1}{4\pi}\int dt \int_{-\infty}^{+\infty} dx \left[2\partial_t\Phi_\rho^F\partial_x\Phi_\rho^F + 2v_\rho\partial_x\Phi_\rho^F\partial_x\Phi_\rho^F\right], \tag{2.35}$$

where the coefficient 2 reflects [5] the FQH conductance $\frac{e^2}{2h}$. The quasiparticle operator contains Φ_ρ^F in the exponential factor $\exp(i\Phi_\rho^F/[4\times\frac{1}{2}]) = \exp(i\Phi_\rho^F/2)$. Hence, Eq. (2.27) yields

$$g_B - g_C = \Delta g = \frac{1}{16}\left[\sqrt{\frac{v_\rho+\lambda_2}{v_\rho-\lambda_2}} - 1\right]. \tag{2.36}$$

Substituting the experimental $g_B - g_C = 0.04$ in Eqs. (2.34,2.36) we find $\lambda_1/v_\rho \sim 0.9$ and $\lambda_2/v_\rho \sim 0.45$. These values are similar to the estimate [93] in a related geometry in the 1/3 state. Certainly, the above two models are not very realistic.

Besides, even small uncertainties in g_B and g_C result in major uncertainties in $\lambda_{1,2}$. Note also that we neglect the repulsive interaction between the upper and lower edges of the 2200 nm-wide constriction in the geometry 2.1c since the constriction width is much shorter than the relevant thermal length. This interaction decreases g_C and hence decreases the estimates (2.34,2.36) for $\lambda_{1,2}$. Finally, in the above discussion we disregarded the repulsive interaction between the edge modes on the inner and outer sides of the gates in the geometry 2.1c and the lower gate in the geometry 2.1b (Fig. 2.3). This interaction increases both g_B and g_C compared to the situation without an inner edge. In the next subsection we show that it is safe to neglect the interaction of the inner and outer channels unless it is so strong that the system is on the verge of instability. This possibility is not a concern for us here because our goal is to demonstrate that the interaction is not weak. Overall, it appears safe to conclude that physical λ/v_ρ is within an order of magnitude from the above values. This corresponds to a significant interaction across the gate.

2.4.4 Interaction of inner and outer edge channels

In this subsection we address the interaction between the inner and outer edge channels, Fig. 2.3, in the geometry 2.1c and around the lower gate in the geometry 2.1b. We find that for most values of parameters this interaction has considerably less effect on the tunneling exponents g_B and g_C than the interaction discussed in the previous subsection. This justifies neglecting the interaction of the inner and outer channels.

To estimate the change in the exponents g_B and g_C we consider a model, similar

to the second model of the previous subsection. The action reads

$$L = -\frac{2}{4\pi}\int dt \int_{-\infty}^{+\infty} dx[\partial_t \Phi^F_{\rho O}\partial_x \Phi^F_{\rho O} + v_\rho \partial_x \Phi^F_{\rho O}\partial_x \Phi^F_{\rho O} \\ -\partial_t \Phi^F_{\rho I}\partial_x \Phi^F_{\rho I} + v_\rho \partial_x \Phi^F_{\rho I}\partial_x \Phi^F_{\rho I} + 2\lambda_2 \partial_x \Phi^F_{\rho O}\partial_x \Phi^F_{\rho I}], \tag{2.37}$$

where $\Phi^F_{\rho O}$ and $\Phi^F_{\rho I}$ describe the charge density in the outer and inner fractional edge channels. We are interested in the tunneling into the outer channel. $\Phi^F_{\rho O}$ enters the tunneling operator through the factor $\exp(i\Phi^F_{\rho O}/2)$. Thus, we wish to compute the correction δg to the scaling dimension of the above operator due to a nonzero λ_2.

It is convenient to change the variables:

$$\Phi^F_{\rho O} = \frac{(z+1/z)}{2}\phi_+ + \frac{(z-1/z)}{2}\phi_-; \\ \Phi^F_{\rho I} = \frac{(z-1/z)}{2}\phi_+ + \frac{(z+1/z)}{2}\phi_-, \tag{2.38}$$

where $z = \sqrt[4]{\frac{v_\rho - \lambda_2}{v_\rho + \lambda_2}}$. In the new variables, we discover the action of two noninteracting chiral fields:

$$L = -\frac{2}{4\pi}\int dt \int dx\{\partial_t \phi_+ \partial_x \phi_+ - \partial_t \phi_- \partial_x \phi_- + \sqrt{v_\rho^2 - \lambda_2^2}[(\partial_x \phi_+)^2 + (\partial_x \phi_-)^2]\}. \tag{2.39}$$

Computing δg is now easy. One finds

$$\delta g = \frac{1}{16}\left(\frac{1}{\sqrt{1-(\lambda_2/v_\rho)^2}} - 1\right). \tag{2.40}$$

The experimentally measured g differs from the universal value $g_{\text{universal}}$ for a system without an inner channel along a wide gate and Coulomb interaction across a narrow gate: $g_C = g_{\text{universal}} + 2\delta g$ and $g_B = g_{\text{universal}} + \delta g + \Delta g$, where Δg is

given by Eq. (2.36) and reflects the effect of the interaction across the upper gate in Fig. 2.1b. In the previous subsection we estimated $\lambda_2/v_\rho \sim 0.45$. This corresponds to $\Delta g \sim 0.04$. Substituting the same value of λ_2 in Eq. (2.40), one finds $\delta g \sim 0.007$. This justifies neglecting δg above. It is easy to see that δg is much less than 1 and considerably smaller than Δg as long as λ_2/v_ρ is not close to 1. The unlikely regime $\lambda_2/v_\rho \approx 1$ describes a system on the verge of an instability due to Coulomb interaction. Even in that regime $\delta g < \Delta g/2$ for all λ_2 and hence δg can be ignored in crude estimates of, e.g., the Coulomb interaction strength. At the same time, the expressions (2.34), (2.36) and (2.40) all diverge as $\lambda_{1,2}/v_\rho \to 1$ and all three experimental exponents g_A, g_B and g_C provide only upper bounds for $g_{\text{universal}}$ in that unlikely limit.

One can avoid complications due to the inner channel by changing the geometry of the gates. Instead of Π-shaped gates, one can use gates that contain not only the perimeter but also the inside of a rectangle.

2.5 Discussion

We find that the 331 state with the theoretical $g_C = 3/8$ gives the best fit to the experimental $g_C = 0.38$. It is instructive to compare this conclusion with the lessons from other types of experiments. The data on the spin polarization are controversial [17–20]. There is support for both 0 and 100% polarization. The 331 state comes in both spinal-polarized and unpolarized versions with identical transport signatures in the tunneling experiment. Most other proposed 5/2 states are spin-polarized. Some features of the thermopower data [21] are qualitatively compatible with theoretical predictions for the Pfaffian state [91]. However, even Abelian states may exhibit

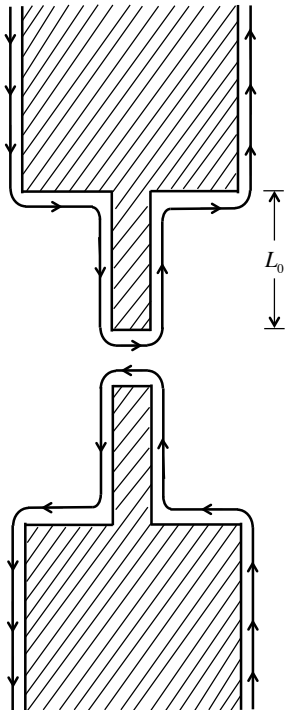

Figure 2.5: Setup of the "smoking gun" experiment. The width of the gates depends on the distance from the tunneling contact.

qualitatively similar behavior, if different quasiparticle species are degenerate or close in energy. The Fabry-Perot interference experiments [14, 15] were interpreted [100] as supporting the Pfaffian or anti-Pfaffian state. At the same time, it was shown that the 331 state can produce identical signatures in a Fabry-Perot interferometer [101] (but interestingly, not in a Mach-Zehnder interferometer [102]). The anti-331 state may also exhibit identical signatures. The results of the transport experiment [16] were explained as a sign of an upstream neutral mode. Such interpretation is incompatible with all proposed states except anti-Pfaffian, anti-331 and anti-$SU(2)_2$. In particular, the 331 state has no upstream edge modes. As discussed in Section 2.3, in the unlikely case of a system on the verge of Coulomb-interaction driven instability, the data [24] do not exclude the Pfaffian state. That state also does not possess contra-propagating edge modes.

Thus, a conflict appears between the interpretation of the experiments from

Refs. [16] and [23, 24]. Our explanation of the data [23, 24] is based on the assumption that the system is in the scaling regime, where universal predictions apply. We also assume that the edges can be described by a chiral Luttinger liquid model. It may happen that such description fails due to, e.g., dissipation [103]. At the same time, edge reconstruction [46] or bulk transport [104] may affect the interpretation of the experiments on upstream modes. On the other hand, various proposed 5/2 states are rather close in energy [105] and it was suggested that more than one 5/2 state might be present at different conditions or in different samples [106]. It is also possible that the true 5/2 state is not one of the simplest states considered above. More light could be shed on the nature of the 5/2 state by tunneling experiments at lower temperatures. To reduce the effect of Coulomb interaction across the gate, one needs to modify the 2.1c setup, Fig. 2.3. The inner edge channel can be eliminated by filling the inside of the Π-shaped gate, Fig. 2.3, with metal. Other methods that could show unique signatures of Abelian and non-Abelian states include thermopower measurements [21, 91] and Mach-Zehnder interferometry [61, 81, 102, 107–112]. The non-equilibrium fluctuation-dissipation theorem [113,114] would provide an independent test of the existence of upstream modes.

Our key idea about the role of gating in the experiments [23,24] can be tested with a "smoking gun" experiment illustrated in Fig. 2.5. The width of the gate is different at short distances $x < L_0$ and long distances $x > L_0$ from the gate. The Coulomb interaction across the gate is strong at $x < L_0$ and negligible at large x. In such situation our theory predicts two different power dependencies of the conductance on the temperature at $T < \hbar v/k_B L_0$ and $T > \hbar v/k_B L_0$, where v is the excitation speed on the edges. The higher temperature regime is similar to the geometry 2.1a and the low temperature limit corresponds to the geometry 2.1c. Thus, one can go between two fixed points by simply changing the temperature (or voltage).

Even though the agreement between the experimental $g_C = 0.38$ and theoretical $g_C = 3/8$ looks excellent, one should be cautious about data accuracy. For example, electron tunneling experiments into the 1/3 edge have routinely shown a 10% discrepancy with the theory [115]. A relative fragility of the 5/2 edge may lead to even lower experimental resolution. Nevertheless, the difference between g_C in the 331 and other competing states exceeds 30% in all cases and this lends credibility to the 331 state as the best fit.

A considerable body of numerical work supports Pfaffian or anti-Pfaffian states (see, e.g., Refs. [116–119]). As discussed above, the data [23, 24] are not compatible with the anti-Pfaffian state but do not exclude the Pfaffian state in the unlikely case of the system on the verge of instability. On the other hand, numerical studies of small simplified model systems have limitations and only experiment can determine the right state. In particular, the existing numerical results [120–123] for the energy gap at $\nu = 5/2$ significantly exceed experimental findings. One limitation of numerics is due to the fact that most studies assume full spin polarization outright. This would exclude the spin-unpolarized 331 state. At the same time, several papers [105, 116, 124, 125] lend support to a spin-polarized ground state. Another limitation comes from the incomplete understanding of the Landau-level mixing effects [126–129]. Disorder apparently plays a major role in the discrepancy of the theoretical and experimental results for the energy gap [121, 130] and may affect the nature of the ground state. We are not aware on any numerical studies that include disorder. Moreover, the numerical energy difference between competing states [105] is so small that even a tiny and generally neglected effect of the spin-orbit interaction [131, 132] might be relevant.

In conclusion, we have proposed an explanation of the discrepancy of the tunneling exponents in Refs. [23, 24]. Two of the three geometries used in Refs. [23, 24] are

affected by the electrostatic interaction across the gates that changes the exponent g. We compare the exponent g_C in the third geometry 2.1c with the theoretical predictions for seven states with the simplest topological orders at $\nu = 5/2$, Eqs. (2.1-2.14). We find that the 331 state gives the best fit for the experiments.

Chapter Three

Particle-Hole Symmetry and Construction of $\nu = \frac{5}{2}$ Quantum Hall States with Upstream Neutral Edge Transport

3.1 Particle-hole symmetry in fractional quantum Hall systems

In a fractional quantum Hall (FQH) system, the uppermost Landau level is partially filled. The ratio of the number N of electrons to the number N_0 of available states in a Landau level is defined as the filling factor $\nu = N/N_0$, Eq. (1.10). If we ignore Landau level mixing and focus only on the partially filled Landau level, there is a particle-hole symmetry [133] in the electron system: the particle-hole transformation takes a FQH liquid at filling factor $\nu < 1$ into a FQH liquid at filling factor $1-\nu$ which has an identical excitation spectrum to the FQH liquid before the transformation. As pointed out by Girvin [133], the particle-hole symmetry is useful for constructing new hierarchical FQH states.

Fig. 3.1 shows the particle-hole transformation schematically. The upper left panel and the lower left panel are the side view and the top view of a FQH liquid at filling factor $\nu < 1$, respectively. We assume the edge states of this FQH liquid propagate clockwise. The side view and the top view of the FQH liquid after the particle-hole transformation are shown in the upper right panel and the lower right panel, respectively. As we can see, the particle-hole transformation is the operation which removes electrons from previously occupied state and fills with electrons the previously unoccupied states. Hence, the resulting FQH liquid, called the particle-hole conjugate of the original FQH liquid, has a filling factor $1 - \nu$. Intuitively, the shape of the two-dimensional electron gas (2DEG) changes from a solid circular disk into an annulus, where the propagation of the original edge modes is inverted and a new integer edge mode at filling factor 1 appears.

The particle-hole symmetry is more easily understood in the language of second

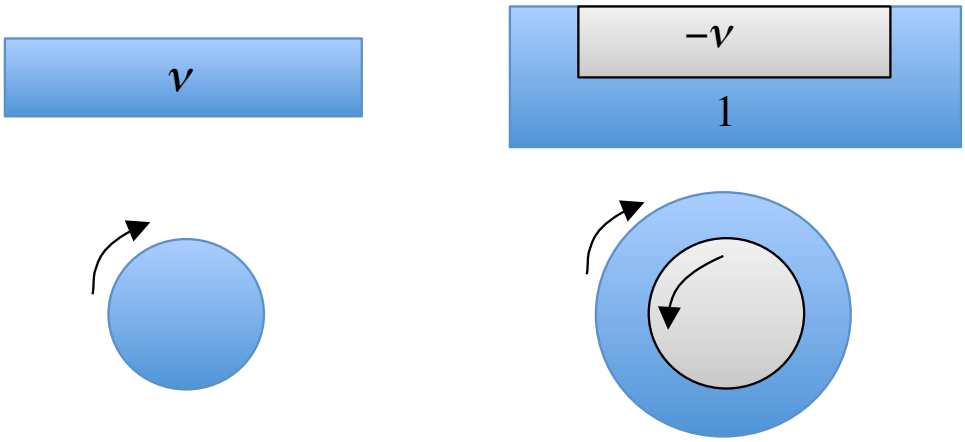

Figure 3.1: A schematic picture of particle-hole transformation in a FQH system. Upper left and lower left panels: side view and top view of a FQH liquid at filling factor ν. Upper right and lower right panels: side view and top view of the FQH liquid after the transformation, at filling factor $1-\nu$. Arrows follow the propagation of edge states. Light grey region indicates the unoccupied states for electrons (or occupied states for holes) in the Landau level.

quantization [28]. In Fock space, a FQH liquid at filling factor ν has the Hamiltonian

$$H = \frac{1}{2} \sum_{m_1,m_2,m_1',m_2'} c^\dagger_{m_1'} c^\dagger_{m_2'} c_{m_2} c_{m_1} \langle m_1', m_2' | V | m_1, m_2 \rangle, \tag{3.1}$$

where c_m and $c^\dagger_m$ are the annihilation and creation operators of the single particle state with definite angular momentum m, Eq. (1.15). V is the electron-electron interaction whose expectation was evaluated in Eq. (1.17) for a two-electron system and approximated in Eq. (1.19) using two-electron eigenfunctions as the basis. Let h_m and $h^\dagger_m$ be the annihilation and creation operators of a hole state with angular momentum m. Then, $h^\dagger_m = c_m$ and $h_m = c^\dagger_m$. The vacuum state $|0\rangle$ for electrons is identified as the completely occupied Landau level for holes,

$$|0\rangle = \prod_{m=0}^{N_0-1} h^\dagger_m |0\rangle_h, \tag{3.2}$$

where $|0\rangle_h$ is the vacuum state for holes. By definitions of h_m and $h^\dagger_m$ and that $\{c_m, c^\dagger_{m'}\} = \delta_{m,m'}$, we have $\{h_m, h^\dagger_{m'}\} = \delta_{m,m'}$. Using anti-commutation relations for

holes, we can write Eq. (3.1) in terms of hole degrees of freedom

$$\begin{aligned} H =& \frac{1}{2} \sum_{m_1,m_2,m_1',m_2'} h^\dagger_{m_1} h^\dagger_{m_2} h_{m_2'} h_{m_1'} \langle m_1', m_2'|V|m_1, m_2\rangle \\ &- \sum_{m_1,m_2,m_1'} h^\dagger_{m_1} h_{m_1'} \langle m_1', m_2|V|m_1, m_2\rangle + \sum_{m_1,m_2,m_2'} h_{m_2'} h^\dagger_{m_2} \langle m_1, m_2'|V|m_1, m_2\rangle \\ &- \sum_{m_1,m_2,m_1'} h_{m_1'} h^\dagger_{m_2} \langle m_1', m_1|V|m_1, m_2\rangle + \sum_{m_1,m_2,m_2'} h^\dagger_{m_1} h_{m_2'} \langle m_2, m_2'|V|m_1, m_2\rangle. \end{aligned} \tag{3.3}$$

It can be shown [28] that

$$\begin{aligned} \sum_{m_1} \langle m_1, m_2'|V|m_1, m_2\rangle &= \delta_{m_2,m_2'} 2\epsilon_H \\ \sum_{m_1} \langle m_1', m_1|V|m_1, m_2\rangle &= \delta_{m_2,m_1'} 2\epsilon_X, \end{aligned} \tag{3.4}$$

where ϵ_H and ϵ_X are constants. Physically, ϵ_H and $-\epsilon_X$ are the Hartree and exchange energies per electron, respectively, of the ground state of a completely filled Landau level. Substituting Eq. (3.4) into Eq. (3.3), we find

$$\begin{aligned} H =& \frac{1}{2} \sum_{m_1,m_2,m_1',m_2'} h^\dagger_{m_1} h^\dagger_{m_2} h_{m_2'} h_{m_1'} \langle m_1', m_2'|V|m_1, m_2\rangle \\ &+ (N - N_h)(\epsilon_H - \epsilon_X) \end{aligned} \tag{3.5}$$

where $N_h = N_0 - N$ is the number of holes (unoccupied states for electrons) in the Landau level. The first term in Eq. (3.5) is the Hamiltonian of holes in a FQH liquid at filling factor ν. But it can also be interpreted as the Hamiltonian of electrons in the particle-hole conjugate system at filling factor $1 - \nu$, if we identify h_m and $h^\dagger_m$ with the annihilation and creation operators of an electron state with angular momentum m in the particle-hole conjugate system. Since the matrix elements $\langle m_1', m_2'|V|m_1, m_2\rangle$ are real, the Hilbert space of the particle-hole conjugate system

is isomorphic (identical apart from a constant $(N - N_h)(\epsilon_H - \epsilon_X)$) to the Hilbert space of the original FQH system. The dimensions of the two Hilbert spaces are certainly the same: $\frac{N_0!}{N!(N_0-N)!} = \frac{N_0!}{N_h!(N_0-N_h)!}$.

Let $E(\nu)$ and $E(1-\nu)$ be the ground state (Coulomb) energies of a FQH liquid at filling factors ν and $1-\nu$, respectively. By Eqs. (3.1)(3.5),

$$E(\nu) = E(1-\nu) + (N - N_h)(\epsilon_H - \epsilon_X). \tag{3.6}$$

Dividing Eq. (3.6) by the number N of electrons, we find

$$\nu\epsilon(\nu) = (1-\nu)\epsilon(1-\nu) + (2\nu - 1)(\epsilon_H - \epsilon_X), \tag{3.7}$$

where $\epsilon(\nu) = E(\nu)/N$ is the energy per electron as a function of the filling factor ν. Taking derivative of Eq. (3.6) with respect to N, we find

$$\mu(\nu) + \mu(1-\nu) = 2(\epsilon_H - \epsilon_X), \tag{3.8}$$

where $\mu(\nu) = \partial E(\nu)/\partial N$ is the chemical potential as a function of the filling factor ν. The chemical potential discontinuity at filling factors ν and $1-\nu$ are identical.

Interesting things happen when the Landau level is at half filling $\nu = 1/2$. In such a case, the ground state energies of a FQH liquid and its particle-hole conjugate are exactly the same, by Eqs. (3.6)(3.7). Moreover, by Eqs. (3.1)(3.5), the Hilbert spaces of the two FQH systems are identical. In Section 3.2, we use these properties to construct new FQH states at filling factor $\nu = 5/2$.

3.2 Construction of particle-hole conjugate states

In this section, we construct particle-hole conjugate states at filling factor $\nu = 5/2$. This work is motivated by the recent observation of upstream neutral edge modes in Ref. [16]. The upstream neutral edge modes are a common feature of particle-hole conjugate states in the presence of many disorders on the edge. Among the existing proposals, the anti-Pfaffian state [44, 45] is the only particle-hole conjugate state. However, we have seen in Chapter 2 that the anti-Pfaffian state does not agree with quasiparticle tunneling experiments [23, 24]. Hence, we need to construct new particle-hole conjugate states to account for the observation in Ref. [16].

Assuming no Landau level mixing, we can treat the completely filled first Landau level as an inert background and focus on the $\nu = 1/2$ FQH state in the second Landau level. We perform particle-hole transformation for the following $\nu = 1/2$ FQH states: the spin-polarized 331 state [52], the $SU(2)_2$ state [49] and the $K = 8$ state [12]. We call the resulting new states the anti-331 state, the anti-$SU(2)_2$ state and the anti-$K = 8$ state. We do not consider the spin-unpolarized 331 state since its particle-hole conjugate has a filling factor $\nu = 3/2$ ($\nu = 7/2$ including the first Landau level). As shown in Section 3.1, at half filling, the two particle-hole dual states have identical Hilbert space and the same ground state energy: They are equally favorable to the FQH Hamiltonian.

We focus on building edge theories for the new particle-hole conjugate states, which can be used to calculate current-voltage characteristics in transport experiments. We only consider the FQH edge between the $\nu = 2$ and $\nu = 5/2$ regions. The two integer edge modes in the first Landau level play little role in our discussion.

It should be noted that, in reality, the particle-hole symmetry is not exact for the

$\nu = 5/2$ FQH liquid. The $\nu = 5/2$ FQH liquid is typically observed at magnetic field $B \sim 4 - 6$T, where Landau level mixing, proportional to $B^{-1/2}$, is not negligible. Landau level mixing renormalizes the two-body interactions (Eq. (3.1)) in the uppermost $\nu = 1/2$ Landau level and produces effective three-body interactions [134, 135] which break the particle-hole symmetry and stabilize one of the two particle-hole dual states as the true ground state.

Our construction uses an approach similar to the treatment of the disorder-dominated $\nu = 2/3$ state [136] and the anti-Pfaffian state [44, 45].

3.2.1 The anti-331 state

In this subsection we formulate the edge theory of the anti-331 state.

We start from a clean particle-hole conjugate of the 331 state which is obtained by condensing hole excitations of the $\nu = 1$ quantum Hall state into the 331 state. In our picture, the 2DEG has an annular shape with the inner edge being the interface between the hole 331 state and its parental $\nu = 1$ IQH state and the outer edge being the interface between the $\nu = 1$ quantum Hall state and the vacuum. The edge is the combination of a right-moving $\nu = 1$ edge and a left-moving FQH edge of the 331 state with the Lagrangian density

$$\mathcal{L}_0 = -\frac{1}{4\pi} \sum_{I,J=0,1,2} [K_{IJ}\partial_t\phi_I\partial_x\phi_J + V_{IJ}\partial_x\phi_I\partial_x\phi_J], \tag{3.9}$$

where the K-matrix [5] and the potential matrix are

$$K = \begin{pmatrix} 1 & 0 & 0 \\ 0 & -3 & 2 \\ 0 & 2 & -4 \end{pmatrix} \text{ and } V = \begin{pmatrix} V_{00} & V_{01} & V_{02} \\ V_{01} & V_{11} & V_{12} \\ V_{02} & V_{12} & V_{22} \end{pmatrix}, \tag{3.10}$$

ϕ_0 is the right-moving $\nu = 1$ charge density mode, ϕ_1 and ϕ_2 are two left-moving modes in the edge theory of the 331 state. The charge vector that determines how the modes (ϕ_0, ϕ_1, ϕ_2) couple to the external gauge field and contribute to the electric current is $\mathbf{t}^T = (1, 1, 0)$. The K-matrix and the charge vector $\mathbf{t}$ together characterize the topological order of the FQH state. To simplify the discussion, we assume at this point that $V_{12} = -V_{22}/2$. We will also assume that the $\nu = 1$ edge mode only couples with the edge mode in the bottom hierarchy of the hole 331 state so that $V_{02} = 0$. This approximation reflects the fact that only the bottom level hierarchy contains electrons which interact with the $\nu = 1$ IQH liquid through the Coulomb potential. At the end of the discussion, we will relax the above assumptions and will see that they do not change any conclusions.

The Lagrangian $\mathcal{L}_0$ describes the low energy edge physics of a clean particle-hole conjugate of the 331 state. In reality, there are always impurities on the edge. They destroy the translational invariance on the FQH edge and cause inter-edge tunneling which leads to the edge mode equilibration. Nontrivial topological charges cannot travel between the hole 331 edge and the $\nu = 1$ channel. Hence, only electrons can tunnel. The electron operator on the $\nu = 1$ edge is $e^{i\phi_0}$. The most relevant electron operators on the hole 331 edge are $e^{-i(3\phi_1 - 2\phi_2)}$ and $e^{-i(\phi_1 + 2\phi_2)}$. The appropriate term for the electron tunneling in the Lagrangian density is

$$\mathcal{L}_{\text{tun}} = \xi_1(x) e^{i(\phi_0 + 3\phi_1 - 2\phi_2)} + \xi_2(x) e^{i(\phi_0 + \phi_1 + 2\phi_2)} + \text{H.c.}, \tag{3.11}$$

where we have suppressed the Klein factors that are necessary to ensure correct statistics among different electron operators. $\xi_1(x)$ and $\xi_2(x)$ are complex variables characterizing the strength of random impurities. We assume for simplicity that their distribution is Gaussian and they are δ-correlated: $\langle \xi_1(x)\xi_1^*(x')\rangle = W_1\delta(x-x')$ and $\langle \xi_2(x)\xi_2^*(x')\rangle = W_2\delta(x-x')$.

At weak disorder W_1 and W_2, the effect of electron tunneling on the FQH edge is determined by the scaling behavior of the tunneling operators. Using $\mathcal{L}_0$, we find that the two tunneling operators have the same scaling dimension

$$\Delta = \frac{1}{2} + \frac{3-2\sqrt{2}c}{2\sqrt{1-c^2}}, \tag{3.12}$$

where $c = 8\sqrt{2}V_{01}/(8V_{00}+4V_{11}-V_{22})$. The leading order renormalization group (RG) equations for the disorder strength are [137]

$$\frac{dW_i}{dl} = (3-2\Delta)W_i, \tag{3.13}$$

where $i = 1, 2$. For $\Delta > 3/2$, the electron tunneling is irrelevant and the low temperature edge physics is described by $\mathcal{L}_0$ in Eq. (3.9) in which no equilibration occurs between the $\nu = 1$ edge and the hole 331 edge. The physics is very similar to the physics of the anti-$K = 8$ state, which will be addressed in Subsection 3.2.3. Quasiparticle tunneling is nonuniversal. At low voltages and temperatures the quantum Hall conductance is quantized at $7e^2/2h$ instead of the right value $5e^2/2h$. This happens because the integer mode conductance $3e^2/h$ and the conductance $e^2/2h$ of the fractional edge must be added and not subtracted in the quantum Hall bar geometry. A detailed discussion of a similar point can be found in Ref. [90]. On the other hand, if $\Delta < 3/2$ the electron tunneling is relevant and we end up with a disorder-dominated phase with equilibrated edge modes at low temperatures. This

is the situation we consider below.

To study the disorder-dominated phase, it is useful to rewrite the edge dynamics in terms of a charged mode, represented by the charge vector $\mathbf{t}$, and two independent neutral modes, represented by the neutral vectors $\mathbf{n_1}$, $\mathbf{n_2}$. If we treat the matrix K^{-1} as a metric then neutral vectors are those with vanishing inner products with the charge vector, $\mathbf{n}_1^T K^{-1}\mathbf{t} = 0$, $\mathbf{n}_2^T K^{-1}\mathbf{t} = 0$. We choose $\mathbf{n}_1^T = (1, 2, 0)$, $\mathbf{n}_2^T = (0, -1, 2)$. The corresponding charged ϕ_ρ and neutral ϕ_{n_1}, ϕ_{n_2} boson fields are

$$\begin{aligned} \mathbf{t} &\rightarrow \phi_\rho = \phi_0 + \phi_1 \\ \mathbf{n}_1 &\rightarrow \phi_{n_1} = \phi_0 + 2\phi_1 \\ \mathbf{n}_2 &\rightarrow \phi_{n_2} = -\phi_1 + 2\phi_2. \end{aligned} \tag{3.14}$$

In the basis $(\phi_\rho, \phi_{n_1}, \phi_{n_2})$, the Lagrangian density of the tunneling problem $\mathcal{L}_0 + \mathcal{L}_{\text{tun}} = \mathcal{L}_\rho + \mathcal{L}_{\text{Sym}} + \mathcal{L}_{\text{SB}}$, where

$$\mathcal{L}_\rho = -\frac{2}{4\pi}[\partial_t\phi_\rho\partial_x\phi_\rho + v_\rho(\partial_x\phi_\rho)^2] \tag{3.15}$$

and

$$\begin{aligned} \mathcal{L}_{\text{Sym}} =& -\frac{1}{4\pi}\sum_{i=1,2}[-\partial_t\phi_{n_i}\partial_x\phi_{n_i} + \bar{v}_n(\partial_x\phi_{n_i})^2] \\ &+ [\xi_1(x)e^{i(\phi_{n_1}-\phi_{n_2})} + \xi_2(x)e^{i(\phi_{n_1}+\phi_{n_2})} + \text{H.c.}]; \\ \mathcal{L}_{\text{SB}} =& -\frac{1}{4\pi}\sum_{i=1,2}\delta v_{n_i}(\partial_x\phi_{n_i})^2 - \frac{2}{4\pi}v_{\rho n_1}\partial_x\phi_\rho\partial_x\phi_{n_1}. \end{aligned} \tag{3.16}$$

The velocities of ϕ_ρ, ϕ_{n_1} and ϕ_{n_2} are $v_\rho = 2V_{00} - 2V_{01} + \frac{1}{2}V_{11} - \frac{1}{8}V_{22}$, $v_{n_1} = V_{00} - 2V_{01} + V_{11} - \frac{1}{4}V_{22}$ and $v_{n_2} = \frac{1}{4}V_{22}$, respectively. In writing the Lagrangians, we have defined the average velocity $\bar{v}_n = \frac{1}{2}(v_{n_1} + v_{n_2})$ and moved the anisotropic part of the velocities

$\delta v_{n_i} = v_{n_i} - \bar{v}_n$ into $\mathcal{L}_{\rm SB}$. The reason for this is that $\mathcal{L}_{\rm Sym}$ now has a hidden $SO(4)$ symmetry whereas $\mathcal{L}_{\rm SB}$ is the symmetry-breaking term. The interaction between the charged mode ϕ_ρ and the neutral mode ϕ_{n_1} is $v_{\rho n_1} = -2V_{00} + 3V_{01} - V_{11} + \frac{1}{4}V_{22}$. Note that after the basis change the electron tunneling only couples the neutral modes and contributes to their equilibration. The charged mode is left alone with its own velocity v_ρ.

To view the $SO(4)$ symmetry in $\mathcal{L}_{\rm Sym}$ more clearly, we fermionize ϕ_{n_1} and ϕ_{n_2} into chiral fermions by setting $\Psi_{n_1} = \frac{1}{\sqrt{2\pi}} e^{-i\phi_{n_1}}$ and $\Psi_{n_2} = \frac{1}{\sqrt{2\pi}} e^{-i\phi_{n_2}}$. We then further break the two chiral fermions into four real Majorana fermions defined as $\psi_1 = {\rm Re}\Psi_{n_1}$, $\psi_2 = {\rm Im}\Psi_{n_1}$, $\psi_3 = {\rm Re}\Psi_{n_2}$ and $\psi_4 = {\rm Im}\Psi_{n_2}$. In terms of the Majorana fermions, the Lagrangians $\mathcal{L}_{\rm Sym}$ and $\mathcal{L}_{\rm SB}$ are

$$\begin{aligned} \mathcal{L}_{\rm Sym} &= i\psi^T(\partial_t - \bar{v}_n\partial_x)\psi + \sum_{a,b} \psi^T(\xi_{ab}L_{ab})\psi; \\ \mathcal{L}_{\rm SB} &= -i\psi^T(\delta v\partial_x)\psi - v_{\rho n_1}(\partial_x\phi_\rho)\psi^T M\psi, \end{aligned} \tag{3.17}$$

where $\psi^T \equiv (\psi_1, \psi_2, \psi_3, \psi_4)$ and $a, b = 1, 2, 3, 4$. The new random variables are defined as $\xi_{13} = -2\pi({\rm Im}\xi_1 + {\rm Im}\xi_2)$, $\xi_{14} = -2\pi({\rm Re}\xi_1 - {\rm Re}\xi_2)$, $\xi_{23} = 2\pi({\rm Re}\xi_1 + {\rm Re}\xi_2)$, $\xi_{24} = -2\pi({\rm Im}\xi_1 - {\rm Im}\xi_2)$, and all other $\xi_{ab} = 0$. The Hermitian matrices L_{ab} are the generators of the $SO(4)$ group in the fundamental representation,

$$(L_{ab})_{kl} = i(\delta_{al}\delta_{bk} - \delta_{ak}\delta_{bl}) \tag{3.18}$$

with $k, l = 1, 2, 3, 4$. The other matrices in Eq. (3.17): $\delta v = {\rm Diag}(\delta v_{n_1}, \delta v_{n_1}, \delta v_{n_2}, \delta v_{n_2})$ and $M = -L_{12}$.

As the last step, we perform a local rotation of the Majorana fermions $\tilde{\psi}(x) =$

$R(x)\psi(x)$, where

$$R(x) = \mathcal{P}\exp\Big(\frac{i}{\bar{v}_n}\sum_{a,b}\int_{-\infty}^{x} dx'\xi_{ab}(x')L_{ab}\Big) \tag{3.19}$$

and $\mathcal{P}$ is the path-ordering operator. Clearly, $R^T R = \mathbb{1}_{4\times 4}$ and $\det(R) = 1$. After the rotation, the Lagrangians become

$$\begin{aligned}\mathcal{L}_{\rm Sym} &= i\tilde{\psi}^T(\partial_t - \bar{v}_n\partial_x)\tilde{\psi};\\ \mathcal{L}_{\rm SB} &= -i\tilde{\psi}^T(\widetilde{\delta v}\partial_x)\tilde{\psi} - v_{\rho n_1}(\partial_x\phi_\rho)\tilde{\psi}^T\widetilde{M}\tilde{\psi},\end{aligned} \tag{3.20}$$

where $\widetilde{\delta v} = R(x)\delta v R^{-1}(x)$ and $\widetilde{M} = R(x)MR^{-1}(x)$ are spatially random matrices. On the second line of the above equation we omit a term with the derivative $\partial_x R^{-1}$. Its structure is similar to the second term on the first line of Eq. (3.17) and it can be removed with a variable change, similar to Eq. (3.19). The $SO(4)$ symmetry in $\mathcal{L}_{\rm Sym}$ is now clearly manifest. Let us study the symmetry-breaking terms in $\mathcal{L}_{\rm SB}$. Naively, both operators in $\mathcal{L}_{\rm SB}$ have scaling dimension 2 and they are marginal. However, the random coefficients $\widetilde{\delta v}$ and $\widetilde{M}$ make them irrelevant under a perturbative RG analysis. [137] Hence, both terms in $\mathcal{L}_{\rm SB}$ scale to zero at low temperature.

In general, our initial simplifying assumptions for the potential matrix may not hold and we will have two more terms in the Lagrangian,

$$\begin{aligned}\mathcal{L}'_{\rm Sym} &= -\frac{1}{4\pi}v_{n_1n_2}\partial_x\phi_{n_1}\partial_x\phi_{n_2} = \frac{\pi}{6}v_{n_1n_2}\sum_{ijkl}\varepsilon_{ijkl}\tilde{\psi}_i\tilde{\psi}_j\tilde{\psi}_k\tilde{\psi}_l,\\ \mathcal{L}'_{\rm SB} &= -\frac{1}{4\pi}v_{\rho n_2}\partial_x\phi_\rho\partial_x\phi_{n_2} = -v_{\rho n_2}(\partial_x\phi_\rho)\tilde{\psi}^T N\tilde{\psi},\end{aligned} \tag{3.21}$$

where ε_{ijkl} is the Levi-Civita tensor with $i,j,k,l = 1,2,3,4$, and N is a spatially random matrix. $\mathcal{L}'_{\rm Sym}$ is a marginal term that respects the $SO(4)$ symmetry. It should be retained in the edge theory of the anti-331 state. On the other hand, the operator in $\mathcal{L}'_{\rm SB}$ is irrelevant.

Any $SO(4)$-invariant combination of the Majorana fermions can be constructed from the Majorana operators and their derivatives, the Kronecker tensor δ_{ij} and the Levi-Civita tensor ε_{ijkl}. Keeping all possible relevant terms we find the full Lagrangian that describes the low energy edge physics of the anti-331 state:

$$\begin{aligned}\mathcal{L} = &-\frac{2}{4\pi}[\partial_t\phi_\rho\partial_x\phi_\rho + v_\rho(\partial_x\phi_\rho)^2] + i\tilde{\psi}^T(\partial_t - \bar{v}_n\partial_x)\tilde{\psi} \\ &+ \frac{\pi}{6}v_{n_1n_2}\sum_{ijkl}\varepsilon_{ijkl}\tilde{\psi}_i\tilde{\psi}_j\tilde{\psi}_k\tilde{\psi}_l. \end{aligned} \tag{3.22}$$

The edge theory consists of one right-moving charged density mode and four left-moving Majorana fermions obeying an explicit $SO(4)$ symmetry. The density mode and the Majorana fermions decouple.

The thermal conductance of a FQH state is a universal quantity that is determined by the bulk topological order. It depends only on the numbers of right-moving and left-moving edge modes and is robust [138] with respect to interactions (for example, the off-diagonal elements in the potential matrix) and disorder. Using the Lagrangian in Eq. (3.9) or Eq. (3.22), we obtain the thermal conductance in the anti-331 state as $\kappa_{\overline{331}} = 2+1-1-1 = 2+1-4\times\frac{1}{2} = 1$, in units of $\pi^2k_B^2T/3h$ (the first factor of 2 comes from the two integer modes). This is different from the thermal conductance $\kappa_{331} = 2+1+1 = 4$ in the 331 state, indicating different topological orders of the 331 and anti-331 state.

A generic quasiparticle operator on the edge of the anti-331 state is $\Psi_{qp} = e^{i(l_0\phi_0+l_1\phi_1+l_2\phi_2)}$ with the electric charge $Q_{qp} = l_0-\frac{1}{2}l_1-\frac{1}{4}l_2$ in units of e, where l_0, l_1, l_2 are independent integers. Its scaling dimension g_{qp} can be obtained by computing the correlation function, $\langle\Psi^\dagger_{qp}(t)\Psi_{qp}(0)\rangle \sim t^{-2g_{qp}}$ at zero temperature, using the $SO(4)$ invariant Lagrangian from Eq. (3.22). Equivalently yet more easily, we can use the boson Lagrangians from Eqs. (3.15,3.16,3.21) by setting $\delta v_1 = \delta v_2 = v_{\rho n_1} = v_{\rho n_2} = 0$

and $\xi_1 = \xi_2 = 0$. This is because the rotation $R(x)$ is local and does not change the equal-space correlation functions of quasiparticle operators. The interaction $v_{n_1 n_2}$ between copropagating neutral bosons cannot modify the scaling behavior of a quasiparticle [5]. Using $\phi_0 = 2\phi_\rho - \phi_{n_1}$, $\phi_1 = -\phi_\rho + \phi_{n_1}$ and $\phi_2 = -\frac{1}{2}(\phi_\rho - \phi_{n_1} - \phi_{n_2})$, we obtain the universal scaling dimension of Ψ_{qp} as

$$g_{qp} = \frac{(4l_0 - 2l_1 - l_2)^2}{16} + \frac{(2l_0 - 2l_1 - l_2)^2}{8} + \frac{l_2^2}{8}. \tag{3.23}$$

The most relevant quasiparticles are those with the minimal scaling dimension (3.23). Here, it is $e^{i(\phi_0+\phi_1)}$ with the electric charge $e/2$ and scaling dimension $1/4$. The next-most relevant quasiparticles are $e^{i(\phi_0+2\phi_1-\phi_2)}$, $e^{i(\phi_0+\phi_1+\phi_2)}$, $e^{i(\phi_2-\phi_1)}$ and $e^{-i\phi_2}$ with the electric charge $e/4$ and scaling dimension $5/16$. The above quasiparticle operators can all be represented in the form $e^{i\phi_\rho/2}e^{\pm i\phi_{n_1}/2}e^{\pm i\phi_{n_2}/2}$, where the last two exponential factors correspond to the operators σ_α in Subsection 2.2.6.

3.2.2 The anti-$SU(2)_2$ state

In this subsection we obtain the edge theory of the anti-$SU(2)_2$ state.

Our approach is the same as in Subsection 3.2.1. As a starting point, we write down the edge Lagrangian of a clean particle-hole conjugate of the $SU(2)_2$ phase

$$\begin{aligned}\mathcal{L}_0 = &-\frac{1}{4\pi}[\partial_t\phi_0\partial_x\phi_0 - 2\partial_t\phi_\rho\partial_x\phi_\rho - \partial_t\phi_n\partial_x\phi_n + v_0(\partial_x\phi_0)^2 + 2v_\rho(\partial_x\phi_\rho)^2 + v_n(\partial_x\phi_n)^2] \\ &-\frac{2}{4\pi}v_{0\rho}\partial_x\phi_0\partial_x\phi_\rho + i\psi(\partial_t - v_\psi\partial_x)\psi,\end{aligned} \tag{3.24}$$

where ϕ_0 is the right-moving $\nu = 1$ edge mode and ϕ_ρ, ϕ_n, ψ are left-moving $SU(2)_2$ FQH edge modes. We first assume that only charged modes interact via Coulomb

potential $v_{0\rho}$. At the end of the discussion we will see that our conclusions do not depend on that assumption. The charge vector of the boson fields $(\phi_0, \phi_\rho, \phi_n)$ is $\mathbf{t}^T = (1, 1, 0)$. The Majorana fermion ψ is neutral.

In the presence of disorder, electrons may tunnel between the integer edge and the FQH edge. The electron operator on the $\nu = 1$ edge is $e^{i\phi_0}$. The most relevant electron operators on the FQH edge are $\psi e^{-i2\phi_\rho}$, $\mathrm{Re}\{e^{-i\phi_n}\}e^{-i2\phi_\rho}$ and $\mathrm{Im}\{e^{-i\phi_n}\}e^{-i2\phi_\rho}$. The Lagrangian density that describes the electron tunneling due to impurities on the edge is

$$\begin{aligned}\mathcal{L}_{\mathrm{tun}} =&\xi_1(x)\psi e^{i(\phi_0+2\phi_\rho)} + \xi_2(x)\mathrm{Re}\{e^{-i\phi_n}\}e^{i(\phi_0+2\phi_\rho)} \\ &+ \xi_3(x)\mathrm{Im}\{e^{-i\phi_n}\}e^{i(\phi_0+2\phi_\rho)} + \mathrm{H.c.},\end{aligned} \tag{3.25}$$

where $\xi_i(x)$ are complex Gaussian variables characterizing the strength of disorder, $\langle \xi_i(x)\xi_j^*(x')\rangle = W_i\delta(x-x')\delta_{ij}$, where $i, j = 1, 2, 3$. To simplify notation we suppress Klein factors as in Subsection 3.2.1.

From $\mathcal{L}_0$ in Eq. (3.24), we find that the tunneling operators in Eq. (3.25) have the same scaling dimension $\Delta = 1/2+(3-2\sqrt{2}c)/(2\sqrt{1-c^2})$, where $c = \sqrt{2}v_{0\rho}/(v_0+v_\rho)$. The scaling dimension Δ determines the edge physics at low temperatures. The leading order RG equations [137] are $dW_i/dl = (3-2\Delta)W_i$. When $\Delta > 3/2$, the electron tunneling is irrelevant and the low temperature edge physics is described by $\mathcal{L}_0$. When $\Delta < 3/2$, we arrive at the disorder-dominated phase with equilibrated edges at low temperature.

The physics of the non-equilibrated case $\Delta < 3/2$ is nonuniversal. Just like in Subsection 3.2.3, we find that the quasiparticle tunneling exponent g can assume a broad range of values. Moreover, the quantum Hall conductance at low tempera-

tures and voltages does not assume the correct value $5e^2/2h$. It becomes $7e^2/2h$ in the quantum Hall bar geometry. This happens for the same reasons as in Subsections 3.2.1 and 3.2.3: One has to add the conductance $3e^2/h$ of the integer quantum Hall subsystem and the conductance $e^2/2h$ of the FQH subsystem. Below we focus on the disorder dominated equilibrated phase.

Let us separate the charged and neutral degrees of freedom on the edge by defining $\phi_{\tilde{\rho}} = \phi_0 + \phi_\rho$, $\phi_{n_1} = \phi_0 + 2\phi_\rho$ and $\phi_{n_2} = \phi_n$. The full Lagrangian $\mathcal{L}_0 + \mathcal{L}_{\rm tun} = \mathcal{L}_{\tilde{\rho}} + \mathcal{L}_{\rm Sym} + \mathcal{L}_{\rm SB}$, where

$$\begin{aligned}
\mathcal{L}_{\tilde{\rho}} =& -\frac{2}{4\pi}[\partial_t\phi_{\tilde{\rho}}\partial_x\phi_{\tilde{\rho}} + v_{\tilde{\rho}}(\partial_x\phi_{\tilde{\rho}})^2];\\
\mathcal{L}_{\rm Sym} =& -\frac{1}{4\pi}\sum_{i=1,2}[-\partial_t\phi_{n_i}\partial_x\phi_{n_i} + \bar{v}_n(\partial_x\phi_{n_i})^2]\\
&+ [\xi_1\psi e^{i\phi_{n_1}} + \xi_2 {\rm Re}\{e^{-i\phi_{n_2}}\}e^{i\phi_{n_1}} + \xi_3 {\rm Im}\{e^{-i\phi_{n_2}}\}e^{i\phi_{n_1}} + {\rm H.c.}]\\
&+ i\psi(\partial_t - \bar{v}_n\partial_x)\psi;\\
\mathcal{L}_{\rm SB} =& -\frac{1}{4\pi}\sum_{i=1,2}\delta v_{n_i}(\partial_x\phi_{n_i})^2 - \frac{2}{4\pi}v_{\tilde{\rho}n_1}\partial_x\phi_{\tilde{\rho}}\partial_x\phi_{n_1}\\
&- i\psi(\delta v_\psi\partial_x)\psi.
\end{aligned} \tag{3.26}$$

The velocities of $\phi_{\tilde{\rho}}$, ϕ_{n_1}, ϕ_{n_2} are $v_{\tilde{\rho}} = 2v_0 + v_\rho - 2v_{0\rho}$, $v_{n_1} = v_0 + 2v_\rho - 2v_{0\rho}$ and $v_{n_2} = v_n$, respectively. The interaction parameter $v_{\tilde{\rho}n_1} = -2v_0 - 2v_\rho + 3v_{0\rho}$. Here we have split the Lagrangian into $\mathcal{L}_{\rm Sym}$, which respects a hidden symmetry, and the symmetry-breaking part $\mathcal{L}_{\rm SB}$. The velocity anisotropies $\delta v_\psi = v_\psi - \bar{v}_n$ and $\delta v_{n_i} = v_{n_i} - \bar{v}_n$ $(i = 1, 2)$ are defined with respect to the average velocity $\bar{v}_n = \frac{1}{5}(v_\psi + 2v_{n_1} + 2v_{n_2})$.

We now fermionize the neutral bosons into Majorana fermions according to $\psi_2 = \frac{1}{\sqrt{2\pi}}{\rm Re}\{e^{-i\phi_{n_1}}\}$, $\psi_3 = \frac{1}{\sqrt{2\pi}}{\rm Im}\{e^{-i\phi_{n_1}}\}$, $\psi_4 = \frac{1}{\sqrt{2\pi}}{\rm Re}\{e^{-i\phi_{n_2}}\}$, $\psi_5 = \frac{1}{\sqrt{2\pi}}{\rm Im}\{e^{-i\phi_{n_2}}\}$ and

define $\psi_1 = \psi$. In terms of the Majorana fermions,

$$\begin{aligned} \mathcal{L}_{\rm Sym} &= i\psi^T(\partial_t - \bar{v}_n\partial_x)\psi + \sum_{a,b}\psi^T(\xi_{ab}K_{ab})\psi \\ \mathcal{L}_{\rm SB} &= -i\psi^T(\delta v\partial_x)\psi - v_{\tilde{\rho}n_1}(\partial_x\phi_{\tilde{\rho}})\psi^T M\psi, \end{aligned} \tag{3.27}$$

where $\psi^T \equiv (\psi_1, \psi_2, \psi_3, \psi_4, \psi_5)$ and $a, b = 1, 2, 3, 4, 5$. Random variables ξ_{ab} are defined as $\xi_{12} = -\sqrt{2\pi}{\rm Im}\xi_1$, $\xi_{13} = \sqrt{2\pi}{\rm Re}\xi_1$, $\xi_{24} = 2\pi{\rm Im}\xi_2$, $\xi_{25} = 2\pi{\rm Im}\xi_3$, $\xi_{34} = -2\pi{\rm Re}\xi_2$, $\xi_{35} = -2\pi{\rm Re}\xi_3$ and all other $\xi_{ab} = 0$. Hermitian matrices K_{ab} are the generators of the $SO(5)$ group in the fundamental representation, $(K_{ab})_{kl} = i(\delta_{al}\delta_{bk} - \delta_{ak}\delta_{bl})$ with $k, l = 1, 2, 3, 4, 5$. The other matrices in the Lagrangians are $\delta v = {\rm Diag}(\delta v_\psi, \delta v_{n_1}, \delta v_{n_1}, \delta v_{n_2}, \delta v_{n_2})$ and $M = -K_{23}$.

Finally, we make a local rotation of the Majorana fermions $\tilde{\psi}(x) = R(x)\psi(x)$, where

$$R(x) = \mathcal{P}\exp\Big(\frac{i}{\bar{v}_n}\sum_{a,b}\int_{-\infty}^{x} dx'\xi_{ab}(x')K_{ab}\Big) \tag{3.28}$$

and $\mathcal{P}$ is the path-ordering operator. The Lagrangians after the rotation are

$$\begin{aligned} \mathcal{L}_{\rm Sym} &= i\tilde{\psi}^T(\partial_t - \bar{v}_n\partial_x)\tilde{\psi} \\ \mathcal{L}_{\rm SB} &= -i\tilde{\psi}^T(\widetilde{\delta v}\partial_x)\tilde{\psi} - v_{\tilde{\rho}n_1}(\partial_x\phi_{\tilde{\rho}})\tilde{\psi}^T\widetilde{M}\tilde{\psi}, \end{aligned} \tag{3.29}$$

where $\widetilde{\delta v} = R(x)\delta v R^{-1}(x)$ and $\widetilde{M} = R(x)MR^{-1}(x)$ are spatially random matrices. As in Subsection 3.2.1, we omit a term with $\partial_x R^{-1}$. It can be removed with another transformation of the type (3.28). Now, the $SO(5)$ symmetry in $\mathcal{L}_{\rm Sym}$ is clear. The symmetry-breaking terms in $\mathcal{L}_{\rm SB}$ are irrelevant due to their random coefficients, in exactly the same way as in the anti-331 state, Subsection 3.2.1.

In the most general case, the neutral boson ϕ_n in Eq. (3.24) may interact with

charged bosons ϕ_0 and ϕ_ρ. This gives rise to two more symmetry-breaking terms in the Lagrangian. However, both terms are irrelevant and disappear at low temperatures. The edge physics of the anti-$SU(2)_2$ state is described by $\mathcal{L}_{\tilde{\rho}} + \mathcal{L}_{\text{Sym}}$ that contains all relevant operators allowed by the symmetry. In contrast to the anti-331 case with its $SO(4)$ symmetry group, we do not need to keep any four-fermion operators in the action.

A generic quasiparticle operator on the edge of the anti-$SU(2)_2$ state is $\Psi_{qp} = \zeta e^{i(l_0\phi_0 + l_\rho\phi_\rho + l_n\phi_n)}$ with the electric charge $Q_{qp} = l_0 - \frac{1}{2}l_\rho$ in units of e, where ζ is one of the three fields $\mathbf{1}$, σ, and ψ with the scaling dimensions $g_{\mathbf{1}} = 0$, $g_\sigma = \frac{1}{16}$ and $g_\psi = \frac{1}{2}$. l_0 is an arbitrary integer. l_ρ and l_n are integers or half integers. We are interested in $\pm e/4$ charged quasiparticles. The quasiparticle charge gives the constraint $l_0 = \frac{1}{2}l_\rho \pm \frac{1}{4}$, which is satisfied only if l_ρ is a half integer given that l_0 is an integer. In addition, we must require that the quasiparticle is local with respect to electrons, which means there is no branch cut in the correlation function between the quasiparticle operator and any of the electron operators in the theory [5]. Hence, l_n must also be a half integer and $\zeta = \sigma$. The most general $\pm e/4$ charged quasiparticle is then $\Psi_{\pm e/4} = \sigma e^{i(l_0\phi_0 + l_\rho\phi_\rho + l_n\phi_n)}$ with l_ρ and l_n being half integers and $l_0 = \frac{1}{2}l_\rho \pm \frac{1}{4}$ an integer. The scaling dimension $g_{\pm e/4}$ can be computed using the boson Lagrangians in Eq. (3.26) by setting $\delta v_\psi = \delta v_1 = \delta v_2 = v_{\tilde{\rho}n_1} = 0$ and $\xi_1 = \xi_2 = \xi_3 = 0$. This gives

$$g_{\pm e/4} = \frac{1}{2}(l_0 \mp \frac{1}{2})^2 + \frac{1}{2}l_n^2 + \frac{1}{8}. \tag{3.30}$$

The most relevant $e/4$ and $-e/4$ charged quasiparticles are $\sigma e^{i(\phi_0 + \frac{3}{2}\phi_\rho \pm \frac{1}{2}\phi_n)}$, $\sigma e^{-i(\frac{1}{2}\phi_\rho \pm \frac{1}{2}\phi_n)}$ and $\sigma e^{-i(\phi_0 + \frac{3}{2}\phi_\rho \pm \frac{1}{2}\phi_n)}$, $\sigma e^{i(\frac{1}{2}\phi_\rho \pm \frac{1}{2}\phi_n)}$, all with the scaling dimension 3/8. All these operators are products of a factor $e^{\pm i\phi_{\tilde{\rho}}/2}$ and one of the twist operators σ_α, Subsection 2.2.8.

3.2.3 The anti-$K = 8$ state

The anti-$K = 8$ state is the particle-hole conjugate of the $K = 8$ state, with the FQH edge Lagrangian density

$$\mathcal{L}_0 = -\frac{1}{4\pi}[\partial_t\phi_0\partial_x\phi_0 - 8\partial_t\phi_1\partial_x\phi_1 + v_0(\partial_x\phi_0)^2 + 8v_1(\partial_x\phi_1)^2] - \frac{1}{\pi}v_{01}\partial_x\phi_0\partial_x\phi_1, \tag{3.31}$$

where ϕ_0 is the right-moving integer edge mode and ϕ_1 is the left-moving fractional edge mode from the $K = 8$ state. As in Subsections 3.2.1 and 3.2.2 we focus on the FQH edge between the $\nu = 2$ and $\nu = 5/2$ regions. The charge vector of (ϕ_0, ϕ_1) is $\mathbf{t}^T = (1, 2)$, which reflects that the $K = 8$ state is a Laughlin state of electron pairs. The Lagrangian that describes the tunneling of electron pairs between the integer and fractional edges due to impurities is

$$\mathcal{L}_{\text{tun}} = \xi(x)e^{i(2\phi_0+8\phi_1)} + \text{H.c.}, \tag{3.32}$$

where $\xi(x)$ is a complex Gaussian random variable that describes local disorder, $\langle\xi(x)\xi^*(x')\rangle = W\delta(x - x')$. The scaling dimension of the tunneling operators is $\Delta = (6 - 4\sqrt{2}c)/\sqrt{1 - c^2}$, where $c = \sqrt{2}v_{01}/(v_0 + v_1)$. Positive-definiteness of the Hamiltonian requires $v_0v_1 > v_{01}^2/2$, and hence $|c| < 1$. The leading order RG equation [137] for the disorder strength W is $dW/dl = (3 - 2\Delta)W$. By inspection, the scaling dimension Δ is always greater than 3/2. Hence, electron-pair tunneling is always irrelevant and a disorder-dominated phase does not exist. The edge physics of the anti-$K = 8$ state is described by $\mathcal{L}_0$.

A generic quasiparticle $\Psi_{qp} = e^{i(l_0\phi_0+l_1\phi_1)}$ (l_0, l_1 are independent integers) on the edge of the anti-$K = 8$ state has the electric charge $Q_{qp} = l_0 - \frac{1}{4}l_1$ in units of

e. Its scaling dimension g_{qp} is nonuniversal and depends on the parameters in the Hamiltonian. With $\mathcal{L}_0$, we find

$$g_{qp} = \frac{1}{2\sqrt{1-c^2}}(l_0^2 + \frac{l_1^2}{8} - \frac{l_0 l_1}{\sqrt{2}}c). \tag{3.33}$$

Possible values of g_{qp} for charge-$e/4$ excitations range between $1/16$ and $+\infty$. The low temperature quantum Hall bar conductance is quantized at $7e^2/2h$ just like in other nonequilibrated states with the same filling factor, Ref. [90].

The above discussion ignores the two integer edge modes ϕ_1^0, ϕ_2^0 always present in the second Landau level states. If we allow tunneling between those modes and the FQH modes and include operators that transmit three or more electrons then it is possible to find relevant tunneling operators at certain choices of the interaction constants in the Hamiltonian. One example would be the operator $O_3 = \exp(i[8\phi_1 + 3\phi_0 - \phi_1^0])$, where ϕ_1^0 describes the integer mode with the same spin polarization as the FQH edge. We expect the amplitude of such many-body operators to be small and neglect them even if the interaction constants are such that they are relevant.

Chapter Four

The 113 State: A New Topological Order at Filling Factor $\nu = \frac{5}{2}$

4.1 Charge-neutral separation

The quantized Hall conductance plateau at filling factor $\nu = 5/2$ is a well-known exception of the conventional series of fractional quantum Hall (FQH) states based on hierarchical extensions [5] of Laughlin's variational wave function. The fact that the filling factor has an even denominator indicates the possibility of a paired state. Based on such assumption, both Abelian [11,12] and non-Abelian [10,44,45,49] models are proposed to describe the $\nu = 5/2$ FQH state. In all these candidate models, a fundamental quasiparticle charge of $e/4$ is predicted and has been confirmed experimentally by shot-noise measurement [13] and local electrometry [139]. On the other hand, different models have different implications on the topological nature of the quantum liquid.

The physics on the edge of a FQH liquid contains information about the topological order in the bulk. Measurement of edge transport characteristics therefore helps identify the best candidate model for the $\nu = 5/2$ FQH state. In two recent experiments [23, 24], the temperature dependence of tunneling current was measured for quasiparticle tunneling at a quantum point contact (QPC). The seemingly conflicting data were understood after a close look at the effect of electrostatic interaction near the tunneling point (Chapter 2), which provided the support for the Abelian Halperin 331 state and excluded the possibility of the non-Abelian anti-Pfaffian state. This conclusion from the tunneling experiments, however, contradicts the observation [16] of "upstream" neutral edge modes. A common feature of particle-hole conjugate states, the existence of upstream edge modes points to the anti-Pfaffian state as the only probable candidate. All together, none of the existing models is completely satisfactory from experimental point of view.

In this section, we show that a long overlooked simple topological order offers a good phenomenological description of the FQH liquid at filling factor $\nu = 5/2$. By analyzing the electron density profile and the microscopic details of interactions on the edge of the FQH liquid, we argue that the physical degrees of freedom participating in transport are charged and neutral edge modes propagating in opposite directions and at different velocities. The key point in our argument is the existence of two distinct types of interactions on the edge of the FQH liquid: The long-ranged Coulomb interaction between charge densities and the ubiquitous short-ranged interaction between neighboring edge states due to the overlap of electron wave functions. Their difference in interaction range leads to the decoupling and the large velocity difference between charged and neutral edge modes. The separation of charged and neutral degrees of freedom in transport has been observed [140, 141] in the integer quantum Hall regime. Here we extend such a scenario to physics in the second Landau level. With this scenario, we demonstrate that our model reconciles all transport experiments in the $\nu = 5/2$ FQH liquid.

We neglect Landau-level mixing and assume that the physics of the $\nu = 5/2$ FQH liquid is captured by a $\nu = 1/2$ FQH state in the second Landau level. Our model describes an Abelian state formed by condensing charge-$2e$ quasihole excitations of a $\nu = 1$ integer Hall state into a $\nu = 1/4$ Laughlin state. The state is spin-polarized. At low energy, the effective Lagrangian for the bulk is an Abelian Chern-Simons theory,

$$\mathcal{L}_{\text{bulk}} = -\sum_{I,J} \frac{1}{4\pi} K_{IJ} \epsilon_{\mu\nu\lambda} a_{I\mu} \partial_\nu a_{J\lambda} + \sum_I \frac{e}{2\pi} q_I \epsilon_{\mu\nu\lambda} A_\mu \partial_\nu a_{I\lambda}, \tag{4.1}$$

where $K = \left(\begin{smallmatrix} 1 & 2 \\ 2 & -4 \end{smallmatrix}\right)$ and $q = \left(\begin{smallmatrix} 1 \\ 0 \end{smallmatrix}\right)$ are the K matrix and charge vector that characterize the topological order, A_μ is the electromagnetic field and $a_{I\mu}$ are the effective gauge fields describing conserved densities of condensates. The low-energy edge dynamics is dominated by the shape distortion of the incompressible quantum Hall droplet

and is effectively a Luttinger liquid theory with two elementary density modes ϕ_1 and ϕ_2,

$$\mathcal{L}_{\text{edge}} = -\frac{1}{4\pi}\sum_{I,J}[K_{IJ}\partial_t\phi_I\partial_x\phi_J + V_{IJ}\partial_x\phi_I\partial_x\phi_J], \tag{4.2}$$

where $V = \left(\begin{smallmatrix} v_1 & v_{12} \\ v_{12} & v_2 \end{smallmatrix}\right)$. To facilitate later discussion, we make a change of variables to rewrite the edge Lagrangian in terms of the physical charge density mode $\phi_\rho = \phi_1$ and a neutral density mode $\phi_n = -\phi_1 + 2\phi_2$,

$$\begin{aligned}\mathcal{L}_{\text{edge}} = -\frac{1}{4\pi}[&2\partial_t\phi_\rho\partial_x\phi_\rho - \partial_t\phi_n\partial_x\phi_n + 2v_\rho(\partial_x\phi_\rho)^2 \\ &+ v_n(\partial_x\phi_n)^2 + 2v_{\rho n}\partial_x\phi_\rho\partial_x\phi_n],\end{aligned} \tag{4.3}$$

where $v_\rho = \frac{1}{2}v_1 + \frac{1}{8}v_2 + \frac{1}{2}v_{12}$, $v_n = \frac{1}{4}v_2$, and $v_{\rho n} = \frac{1}{4}v_2 + \frac{1}{2}v_{12}$. The physics of $\mathcal{L}_{\text{edge}}$ is nonuniversal because of the nonzero interaction $v_{\rho n}$ between the charged mode ϕ_ρ and the neutral mode ϕ_n.

The three physical parameters $v_\rho, v_n, v_{\rho n}$ have different origins. The charged mode velocity v_ρ is a manifestation of the Coulomb interaction between charged degrees of freedom in the edge channel. Its magnitude is determined by the two electrostatic length scales in the system: the width of the edge channel and the distance from the 2D electron gas to the metallic gate defining the edge. The other two parameters $v_n, v_{\rho n}$, on the other hand, arise from the overlap of nearby electron wave functions. In a FQH system, the pertinent length scale to the size of electron wave packets is the magnetic length. It is useful to compare these length scales. For this end, we recall the physical picture [142] of edge channels in a FQH system. As shown in Fig. 4.1, the edge of the $\nu = 5/2$ FQH liquid is composed of alternating compressible and incompressible liquid strips. The compressible strips are the conductive edge channels while the incompressible strips, occurring when the local electron density reaches integer filling factors, do not contribute to transport. The edge channel in the

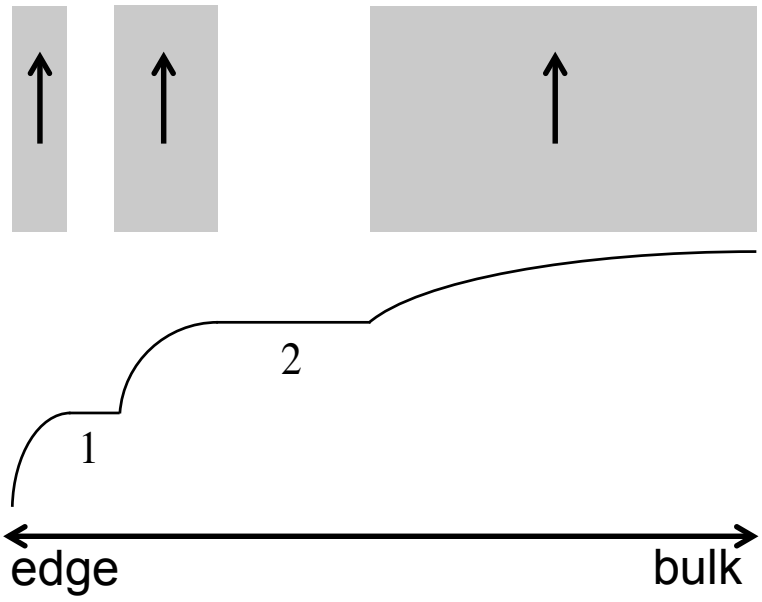

Figure 4.1: Electron density profile on the edge of the $\nu = 5/2$ FQH liquid. Shaded areas are compressible liquid strips contributing to transport. White gaps are incompressible liquid strips at integer filling factors 1 and 2. Arrows follow the direction of charge current. The curve shows local filling factor versus position.

second Landau level is the compressible strip restricted by the incompressible strip at filling factor 2. Its width can be estimated based on an electrostatic argument [99] to be $\sim 10^3$nm for a typical $\nu = 5/2$ FQH state realized at magnetic field $B \sim 5$T, which was the case in the quasiparticle tunneling experiments. The magnetic length under the same experimental conditions is $\sim 10^1$nm, much shorter than the width of the edge channel and the typical distance $\sim 10^2$nm between the FQH liquid and the gate. Hence, we expect that the charged mode velocity v_ρ, set by the electrostatic length scales, is considerably larger than the neutral mode velocity v_n and the interaction strength $v_{\rho n}$, both set by the magnetic length.

Experimental evidence on the ratios between $v_\rho, v_n, v_{\rho n}$ is lacking. However, for the $\nu = 2$ integer Hall state, Refs. [140, 141] concluded that the velocity of the charged edge mode is at least one order of magnitude larger than that of the neutral edge mode and the interaction between two edge modes. Their data also showed an increase of the charged mode velocity as the bulk filling factor grew from $\nu = 2$

to $\nu = 3$, passing the $\nu = 5/2$ plateau. At the same time, the magnetic length remained the same during the variation of the bulk filling factor since the electron density in the bulk did not change. Hence, it is legitimate to assume $v_\rho/v_n \gtrsim 10$ and $v_\rho/v_{\rho n} \gtrsim 10$ for our new $\nu = 5/2$ FQH state, as analytical continuation of the large ratios between parameters in the $\nu = 2$ integer Hall state.

We note that because of the large difference in magnitude between v_ρ and $v_n, v_{\rho n}$, the charged edge mode ϕ_ρ exhibits the features of an independent edge mode, very weakly coupled to the much slower neutral edge mode ϕ_n. The near decoupling of the physical edge modes is consistent with the observation in Ref. [16].

A generic quasiparticle operator on the edge of the $\nu = 5/2$ FQH state in Eqs. (4.2)(4.3) is $O = e^{i[l_1\phi_1 + l_2\phi_2]}$ with electric charge $Q = (\frac{1}{2}l_1 + \frac{1}{4}l_2)e$, where l_1, l_2 are integers. Its scaling dimension Δ can be extracted from the equal-position correlation function $\langle O(x,t)O(x,0)\rangle \sim t^{-2\Delta}$ at zero temperature. With the change of variables $\tilde{\phi}_\rho = \frac{\sqrt{2}}{2}(\sqrt[4]{\frac{1+c}{1-c}} + \sqrt[4]{\frac{1-c}{1+c}})\phi_\rho + \frac{1}{2}(\sqrt[4]{\frac{1+c}{1-c}} - \sqrt[4]{\frac{1-c}{1+c}})\phi_n$ and $\tilde{\phi}_n = \frac{\sqrt{2}}{2}(\sqrt[4]{\frac{1+c}{1-c}} - \sqrt[4]{\frac{1-c}{1+c}})\phi_\rho + \frac{1}{2}(\sqrt[4]{\frac{1+c}{1-c}} + \sqrt[4]{\frac{1-c}{1+c}})\phi_n$, where $c = \frac{\sqrt{2}v_{\rho n}}{v_\rho + v_n}$, we can diagonalize $\mathcal{L}_{\text{edge}}$ and obtain

$$2\Delta = \frac{1}{\sqrt{1-c^2}}[\frac{l_\rho^2}{2} + l_n^2 - \sqrt{2}l_\rho l_n c], \tag{4.4}$$

where $l_\rho = l_1 + \frac{1}{2}l_2$ and $l_n = \frac{1}{2}l_2$. From above discussion on the magnitudes of parameters, $c \approx \frac{1}{10}$. Using the smallness of c, it is easily seen that the most relevant quasiparticle operators correspond to $l_\rho = \pm\frac{1}{2}, l_n = \pm\frac{1}{2}$ and $l_\rho = \pm\frac{1}{2}, l_n = \mp\frac{1}{2}$, or $l_1 = 0, l_2 = \pm 1$ and $l_1 = \pm 1, l_2 = \mp 1$. These quasiparticles all have $e/4$ electric charge (up to a sign), in accordance with experiments [13, 139]. The scaling dimension of the most relevant quasiparticles

$$2\Delta_{\min} = \frac{1}{\sqrt{1-c^2}}[\frac{3}{8} \pm \frac{\sqrt{2}}{4}c] = \frac{3}{8} \pm \frac{\sqrt{2}}{4}c + \frac{3}{16}c^2 \pm \cdots, \tag{4.5}$$

where in the second line we have expanded the prefactor $\frac{1}{\sqrt{1-c^2}} = \sum_{m=0}^{\infty} \frac{(2m-1)!!}{2^m \cdot m!} c^{2m}$. The first term in the expansion agrees with the measured [23, 24] scaling behavior of the zero-bias tunneling conductance G with temperature T in the $\nu = 5/2$ FQH liquid, $G \sim T^{2g-2}$, where the tunneling exponent $g \approx 0.38$. The second term gives the leading order correction $|\delta g| \approx 0.04$ to the tunneling exponent, which is beyond the precision of measurement in the experiments.

So far we have ignored the two integer edge modes in the first Landau level. Like the fractional edge modes ϕ_1, ϕ_2 in the second Landau level, the integer edge modes couple strongly with each other and resolve [140] into charged and neutral edge modes during transport. The integer edge modes are separated from the fractional edge modes by the incompressible liquid strip at filling factor 2. Through Coulomb interaction across the incompressible strip, integer edge modes affect transport in the second Landau level. For example, they modify the scaling dimensions of quasiparticles and their tunneling behaviors at a QPC. In Section 4.2, we show that a moderate interaction between the integer modes and the fractional modes gives rise to a correction to the tunneling exponent that is much smaller than the leading order correction $|\delta g|$. In such a case, the interaction does not change the fact that our new FQH state predicts the correct tunneling exponent.

There is yet another complication in the quasiparticle tunneling experiments [23, 24]. There, the metallic gates used to define the edges of the FQH liquid are Π-shaped (Fig. 2.3), rather than solid slabs of metal. In such a case, quantum Hall edge channels exist inside the metallic gates. The Coulomb interaction between the inner edge channels and the outer edge channels in the Π-shaped gates modifies the scaling dimensions of quasiparticles in the outer edge channels and hence changes the tunneling exponent measured in the experiments. In Section 4.3, we show that this change of the tunneling exponent due to the shape of the devices is negligible.

Experimentally, our new $\nu = 5/2$ FQH state can be identified with the help of an electronic Mach-Zehnder interferometer [61]. The interferometer consists of two QPCs, through which quasiparticles can tunnel and propagate following two electronic paths that differ in quantum phase, defined by the edges of the FQH liquid. The quasiparticles are eventually trapped in the area enclosed by the electronic paths. Interference of quasiparticle wave functions from different paths gives rise to Aharonov-Bohm oscillation in charge current that depends on the magnetic flux passing through the interferometer and the accumulated statistical phase of the trapped quasiparticles.

At low temperature, the most relevant quasiparticles dominate in the interference pattern. In our new $\nu = 5/2$ state, there are two (up to a sign) most relevant quasiparticles, corresponding to $l_1 = 0, l_2 = 1$ and $l_1 = 1, l_2 = -1$. We label them with superscripts a and b. These two quasiparticles can combine to give eight topologically distinct phases in the interferometer. The transition rates among different topological phases due to the tunneling of quasiparticles a or b are

$$p_k^x = A^x[1 + u^x \cos(\frac{\pi}{2}\frac{\Phi}{\Phi_0} + \frac{\pi}{4}k + \delta^x)], \tag{4.6}$$

where Φ_0 is the magnetic flux quantum, Φ/Φ_0 is the number of flux quanta passing through the enclosed area in the interferometer, $x = a, b$ and $k = 0, 1, \ldots, 7$ labels the eight topological phases. The parameters A^x, u^x and δ^x depend on experimental realization of the interferometer, including temperature, the bias voltage and the transmission amplitudes at the two QPCs. The steady charge current reflects the averaged interference pattern over all eight topological phases. At zero temperature and with the assumption that the parameters are symmetric for both flavors of quasiparticles, $A^a = A^b = A$, $u^a = u^b = u$, $\delta^a = \delta^b = \delta$ and $p_k^a = p_k^b = p_k$, it

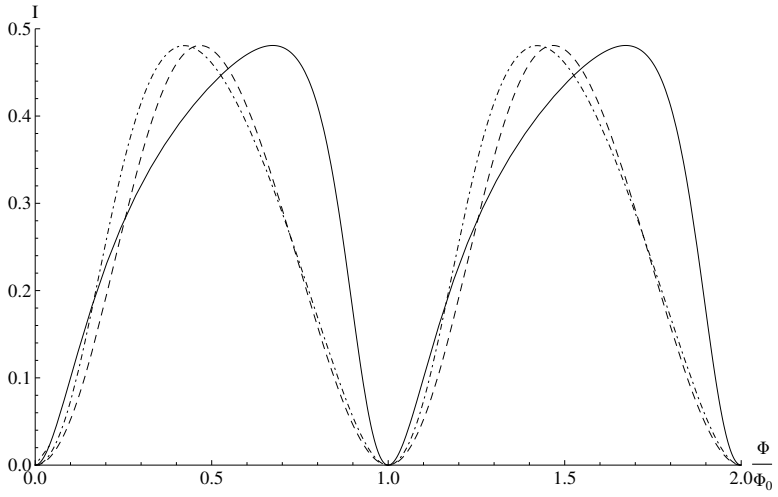

Figure 4.2: Comparison of steady currents in Mach-Zehnder interferometer for various $\nu = 5/2$ quantum Hall states: the Pfaffian state (dotdashed), the 331 state (dashed) and the 113 state (solid). For the 331 state and the 113 state, we assume flavor symmetry and set $u = 1$, $\delta = 0$. The current for the Pfaffian state is acquired from Eq. (8) in Ref. [81], with the setting $r_{11}^{+} = r_{12}^{+} = 1$, $\Gamma_1 = \Gamma_2$. The current for the 331 state is acquired from Eq. (9) in Ref. [102]. We tune the peaks of the currents in different states to the same height for a better comparison.

simplifies to

$$I = 4eA/(4 + \sum_{k=0}^{3} \frac{p_{2k+1}}{p_{2k}}). \tag{4.7}$$

The current in Mach-Zehnder interferometer distinguishes different topological orders proposed for the $\nu = 5/2$ FQH liquid. In Fig. 4.2, we compare the currents in the Pfaffian state, the 331 state and the new $\nu = 5/2$ state, assuming flavor symmetry for the two latter states. The currents in all three states oscillate with the period of a magnetic flux quantum, in agreement with Byers-Yang theorem [143]. Among three states, the current in the 331 state exhibits the most symmetric shape. It is also interesting to look at the current with a varying ratio $\gamma = A^b/A^a$ between the amplitudes of tunneling of two quasiparticles. We show such a situation in Fig. 4.3. An immediate doubling of the period of current is observed at the onset of the tunneling of the second quasiparticle, indicating the paired-state nature of the new $\nu = 5/2$ state.

The steady current I and the shot noise S in Mach-Zehnder interferometer are

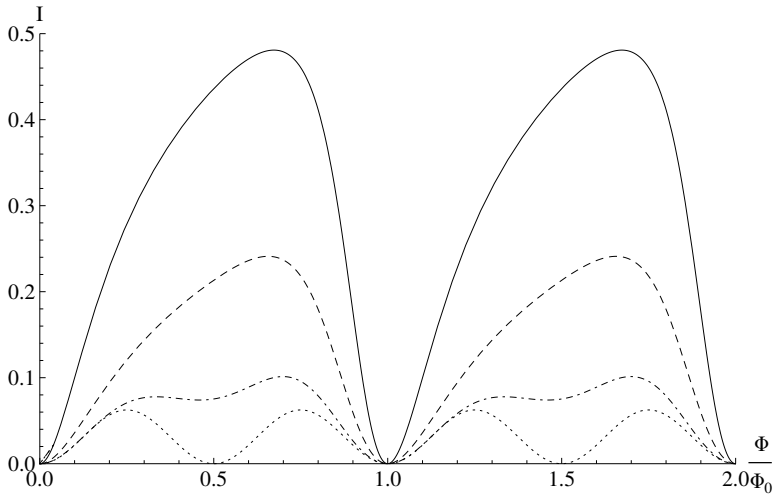

Figure 4.3: Comparison of steady currents in Mach-Zehnder interferometer for different $\gamma = A^b/A^a$ values in the 113 state: $\gamma = 0$ (dotted), $\gamma = 0.05$ (dotdashed), $\gamma = 0.25$ (dashed), and $\gamma = 1$ (solid), where we have set $A^a = 1$, $u^a = u^b = 1$ and $\delta^a = \delta^b = 0$.

related as $S = 2e^*I$, where e^* is the Fano factor. In our new $\nu = 5/2$ state, e^* has an upper bound of $13.6e$, much larger than the upper bound $2.3e$ in the 331 state and the value $3.2e$ in the Pfaffian state. The large Fano factor reflects the excess noise at the two QPCs in the interferometer, due to counter-propagating edge modes participating in the tunneling process.

The spin polarization of the $\nu = 5/2$ FQH liquid has been controversial [17, 19, 20, 144]. Here, we note a spin-unpolarized counterpart of the above-discussed new $\nu = 5/2$ state, described by $K = \left(\begin{smallmatrix} 1 & 3 \\ 3 & 1 \end{smallmatrix}\right)$ and $q = \left(\begin{smallmatrix} 1 \\ 1 \end{smallmatrix}\right)$. Physically, this spin-unpolarized state is formed by topologically coupling one layer of spin-up electrons with another layer of spin-down electrons, both layers in the $\nu = 1$ integer Hall state. These two $\nu = 5/2$ FQH states we have obtained differ in spin wave functions but share the same topological order [5]: The K matrices and charge vectors of the two states are connected by a special linear transformation $U = \left(\begin{smallmatrix} 0 & 1 \\ 1 & -1 \end{smallmatrix}\right)$. For this reason, the two states show identical signatures in transport experiments and cannot be discriminated by a Mach-Zehnder interferometer. We will call our new $\nu = 5/2$ FQH state the 113 state.

In sum, we have proposed a new Abelian description of the FQH state at filling factor $\nu = 5/2$, called the 113 state. The 113 state has the advantage of being compatible with all existing transport experiments. The 113 state assumes quite different signatures in Mach-Zehnder interferometer from the Pfaffian state and the 331 state.

4.2 Influence of integer edge channels

In this section, we consider the interaction between the integer edge modes in the first Landau level and the fractional edge modes in the second Landau level. We show that a moderate interaction gives rise to a correction to the tunneling exponent g that is much smaller than the leading order correction $|\delta g|$ found in Eq. (4.5).

The integer edge modes ϕ_1^o, ϕ_2^o are described by the Lagrangian density

$$\mathcal{L}^o = -\frac{1}{4\pi}[\partial_t\phi_1^o\partial_x\phi_1^o + \partial_t\phi_2^o\partial_x\phi_2^o + u_1(\partial_x\phi_1^o)^2 + u_2(\partial_x\phi_2^o)^2 + 2u_{12}\partial_x\phi_1^o\partial_x\phi_2^o]. \quad (4.8)$$

As illustrated in Fig. 4.1, ϕ_1^o and ϕ_2^o lie in different edge channels separated by the incompressible liquid strip at filling factor 1. By Ref. [99], the width w_1 of this incompressible strip is comparable to the magnetic length. Hence, in reality, ϕ_1^o and ϕ_2^o strongly couple with each other. The physical edge modes participating in transport are the charged mode $\phi_\rho^o = \frac{1}{\sqrt{2}}(\phi_1^o + \phi_2^o)$ and the neutral mode $\phi_n^o = \frac{1}{\sqrt{2}}(\phi_1^o - \phi_2^o)$. ϕ_ρ^o interacts with the charged mode ϕ_ρ in the second Landau level through Coulomb interaction λ_1 across the width w_2 of the incompressible strip at filling factor 2, described by $\mathcal{L}_{\lambda_1} = -\frac{2\lambda_1}{4\pi}\partial_x\phi_1(\partial_x\phi_1^o + \partial_x\phi_2^o) = -\frac{2\sqrt{2}\lambda_1}{4\pi}\partial_x\phi_\rho\partial_x\phi_\rho^o$. After

incorporating $\mathcal{L}^o$ and $\mathcal{L}_{\lambda_1}$, the K matrix and the potential matrix extend to

$$K = \begin{pmatrix} 2 & 0 & 0 & 0 \\ 0 & -1 & 0 & 0 \\ 0 & 0 & 1 & 0 \\ 0 & 0 & 0 & 1 \end{pmatrix} \quad \text{and} \quad V = \begin{pmatrix} 2v_\rho & v_{\rho n} & \sqrt{2}\lambda_1 & 0 \\ v_{\rho n} & v_n & 0 & 0 \\ \sqrt{2}\lambda_1 & 0 & u_\rho & u_{\rho n} \\ 0 & 0 & u_{\rho n} & u_n \end{pmatrix}, \tag{4.9}$$

written in the basis $(\phi_\rho, \phi_n, \phi^o_\rho, \phi^o_n)$, where $u_{\rho,n} = \frac{1}{2}u_1 + \frac{1}{2}u_2 \pm u_{12}$ are the velocities of ϕ^o_ρ, ϕ^o_n, respectively. An estimate based on Ref. [99] gives $w_2/w_1 \approx 4$. Hence, we expect that the inter-Landau-level Coulomb interaction λ_1 is weaker than the Coulomb interactions v_ρ, u_ρ within the Landau levels. This is guaranteed by the stability condition $\lambda_1^2 < v_\rho u_\rho$ and the assumption that the charge velocities in the first and the second Landau levels are comparable: $v_\rho \approx u_\rho$. Also, we assume that $u_{\rho n} \approx u_n \approx v_{\rho n} \approx v_n$, since the magnitudes of these parameters are all set by the magnetic length. Let us define $c_1 = \frac{\lambda_1}{v_\rho} \approx \frac{\lambda_1}{u_\rho}$ to be ratio which characterizes the strength of Coulomb interaction λ_1. The stability condition can be written as $c_1 < 1$.

We want to compute the tunneling exponent, or equivalently, twice the scaling dimension of the most relevant quasiparticle operators, in the presence of Coulomb interaction λ_1. Hence, we need to simultaneously diagonalize the K matrix and the potential matrix in Eq. (4.9). Let us first diagonalize the two matrices in subspaces (ϕ_ρ, ϕ_n) and (ϕ^o_ρ, ϕ^o_n). This is done using the change of variables that led to Eq. (4.4), $\tilde{\phi}_\rho = \sqrt{2}\cosh\theta\phi_\rho + \sinh\theta\phi_n$, $\tilde{\phi}_n = \sqrt{2}\sinh\theta\phi_\rho + \cosh\theta\phi_n$, where $\tanh 2\theta = \frac{\sqrt{2}v_{\rho n}}{v_\rho + v_n} = c \approx \frac{1}{10}$, and the rotation: $\tilde{\phi}^o_\rho = \cos\varphi\phi^o_\rho + \sin\varphi\phi^o_n$, $\tilde{\phi}^o_n = -\sin\varphi\phi^o_\rho + \cos\varphi\phi^o_n$, where

$\tan 2\varphi = \frac{2u_{\rho n}}{u_\rho - u_n} \ll 1$. Then,

$$K = \begin{pmatrix} 1 & 0 & 0 & 0 \\ 0 & -1 & 0 & 0 \\ 0 & 0 & 1 & 0 \\ 0 & 0 & 0 & 1 \end{pmatrix} \tag{4.10}$$

and

$$V = \begin{pmatrix} \tilde{v}_\rho & 0 & \lambda_1 \cosh\theta \cos\varphi & -\lambda_1 \cosh\theta \sin\varphi \\ 0 & \tilde{v}_n & -\lambda_1 \sinh\theta \cos\varphi & \lambda_1 \sinh\theta \sin\varphi \\ \lambda_1 \cosh\theta \cos\varphi & -\lambda_1 \sinh\theta \cos\varphi & \tilde{u}_\rho & 0 \\ -\lambda_1 \cosh\theta \sin\varphi & \lambda_1 \sinh\theta \sin\varphi & 0 & \tilde{u}_n \end{pmatrix} \tag{4.11}$$

in the basis $(\tilde{\phi}_\rho, \tilde{\phi}_n, \tilde{\phi}^o_\rho, \tilde{\phi}^o_n)$. The velocities $\tilde{u}_\rho = \frac{1}{\cos 2\varphi}(\cos^2\varphi u_\rho - \sin^2\varphi u_n)$, $\tilde{u}_n = \frac{1}{\cos 2\varphi}(\cos^2\varphi u_n - \sin^2\varphi u_\rho)$, $\tilde{v}_\rho = \frac{1}{\cosh 2\theta}(\cosh^2\theta v_\rho - \sinh^2\theta v_n)$, $\tilde{v}_n = \frac{1}{\cosh 2\theta}(\cosh^2\theta v_n - \sinh^2\theta v_\rho)$. By smallness of c, we know that θ and φ are both very small angles such that $\sinh^2\theta \ll 1$ and $\sin^2\varphi \ll 1$. Hence, $\tilde{v}_\rho \approx v_\rho \approx u_\rho \approx \tilde{u}_\rho$ and $\tilde{v}_n \approx v_n \approx u_n \approx \tilde{u}_n$. Also, $c_1 = \frac{\lambda_1}{v_\rho} \approx \frac{\lambda_1}{u_\rho} \approx \frac{\lambda_1}{\tilde{v}_\rho} \approx \frac{\lambda_1}{\tilde{u}_\rho}$. To simplify the discussion, we set in the following: $\tilde{u}_\rho \to \tilde{v}_\rho$ and $\tilde{u}_n \to \tilde{v}_n$.

Next, we diagonalize the subspace $(\tilde{\phi}_\rho, \tilde{\phi}^o_\rho)$ by defining $\Phi_\pm = \frac{1}{\sqrt{2}}(\tilde{\phi}_\rho \pm \tilde{\phi}^o_\rho)$. In the basis $(\Phi_+, \tilde{\phi}_n, \Phi_-, \tilde{\phi}^o_n)$, the K matrix remains unchanged while the potential matrix

$$V = \begin{pmatrix} V_+ & -a_1 & 0 & -a_2 \\ -a_1 & \tilde{v}_n & a_1 & a_3 \\ 0 & a_1 & V_- & -a_2 \\ -a_2 & a_3 & -a_2 & \tilde{v}_n \end{pmatrix}, \tag{4.12}$$

where $V_\pm = \tilde{v}_\rho(1 \pm \frac{\lambda_1 \cosh\theta\cos\varphi}{\tilde{v}_\rho}) \approx \tilde{v}_\rho(1 \pm \frac{\lambda_1}{\tilde{v}_\rho}) \approx \tilde{v}_\rho(1 \pm c_1)$, $a_1 = \frac{1}{\sqrt{2}}\lambda_1 \sinh\theta\cos\varphi$, $a_2 = \frac{1}{\sqrt{2}}\lambda_1 \cosh\theta\sin\varphi$ and $a_3 = \lambda \sinh\theta\sin\varphi$. $V_+ \gg \tilde{v}_n$. The generic quasiparticle operator can be written as

$$e^{i[l_1\phi_1 + l_2\phi_2]} = e^{i[l_\rho\phi_\rho + l_n\phi_n]} = e^{i[\tilde{l}_\rho\tilde{\phi}_\rho + \tilde{l}_n\tilde{\phi}_n]} = e^{i[\frac{1}{\sqrt{2}}\tilde{l}_\rho(\Phi_+ + \Phi_-) + \tilde{l}_n\tilde{\phi}_n]}, \tag{4.13}$$

where $l_\rho = l_1 + \frac{l_2}{2}$, $l_n = \frac{l_2}{2}$, $\tilde{l}_\rho = \frac{l_\rho}{\sqrt{2}}\cosh\theta - l_n \sinh\theta$ and $\tilde{l}_n = l_n \cosh\theta - \frac{l_\rho}{\sqrt{2}}\sinh\theta$.

Let us set $a_1 = a_2 = a_3 = 0$ for now to compute the scaling dimension Δ' of the generic quasiparticle in Eq. (4.13). One finds that $\Delta' = \Delta$ such that $\Delta'_{\min} = \Delta_{\min}$, where $\Delta'_{\min}$ is the scaling dimension of the most relevant quasiparticles and $\Delta, \Delta_{\min}$ are given in Eqs. (4.4)(4.5). We refer to the difference $2\Delta'_{\min} - 2\Delta_{\min}$ as the "zeroth-generation" correction to the tunneling exponent, due to the interaction λ_1 between integer modes and fractional modes. We see it is zero. For higher-generation corrections, we consider the off-diagonal elements a_1, a_2, a_3.

The term $a_1 = \frac{1}{\sqrt{2}}\lambda_1 \sinh\theta\cos\varphi$ couples the fields Φ_+ and $\tilde{\phi}_n$. If we want to remove this coupling, we need to "rotate" the two fields by an angle η: $\Phi_+ \to \cosh\eta\Phi_+ + \sinh\eta\tilde{\phi}_n$, $\tilde{\phi}_n \to \sinh\eta\Phi_+ + \cosh\eta\tilde{\phi}_n$, where

$$\begin{aligned}
\sinh\eta \approx \frac{1}{2}\tanh 2\eta &= -\frac{1}{\sqrt{2}}\frac{\lambda}{V_+ + \tilde{v}_n}\sinh\theta\cos\varphi \approx -\frac{1}{\sqrt{2}}\frac{\lambda}{V_+}\sinh\theta\cos\varphi \\
&\approx -\frac{1}{\sqrt{2}}\frac{\lambda}{\tilde{v}_\rho}\frac{1}{1+c_1}\sinh\theta\cos\varphi \\
&\approx -\frac{1}{2\sqrt{2}}\frac{c_1}{1+c_1}c,
\end{aligned} \tag{4.14}$$

where we have used $V_+ \approx \tilde{v}_\rho(1+c_1) \gg \tilde{v}_n$, $\frac{\lambda}{\tilde{v}_\rho} \approx c_1$, $\sinh\theta \approx \frac{1}{2}\tanh 2\theta \approx \frac{1}{2}c$ and $\cos\varphi \approx 1$. By $c_1 > 0$, we know η is a very small angle. Let us study how this "rotation" affects the tunneling exponent (or $2\Delta_{\min}$). We consider the "first-generation" correction due to this "rotation" by setting all off-diagonal elements in

Eq. (4.12) to zero, except this coupling between Φ_+ and $\tilde{\phi}_n$. The leading order terms come from the cross terms in the square of the prefactor of Φ_+ and the square of the prefactor of $\tilde{\phi}_n$, after the "rotation". The two cross terms both equal $-\frac{1}{\sqrt{2}}\tilde{l}_\rho\tilde{l}_n\sinh 2\eta$. Consider one of the four most relevant quasiparticle operators in the 113 state, defined by $l_\rho = l_n = \frac{1}{2}$ (see Section 4.1). We have $\tilde{l}_\rho = \frac{1}{2\sqrt{2}}\cosh\theta - \frac{1}{2}\sinh\theta \approx \frac{1}{2\sqrt{2}}$ and $\tilde{l}_n = \frac{1}{2}\cosh\theta - \frac{1}{2\sqrt{2}}\sinh\theta \approx \frac{1}{2}$, using $\sinh\theta \approx \frac{c}{2} \ll 1, \cosh\theta \approx 1$. Then, $-\frac{1}{\sqrt{2}}\tilde{l}_\rho\tilde{l}_n\sinh 2\eta \approx -\frac{1}{8}\sinh 2\eta \approx -\frac{1}{4}\sinh\eta \approx \frac{1}{8\sqrt{2}}\frac{c_1}{1+c_1}c$. The two cross terms add up to the leading order term $\approx \frac{1}{4\sqrt{2}}\frac{c_1}{1+c_1}c < \frac{1}{4\sqrt{2}}c$ in the "first-generation" correction.

a_1 also couples the fields Φ_- and $\tilde{\phi}_n$. The "rotation" needed to remove this coupling is: $\Phi_- \to \cosh\eta'\Phi_- + \sinh\eta'\tilde{\phi}_n$, $\tilde{\phi}_n \to \sinh\eta'\Phi_- + \cosh\eta'\tilde{\phi}_n$, where

$$\begin{aligned}\sinh\eta' \approx \frac{1}{2}\tanh 2\eta' &= \frac{1}{\sqrt{2}}\frac{\lambda}{V_- + \tilde{v}_n}\sinh\theta\cos\varphi \approx \frac{1}{\sqrt{2}}\frac{\lambda}{\tilde{v}_\rho}\frac{1}{1-c_1+\tilde{v}_n/\tilde{v}_\rho}\sinh\theta\cos\varphi \\ &\approx \frac{1}{2\sqrt{2}}\frac{c_1}{1-c_1+c}c, \end{aligned} \tag{4.15}$$

where we have used $V_- \approx \tilde{v}_\rho(1-c_1)$, $\frac{\lambda}{\tilde{v}_\rho} \approx c_1$, $\frac{v_n}{v_\rho} \approx \frac{\tilde{v}_n}{\tilde{v}_\rho} \approx c$, $\sinh\theta \approx \frac{1}{2}c$ and $\cos\varphi \approx 1$. Two extreme cases are interesting. For weak Coulomb interaction λ_1 such that $1-c_1 \gg c \approx \frac{1}{10}$, we have $\sinh\eta' \approx \frac{1}{2\sqrt{2}}\frac{c_1}{1-c_1}c$. On the other hand, for very strong λ_1 such that $1-c_1 \ll c \approx \frac{1}{10}$, we have $\sinh\eta' \approx \frac{1}{2\sqrt{2}}\frac{c_1}{c}c = \frac{1}{2\sqrt{2}}c_1$. The "rotation" gives rise to a leading order term $-\sqrt{2}\tilde{l}_\rho\tilde{l}_n\sinh 2\eta' \approx -\frac{1}{2}\sinh\eta'$ in the "first-generation" correction, using $\tilde{l}_\rho \approx \frac{1}{2\sqrt{2}}$ and $\tilde{l}_n \approx \frac{1}{2}$. This term $\approx -\frac{1}{4\sqrt{2}}\frac{c_1}{1-c_1}c$ for $1-c_1 \gg c$ and $\approx -\frac{1}{4\sqrt{2}}c_1$ for $1-c_1 \ll c$.

In the potential matrix in Eq. (4.12), a_1 couples Φ_+, $\tilde{\phi}_n$ and Φ_-, $\tilde{\phi}_n$ at the same time. As a result, "second-generation" corrections arise from the combination of two a_1 couplings, in addition to the "first-generation" corrections, even if we assume $a_2 = a_3 = 0$. These "second-generation" corrections are however negligible. To see this, imagine we first make the "rotation" by η and then the "rotation" by η'. After

the first "rotation" which generates the "first-generation" correction discussed after Eq. (4.14), $\tilde{\phi}_n$ is almost unchanged, since the angle η is very small. Hence, to a good approximation, we assume that the fields participating in the second "rotation" are Φ_- and $\tilde{\phi}_n$, which produce the "first-generation" correction discussed after Eq. (4.15). The total correction due to a_1, assuming $a_2 = a_3 = 0$, is the sum of the two "first-generation" corrections, up to an negligible error. In the limit that $1 - c_1 \gg c \approx \frac{1}{10}$, the sum is

$$-\frac{1}{4\sqrt{2}}(\frac{c_1}{1-c_1} - \frac{c_1}{1+c_1})c = -\frac{\sqrt{2}}{4}c \times \frac{c_1^2}{1-c_1^2}, \tag{4.16}$$

which is much smaller than the leading order correction $|\delta g| \approx \frac{\sqrt{2}}{4}c$ in Eq. (4.5), due to the small factor $\frac{c_1^2}{1-c_1^2}$. On the other hand, in the unlikely case that $1-c_1 \ll c \approx \frac{1}{10}$, $c_1 \approx 1$, the sum is

$$-\frac{1}{4\sqrt{2}}(1 - \frac{c}{1+c_1})c_1 \approx -\frac{1}{4\sqrt{2}}c_1 \approx -\frac{\sqrt{2}}{4}c \times \frac{c_1}{2c}. \tag{4.17}$$

Using $c_1 \approx 1, c \approx \frac{1}{10}$, the factor $\frac{c_1}{2c} \approx 5$. Hence, for extremely strong Coulomb interaction λ_1, the correction to the tunneling exponent due to a_1 can be as large as $5 \times |\delta g| \approx \frac{5\sqrt{2}}{4}c$. This destroys our claim that the 113 state predicts the correction tunneling exponent ≈ 0.38 measured in the experiments. Certainly, neither of the above extreme cases is practical. The more likely case is a moderate Coulomb interaction λ_1, for example $c_1 \approx 0.5$. In such a case, Eq. (4.16) is applicable. We find that the correction due to a_1 couplings is much smaller than $|\delta g| \approx \frac{\sqrt{2}}{4}c$.

The off-diagonal elements a_2, a_3 couple Φ_+ with $\tilde{\phi}_n^o$, Φ_- with $\tilde{\phi}_n^o$, and $\tilde{\phi}_n$ with $\tilde{\phi}_n^o$, respectively. For all of these couplings, the "first-generation" corrections are quadratic in c. This is because the field $\tilde{\phi}_n^o$ does not show up in the definition of quasiparticle operators, Eq. (4.13). In general, the combination of a_2, a_3 with a_1 may generate negligible "higher-generation" corrections.

In conclusion, for a moderate interaction between the integer edge modes in the first Landau level and the fractional edge modes in the second Landau level, the correction to the tunneling exponent is much smaller than the leading order correction $|\delta g|$ in Eq. (4.5).

4.3 The Π-shaped gate

In this section, we consider quasiparticle tunneling between two Π-shaped gates. We show that the interaction between the inner edge channels and the outer edge channels in the Π-shaped gates gives a correction to the tunneling exponent g that is much smaller than the leading order correction $|\delta g| \approx 0.04$ found in Eq. (4.5). This correction does not change the fact that the 113 state predicts the correct tunneling exponent $g \approx 0.38$ measured in the quasiparticle tunneling experiments.

Our argument parallels the logic of the discussion of integer edge modes in Section 4.2, with slight changes in the details.

We start by writing down the K matrix and the potential matrix, including both the outer and the inner edge channels in a Π-shaped gate, as well as their interactions. We will study the two models discussed in Subsection 2.4.3. Model 1 includes both integer edge modes and fractional edge modes, while model 2 only includes fractional edge modes. We first consider model 2, and then model 1.

Model 2

We assume that the inner edge channels are an identical copy of the outer edge channels. In model 2, the Coulomb interaction between the inner channels and the outer channels is described by a term $\mathcal{L}_\lambda = -\frac{4\lambda}{4\pi}\partial_x\phi_{\rho O}\partial_x\phi_{\rho I}$ in the Lagrangian density, where $\phi_{\rho O}$ and $\phi_{\rho I}$ are the charged modes in the outer and inner edge channels, respectively. The K matrix and the potential matrix are

$$K = \begin{pmatrix} 2 & 0 & 0 & 0 \\ 0 & -1 & 0 & 0 \\ 0 & 0 & -2 & 0 \\ 0 & 0 & 0 & 1 \end{pmatrix} \quad \text{and} \quad V = \begin{pmatrix} 2v_\rho & v_{\rho n} & 2\lambda & 0 \\ v_{\rho n} & v_n & 0 & 0 \\ 2\lambda & 0 & 2v_\rho & v_{\rho n} \\ 0 & 0 & v_{\rho n} & v_n \end{pmatrix}, \tag{4.18}$$

written in the basis $(\phi_{\rho O}, \phi_{nO}, \phi_{\rho I}, \phi_{nI})$, where the parameters $v_\rho, v_n, v_{\rho n}$ are defined after Eq. (4.3). To simplify the notation, let us define $c' = \frac{\lambda}{v_\rho}$ to be the ratio which characterizes the strength of Coulomb interaction λ. Stability condition requires $c' < 1$. In Subsection 2.4.3, we estimated $c' \approx 0.45$ for model 2.

The tunneling exponent between two Π-shaped gates is simply twice the scaling dimension of the most relevant quasiparticles in the outer edge channels. To compute it, we need to simultaneously diagonalize the K matrix and the potential matrix in Eq. (4.18). We first diagonalize the two matrices in subspace $(\phi_{\rho O}, \phi_{nO})$ and subspace $(\phi_{\rho I}, \phi_{nI})$. This can be done by the change of variables introduced before Eq. (4.4),

$$\begin{aligned} \tilde{\phi}_{\rho O,\rho I} &= \sqrt{2}\cosh\theta\phi_{\rho O,\rho I} + \sinh\theta\phi_{nO,nI} \\ \tilde{\phi}_{nO,nI} &= \sqrt{2}\sinh\theta\phi_{\rho O,\rho I} + \cosh\theta\phi_{nO,nI}, \end{aligned} \tag{4.19}$$

where $\tanh 2\theta = c = \frac{\sqrt{2}v_{\rho n}}{v_\rho + v_n} \approx \frac{1}{10}$. By smallness of c, we know θ is a very small angle

such that $\sinh\theta \approx \tanh\theta \approx \frac{1}{2}\tanh 2\theta = \frac{1}{2}c$. After the change of variables,

$$K = \begin{pmatrix} 1 & 0 & 0 & 0 \\ 0 & -1 & 0 & 0 \\ 0 & 0 & -1 & 0 \\ 0 & 0 & 0 & 1 \end{pmatrix} \tag{4.20}$$

and

$$V = \begin{pmatrix} \tilde{v}_\rho & 0 & \lambda\cosh^2\theta & -\frac{1}{2}\lambda\sinh 2\theta \\ 0 & \tilde{v}_n & -\frac{1}{2}\lambda\sinh 2\theta & \lambda\sinh^2\theta \\ \lambda\cosh^2\theta & -\frac{1}{2}\lambda\sinh 2\theta & \tilde{v}_\rho & 0 \\ -\frac{1}{2}\lambda\sinh 2\theta & \lambda\sinh^2\theta & 0 & \tilde{v}_n \end{pmatrix} \tag{4.21}$$

in the basis $(\tilde{\phi}_{\rho O}, \tilde{\phi}_{nO}, \tilde{\phi}_{\rho I}, \tilde{\phi}_{nI})$, where $\tilde{v}_\rho = \frac{1}{\cosh 2\theta}(\cosh^2\theta v_\rho - \sinh^2\theta v_n)$, $\tilde{v}_n = \frac{1}{\cosh 2\theta}(\cosh^2\theta v_n - \sinh^2\theta v_\rho)$. Since $\sinh^2\theta \approx \frac{1}{4}c^2 \ll 1$, we know that $\tilde{v}_\rho \approx v_\rho$, $\tilde{v}_n \approx v_n$ so that $\tilde{v}_\rho \gg \tilde{v}_n$. Also, $c' = \frac{\lambda}{v_\rho} \approx \frac{\lambda}{\tilde{v}_\rho}$.

Next, we diagonalize the subspace $(\tilde{\phi}_{\rho O}, \tilde{\phi}_{\rho I})$ by the change of variables: $\Phi_{\rho 1} = \cosh\beta\tilde{\phi}_{\rho O} + \sinh\beta\tilde{\phi}_{\rho I}$ and $\Phi_{\rho 2} = \sinh\beta\tilde{\phi}_{\rho O} + \cosh\beta\tilde{\phi}_{\rho I}$, where $\tanh 2\beta = \frac{\lambda\cosh^2\theta}{\tilde{v}_\rho} \approx \frac{\lambda}{\tilde{v}_\rho} \approx c'$, since $\cosh^2\theta \approx 1$. Using $c' \approx 0.45$, we find $2\beta \approx 0.4847$ such that $\sinh\beta \approx 0.245$, $\cosh\beta \approx 1.03$, $\sinh 2\beta \approx 0.504$ and $\cosh 2\beta \approx 1.12$.

In the basis $(\Phi_{\rho 1}, \tilde{\phi}_{nO}, \Phi_{\rho 2}, \tilde{\phi}_{nI})$, the K matrix remains unchanged while the potential matrix

$$V = \begin{pmatrix} V_\rho & b_2 & 0 & b_1 \\ b_2 & \tilde{v}_n & b_1 & b_3 \\ 0 & b_1 & V_\rho & b_2 \\ b_1 & b_3 & b_2 & \tilde{v}_n \end{pmatrix}, \tag{4.22}$$

where $V_\rho = \frac{1}{\cosh 2\beta}\tilde{v}_\rho \approx 0.9\tilde{v}_\rho \gg \tilde{v}_n$, $b_1 = -\frac{1}{2}\lambda \sinh 2\theta \cosh\beta$, $b_2 = \frac{1}{2}\lambda \sinh 2\theta \sinh\beta$ and $b_3 = \lambda \sinh^2\theta$. The generic quasiparticle operator can be written as

$$e^{i[l_1\phi_1 + l_2\phi_2]} = e^{i[l_\rho\phi_{\rho O} + l_n\phi_{nO}]} = e^{i[\tilde{l}_\rho\tilde{\phi}_{\rho O} + \tilde{l}_n\tilde{\phi}_{nO}]} = e^{i[\tilde{l}_\rho \cosh\beta\Phi_{\rho 1} - \tilde{l}_\rho \sinh\beta\Phi_{\rho 2} + \tilde{l}_n\tilde{\phi}_{nO}]}, \quad (4.23)$$

where $l_\rho = l_1 + \frac{l_2}{2}$, $l_n = \frac{l_2}{2}$, $\tilde{l}_\rho = \frac{l_\rho}{\sqrt{2}}\cosh\theta - l_n \sinh\theta$ and $\tilde{l}_n = l_n \cosh\theta - \frac{l_\rho}{\sqrt{2}}\sinh\theta$.

At this point, we set $b_1 = b_2 = b_3 = 0$ in the potential matrix to compute the scaling dimension Δ'' of the generic quasiparticle in Eq. (4.23). Later, we will consider the corrections due to these off-diagonal elements. We have

$$\begin{aligned} 2\Delta'' &= \tilde{l}_\rho^2(\cosh^2\beta + \sinh^2\beta) + \tilde{l}_n^2 \\ &= 2\Delta + \tilde{l}_\rho^2(\cosh 2\beta - 1) \\ &\approx 2\Delta + 0.12\tilde{l}_\rho^2, \end{aligned} \quad (4.24)$$

where $2\Delta = \tilde{l}_\rho^2 + \tilde{l}_n^2$ by Eq. (4.4). As discussed in Section 4.1, the four most relevant quasiparticles correspond to $l_\rho = \pm\frac{1}{2}, l_n = \pm\frac{1}{2}$ and $l_\rho = \pm\frac{1}{2}, l_n = \mp\frac{1}{2}$. We pick one of these quasiparticles, defined by $l_\rho = l_n = \frac{1}{2}$, and evaluate its scaling dimension $\Delta''_{\min}$. We have $\tilde{l}_\rho = \frac{1}{2\sqrt{2}}\cosh\theta - \frac{1}{2}\sinh\theta$ and $\tilde{l}_n = \frac{1}{2}\cosh\theta - \frac{1}{2\sqrt{2}}\sinh\theta$. Hence,

$$\begin{aligned} 2\Delta''_{\min} &= 2\Delta_{\min} + 0.12\left(\frac{1}{8}\cosh 2\theta + \frac{1}{8}\sinh^2\theta - \frac{1}{4\sqrt{2}}\sinh 2\theta\right) \\ &\approx 2\Delta_{\min} + 0.12\left(\frac{1}{8} - \frac{1}{4\sqrt{2}}c\right) \\ &\approx 2\Delta_{\min} + 0.015 - 0.021c \\ &\approx 2\Delta_{\min} + 0.013, \end{aligned} \quad (4.25)$$

where $2\Delta_{\min}$ is given in Eq. (4.5) by picking up the minus sign. We have ignored the terms that are quadratic or of higher orders in c by taking the limit $\sinh 2\theta =$

$\frac{c}{\sqrt{1-c^2}} \to c$, $\cosh 2\theta = \frac{1}{\sqrt{1-c^2}} \to 1$, $\sinh^2\theta \approx \frac{c^2}{4} \to 0$. In the last line, we set explicitly $c = \frac{1}{10}$. We refer to the difference $2\Delta''_{\min} - 2\Delta_{\min} \approx 0.013$ as the "zeroth-generation" correction to the tunneling exponent, due to the shape of the Π-gates.

Now, we study the corrections to the tunneling exponent (or to $2\Delta''_{\min}$) due to the off-diagonal elements b_1, b_2, b_3 in Eq. (4.22).

The term $b_1 = -\frac{1}{2}\lambda \sinh 2\theta \cosh\beta$ couples the fields $\Phi_{\rho 2}$ and $\tilde{\phi}_{nO}$. If we were to remove this coupling, we must rotate the two fields by a small angle γ: $\Phi_{\rho 2} \to \cos\gamma\Phi_{\rho 2} + \sin\gamma\tilde{\phi}_{nO}$, $\tilde{\phi}_{nO} \to -\sin\gamma\Phi_{\rho 2} + \cos\gamma\tilde{\phi}_{nO}$, where

$$\begin{aligned}
\sin\gamma \approx \frac{1}{2}\tan 2\gamma &= -\frac{1}{2}\frac{\lambda}{V_\rho - \tilde{v}_n}\cosh\beta\sinh 2\theta \approx -\frac{1}{2}\frac{\lambda}{V_\rho}\cosh\beta\sinh 2\theta \\
&= -\frac{1}{2}\frac{\lambda}{\tilde{v}_\rho}\cosh 2\beta\cosh\beta\sinh 2\theta \\
&= -\frac{1}{2}\sinh 2\beta\cosh\beta\sinh 2\theta \\
&\approx -0.26c, \qquad (4.26)
\end{aligned}$$

where we have used $V_\rho = \frac{1}{\cosh 2\beta}\tilde{v}_\rho \approx 0.9\tilde{v}_\rho \gg \tilde{v}_n$, $\tanh 2\beta \approx \frac{\lambda}{\tilde{v}_\rho} \approx c'$, $\sinh 2\theta \approx c$ and the numerical value of β. How does this rotation affect $2\Delta''_{\min}$? The leading order correction comes from the cross terms in the square of the prefactor of $\Phi_{\rho 2}$ and the square of the prefactor of $\tilde{\phi}_{nO}$, after the rotation. By Eq. (4.23), the two cross terms both equal $\tilde{l}_\rho \tilde{l}_n \sinh\beta \sin 2\gamma$, up to a sign. Consider the most relevant quasiparticle $l_\rho = l_n = \frac{1}{2}$. We have $\tilde{l}_\rho = \frac{1}{2\sqrt{2}}\cosh\theta - \frac{1}{2}\sinh\theta \approx \frac{1}{2\sqrt{2}}$ and $\tilde{l}_n = \frac{1}{2}\cosh\theta - \frac{1}{2\sqrt{2}}\sinh\theta \approx \frac{1}{2}$, using $\sinh\theta \approx \frac{c}{2} \ll 1, \cosh\theta \approx 1$. Hence, $\tilde{l}_\rho\tilde{l}_n \sinh\beta\sin 2\gamma \approx 2\tilde{l}_\rho\tilde{l}_n \sinh\beta\sin\gamma \approx \frac{0.245}{2\sqrt{2}}\sin\gamma \approx -0.023c \approx -0.002$. Moreover, one can show that the two cross terms are actually opposite in sign. Hence, the "first-generation" correction, due to solely the coupling between $\Phi_{\rho 2}$ and $\tilde{\phi}_{nO}$, vanishes. (This is expected since the coupled two modes $\Phi_{\rho 2}$ and $\tilde{\phi}_{nO}$ propagate in the same direction and both appear in the

definition of a quasiparticle operator, Eq. (4.23)). Certainly, there may be "second-generation" corrections, linear in $\sin\gamma \propto c$, due to the combination of this coupling with other off-diagonal elements in Eq. (4.22). But their magnitudes cannot exceed the upper bound $|\tilde{l}_\rho \tilde{l}_n \sinh\beta \sin 2\gamma| \approx 0.002$, set by the magnitude of the cross terms in the "first-generation" correction.

We note that b_1 also couples the fields $\Phi_{\rho 1}$ and $\tilde{\phi}_{nI}$. The fact that $\tilde{\phi}_{nI}$ does not show up in the definition of a quasiparticle operator, Eq. (4.23), means that the "first-generation" correction due to solely this coupling does not contain terms linear in $\sin\gamma \propto c$. Taking into account all off-diagonal elements in Eq. (4.22), "second-generation" corrections linear in $\sin\gamma \propto c$ may be generated, whose magnitudes are subject to the upper bound $|\tilde{l}_\rho \tilde{l}_n \sinh\beta \sin 2\gamma| \approx 0.002$.

The term $b_2 = \frac{1}{2}\lambda \sinh 2\theta \sinh\beta$ couples the fields $\Phi_{\rho 1}$ and $\tilde{\phi}_{nO}$. One needs to "rotate" the two fields by a small angle γ', $\Phi_{\rho 1} \to \cosh\gamma' \Phi_{\rho 1} + \sinh\gamma' \tilde{\phi}_{nO}$, $\tilde{\phi}_{nO} \to \sinh\gamma' \Phi_{\rho 1} + \cosh\gamma' \tilde{\phi}_{nO}$, where

$$\begin{aligned}
\sinh\gamma' \approx \frac{1}{2}\tanh 2\gamma' &= \frac{1}{2}\frac{\lambda}{V_\rho + \tilde{v}_n}\sinh\beta \sinh 2\theta \approx \frac{1}{2}\frac{\lambda}{V_\rho}\sinh\beta \sinh 2\theta \\
&= \frac{1}{2}\frac{\lambda}{\tilde{v}_\rho}\cosh 2\beta \sinh\beta \sinh 2\theta \\
&= \frac{1}{2}\sinh 2\beta \sinh\beta \sinh 2\theta \\
&\approx 0.062c, \qquad (4.27)
\end{aligned}$$

to remove this coupling. There are two cross terms in the square of the prefactor of $\Phi_{\rho 1}$ and the square of the prefactor of $\tilde{\phi}_{nO}$, after the rotation. The two terms are equal in magnitude and have the same sign. They add up to the leading order term $\approx -2\tilde{l}_\rho \tilde{l}_n \cosh\beta \sinh 2\gamma' \approx -\frac{1.03}{\sqrt{2}} \sinh\gamma' \approx -0.005$ in the "first-generation" correction, which balances the positive "zeroth-generation" correction in Eq. (4.25).

b_2 also couples the fields $\Phi_{\rho 2}$ and $\tilde{\phi}_{nI}$. Terms in the resulting "first-generation" correction are at most quadratic in $\sinh\gamma' \propto c$, again since $\tilde{\phi}_{nI}$ does not appear in the definition of a quasiparticle operator.

The term $b_3 = \lambda \sinh^2\theta$ mixes the fields $\tilde{\phi}_{nO}, \tilde{\phi}_{nI}$ with each other by small parts

$$\sinh\gamma'' \approx \frac{1}{2}\tanh 2\gamma'' = \frac{1}{2}\frac{\lambda}{\tilde{v}_n}\sinh^2\theta \approx \frac{1}{8}\frac{\lambda}{\tilde{v}_n}c^2 \approx \frac{1}{8}\frac{\lambda}{\tilde{v}_\rho}\frac{\tilde{v}_\rho}{\tilde{v}_n}c^2 \approx \frac{1}{8}c'c \approx 0.056c, \quad (4.28)$$

where we have used $\sinh^2\theta \approx \frac{c^2}{4}$, $\frac{1}{c} \approx \frac{v_\rho}{v_n} \approx \frac{\tilde{v}_\rho}{\tilde{v}_n}$ and $c' \approx \frac{\lambda}{\tilde{v}_\rho} \approx 0.45$. The leading order term in the "first-generation" correction is quadratic in $\sinh\gamma'' \propto c$. In general, there may be "second-generation" corrections linear in $\sinh\gamma'' \propto c$, due to the combination of b_3 with b_1, b_2, whose magnitudes are subject to the upper bound $\approx |\tilde{l}_\rho \tilde{l}_n \sinh 2\gamma''| \approx |\frac{1}{2\sqrt{2}}\sinh\gamma''| \approx 0.02c \approx 0.002$.

The total correction to the tunneling exponent due to the shape of the Π-gates is the sum of terms in Eq. (4.25) and after Eqs. (4.26)(4.27)(4.28). It is much smaller than the leading order correction $|\delta g| \approx 0.04$ in Eq. (4.5).

Model 1

Next, we study model 1. We assume that there is only one neutral edge mode, propagating in the opposite direction to the charged edge mode. Let ϕ_{nO}, ϕ_{nI} be the neutral edge modes outside and inside the Π-shaped gate, respectively. Let $\phi_{\rho O}, \phi_{\rho I}$ be the charged edge modes outside and inside the gate, respectively. The Coulomb interaction between $\phi_{\rho O}, \phi_{\rho I}$ is described by $\mathcal{L}_\lambda = -\frac{1}{4\pi}\frac{4\lambda}{5}\partial_x\phi_{\rho O}\partial_x\phi_{\rho I}$. The complete

K matrix and potential matrix are

$$K = \begin{pmatrix} \frac{2}{5} & 0 & 0 & 0 \\ 0 & -1 & 0 & 0 \\ 0 & 0 & -\frac{2}{5} & 0 \\ 0 & 0 & 0 & 1 \end{pmatrix} \quad \text{and} \quad V = \begin{pmatrix} \frac{2}{5}v_\rho & v_{\rho n} & \frac{2}{5}\lambda & 0 \\ v_{\rho n} & v_n & 0 & 0 \\ \frac{2}{5}\lambda & 0 & \frac{2}{5}v_\rho & v_{\rho n} \\ 0 & 0 & v_{\rho n} & v_n \end{pmatrix}, \tag{4.29}$$

written in the basis $(\phi_{\rho O}, \phi_{nO}, \phi_{\rho I}, \phi_{nI})$. We again define $c' = \frac{\lambda}{v_\rho}$ to be the ratio which characterizes the strength of Coulomb interaction λ between $\phi_{\rho O}, \phi_{\rho I}$. Stability condition requires $c' < 1$. In Subsection 2.4.3, we found $c' \approx 0.9$ for model 1.

For model 1, a different transformation is needed to diagonalize the two matrices in subspace $(\phi_{\rho O}, \phi_{nO})$ and in subspace $(\phi_{\rho I}, \phi_{nI})$. Eq. (4.19) modifies to

$$\begin{aligned} \tilde{\phi}_{\rho O,\rho I} &= \sqrt{\frac{2}{5}} \cosh\theta \phi_{\rho O,\rho I} + \sinh\theta \phi_{nO,nI} \\ \tilde{\phi}_{nO,nI} &= \sqrt{\frac{2}{5}} \sinh\theta \phi_{\rho O,\rho I} + \cosh\theta \phi_{nO,nI}, \end{aligned} \tag{4.30}$$

where $\tanh 2\theta = c = \frac{\sqrt{10}v_{\rho n}}{v_\rho + v_n}$. Here we make use of the estimate of parameters in Section 4.1: $\frac{\sqrt{2}v_{\rho n}}{v_\rho + v_n} \approx \frac{1}{10}$. Hence, we have $c \approx \frac{\sqrt{5}}{10} \approx 0.22$ for model 1.

After the transformation in Eq. (4.30), the K matrix and potential matrix in Eq. (4.29) reduce to Eq. (4.20) and Eq. (4.22), respectively. The rest of the arguments are the same as those in model 2. Neglecting the off-diagonal elements in Eq. (4.22), the scaling dimension of a generic quasiparticle is given in Eq. (4.24), except that here the numerical values of c and c' are different: $c \approx 0.22$ and $c' \approx 0.9$. We have

$$2\Delta'' - 2\Delta \approx \tilde{l}_\rho^2(\cosh 2\beta - 1) \approx 1.3\tilde{l}_\rho^2 \tag{4.31}$$

where $\tanh 2\beta \approx c' \approx 0.9$ such that $2\beta \approx 1.47$, $\sinh 2\beta \approx 1.0$, $\cosh 2\beta \approx 2.3$,

$\sinh\beta \approx 0.8$, $\cosh\beta \approx 1.3$.

In model 1, the coefficients $\tilde{l}_\rho, \tilde{l}_n$ defined in Eq. (4.23) are: $\tilde{l}_\rho = \sqrt{\frac{5}{2}} l_\rho \cosh\theta - l_n \sinh\theta$ and $\tilde{l}_n = l_n \cosh\theta - \sqrt{\frac{5}{2}} l_\rho \sinh\theta$. As discussed in Subsection 2.4.3, we set $l_\rho = \frac{1}{10}$ to reproduce the $e/4$ electric charge of the most relevant quasiparticles. We assume this is the only difference, between model 1 and model 2: We still set $l_n = \frac{1}{2}$. Hence, for the most relevant quasiparticle $l_\rho = l_n = \frac{1}{2}$, we have $\tilde{l}_\rho = \frac{1}{2\sqrt{10}} \cosh\theta - \frac{1}{2} \sinh\theta$ and $\tilde{l}_n = \frac{1}{2} \cosh\theta - \frac{1}{2\sqrt{10}} \sinh\theta$. Substituting $\tilde{l}_\rho$ into Eq. (4.31), the "zeroth-generation" correction

$$\begin{aligned} 2\Delta''_{\min} - 2\Delta_{\min} &= 1.3\left(\frac{1}{40}\cosh 2\theta + \frac{9}{40}\sinh^2\theta - \frac{1}{4\sqrt{10}}\sinh 2\theta\right) \\ &\approx 1.3\left(\frac{1}{40} - \frac{1}{4\sqrt{10}}c\right) \\ &\approx 0.0325 - 0.103c \\ &\approx 0.01, \end{aligned} \tag{4.32}$$

where we have ignored the terms that are quadratic in c by setting $\sinh 2\theta = \frac{c}{\sqrt{1-c^2}} \to c$, $\cosh 2\theta = \frac{1}{\sqrt{1-c^2}} \to 1$ and $\sinh^2\theta \approx \frac{c^2}{4} \to 0$. In the last line, we set $c \approx 0.22$.

Higher-generation corrections come from the neglected off-diagonal elements in Eq. (4.22). These terms mix field operators with other field operators by small parts, whose magnitudes are estimated in Eqs. (4.26)(4.27)(4.28). The resulting corrections are small. For example, the "first-generation" correction due to the "rotation" in Eq. (4.27) can be estimated to be $\approx -2\tilde{l}_\rho \tilde{l}_n \cosh\beta \sinh 2\gamma' \approx -\frac{1.3}{\sqrt{10}} \sinh\gamma' \approx -0.006$, using $\tilde{l}_\rho \approx \frac{1}{2\sqrt{10}}$, $\tilde{l}_n \approx \frac{1}{2}$, $\cosh\beta \approx 1.3$, $\sinh\gamma' \approx 0.062c$ and $c \approx 0.22$ for model 1. This term balances the positive "zeroth-generation" correction in Eq. (4.32). The total correction due to the shape of the Π-gates is much smaller than the leading order correction $|\delta g| \approx 0.04$ in Eq. (4.5).

Chapter Five

Optimizing Reliability of Topological Quantum Computation with Majorana Fermions

5.1 Introduction

The beautiful idea of topological quantum computation [7, 8] offers a conceptually simple and straightforward approach to quantum information processing: Logical operations can be performed by braiding topological excitations; The memory remains protected from errors as long as the ground state manifold is separated from the excitation by a sufficient gap. Several systems are expected to host non-Abelian particles which can be used to implement topological quantum computation. In particular, much attention has focused on fractional quantum Hall states in the second Landau level [8], p-wave superconductors [25, 59], and heterostructures of superconductors and topological insulators [60]. In a majority of those systems, topological excitations are bound states of Majorana fermions. Majorana fermions are insufficient for the universal quantum computation [8,145,146] but they do provide a route to topologically protected memory.

A Majorana fermion can be thought of as a half of a complex fermion. Thus, a system of two distant Majorana fermions γ_1 and γ_2 possesses two degenerate quantum states which differ by their fermion parity. Those two states can be used to form a qbit (strictly speaking, one needs four Majorana fermions but this will not be important below). No local operators that affect parity can be constructed from γ_1 and γ_2 and hence the qbit enjoys topological protection. The situation changes, if other low-energy fermionic excitations are present. For example, a Majorana fermion in the core of a superconducting vortex is separated from other excitations in the vortex by a tiny minigap [62, 63]. Within the mean-field approximation those excitations do not interact with Majorana fermions but corrections to the mean-field theory are always present and can be significant and comparable to the minigap [1].

[1] A crude estimate of the interaction between fermions, localized in a vortex core, can be obtained from the following model. We describe the core as a disk of normal metal, separated by an infinite

As a result, the parity of the Majorana qbit no longer conserves.

An elegant way around this problem was proposed by Akhmerov in Ref. [147]. The topological charge of a closed subsystem that contains a Majorana fermion must always conserve. As a consequence, the local part Γ of the fermion parity operator can be used in place of the original Majorana fermion to obtain a protected qbit. The form of the local parity operator Γ does not depend on any details of the closed system except the number of its degrees of freedom. Thus, the same solution works for any interaction, weak or strong, and even time-dependent Hamiltonians. The only weakness of the proposal is related to the fact that a Majorana qbit is never an ideal closed system [64–67]. For example, it can exchange fermions with metallic gates used to control the system [68]. Another problem comes from quasiparticle poisoning [69–78]. In the ideal equilibrium limit, the number of bulk excitations scales as $\exp(-\Delta/T)$, where Δ is the energy gap, and hence is vanishingly small at low temperatures. However, in real low-temperature superconductors a nonequilibrium quasiparticle population is present and may considerably limit the qbit lifetime. The local parity Γ is much more vulnerable to these and other decoherence mechanisms than an individual Majorana fermion.

Ref. [148] has argued that other fermionic zero modes can be used to build a qbit with a longer lifetime than in Akhmerov's proposal. An appropriate zero mode has been identified for a quadratic Hamiltonian. Its use significantly increases the decoherence time indeed. That observation could be anticipated from the fact that quadratic Hamiltonians correspond to the mean-field approximation. One can ex-

barrier from the rest of the system. The radius of the disk $r \sim \hbar v_F/\Delta$, where v_F is the Fermi velocity and Δ the bulk gap. Bogoliubov quasiparticles do not participate in the long-range Coulomb interaction. Their short-range screened Coulomb interaction has the radius of $l \sim 1/k_F$, where k_F is the Fermi momentum. Its strength $U \sim \hbar v_F k_F$. Hence, the interaction energy of two quasiparticles can be estimated as $U(l/r)^2$ and is comparable with the minigap. Additional contributions to the interaction come from the BCS attraction between electrons.

pect similar behavior in the limit of weak interactions. What happens beyond that limit remains an open question. We answer that question below. We find simple analytic expressions for all zero modes of a general fermionic Hamiltonian, use those expressions to estimate the maximum decoherence time, and give an algorithm for designing a qbit with the longest lifetime. At weak interaction, in a system of $2N+2$ Majorana fermions, the lifetime τ can be increased to about $2N\tau_\Gamma$, where τ_Γ is the decoherence time of the qbit, based on the local parity operator Γ. At strong interaction the gain in the lifetime is less spectacular: $\tau \lesssim 10\tau_\Gamma$.

This chapter is organized as follows. As a warming-up exercise, in Section 5.2, we consider the simplest case of one Majorana and one complex fermion. In Section 5.3 we classify all zero modes of a general interacting fermionic Hamiltonian and describe those modes which can be used in a qbit. A general expression for their decoherence time is obtained in Section 5.4. We estimate the maximal decoherence time for strongly interacting systems in Section 5.5. Sections 5.2-5.5 focus on systems made of fermions only. This is the main question addressed in this article. What happens in the presence of additional bosonic modes, such as phonons, is briefly discussed in Section 5.6. We summarize our results in Section 5.7.

In this chapter, we focus on explaining the physical picture and summarizing our results. We refer all technical details to Appendix C.

5.2 One real and one complex fermion

This case is easy and always reduces to the mean-field limit considered in Ref. [148]. We will generalize for an arbitrary number of degrees of freedom in subsequent

sections.

One complex fermion is equivalent to two real fermions: $c^\dagger = (\gamma_1 + i\gamma_2)/2$. Thus, it is sufficient to study the problem with three Majorana fermions $\gamma_0, \gamma_1, \gamma_2$ with the anticommutation relations $\{\gamma_i, \gamma_j\} = 2\delta_{ij}$.

Let f be another Majorana operator, localized far away from the subsystem, where γ_i live. Consider a Majorana operator F, constructed from γ_i. Since F obeys the Fermi statistics and anticommutes with f, it is a polynomial of an odd degree as a function of γ_i, $i = 0, 1, 2$. F must also be Hermitian and satisfy the Majorana condition $F^2 = 1$. Then the operator iFf has two parity eigenvalues ± 1 which can be used to store quantum information. The information is preserved as long as the parity does not change. In a closed system, the parity conserves indefinitely as long as F commutes with the Hamiltonian, i.e., is a zero mode. Thus, as the first step, we classify fermionic zero modes.

The Hamiltonian that controls the γ_i degrees of freedom is a Bose-operator and reduces to a sum of products of even numbers of Majorana fermions. Since $\gamma_i^2 = 1$, the Hamiltonian is quadratic:

$$H = 2i(a_0\gamma_1\gamma_2 + a_1\gamma_2\gamma_0 + a_2\gamma_0\gamma_1) = i\sum_{ij} A_{ij}\gamma_i\gamma_j, \tag{5.1}$$

where A_{ij} is a skew-symmetric matrix. Any three-dimensional skew symmetric matrix can be reduced to a block diagonal form

$$\tilde{A} = \begin{pmatrix} 0 & 0 & 0 \\ 0 & 0 & a \\ 0 & -a & 0 \end{pmatrix}, \tag{5.2}$$

by an orthogonal transformation $\tilde{\gamma}_i = \sum_j O_{ij}\gamma_j$, where $\tilde{\gamma}_i$ is a new set of Majorana operators. Hence, the Hamiltonian can be rewritten as $H = 2ia\tilde{\gamma}_1\tilde{\gamma}_2$. In order to identify fermionic zero modes F we need to compute the commutator $[H, F] = 0$. We find that all (Hermitian) zero modes F reduce to linear combinations $F = \alpha\tilde{\gamma}_0 + \beta\Gamma$ with real coefficients α and β, where $\Gamma = i\tilde{\gamma}_0\tilde{\gamma}_1\tilde{\gamma}_2$ is the local parity operator. Since F is a Majorana fermion, $F^2 = 1$. Therefore there are only two possibilities for F (up to an overall sign): $F = \pm\tilde{\gamma}_0$ or $F = \pm\Gamma$. The first choice corresponds to Ref. [148] and the second choice coincides with Akhmerov's proposal [147].

Both choices would work equally well in a closed system. We now wish to include decoherence effects due to external degrees of freedom. As argued in Ref. [148], the decoherence time τ_Γ for $F = \Gamma$ is shorter than the decoherence time τ_0 for $F = \tilde{\gamma}_0$. We review the estimate of the lifetimes below. We generalize it for larger systems in subsequent sections.

The lifetime depends on the details of the interaction with the bath. Thus, for the most general case, only a crude estimate can be obtained for the ratio of τ_0 and τ_Γ. Our estimate is based on a simple model of a bath as a system of noninteracting electrons $c_{k,i}$ with the Hamiltonian $H_b = \sum_{k,i} \epsilon_{k,i} c^\dagger_{k,i} c_{k,i}$. The index k is continuous and i labels various discrete degrees of freedom. The calculations simplify slightly, if we assume that each operator $\tilde{\gamma}_i$ couples only with the bath fermions labeled by the same index i. Thus, the interaction with the bath is described by the Hamiltonian $H_I = \sum_{i,k} M_{k,i}(t)\tilde{\gamma}_i c_{k,i} + H.c.$

We will estimate the lifetime τ of a qbit by computing how long it takes until the bath flips the sign of the parity eigenvalue $iFf = \pm 1$. A similar estimate can be extracted from the time dependence of the parity correlation function $C(s) = \langle iF(t = 0)fiF(t = s)f\rangle$ and the condition $C(\tau) \sim C(0)/e = e^{-1}$. Both approaches also lead

to similar results in a system with an arbitrary number of Majorana fermions.

Let the system be in an initial state $|0\rangle$ with a definite parity of the qbit $q(t=0) = \langle 0|iFf|0\rangle$. $q(0)$ can be set equal to one without loss of generality. In order to compute the qbit lifetime we need to estimate the time-dependence of $q(t) = \langle\psi(t)|iFf|\psi(t)\rangle$, where $\psi(t)$ is the time-dependent wave function with the initial condition $|\psi(0)\rangle = |0\rangle$. Let us find the probability of the transition to the state $|\psi_q\rangle|\psi_b\rangle$ during the time interval t, where $|\psi_q\rangle$ is a wave function of the qbit and $|\psi_b\rangle$ a state of the bath. The probability is given by Fermi's golden rule, $p \sim t|\langle\psi_q|\langle\psi_b|H_{I,\omega}|0\rangle|^2$, where $H_{I,\omega}$ is the Fourier harmonic of the interaction at the frequency ω, determined by the energy conservation: $\hbar\omega = E_{\text{final}} - E_{\text{initial}}$. The matrix element in the above formula is a linear combination of the products of the matrix elements $\langle\psi_q|\tilde{\gamma}_i|0\rangle$ and matrix elements of the fermion operators in the bath. The relevant matrix elements and densities of states depend on the details of the physical realization. For the sake of a general estimate, we use the simplest assumption that the probability to find the qbit in a common energy and total parity eigenstate $|\psi_q\rangle$ is $P_q = At\sum_i |\langle\psi_q|\tilde{\gamma}_i|0\rangle|^2$, where A does not depend on $|\psi_q\rangle$. It is easy to compute $q(t)$ now:

$$\begin{aligned} q(t) &= 1 - At\sum_{i,\psi_q} |\langle\psi_q|\tilde{\gamma}_i|0\rangle|^2 + At\sum_{i,\psi_q}\langle\psi_q|iFf|\psi_q\rangle|\langle\psi_q|\tilde{\gamma}_i|0\rangle|^2 \\ &= 1 - At\sum_i[\langle 0|\tilde{\gamma}_i^2|0\rangle - \langle 0|\tilde{\gamma}_i iFf\tilde{\gamma}_i|0\rangle], \end{aligned} \tag{5.3}$$

where it is legitimate to include $|\psi_q\rangle = |0\rangle$ in the sums in the first line. By setting $F = \tilde{\gamma}_0$ we get $q(t) = q_0(t) = 1 - 2At$ at $t \ll 1/A$. By setting $F = \Gamma$ we find $q(t) = q_\Gamma(t) = 1 - 6At$. This shows that $\tau_0 = 3\tau_\Gamma \sim 1/[2A]$.

The above results crucially depend on the existence of a linear zero mode in any system of three Majorana particles. Such modes do not exist [149] in a generic

system with more than three Majorana fermions. We address the structure of the zero modes for an arbitrary number of the degrees of freedom in the next section.

5.3 Zero modes

We consider a system of an arbitrary odd number $2N+1$ of interacting Majorana fermions $\gamma_0, \ldots, \gamma_{2N}$. This is equivalent to a system of one Majorana and N complex fermions. We first neglect the interaction with the bath. Then the Hamiltonian H is a linear combination of various products of even numbers of Majorana operators.

As the discussion in the previous section shows, in order to construct a qbit, we need to identify a fermionic zero mode operator F, constructed from γ_i, such that $F = F^\dagger$, $[H, F] = 0$ and $F^2 = 1$. Then quantum information can be encoded in the total parity operator iFf, where f is a Majorana fermion far away from γ_i. We start with finding all fermionic zero modes O, commuting with H, and impose the Majorana condition $O^2 = 1$ later.

Obviously, $\Gamma = i^N \Pi_{i=0}^{2N} \gamma_i$ is Hermitian and commutes with any Hamiltonian H. The operator H also commutes with itself. Thus, any operator of the form

$$O = P(H)\Gamma, \tag{5.4}$$

where $P(x)$ is a polynomial, is a fermionic zero mode. We show in Appendix C.2 that there are no other fermionic zero modes for a generic Hamiltonian H. We also find that for a generic Hamiltonian, there are exactly 2^N linear independent integrals of motion of the above form. Note that the number 2^N of fermionic zero modes has been identified in Ref. [148] for non-interacting Hamiltonians and in the case of

infinitesimal interactions. On the other hand, we establish a general result.

The number of the linear independent zero modes is easy to understand. We first note that any fermionic zero mode can be obtained by multiplying a bosonic zero mode by Γ. This establishes a one-to-one correspondence between bosonic and fermionic zero modes. Thus, it is sufficient to establish that there are exactly 2^N linear independent bosonic zero modes. For this end, we notice that the Hamiltonian acts in the Hilbert space of dimension 2^{N+1}, defined by the $(2N+2)$ Majorana operators γ_k and f. There are 2^N states of even parity $i\Gamma f$ and 2^N states of odd parity $i\Gamma f$ in the Hilbert space. The two subspaces are connected by the operator Γ. The Hamiltonian and all bosonic zero modes commute with Γ as well as with the parity operator $i\Gamma f$. Hence, they can be represented in the form of block operators with two identical blocks in the even and odd subspaces. This means, in turn, that it is sufficient to classify bosonic zero modes of the restriction of H to the even subspace. After the diagonalization of the Hamiltonian in that subspace, we obtain a diagonal matrix of size 2^N. Clearly, such matrix commutes with at least 2^N linear independent Hermitian operators that preserve the parity $i\Gamma f$ and commute with Γ, i.e., bosonic zero modes. Moreover, there are exactly 2^N linear independent modes in the generic case of the Hamiltonian without degenerate eigenvalues.

Appendix C.2 contains a different proof, based on an explicit construction of the zero modes for particular Hamiltonians.

It is also easy to see that for a generic Hamiltonian, 2^N linear independent fermionic zero modes can be selected in the form $O_k = H^k\Gamma$, $k = 0, \ldots, 2^N - 1$. Indeed, if those modes were linear dependent then one could find a polynomial $P(x)$ of a degree $n < 2^N$ such that $P(H) = 0$. Thus, $P(E_k) = 0$ for all eigenvalues E_k of the Hamiltonian. However, in a generic situation there are 2^N different energy levels

E_k in contradiction with the fundamental theorem of algebra. Hence, the modes O_k are linear independent. Any other fermionic zero mode is a linear combination of the modes O_k, i.e., satisfies Eq. (5.4), where the degree of the polynomial $P(H)$ is less than 2^N.

Not all zero modes $O = P(H)\Gamma$, deg $[P(x)] < 2^N$, are suitable to build a qbit. We need to impose the condition

$$O^2 = 1. \tag{5.5}$$

This is equivalent to $P^2(H) = 1$. In turn, the former condition simplifies to $P(E_k) = \pm 1$ where E_k, $k = 1, \ldots, N_E = 2^N$, are the eigenenergies of H. All allowed polynomials P can be written in terms of E_k with the use of standard interpolation formulas, e.g.,

$$P(x) = \sum_k P(E_k)\Pi_{n=1}^{k-1}\frac{x - E_n}{E_k - E_n}\Pi_{n=k+1}^{N_E}\frac{x - E_n}{E_k - E_n}. \tag{5.6}$$

The number of the possible choices of P depends on the number $N_E = 2^N$ of the energy levels of H and equals 2^{N_E}. This set is made of 2^{N_E-1} pairs of opposite polynomials P and $-P$. Thus, there are 2^{N_E-1} ways to build a topological qbit.

The goal of the next two sections is to estimate the maximal lifetime for such qbits in the presence of a bath.

5.4 Dephasing

In this section we derive a general formula for the lifetime of a qbit. We will use it to estimate the maximal possible lifetime in a system of $2N + 1$ interacting Majorana modes in the next section. The exact value of the lifetime depends on many details

of the Hamiltonian and cannot be computed in a general situation. Thus, we limit ourself to an estimate based on a simple model in the spirit of Section 5.2.

Our model Hamiltonian is the sum of three pieces, $H+H_b+H_I$, where H describes the Majorana degrees of freedom, $H_b = \sum_{k,i} \epsilon_{k,i} c^\dagger_{k,i} c_{k,i}$ is the bath Hamiltonian, and $H_I = \sum_{i,k} M_{k,i}(t)\gamma_i c_{k,i} + H.c.$ describes the interaction of the qbit with the bath. Quantum information is encoded in the total parity operator $P = iFf$, where F is a fermionic zero mode (Section 5.3) and f is a Majorana fermion, located far away from the Majorana fermions $\gamma_0, \ldots, \gamma_{2N}$. As discussed above, F is a polynomial of γ's:

$$F = \sum_{n=0}^{N} i^n \sum_{\{k_l\}} a_{k_1,\ldots,k_{2n+1}} \Pi_{s=1}^{2n+1} \gamma_{k_s}, \tag{5.7}$$

where $k_1 < k_2 < \cdots < k_{2n+1}$ and $\{k_l\}$ is the shorthand for the set of the indices $k_1, \ldots, k_{2n+1}$. The fact that F is Hermitian implies that the coefficients $a_{k_1,\ldots,k_{2n+1}}$ are real. The normalization condition (5.5) means that

$$\frac{\mathrm{Tr} F^2}{2^{N+1}} = \sum a^2_{\{k_l\}} = 1. \tag{5.8}$$

In what follows we ignore the interaction between f and the bath and only compute the lifetime due to the interaction of the bath with the Majorana modes γ_k. Assuming that the physics is similar in the regions, where F and f are localized, one can expect that the interaction of f with the bath cuts the lifetime in half.

We assume that initially the qbit is in a common eigenstate $|q_k\rangle$ of the total parity operator P and the Hamiltonian H, $P|q_k\rangle = \pm|q_k\rangle$. The 2^{N+1} states $|q_k\rangle$ form an orthonormal basis in the Hilbert space on which P and F act. Due to the interaction with the bath, the average $q(t) = \langle P(t)\rangle$ depends on time and eventually approaches 0. Since $P^2 = 1$ for any choice of $|q_k\rangle$, a convenient definition of the relaxation time

is

$$\tau = \frac{2P^2(0)}{-\frac{d}{dt}\overline{\langle P(t)\rangle^2}\Big|_{t=0}} = -\frac{2}{\frac{d}{dt}\overline{\langle P(t)\rangle^2}\Big|_{t=0}}, \tag{5.9}$$

where the bar denotes the average with respect to all possible choices of $|q_k\rangle$ and the angular brackets denote the average with respect to the time-dependent wave function.

In order to compute $q(t) = \langle P(t)\rangle$ we need to know the density matrix of the qbit at the time t. This reduces to the calculation of the transition probabilities from the initial state to all other states $|q_i\rangle$. The probabilities can be computed with Fermi's golden rule and depend on many features of the system. Following Section 5.2, we make the simplest assumption that the transition probability between the states $|q_i\rangle$ and $|q_j\rangle$, $i \neq j$, has the form $P_{i\to j} = At\sum_k |\langle q_i|\gamma_k|q_j\rangle|^2$, where A does not depend on i and j. Then

$$\begin{aligned} q(t) &= q(0)[1 - \sum_{i,j} At|\langle q_i|\gamma_j|q_k\rangle|^2] + \sum_{i,j} At\langle q_k|\gamma_j|q_i\rangle\langle q_i|P|q_i\rangle\langle q_i|\gamma_j|q_k\rangle \\ &= q(0)[1 - (2N+1)At] + At\sum_j \langle q_k|\gamma_j P\gamma_j|q_k\rangle \\ &= \langle q_k|P_t|q_k\rangle, \end{aligned} \tag{5.10}$$

where we include $i = k$ in the sums, use the fact that P is diagonal in the $|q_i\rangle$ basis, and set $P_t = iQ_t f$ with

$$Q_t = \sum_{n=0}^{N}[1 - 2(2n+1)At]i^n \sum_{\{k_l\}} a_{k_1,\ldots,k_{2n+1}}\Pi_{s=1}^{2n+1}\gamma_{k_s}. \tag{5.11}$$

Note that

$$\frac{d}{dt}\overline{\langle P(t)\rangle^2}\Big|_{t=0} = 2\overline{\langle P(t)\rangle\frac{d\langle P(t)\rangle}{dt}}\Big|_{t=0} = 2\frac{\mathrm{Tr}P_t\frac{dP_t}{dt}}{2^{N+1}}\Big|_{t=0} = 2(Q_t, \frac{dQ_t}{dt})\Big|_{t=0}, \qquad (5.12)$$

where the inner product (A, B) is defined in Appendix C.1 and we use the fact that $P_{t=0}$ is diagonal in the $|q_k\rangle$ basis. From Eqs. (5.12,C.5,5.9) one finds the decoherence time

$$\tau = \frac{1}{2A\sum_{n=0}^{N}(2n+1)\sum_{\{k_l\}} a^2_{k_1,\ldots,k_{2n+1}}}. \qquad (5.13)$$

Eq. (5.13) can be used to estimate the decoherence time and select the most robust of the fermionic zero modes, listed in Section 5.3, for use in a qbit. Longer lifetimes correspond to zero modes, dominated by contributions of lower orders in γ_i's.

5.5 The longest decoherence time

In this section we estimate the longest decoherence time that can be achieved in an interacting system of $2N + 1$ Majorana fermions. As is illustrated in the case of $N = 1$ in Section 5.2, at small N all zero modes can be expected to have comparable decoherence times. Thus, we concentrate on the limit of large N.

Based on Eq. (5.13), one expects that the local parity fermionic zero mode Γ always corresponds to the shortest decoherence time. Thus, any other choice of the zero mode improves the dephasing time. What is the maximal improvement one can achieve? Since the number of the Majorana zero modes is very large at large N, one might think that at least one of the very many Majorana modes has the lifetime,

much greater than τ_Γ. It turns out, however, that such intuition does not work for strongly interacting systems.

We start with an easy case of a noninteracting system, where the qbit Hamiltonian H is quadratic in Majorana operators. Similar to Section 5.2, an orthogonal change of the variables reduces the Hamiltonian to the canonical form $H = i\sum_{n=1}^{N} a_n \tilde{\gamma}_{2n-1}\tilde{\gamma}_{2n}$, where $\tilde{\gamma}_k$ $(k = 0, \ldots, 2N)$ are new Majorana fermions and $\tilde{\gamma}_0$ does not enter the Hamiltonian. The operator $\tilde{\gamma}_0$ is a fermionic zero mode. It is a linear combination of the original Majorana fermions γ_k. Consider a qbit, based on the Majorana mode $\tilde{\gamma}_0$. Eq. (5.13) shows that the decoherence time of such qbit does not depend on the system size N and equals roughly $1/[2A]$. For comparison, the decoherence time τ_Γ for the local parity operator $\Gamma = i^N \Pi_{n=0}^{2N} \gamma_n$ scales as $1/N$. Thus, choosing $\tilde{\gamma}_0$ to build a qbit gives a considerable advantage at large N in agreement with Ref. [148]. Unfortunately, such long lifetime cannot be obtained in a general strongly interacting system.

To see why, we start with a crude simplistic estimate. We will see that it has the same order of magnitude as the rigorous result. The fermionic zero modes, classified in Section 5.3, are linear combinations of products of odd numbers of Majoranas. For our estimate, we will treat the zero modes as random vectors in the linear space of all such products. The total number of linear independent fermionic zero modes is 2^N. In a system with $2N+1$ Majorana fermions, one can construct exactly 2^{2N} linear independent products Π_k of odd numbers $\deg[\Pi_k]$ of Majorana operators. For the sake of a crude estimate, let us make a simplifying assumption that up to constant prefactors a set of 2^N linear independent fermionic zero modes can be chosen from those 2^{2N} products, i.e, monomial functions of Majorana operators. We will denote those linear independent modes $F_1, \ldots, F_{2^N}$.

Let us estimate the decoherence times for the above 2^N modes F_k. Eq. (5.13) shows that this is sufficient to identify the longest possible decoherence time.

A mode F_k is given by a product of $\deg[F_k]$ Majorana operators. As Eq. (5.13) shows, to find the maximal decoherence time we need to identify the mode $F_{\min}$ with the minimum degree $\deg[F_{\min}] = d_{\min}$. The dephasing time can then be extracted from the value of $d_{\min}$. Assuming that each F_n is randomly chosen among Π_l, one expects that $F_{\min}$ is typically one of the $K = 2^{2N}/2^N = 2^N$ operators Π_l of the lowest degrees $\deg[\Pi_l] = d_1 \leq d_2 \leq \cdots \leq d_K$. For a crude estimate we can set $d_{\min} \sim d_K$. Then Eq. (5.13) yields the dephasing time $\sim 1/[2Ad_K]$. The number K of the operators Π_k with $\deg[\Pi_k] \leq d_K$ can be easily found from combinatorics as $K = LC_{2N+1}^{d_K}$, where the binomial coefficient $C_{2N+1}^{d_K} = (2N+1)!/[d_K!(2N+1-d_K)!]$ and $(d_K/2N)^2 < L < (d_K+1)/2$. Since we are interested in large N, the binomial coefficient can be approximated with the Stirling formula and

$$K \approx \frac{L}{\sqrt{2\pi\epsilon N}} \left[\left(\frac{\epsilon}{2}\right)^{\epsilon/2} \left(1 - \frac{\epsilon}{2}\right)^{1-\epsilon/2} \right]^{-2N}, \tag{5.14}$$

where we define $\epsilon = d_K/N$. Next, we use the fact that $K = 2^N$ to obtain $\epsilon \approx 0.22$. Hence, $\deg[F_{\min}] \sim 0.2N$ and the decoherence time (5.13), $\tau_{\max} \sim \frac{5}{2NA}$. This scales as $1/N$ and is only one order of magnitude better than the estimate $\tau_\Gamma \sim 1/[4NA]$ for a qbit, constructed from the local parity operator Γ in place of $F_{\min}$.

The above conclusion agrees with the rigorous estimate from Appendix C.3. The maximal decoherence time depends on the details of the Hamiltonian and can be higher than the result of Appendix C.3 for special Hamiltonians. To formulate our results precisely, we introduce a measure on the ensemble of all possible Hamiltonians H of a system with $2N+1$ Majorana fermions. Specifically, we assume that the measure depends only on the inner product (H, H), defined in Appendix C.1. The

details of the dependence are not important. Then, in the limit of a large N, our estimate applies to all Hamiltonians except a set of measure 0. We find that the dephasing time

$$\tau_{\max} < \frac{5}{NA}. \tag{5.15}$$

5.6 Interaction with bosons

So far, our focus has been on a system of fermions. In realistic systems, interaction with Bose degrees of freedom, such as phonons, is possible. The arguments from Sections 5.3 and 5.4 easily translate to such situation. We first remove physically unimportant high energy states from the Hilbert space of bosons. Let the dimension of the truncated Hilbert space of bosons be D_b. Any operator of the form (5.4), where the Hamiltonian H includes both Fermi and Bose degrees of freedom, is still a fermionic zero mode; All fermionic zero modes satisfy (5.4). The number of the linear independent zero modes changes but can be found with essentially the same argument as in Section 5.3. It equals $D_b 2^N$. Exactly the same prescription (5.6) as in Section 5.3 can be used to construct zero modes, satisfying Eq. (5.5). The number of the ways to build a qbit is given by the same expression as before, 2^{N_E-1}, where the number of the different energy levels expresses now as $N_E = D_b 2^N$ for a generic Hamiltonian.

The discussion of dephasing, Section 5.4, also applies. In particular, only a slight change is necessary in Eq. (5.13). The coefficients $a_{\{k_l\}}$ in Eq. (5.7) should now be understood as Hermitian operators $\hat{a}_{\{k_l\}}$ in the Hilbert space of bosons. In order to compute the dephasing time, $\mathrm{Tr}\hat{a}^2_{\{k_l\}}/D_b$ should be written instead of $a^2_{\{k_l\}}$ in Eqs. (5.8) and (5.13).

We were unable to extend the rigorous proof of the estimate (5.15) from Appendix C.3 to systems with bosons. Nevertheless, we expect the limit on the maximal decoherence time (5.15) to hold irrespective of the presence of Bose degrees of freedom. This expectation is supported by the qualitative argument below.

We first note that there are D_b^2 linear independent Hermitian operators $\hat{A}_k$ in the Hilbert space of bosons. They can be selected so that $\mathrm{Tr}\hat{A}_i\hat{A}_j = \delta_{ij}$. Any of the Majorana zero modes, satisfying Eq. (5.5), can be represented in the form

$$F = \sqrt{D_b}\sum c^{(n)}_{m,\{k_s\}}\hat{A}_m i^n \Pi_{s=1}^{2n+1}\gamma_{k_s}, \tag{5.16}$$

where $k_1 < k_2 < \cdots < k_{2n+1}$, $m = 1, \ldots, D_b^2$ and $\sum[c^{(n)}_{m,\{k_s\}}]^2 = 1$. The dephasing time is given by Eq. (5.13) with $c^{(n)}_{m,\{k_s\}}$ in place of $a_{\{k_s\}}$. For the sake of our qualitative argument we will treat the above Majorana zero modes (5.16) as random vectors in the space of all possible fermionic operators. The dimension of the latter space is $D_b^2 2^{2N}$. It will be convenient to set

$$c^{(n)}_{m,\{k_s\}} = \frac{b^{(n)}_{m,\{k_s\}}}{\sqrt{\sum[b^{(n)}_{m,\{k_s\}}]^2}}. \tag{5.17}$$

This ansatz takes care about appropriate normalization conditions. For simplicity we will assume that $b^{(n)}_{m,\{k_s\}}$ are independent Gaussian variables. The results do not depend on their variance and we select the distribution functions of the form $P(b^{(n)}_{m,\{k_s\}}) \sim \exp[-(b^{(n)}_{m,\{k_s\}})^2 D_b^2 2^{2N}/2]$. This choice implies that $\langle\sum[b^{(n)}_{m,\{k_s\}}]^2\rangle = 1$.

Since there are $2^{D_b 2^N - 1}$ Majorana modes (5.16), we can neglect the choices of the coefficients $b^{(n)}_{m,\{k_s\}}$ whose joint probability is below $2^{-D_b 2^N}$. For example, $\sum[b^{(n)}_{m,\{k_s\}}]^2$, is a random variable with the variance $2/[D_b^2 2^{2N}]$. Thus, we can neglect the probability of the event that $|\sum[b^{(n)}_{m,\{k_s\}}]^2 - 1| \gg 1/\sqrt{D_b 2^N}$. Similar considerations show that

we can neglect the probability of such configurations that $\sum_{2n+1<0.1N}[b^{(n)}_{m,\{k_s\}}]^2 \sim 1$. Eq. (5.13) then immediately leads to the estimate (5.15).

In contrast to Appendix C.3, the above simple argument is not rigorous. In Appendix C.4, we use a rigorous approach to compare dephasing times for Hamiltonians, quadratic in Majoranas, in the absence and presence of bosonic modes. We find that Bose modes shorten the decoherence time. Thus, we expect that interaction with Bose modes improves the decoherence time in neither weakly nor strongly interacting systems.

5.7 Summary

A topological qbit can be constructed from a fermionic zero mode of a system of $2N + 1$ Majorana fermions. We classified such modes F_k for a generic Hamiltonian and found a simple analytical expression for all of them. We also proposed how to design the qbit with the longest decoherence time. One first needs to identify the modes, satisfying the Majorana condition $F_k^2 = 1$. Second, one should use Eq. (5.13) to estimate the decoherence time, corresponding to each choice of the zero mode, and select the most robust Majorana operator. In noninteracting systems, the decoherence times vary greatly, depending on the choice of F_k. We found that the maximum decoherence time does not depend on the system size in the absence of interactions. On the other hand, in strongly interacting systems, the shortest decoherence time $\tau_\Gamma \sim 1/[4NA]$ and the longest decoherence time (5.15) differ by no more than one order of magnitude. The contrast between interacting and noninteracting systems is not surprising. In the absence of interactions, it is possible to find a subsystem that does not feel most excitations in the bath. Such effectively isolated subsystems

cannot exist in the presence of strong interactions.

Many-particle systems can exhibit many-body localization [150] (MBL) in the presence of weak interactions. Localized states may support topological order [151, 152] and it was argued that MBL may be used to build robust topological memory [152] in a large system. This does not conflict with our results in the case of strong interactions, where we find a rapid decrease of the decoherence time as a function of N. First of all, MBL occurs at weak interactions, where our results do not apply. Even more importantly, a typical Hamiltonian in the space of all Hamiltonians, Appendix C.3, involves the interaction of all pairs of Majorana modes. This is natural for Majorana fermions, localized in the same vortex, but quite different from what happens in systems with MBL. Such systems have zero measure in the space of the interacting Hamiltonians at $N \to \infty$.

It was proposed in Ref. [148] that selecting a zero mode with the longest decoherence time is a route to more robust topological quantum computation. Our results show that such strategy is rather limited. The structure of all zero modes, except Γ, is complicated and sensitive to the system details. It is not obvious how to access them experimentally. Taking into account a relatively small gain in the decoherence time from optimizing F_k, we see that the advantages of such optimization are narrow. The only ways to dramatically improve the decay time consist in 1) suppressing the interaction with the bath; 2) reducing the interaction between the fermions that form the qbit or 3) cutting the number of low-energy degrees of freedom by increasing the minigap [153, 154].

Appendix A

Positive-Definiteness of Interaction Matrix U_{ij}

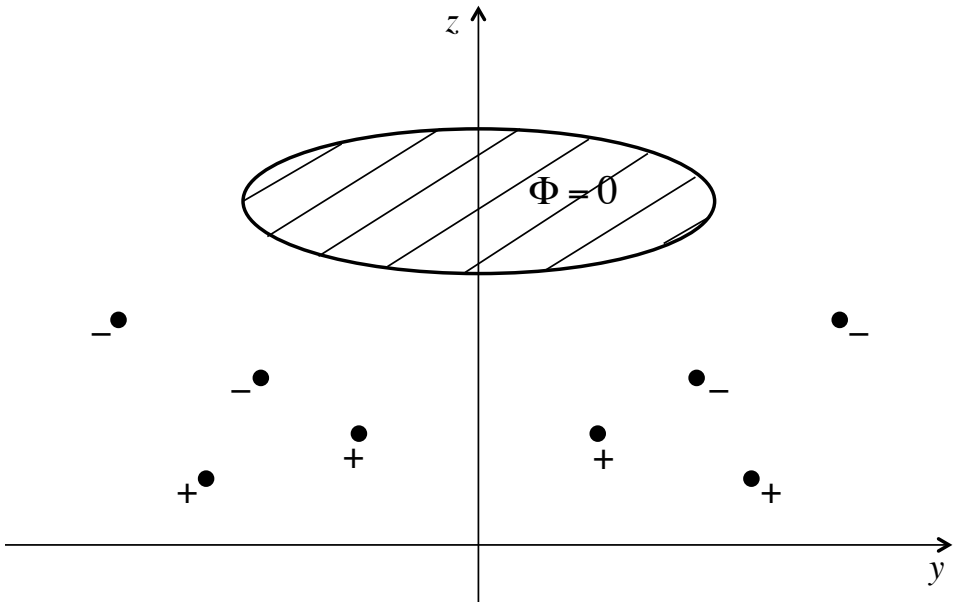

Figure A.1: The charge distribution is mirror symmetric with respect to the $y = 0$ plane. The mirror-symmetric gate with the potential $\Phi = 0$ is shaded.

In this appendix we prove that the interaction matrix U_{ij} in Eq. (2.17) is positive definite. We consider a system with mirror symmetry, Fig. A.1. In Fig. A.1 the x-axis is perpendicular to the plane of the figure and the mirror plane is defined by the equation $y = 0$. The only assumption about the dielectric constant outside the mirror symmetric gates is the mirror symmetry of its coordinate dependence.

Our effective models for edge states are one-dimensional and contain only the coordinate x but the physical charge distribution is always three-dimensional. The energy of the electrostatic interaction between the edge segments on the left and right of the gate, Fig. A.1, depends on the whole three-dimensional distribution of the charges.

The derivatives of the Bose fields $\partial_x \phi_i$ in Eq. (2.17) are determined by the local charge distribution. It will be convenient for us to consider a situation in which the charge density $\rho(\mathbf{r}) = \rho(x, y, z)$ does not depend on x and exhibits the mirror symmetry $\rho(x, y, z) = \rho(x, -y, z)$. Then all $\partial_x \phi_i$ remain constant on the left and right

of the gate with $\partial_x\phi_i$(left of the gate) $= -\partial_x\phi_i$(right of the gate). The interaction energy (2.17) becomes $(+1/4\pi)\int_{-\infty}^{0} dx \sum_{ij} U_{ij}\partial_x\phi_i(x<0)\partial_x\phi_j(x<0)$. The same energy can be found from electrostatics. It is just the interaction energy of the charge distribution on the left of the gate, $\rho(x,y,z)$, $y<0$, with the mirror symmetric charge distribution $\rho(x,y,z)$, $y>0$. It is now clear that to prove the positive definiteness of U it is sufficient to prove that the electrostatic interaction energy of a set of charges on the left of the mirror plane with the mirror symmetric set of charges on the right of the plane is always positive. Below we compute such electrostatic energy in the presence of mirror symmetric metallic gates.

We set the electrostatic potential of the gates to zero. The electrostatic potential $\Phi(\mathbf{r})$ outside the gates can be represented as the sum of two contributions. $\Phi_l(\mathbf{r})$ is the electrostatic potential, created by the charges on the left of the mirror plane (i.e., the charges from the points with negative y). By definition Φ_l includes the effect of the screening charges on the gate surface, i.e., satisfies the boundary condition $\Phi_l(\mathbf{r}$ in the gate$)=0$. $\Phi_r(\mathbf{r})$ is created by the charges on the right of the mirror plane in the presence of a screening gate. The mirror symmetry implies that $\Phi_l(x,y,z) = \Phi_r(x,-y,z)$. The total electrostatic energy is thus

$$E = \int dxdz \int_{-\infty}^{0} dy\rho(x,y,z)[\Phi_l(x,y,z)+\Phi_r(x,y,z)]. \tag{A.1}$$

We wish to prove that the interaction contribution

$$E_{lr} = \int dxdz \int_{-\infty}^{0} dy\rho\Phi_r \tag{A.2}$$

is positive.

Let us investigate the effect of two changes in the charge distribution on the

energy.

1) We remove all charges on the right of the mirror plane, i.e., set $\rho(x, y > 0, z) = 0$. The electrostatic energy becomes

$$E_1 = \int dxdz \int_{-\infty}^{0} \rho(x, y, z)\Phi_l(x, y, z)/2. \tag{A.3}$$

2) Alternatively, let us change the sign of all charges on the right of the mirror plane: $\rho(x, y, z) \to -\rho(x, y, z)$, $y > 0$. The potential becomes $\Phi_l(\mathbf{r}) - \Phi_r(\mathbf{r})$. We have created a situation with $\Phi(x, y = 0, z) = 0$. Hence, the total electrostatic potential at $y < 0$ would not change after all charges with $y > 0$ are removed and the region $y > 0$ is filled with metal. In the latter situation, the total electrostatic energy becomes

$$E_2 = \int dxdz \int_{-\infty}^{0} dy\rho(x, y, z)[\Phi_l(x, y, z) - \Phi_r(x, y, z)]/2, \tag{A.4}$$

where Φ_l and Φ_r are the same as in Eq. (A.1), i.e., $[\Phi_l(x, y, z) + \Phi_r(x, y, z)]$ is the electrostatic potential of a mirror symmetric charge distribution.

According to a theorem of electrostatics [155], the energy always goes down if a piece of metal is introduced into a system at fixed positions of free charges. Hence, $E_2 < E_1$. Subtracting E_2 from E_1 we find that $E_{lr} > 0$ and hence U_{ij} is positive definite.

Appendix B

Effect of Unscreened Coulomb Interaction on Quasiparticle Tunneling in the 331 State

In this appendix, we study the effect of unscreened Coulomb interaction on tunneling exponents in the spin-unpolarized 331 state (Eq. (2.4)). The spin-polarized 331 state (Eq. (2.5)) has the same "orbital" topological order as the spin-unpolarized 331 state. In geometry 2.1c where there is no unscreened Coulomb interaction across the quantum point contact (QPC), the tunneling exponents predicted by the two versions of the 331 state are the same. In geometries 2.1a and 2.1b, unscreened Coulomb interaction couples contra-propagating charge densities on opposite sides of a narrow QPC. The quasiparticle tunneling is hence nonuniversal and the tunneling exponent depends on the details in the Hamiltonian. Nevertheless, the tunneling exponents predicted by the two versions of the 331 state behave qualitatively similar in geometries 2.1a and 2.1b, since the coupling between charged densities across a narrow QPC is purely orbital which cannot distinguish the two states.

The Lagrangian density on the edge of the spin-unpolarized 331 state is

$$\mathcal{L} = -\frac{1}{4\pi} \sum_{I,J=1,2} [K_{IJ} \partial_t \phi_I \partial_x \phi_J + V_{IJ} \partial_x \phi_I \partial_x \phi_J] \tag{B.1}$$

with the K matrix and the potential matrix V

$$K = \begin{pmatrix} 3 & 1 \\ 1 & 3 \end{pmatrix} \quad \text{and} \quad V = \begin{pmatrix} V_{11} & V_{12} \\ V_{12} & V_{22} \end{pmatrix}, \tag{B.2}$$

where ϕ_1, ϕ_2 are two charged bosonic modes, V_{11}, V_{22} are the effective velocities of ϕ_1, ϕ_2, respectively, and V_{12} is the effective interaction between the two edge modes.

Let us study the quasiparticle tunneling in the 331 state. We will consider the three QPC geometries in Fig. 2.1. First of all, we study the physics on a single fractional quantum Hall (FQH) edge. The edge can be either a long line channel or a narrow QPC, depending on the particular geometry it belongs to. If the FQH

edge is a long line channel, Coulomb interaction is absent and its Lagrangian density, denoted by $\mathcal{L}^W$, is simply the bare Lagrangian density in Eq. (B.1). If however, the FQH edge is a narrow QPC, unscreened Coulomb interaction term should be added to $\mathcal{L}^W$ in order to obtain the Lagrangian density $\mathcal{L}^N$ for a narrow QPC, as shown in the following. We choose the point where quasiparticles tunnel to be $x = 0$. Then, we break the FQH edge in consideration into two semi-infinite spatial pieces with respect to the tunneling point by defining edge modes

$$\begin{aligned} \phi_{IR}(x) &= \phi_I(x) \\ \phi_{IL}(x) &= \phi_I(-x), \end{aligned} \tag{B.3}$$

for $x \leq 0$, where $I = 1, 2$. By definition, both two spatial pieces are parameterized in $x \leq 0$. The K matrix in Eq. (B.2) can be diagonalized by making a rotation in boson fields,

$$\phi_\pm = \frac{1}{\sqrt{2}}(\phi_1 \pm \phi_2), \tag{B.4}$$

and correspondingly, $\phi_{\pm R,L} = \frac{1}{\sqrt{2}}(\phi_{1R,L} \pm \phi_{2R,L})$, after which

$$\begin{aligned} \mathcal{L}^W = -\frac{1}{4\pi} \sum_{I,J=+,-} [&\widetilde{K}_{IJ}\partial_t\phi_{IR}\partial_x\phi_{JR} - \widetilde{K}_{IJ}\partial_t\phi_{IL}\partial_x\phi_{JL} \\ &+ \widetilde{V}_{IJ}\partial_x\phi_{IR}\partial_x\phi_{JR} + \widetilde{V}_{IJ}\partial_x\phi_{IL}\partial_x\phi_{JL}] \end{aligned} \tag{B.5}$$

written in term of the split edge modes.

$$\widetilde{K} = \begin{pmatrix} 4 & 0 \\ 0 & 2 \end{pmatrix} \quad \text{and} \quad \widetilde{V} = 4 \begin{pmatrix} \widetilde{V}_{++} & \widetilde{V}_{+-} \\ \widetilde{V}_{+-} & \widetilde{V}_{--} \end{pmatrix} \tag{B.6}$$

are the K matrix and potential matrix after the rotation. $\widetilde{V}_{++} = \frac{1}{8}(V_{11} + V_{22} + 2V_{12})$, $\widetilde{V}_{--} = \frac{1}{8}(V_{11} + V_{22} - 2V_{12})$ and $\widetilde{V}_{+-} = \frac{1}{8}(V_{11} - V_{22})$. $\widetilde{V}_{++}, \widetilde{V}_{--} > 0$ by positive-

definiteness of the potential matrix.

To proceed, we first assume that ϕ_1 and ϕ_2 are equilibrated so they have the same effective velocity, $V_{11} = V_{22}$, in Subsection B.1. Tunneling exponents in this case can be obtained analytically. In Subsection B.2, we will also consider the case when edge velocities are not the same, in which tunneling exponents are studied numerically. Subsection B.3, we study the influence of the underlying $\nu = 2$ integer quantum Hall (IQH) edge on tunneling exponents. We show that the interaction between IQH edge and the 331 edge does not change the behaviors of tunneling exponents qualitatively.

B.1 Equilibrated fractional edge modes

In this case, we have $\widetilde{V}_{+-} = 0$ and hence a diagonal potential matrix $\widetilde{V}$. Let us introduce Coulomb interaction which couples total charge densities between two semi-infinite spatial pieces, which simulates the effect of unscreened Coulomb interaction across a narrow QPC. This amounts to adding a term

$$\mathcal{L}_c = -4\pi\lambda_c(\rho_{1R} + \rho_{2R})(\rho_{1L} + \rho_{2L}) \tag{B.7}$$

to $\mathcal{L}^W$, where λ_c is a positive real parameter characterizing the strength of repulsive Coulomb interaction. We assume locality of the coupling, which is a legitimate approximation since the interaction of charged density fluctuations is dipolar-natured and dies out fast over distance in the presence of screening. Positive-definiteness of the potential matrix after adding $\mathcal{L}_c$ requires $\lambda_c < \widetilde{V}_{++}$. With bosonization identity $\rho_{IR,L} = \frac{1}{2\pi}(\pm\partial_x\phi_{IR,L} + k_{F,I})$, $I = 1, 2$, the Lagrangian density $\mathcal{L}^N = \mathcal{L}^W + \mathcal{L}_c$ for a narrow QPC is expressed in terms of the K matrix, $\widetilde{K} = \mathrm{Diag}(4, -4, 2, -2)$ and the

potential matrix,

$$\widetilde{V} = 4 \begin{pmatrix} \widetilde{V}_{++} & -\lambda_c & 0 & 0 \\ -\lambda_c & \widetilde{V}_{++} & 0 & 0 \\ 0 & 0 & \widetilde{V}_{--} & 0 \\ 0 & 0 & 0 & \widetilde{V}_{--} \end{pmatrix} \tag{B.8}$$

in the basis $(\phi_{+R}, \phi_{+L}, \phi_{-R}, \phi_{-L})$. To compute correlation functions of tunneling operators and obtain the scaling dimensions, we must simultaneously diagonalize these two matrices so that edge modes completely decouple. It suffices to do so in the subspace (ϕ_{+R}, ϕ_{+L}). With a Bogoliubov transformation

$$\begin{aligned} \tilde{\phi}_{+R} &= \frac{\eta+1}{2\sqrt{\eta}}\phi_{+R} + \frac{\eta-1}{2\sqrt{\eta}}\phi_{+L} \\ \tilde{\phi}_{+L} &= \frac{\eta-1}{2\sqrt{\eta}}\phi_{+R} + \frac{\eta+1}{2\sqrt{\eta}}\phi_{+L}, \end{aligned} \tag{B.9}$$

where $\eta = \sqrt{\frac{1-\lambda_c/\widetilde{V}_{++}}{1+\lambda_c/\widetilde{V}_{++}}}$, $\mathcal{L}^N$ is diagonalized to be

$$\begin{aligned} \mathcal{L}^N = -\frac{1}{4\pi}[&4\partial_t\tilde{\phi}_{+R}\partial_x\tilde{\phi}_{+R} - 4\partial_t\tilde{\phi}_{+L}\partial_x\tilde{\phi}_{+L} + 2\partial_t\phi_{-R}\partial_x\phi_{-R} \\ &- 2\partial_t\phi_{-L}\partial_x\phi_{-L} + 4v(\partial_x\tilde{\phi}_{+R})^2 + 4v(\partial_x\tilde{\phi}_{+L})^2 \\ &+ 4\widetilde{V}_{--}(\partial_x\phi_{-R})^2 + 4\widetilde{V}_{--}(\partial_x\phi_{-L})^2], \end{aligned} \tag{B.10}$$

where $v = \sqrt{\widetilde{V}_{++}^2 - \lambda_c^2}$ is the effective velocity of both new fields $\tilde{\phi}_{+R}$ and $\tilde{\phi}_{+L}$. The edge modes ϕ_{-R}, ϕ_{-L}, $\tilde{\phi}_{+R}$ and $\tilde{\phi}_{+L}$ are all free.

The Lagrangian density $\mathcal{L}^N$ describes the edge dynamics of a narrow QPC in the 331 state only after it is subject to the boundary condition

$$\phi_{\pm R} = \phi_{\pm L} = \phi_{\pm} \tag{B.11}$$

at $x = 0$, which removes redundant degrees of freedom at the tunneling point. We thus have

$$\tilde{\phi}_{+R} = \tilde{\phi}_{+L} \equiv \tilde{\phi}_{+} = \sqrt{\eta}\phi_{+} \tag{B.12}$$

at $x = 0$. The Lagrangian density $\mathcal{L}^W$ for a long line channel is subject to the same boundary condition.

Next, we compute the scaling dimensions of the most relevant tunneling operators in the three QPC geometries. In geometry 2.1a, both the upper and the lower edges are described by the Lagrangian density $\mathcal{L}^N$. In geometry 2.1b, the upper edge is described by $\mathcal{L}^N$ while the lower edge is described by $\mathcal{L}^W$. In geometry 2.1c, both two edges are described by $\mathcal{L}^W$. On the edge of the 331 state, the most relevant quasiparticle operators entering tunneling events are associated with $\pm e/4$ charged quasiparticles, namely, $e^{\pm i\phi_1}$ and $e^{\pm i\phi_2}$. This is true both for a long line channel and for a narrow QPC with unscreened Coulomb interaction, as far as the strength of Coulomb interaction is not too strong. The most relevant tunneling operators between the upper edge u and the lower edge d of the FQH liquid are $e^{\pm i\phi_1^u}e^{\mp i\phi_1^d}$, $e^{\pm i\phi_2^u}e^{\mp i\phi_2^d}$, all with the same scaling dimension. To obtain leading temperature dependence of tunneling current, it suffices to pick one of the most relevant tunneling operators and compute its scaling dimensions in different QPC geometries. We consider $O = e^{i\phi_1^u}e^{-i\phi_1^d}$ which describes the tunneling of quasiparticle $e^{i\phi_1}$. Let us denote O in geometries 2.1a, 2.1b and 2.1c to be O_A, O_B and O_C, respectively, with scaling dimensions g_A, g_B and g_C. Invoking boundary condition at $x = 0$, we rewrite O_A in terms of free fields,

$$O_A = e^{i\frac{1}{\sqrt{2}}\phi_-^u}e^{-i\frac{1}{\sqrt{2}}\phi_-^d}e^{i\frac{1}{\sqrt{2\eta}}\tilde{\phi}_+^u}e^{-i\frac{1}{\sqrt{2\eta}}\tilde{\phi}_+^d}. \tag{B.13}$$

The correlation function

$$\langle O_A^\dagger(t)O_A(0)\rangle = e^{\frac{1}{2}\langle\phi_-^u(t)\phi_-^u(0)\rangle}e^{\frac{1}{2}\langle\phi_-^d(t)\phi_-^d(0)\rangle}e^{\frac{1}{2\eta}\langle\tilde{\phi}_+^u(t)\tilde{\phi}_+^u(0)\rangle}e^{\frac{1}{2\eta}\langle\tilde{\phi}_+^d(t)\tilde{\phi}_+^d(0)\rangle} \tag{B.14}$$

can be evaluated with the diagonalized $\mathcal{L}^N$ to give $g_A = \frac{1}{4} + \frac{1}{8\eta}$. Similarly, we rewrite O_B as

$$O_B = e^{i\frac{1}{\sqrt{2}}\phi_-^u}e^{-i\frac{1}{\sqrt{2}}\phi_-^d}e^{i\frac{1}{\sqrt{2\eta}}\tilde{\phi}_+^u}e^{-i\frac{1}{\sqrt{2}}\phi_+^d}, \tag{B.15}$$

whose correlation function is

$$\langle O_B^\dagger(t)O_B(0)\rangle = e^{\frac{1}{2}\langle\phi_-^u(t)\phi_-^u(0)\rangle}e^{\frac{1}{2}\langle\phi_-^d(t)\phi_-^d(0)\rangle}e^{\frac{1}{2\eta}\langle\tilde{\phi}_+^u(t)\tilde{\phi}_+^u(0)\rangle}e^{\frac{1}{2}\langle\phi_+^d(t)\phi_+^d(0)\rangle}. \tag{B.16}$$

The correlation functions of $\phi_\pm^d$ are computed with $\mathcal{L}^W$ while those of ϕ_-^u and $\tilde{\phi}_+^u$ are computed with $\mathcal{L}^N$. The scaling dimension is evaluated to be $g_B = \frac{5}{16} + \frac{1}{16\eta}$. In geometry 2.1c, the tunneling operator is

$$O_C = e^{i\frac{1}{\sqrt{2}}\phi_-^u}e^{-i\frac{1}{\sqrt{2}}\phi_-^d}e^{i\frac{1}{\sqrt{2}}\phi_+^u}e^{-i\frac{1}{\sqrt{2}}\phi_+^d}. \tag{B.17}$$

The correlation function is

$$\langle O_C^\dagger(t)O_C(0)\rangle = e^{\frac{1}{2}\langle\phi_-^u(t)\phi_-^u(0)\rangle}e^{\frac{1}{2}\langle\phi_-^d(t)\phi_-^d(0)\rangle}e^{\frac{1}{2}\langle\phi_+^u(t)\phi_+^u(0)\rangle}e^{\frac{1}{2}\langle\phi_+^d(t)\phi_+^d(0)\rangle} \tag{B.18}$$

and the scaling dimension is $g_C = \frac{3}{8}$.

Lastly, we verify that the general discussion in Sec. II holds for the 331 state so that the scaling dimensions computed above are indeed the tunneling exponents in respective QPC geometries. The total electron number operator on the upper edge

of the 331 state is

$$N^u = \frac{\sqrt{2}}{2\pi}\int dx\partial_x\phi_+^u + \frac{1}{2\pi}(k_{F,1}^u + k_{F,2}^u)L. \tag{B.19}$$

Substituting N^u into Eq. (1.99) and using $[\phi_+^\mu(x), \phi_+^\nu(x')] = i\pi\frac{1}{4}\mathrm{sgn}(x-x')\delta^{\mu\nu}$, $[\phi_-^\mu(x), \phi_-^\nu(x')] = i\pi\frac{1}{2}\mathrm{sgn}(x-x')\delta^{\mu\nu}$ and $[\phi_+(x), \phi_-(x')] = 0$, where $\mu, \nu = u, d$, we recover the expressions of tunneling current operator and tunneling current in Eqs. (1.100) and (1.103).

As we see, the tunneling exponents in geometries 2.1a and 2.1b due to the tunneling of quasiparticle $e^{i\phi_1}$ depend on the velocity V_{11} of ϕ_1 edge, the interaction V_{12} between two edges and the unscreened Coulomb interaction λ_c across the QPC. Specifically, they are functions of $\lambda_c/\widetilde{V}_{++}$, which is the reduced strength of unscreened Coulomb interaction valued in unit of $\widetilde{V}_{++}$. On an edge with large velocity, quasiparticles move fast and do not feel appreciably the Coulomb interaction across the QPC, which obstructs their tunnelings. In the extreme case when edge velocity $V_{11} \to \infty$, quasiparticle dynamics and tunneling are completely unaffected by Coulomb interaction and we have $g_A = g_B = \frac{3}{8}$. In Fig. B.1, we plot tunneling exponents in three QPC geometries as functions of $\lambda_c/\widetilde{V}_{++}$. By fixing $\widetilde{V}_{++}$, we focus on the effect of unscreened Coulomb interaction only. We immediately observe from g_A and g_B that tunneling exponents are increased by Coulomb interaction. On the contrary, g_C remains unchanged as geometry 2.1c involves no narrow QPCs. In addition, the tunneling exponent g_B in geometry 2.1b is the arithmetic mean of the tunneling exponent g_A in geometry 2.1a and the tunneling exponent g_C in geometry 2.1c, which agrees with measurements in tunneling experiments, such that the effect of Coulomb interaction depends additively on the number of narrow QPCs in the geometry. The divergent behaviors of tunneling exponents near $\lambda_c/\widetilde{V}_{++} = 1$ should not be a concern, as our discussion has always been limited to the regime of weak Coulomb interac-

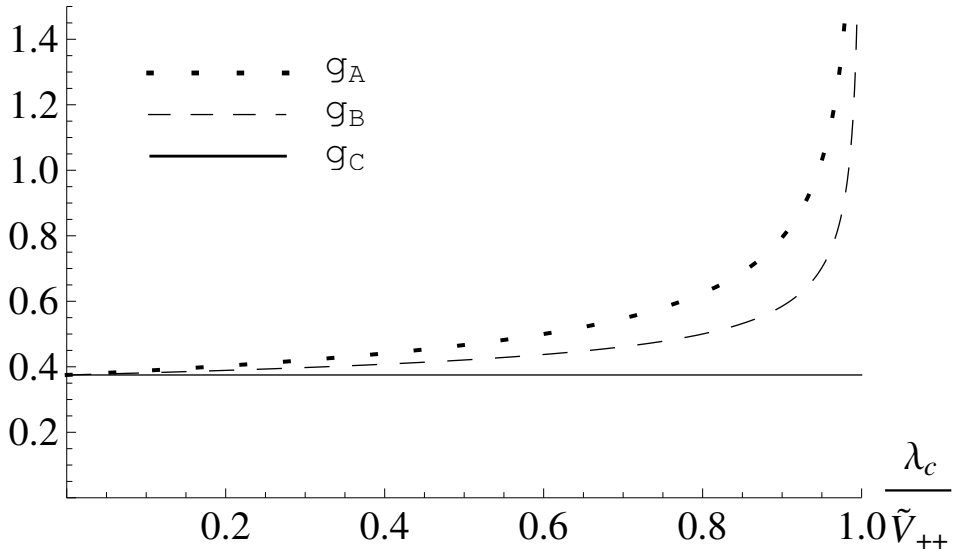

Figure B.1: Tunneling exponents as functions of the reduced strength of unscreened Coulomb interaction (horizontal axis) in the 331 state. $\lambda_c = 0$ and $\lambda_c/\widetilde{V}_{++} = 1$ correspond to vanishing and infinitely strong Coulomb interaction, respectively. At $\lambda_c = 0$, $g_A = g_B = g_C = \frac{3}{8}$.

tion. For a very strong Coulomb interaction, the physics near the QPC may be tremenously altered that a Luttinger liquid theory is no longer a valid description. Locating experimentally measured g_A, g_B on the plots, we find they correspond to $\lambda_c/\widetilde{V}_{++} \sim 0.44, 0.49$, respectively. Hence, the measurements in geometries 2.1a and 2.1b can be explained as obtained in the 331 state under weak unscreened Coulomb interaction across narrow QPCs.

B.2 Non-equilibrated fractional edge modes

In the absence of edge mode equilibration, the effective velocities of ϕ_1 and ϕ_2 do not equal and we have nonvanishing velocity anisotropy, $\widetilde{V}_{+-} \neq 0$. In the basis

$(\phi_{+R}, \phi_{+L}, \phi_{-R}, \phi_{-L})$, the potential matrix is

$$\widetilde{V} = 4 \begin{pmatrix} \widetilde{V}_{++} & -\lambda_c & \widetilde{V}_{+-} & 0 \\ -\lambda_c & \widetilde{V}_{++} & 0 & \widetilde{V}_{+-} \\ \widetilde{V}_{+-} & 0 & \widetilde{V}_{--} & 0 \\ 0 & \widetilde{V}_{+-} & 0 & \widetilde{V}_{--} \end{pmatrix}. \tag{B.20}$$

Tunneling exponents in this case are functions of four parameters: $\widetilde{V}_{++}, \widetilde{V}_{--}, \widetilde{V}_{+-}$ and λ_c. We are primarily interested in three physical linear combinations of these parameters: the mutual interaction V_{12} between two edge modes, the velocity anisotropy $\widetilde{V}_{+-}$ and the unscreened Coulomb interaction λ_c. Below, we study numerically how they affect the tunneling of quasiparticle $e^{i\phi_1}$ in geometry 2.1a. Their effects on tunneling in geometry 2.1b are the same as in geometry 2.1a, but are halfly pronounced. We show that despite various parameters in the potential matrix, (1) the smallest possible value that can be achieved for tunneling exponent g_A is $\frac{3}{8}$, and (2) given fixed other parameters, g_A always increases monotonically as λ_c increases.

As we have seen in the case of equilibrated edges, tunneling exponents diverge when unscreened Coulomb interaction λ_c is too strong to destroy the positive-definiteness of potential matrix. This is also true in the case of non-equilibrated edges. Our discussion must be limited to the situation when the smallest eigenvalue of potential matrix is positive. We ensure this by requiring

$$\lambda_c < \widetilde{V}_{++} - \frac{\widetilde{V}_{+-}^2}{\widetilde{V}_{--}}. \tag{B.21}$$

We first study g_A as a function of the mutual interaction and unscreened Coulomb interaction, at given velocity anisotropy. Noticing the fact that prefactors of the potential matrix do not enter tunneling exponents, we factor an energy scale V_0 out of

the potential matrix so that g_A can be viewed as a function of dimensionless reduced parameters valued in unit of V_0: $\widetilde{V}^r_{++} = \widetilde{V}_{++}/V_0$, $\widetilde{V}^r_{--} = \widetilde{V}_{--}/V_0$, $\widetilde{V}^r_{+-} = \widetilde{V}_{+-}/V_0$ and $\lambda^r_c = \lambda_c/V_0$. Also, $V^r_{12} = V_{12}/V_0$. Then we set a constraint

$$\widetilde{V}^r_{++} = 1 + \frac{(\widetilde{V}^r_{+-})^2}{\widetilde{V}^r_{--}} \tag{B.22}$$

on parameters such that as long as $\lambda^r_c < 1$, Eq. (B.21) is satisfied. The constraint removes one independent parameter in g_A so that at fixed $\widetilde{V}^r_{+-}$, $\widetilde{V}^r_{++}$ and hence V^r_{12} decrease as $\widetilde{V}^r_{--}$ grows. Then, tuning $\widetilde{V}^r_{--}$ is equivalent to tuning V^r_{12} and we can study g_A as a function of V^r_{12} and λ^r_c, as shown in Fig. B.2(a) where we set $\widetilde{V}^r_{+-} = 1$. First, we plot the $\lambda^r_c = 0$ cut of Fig. B.2(a) in Fig. B.2(b), where g_A is a function of $\widetilde{V}^r_{--}$ (V^r_{12}). We see that g_A is a flat line with height $\frac{3}{8}$. This is expected because when $\lambda^r_c = 0$, the only remaining interaction V_{12} couples edge modes propagating in the same direction. g_A in this case is universal and is independent of V_{12}. Next, we look at g_A as a function of $\widetilde{V}^r_{--}$ at nonvanishing Coulomb interaction. Fig. B.2(c) shows the $\lambda^r_c = 0.5$ cut of Fig. B.2(a). A minimum of g_A at intermediate strength of interaction $\widetilde{V}^r_{--}$ is observed. Such a minimum is a common behavior of tunneling exponents when there is interaction coupling counterpropagating edge modes entering the tunneling operator. The g_A minima at various λ^r_c values define the "valley" in Fig. B.2(a). We inspect the suspicious valley to make sure it does not contain g_A values below $\frac{3}{8}$. In Fig. B.2(d), we plot the cut of Fig. B.2(a) inside the valley, as well as two cuts parallel and close to but outside the valley. We see that inside the valley, g_A starts from $\frac{3}{8}$ at $\lambda^r_c = 0$ and increases monotonically as λ^r_c grows, although not as fast as g_A along the cuts outside the valley. Hence, we have confirmed Statements (1)(2) in Fig. B.2(a). In general, at any given velocity anisotropy $\widetilde{V}^r_{+-}$, both statements can be verified, despite that the location of g_A minima valley may change.

To study g_A as a function of the velocity anisotropy and unscreened Coulomb

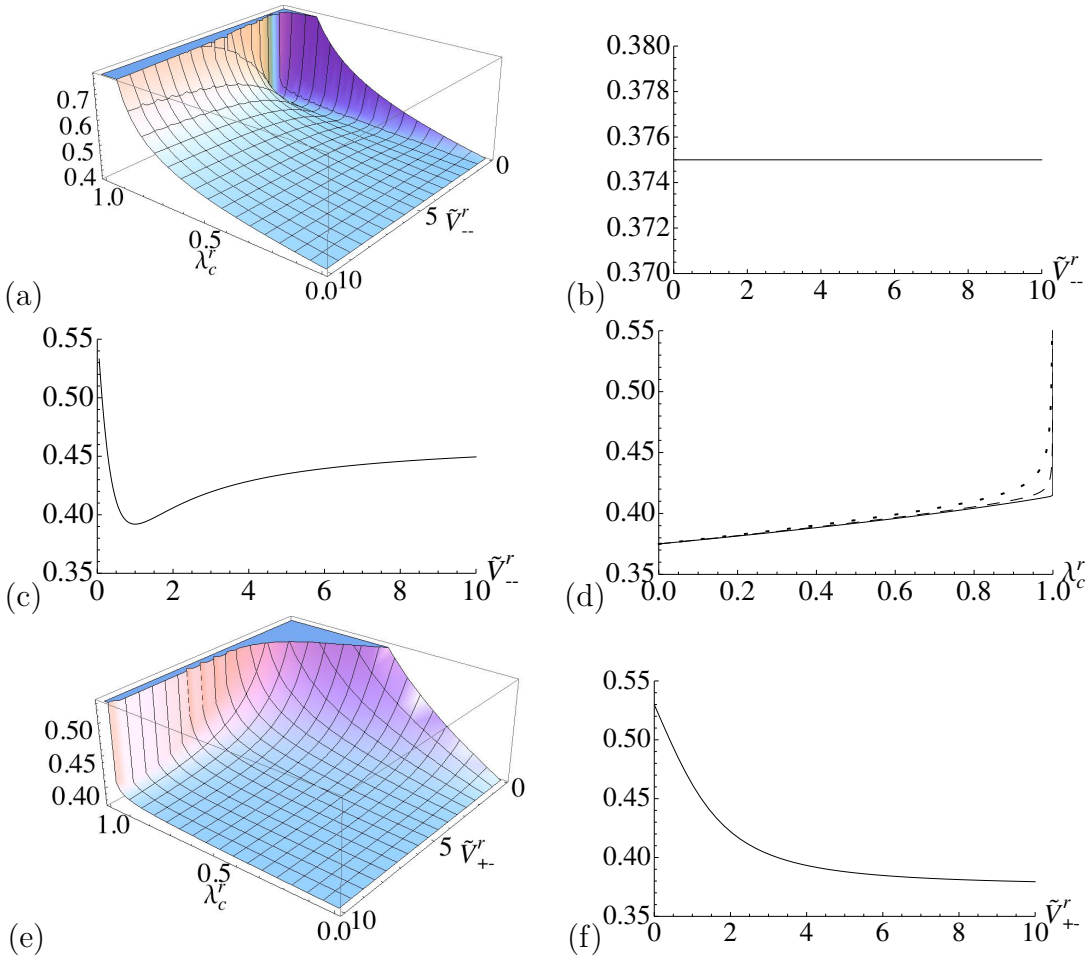

Figure B.2: The tunneling exponent in geometry 2.1a in the absence of edge equilibration: (a) as a function of $\widetilde{V}_{--}^r$ (V_{12}^r) and λ_c^r, at $\widetilde{V}_{+-}^r = 1$; (b) $\lambda_c^r = 0$ cut in (a); (c) $\lambda_c^r = 0.5$ cut in (a); (d) Inside (solid) and near (dashed and dotted) the "valley" in (a), with dotted line more outside; (e) as a function of $\widetilde{V}_{+-}^r$ and λ_c^r, at $V_{12}^r = 10$; (f) $\lambda_c^r = 0.5$ cut in (e).

interaction, we fix $V_{12}^r = 2(\widetilde{V}_{++}^r - \widetilde{V}_{--}^r)$, in addition to Eq. (B.22). In Fig. B.2(e), we plot g_A as a function of $\widetilde{V}_{+-}^r$ and λ_c^r, at $V_{12}^r = 10$. Along any constant-$\widetilde{V}_{+-}^r$ cut, g_A increases monotonically as λ_c^r grows. The global minima of g_A occur at vanishing Coulomb interaction $\lambda_c^r = 0$, or when $\widetilde{V}_{+-}^r \to \infty$. Since both edge velocities $V_{11}, V_{22} > 0$, the latter case implies an infinite velocity V_{11} on ϕ_1 edge. In such a case, quasiparticles on ϕ_1 edge move so fast that they behave and tunnel as if they did not feel Coulomb interaction across the QPC. In Fig. B.2(f), we plot the $\lambda_c^r = 0.5$ cut of Fig. B.2(e), which clearly shows the effect of edge velocity on quasiparticle tunneling. The larger the $\widetilde{V}_{+-}^r$, the slower the rate of growth of g_A with increasing λ_c^r. As $\widetilde{V}_{+-}^r \to \infty$, $g_A \to \frac{3}{8}$.

From above analysis, we see that Statements (1)(2) are satisfied regardless of the velocities and the interaction of two edge modes in the 331 state. The absence of equilibration on the edge of the 331 state does not invalidate the fact that we can attribute the larger measurements in geometries 2.1a and 2.1b to the effect of unscreened Coulomb interaction across narrow QPCs.

B.3 Influence of integer edge modes

We study the influence of $\nu = 2$ IQH edge on tunneling. We still consider the tunneling of quasiparticle $e^{i\phi_1}$. Let Φ_1, Φ_2 be the two integer modes on IQH edge. To reduce the number of parameters in discussion while keeping essential physics, we assume equilibrated integer edge modes at the same velocity v_Φ and equilibrated fractional edge modes in the 331 state, $V_{11} = V_{22}$. The Lagrangian density for $\nu = 2$

IQH edge is

$$\mathcal{L}_{\Phi} = -\frac{1}{4\pi}[\sum_{I=1,2}(\partial_t \Phi_I \partial_x \Phi_I + v_{\Phi}\partial_x \Phi_I \partial_x \Phi_I) + 2v_{\Phi 1\Phi 2}\partial_x \Phi_1 \partial_x \Phi_2], \tag{B.23}$$

where $v_{\Phi 1\Phi 2}$ is the effective interaction between Φ_1, Φ_2. We also assume that the interaction between IQH edge and the 331 edge is Coulomb-natured, which couples total electron densities on respective edges. The corresponding Lagrangian density is

$$\mathcal{L}_{\phi\Phi} = -4\pi V_{\phi\Phi}(\rho_1 + \rho_2)(\rho_{\Phi_1} + \rho_{\Phi_2}), \tag{B.24}$$

where $V_{\phi\Phi}$ characterizes the strength of interaction, $\rho_{\Phi_I} = \frac{1}{2\pi}(\partial_x \Phi_I + k_{F,\Phi_I})$ with k_{F,Φ_I} the Fermi momentum of Φ_I and $I = 1, 2$. To discuss physics at a narrow QPC, we break integer modes into two spatial pieces with respect to tunneling point by defining $\Phi_{IR}(x) = \Phi_I(x)$ and $\Phi_{IL}(x) = \Phi_I(-x)$ for $x \leq 0$, with boundary condition $\Phi_{IR}(x = 0) = \Phi_{IL}(x = 0) = \Phi_I(x = 0)$. The long-range unscreened Coulomb interaction across the QPC couples total electron densities between the two spatial pieces, with a Lagrangian density

$$\mathcal{L}_c = -4\pi\lambda_c(\rho_{1R} + \rho_{2R} + \rho_{\Phi_1 R} + \rho_{\Phi_2 R})(\rho_{1L} + \rho_{2L} + \rho_{\Phi_1 L} + \rho_{\Phi_2 L}), \tag{B.25}$$

where λ_c characterizes the strength of unscreened Coulomb interaction. Physically, $0 < \lambda_c < V_{\phi\Phi}$. It is convenient to define $\Phi_{\pm} = \frac{1}{\sqrt{2}}(\Phi_1 \pm \Phi_2)$, and its split modes $\Phi_{\pm R,L}$ with respect to tunneling point. The K matrix $\widetilde{K}$ and potential matrix $\widetilde{V}$ for a narrow QPC are $\widetilde{K} = \mathrm{Diag}(4, -4, 1, -1) \oplus \mathrm{Diag}(2, -2, 1, -1)$ and

$$\frac{\widetilde{V}}{4} = \begin{pmatrix} \widetilde{V}_{++} & -\lambda_c & V_{\phi\Phi} & -\lambda_c \\ -\lambda_c & \widetilde{V}_{++} & -\lambda_c & V_{\phi\Phi} \\ V_{\phi\Phi} & -\lambda_c & v_+ & -\lambda_c \\ -\lambda_c & V_{\phi\Phi} & -\lambda_c & v_+ \end{pmatrix} \oplus \mathrm{Diag}(\widetilde{V}_{--}, \widetilde{V}_{--}, v_-, v_-) \tag{B.26}$$

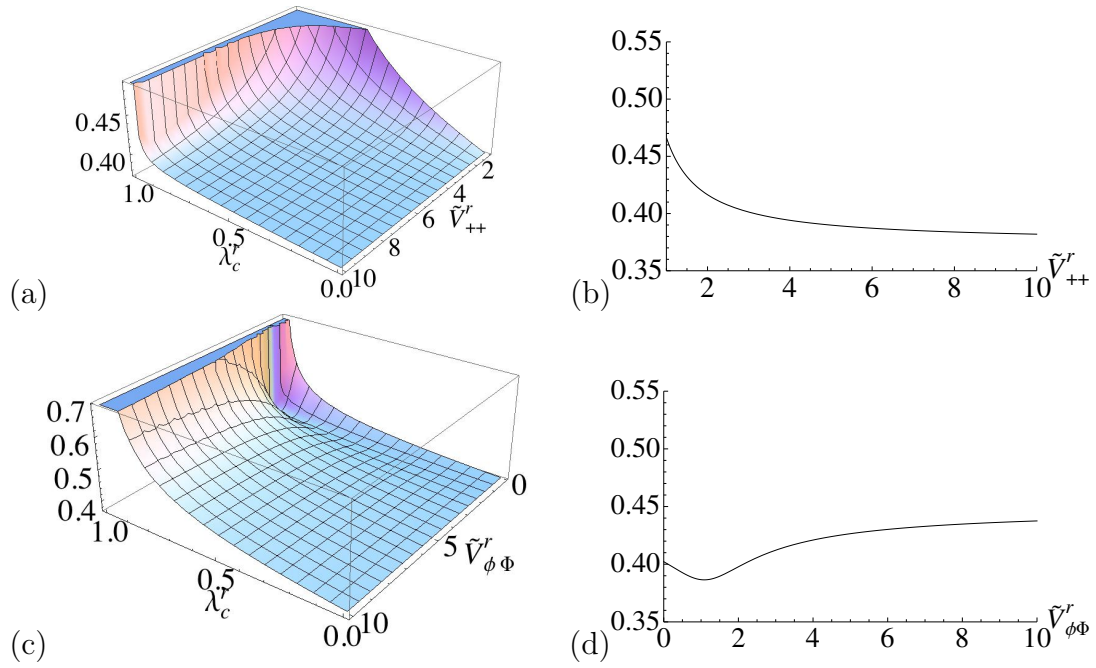

Figure B.3: The tunneling exponent in geometry 2.1a in the presence of $\nu = 2$ IQH edge: (a) as a function of $\widetilde{V}_{++}^r$ and λ_c^r, at $V_{\phi\Phi}^r = 2$; (b) $\lambda_c^r = 0.5$ cut in (a); (c) as a function of $V_{\phi\Phi}^r$ and λ_c^r, at $(\widetilde{V}_{++}^r - v_+^r) = 2$; (d) $\lambda_c^r = 0.5$ cut in (c).

in basis $(\phi_{+R}, \phi_{+L}, \Phi_{+R}, \Phi_{+L}) \oplus (\phi_{-R}, \phi_{-L}, \Phi_{-R}, \Phi_{-L})$, where $v_\pm = \frac{1}{4}(v_\Phi \pm v_{\Phi 1 \Phi 2}) > 0$. Positive-definiteness of the potential matrix requires

$$\lambda_c < \frac{\widetilde{V}_{++} v_+ - V_{\phi\Phi}^2}{\widetilde{V}_{++} + v_+ - 2V_{\phi\Phi}}. \tag{B.27}$$

By further assuming that the interaction between integer modes on IQH edge and the interaction between fractional modes on the 331 edge are of the same strength, $v_{\Phi 1 \Phi 2} = V_{12}$, we study tunneling exponent g_A as a function of three physical parameters: the velocity difference $(\widetilde{V}_{++} - v_+)$ and Coulomb interaction $V_{\phi\Phi}$ between IQH edge and the 331 edge, plus the unscreened Coulomb interaction λ_c. For convenience, we again introduce reduced parameters valued in unit of an energy scale V_0: $\widetilde{V}_{++}^r = \widetilde{V}_{++}/V_0$, $v_+^r = v_+/V_0$, $V_{\phi\Phi}^r = V_{\phi\Phi}/V_0$, $\lambda_c^r = \lambda_c/V_0$, and set

$$(\widetilde{V}_{++}^r - 1)(v_+^r - 1) = (V_{\phi\Phi}^r - 1)^2, \tag{B.28}$$

so that Eq. (B.27) is satisfied for $\lambda_c^r < 1$, and that at fixed $V_{\phi\Phi}^r$, $(\widetilde{V}_{++}^r - v_+^r)$ increases as $\widetilde{V}_{++}^r$ grows. Hence, tuning $\widetilde{V}_{++}^r$ is equivalent to tuning the velocity difference. In Fig. B.3(a), we plot g_A as a function of $\widetilde{V}_{++}^r$ and λ_c^r, at $V_{\phi\Phi}^r = 2$. The fact that $v_+^r > 0$ restricts the range of plot to $\widetilde{V}_{++}^r > 1$. We find that along any constant-$\widetilde{V}_{++}^r$ cut, g_A increases monotonically as λ_c^r grows, with global minima occurring at $\lambda_c^r = 0$ or as $\widetilde{V}_{++}^r$ (or the velocity difference) goes to infinity. Since edge velocities v_Φ, $V_{11} = V_{22} > 0$, the latter case corresponds to an infinite velocity V_{11} of edge ϕ_1 on which the dynamics and tunneling of quasiparticle $e^{i\phi_1}$ are no longer affected by Coulomb interaction across the QPC. Alternatively, we can rewrite $e^{i\phi_1}$ as $e^{i\frac{1}{\sqrt{2}}\phi_-}e^{i\frac{1}{\sqrt{2}}\phi_+}$ and view its tunneling as the combined tunneling of "neutral" quasiparticle $e^{i\frac{1}{\sqrt{2}}\phi_-}$ on unphysical ϕ_- edge at velocity $\widetilde{V}_{--}$ and "charged" quasiparticle $e^{i\frac{1}{\sqrt{2}}\phi_+}$ on unphysical ϕ_+ edge at velocity $\widetilde{V}_{++}$. The tunneling of $e^{i\frac{1}{\sqrt{2}}\phi_-}$ is universal, unaffected by unscreened Coulomb interaction. The tunneling of $e^{i\frac{1}{\sqrt{2}}\phi_+}$ however depends on various parameters $\widetilde{V}_{++}$, v_+, $V_{\phi\Phi}$, λ_c in the potential matrix. Nonetheless, as the velocity of ϕ_+ edge becomes extremely large, quasiparticles on the edge become insensitive to unscreened Coulomb interaction and their tunnelings become universal as well. The combined universal tunneling of quasiparticle $e^{i\frac{1}{\sqrt{2}}\phi_-}$ and $e^{i\frac{1}{\sqrt{2}}\phi_+}$ give rise to the universal global minima of g_A. In Fig. B.3(b), we plot the $\lambda_c^r = 0.5$ cut of Fig. B.3(a). We see that g_A saturates to $\frac{3}{8}$ as $\widetilde{V}_{++}^r \to \infty$. Fig. B.3(c) shows g_A as a function of $V_{\phi\Phi}^r$ and λ_c^r, at fixed velocity difference $(\widetilde{V}_{++}^r - v_+^r) = 2$. When $\lambda_c^r = 0$, $g_A = \frac{3}{8}$. A valley of g_A minima appears at intermediate strength of interaction $V_{\phi\Phi}^r$ between IQH edge and the 331 edge, similar to the one observed in Fig. B.2(a) when we study non-equilibrated 331 edge, along which no values of g_A below $\frac{3}{8}$ are found. Given fixed $V_{\phi\Phi}^r$, g_A grows monotonically with λ_c^r. In Fig. B.3(d), we plot the $\lambda_c^r = 0.5$ cut of Fig. B.3(c).

In the most general case, more independent parameters show up in the potential

matrix. The velocity difference between fractional modes on the 331 edge couples subspaces (ϕ_{+R}, ϕ_{+L}) and (ϕ_{-R}, ϕ_{-L}), as we have seen in the previous discussion. The velocity difference between integer modes on IQH edge couples subspaces (Φ_{+R}, Φ_{+L}) and (Φ_{-R}, Φ_{-L}). A more general form of the interaction between IQH edge and the 331 edge than the one in Eq. (B.24) gives rise to off-diagonal elements coupling subspaces (ϕ_{+R}, ϕ_{+L}) and (Φ_{-R}, Φ_{-L}), subspaces (ϕ_{-R}, ϕ_{-L}) and (Φ_{+R}, Φ_{+L}), and subspaces (ϕ_{-R}, ϕ_{-L}) and (Φ_{-R}, Φ_{-L}). However, all such couplings enter the potential matrix in mathematically the same way as $\widetilde{V}_{+-}$ entering the potential matrix in Eq. (B.20). We hence expect their effects on tunneling exponents to be similar to those observed in Fig. B.2. In general, we conclude that unscreened Coulomb interaction across the QPC always results in larger measured tunneling exponents and that tunneling exponents can never be driven to below the universal value $\frac{3}{8}$ by various interactions. The presence of $\nu = 2$ IQH edge does not affect our interpretation of tunneling exponents in different QPC geometries.

Appendix C

Zero Modes in a System of Interacting Majorana Fermions

In this appendix, we provide a detailed analysis of the zero modes in a system of interacting Majorana fermions.

C.1 Inner product of operators

We first introduce the notion of the inner product of operators, constructed from Majorana fermions. This notion is used in Sections 5.4 and 5.5 and Sections C.2 and C.3.

We consider $2N+2$ Majorana fermions $\gamma_0, \dots \gamma_{2N}$ and f. They act in the Hilbert space of dimension $D = 2^{N+1}$. One can also associate this set of Majoranas with two linear spaces of operators. The space $L_{\rm even}$ includes all Hermitian operators that express as linear combinations of products of even numbers of the operators γ_i. We will denote such products as $E_{\{k_l\}} = E_{k_1,\dots,k_{2n}} = i^n \Pi_{j=1}^{2n} \gamma_{k_j}$, where $n = 0, \dots, N$ and $k_1 < k_2 < \dots < k_{2n}$. The product of zero γ's is defined as $E = 1$. Any vector in $L_{\rm even}$ can be represented as $\sum_{n=0}^{N} \sum_{k_1,\dots,k_{2n}} a_{k_1,\dots,k_{2n}} E_{k_1,\dots,k_{2n}}$. We prove below that $E_{k_1,\dots,k_{2n}}$ form a basis in $L_{\rm even}$. Note that the operator f does not enter any of the expressions for $E_{k_1,\dots,k_{2n}}$. Note also that the Hamiltonian of the qbit is a vector in the space $L_{\rm even}$.

The space of fermionic Hermitian operators $L_{\rm odd}$ is constructed in a similar way. The only difference is that any vector in $L_{\rm odd}$ is a linear combination of the products $O_{\{k_l\}} = O_{k_1,\dots,k_{2n+1}} = i^n \gamma_{k_{2n+1}} \Pi_{j=1}^{2n} \gamma_{k_j}$ of odd numbers of the Majorana operators γ_{k_j}, $k_1 < \dots < k_{2n+1}$.

Consider two vectors in the space L_{even}:

$$A = \sum_n \sum_{k_1,\ldots,k_{2n}} a_{k_1,\ldots,k_{2n}} E_{k_1,\ldots,k_{2n}} \quad \text{and}$$
$$B = \sum_n \sum_{k_1,\ldots,k_{2n}} b_{k_1,\ldots,k_{2n}} E_{k_1,\ldots,k_{2n}}. \tag{C.1}$$

We define their inner product as

$$(A, B) = \mathrm{Tr} AB/2^{N+1}. \tag{C.2}$$

It is easy to see that the product is positive definite and satisfies all other requirements for an inner product in a Euclidean space.

Let us check that $(E_\alpha, E_\beta) = \delta_{\alpha,\beta}$, where $\delta_{\alpha,\beta} = 1$, if the sets of the indices α and β are identical, and $\delta_{\alpha,\beta} = 0$ otherwise. This statement is equivalent to the requirement that

$$\mathrm{Tr} E_{k_1,\ldots,k_{2n}} = 2^{N+1}\delta_{n,0}. \tag{C.3}$$

Proving (C.3) is easy. It follows immediately after we construct the complex fermions $c_m = (\gamma_{k_{2m-1}} + i\gamma_{k_{2m}})/2$ and rewrite $E_{k_1,\ldots,k_{2n}}$ as $\Pi_{m=1}^{n}(2c_m^\dagger c_m - 1)$.

We have thus proved that the Hermitian operators $E_{k_1,\ldots,k_{2n}}$ form an orthonormal basis in the space L_{even}. It then follows that the coefficients $a_{k_1,\ldots,k_{2n}}$ and $b_{k_1,\ldots,k_{2n}}$ in the expansions (C.1) of the Hermitian operators A and B must be real. We also get a simple expression for the inner product in terms of the coordinates: $(A, B) = \sum a_{k_1,\ldots,k_{2n}} b_{k_1,\ldots,k_{2n}}$.

The definition of the inner product in the space $L_{\rm odd}$ is the same: If

$$A = \sum_n \sum_{k_1,\ldots,k_{2n+1}} a_{k_1,\ldots,k_{2n+1}} O_{k_1,\ldots,k_{2n+1}} \quad \text{and}$$
$$B = \sum_n \sum_{k_1,\ldots,k_{2n+1}} b_{k_1,\ldots,k_{2n+1}} O_{k_1,\ldots,k_{2n+1}} \tag{C.4}$$

then

$$(A,B) = {\rm Tr} AB/2^{N+1} = \sum a_{k_1,\ldots,k_{2n+1}} b_{k_1,\ldots,k_{2n+1}}. \tag{C.5}$$

Just as above, the Hermitian operators $O_{\{k_l\}}$ form an orthonormal basis in the Euclidean space $L_{\rm odd}$ and the coordinates $a_{\{k_l\}}$, $b_{\{k_l\}}$ are always real.

C.2 Classification of zero modes

We are looking for Hermitian operators $F = F^\dagger$ that commute with the Hamiltonian H and anticommute with the Fermi operator f which creates excitations far away from the Majorana modes γ_i.

Clearly,

$$F = P(H)\Gamma, \tag{C.6}$$

where $P(H)$ is an arbitrary polynomial of the Hamiltonian and $\Gamma = i^N \Pi_{k=0}^{2N} \gamma_k$ the local parity operator, are integrals of motion that satisfy Fermi statistics. For some Hamiltonians, additional fermionic zero modes are possible. For example, any fermionic operator commutes with the Hamiltonian, if $H = 0$. We show below that for a typical Hamiltonian all fermionic zero modes have the form (C.6) and exactly 2^N of such modes are linear independent. Those statements do not hold for a zero-measure set of Hamiltonians only.

It was stated in Ref. [148] that there are exactly 2^N fermionic zero modes in the absence of interactions and for infinitesimal interactions. Here we find the number of the zero modes for an arbitrary interaction strength. We also give an explicit formula for all integrals of motion.

We first prove the existence of 2^N linear independent integrals of motion of the form (C.6). This is equivalent to finding 2^N linear independent polynomials $P(H)$. We show below that the appropriate polynomials are $P(H) = H^k$ with $k = 0, 1, \ldots, 2^N - 1$.

We start with an example. Let the Hamiltonian be

$$H = \sum_{n=0}^{N} \sum_{0<k_1<k_2<\cdots<k_n<N+1} u_{k_1,\ldots,k_n} \Pi_{j=1}^{n} \alpha_{k_j}, \tag{C.7}$$

where $u_{\{k_l\}}$ are constants and $\alpha_k = i\gamma_{2k-1}\gamma_{2k}$. Note that all α_k commute with each other and square to 1. Hence, the multiplicative group G of all possible products of several operators α_k is $G = \mathbb{Z}_2^N$. The identity operator plays the role of the identity element in the group. The Hamiltonian H is an element of the group algebra $R[G]$ of G. The same is true for any polynomial $P(H)$. The Abelian group G has dim $G = 2^N$ one-dimensional representations R_k, $k = 1, \ldots, 2^N$, whose characters are ± 1. Thus, the group can be faithfully represented by $2^N \times 2^N$ diagonal matrices $M(g_s)$, $g_s \in G$, whose nonzero entries $M_{kk}(g_s)$ equal the characters of the elements of G in the representation R_k. In such representation, H becomes a diagonal matrix whose diagonal elements H_{jj} are linear combinations $\sum_n \sum_{0<k_1<k_2<\cdots<k_n<N+1} \pm u_{k_1,\ldots,k_n}$ with a different set of signs in front of the variables $u_{k_1,\ldots,k_n}$ for each j. For almost any choice of H, all 2^N entries H_{jj} are different from each other. Consider now an arbitrary linear combination $\sum_{k=0}^{2^N-1} c_k H^k = Q(H) \neq 0$, where the degree of the polynomial $Q(x) = \sum c_k x^k$ is $2^N - 1$ or lower. $Q(H)$ is a diagonal matrix with the entries $Q(H_{jj})$.

They could be simultaneously zero only if all the numbers H_{jj} were the roots of $Q(x)$, in contradiction with the fundamental theorem of algebra. Hence, $Q(H) \neq 0$. This proves that the operators H^k, $k = 0, \ldots, 2^N - 1$ are linear independent.

So far the desired property of linear independence was established for a special class of Hamiltonians (C.7) only. We now demonstrate that the result for this special class implies the general statement. Indeed, any Hamiltonian H can be seen as a vector in the space L_{even} (Section C.1) and is defined by its 2^{2N} coordinates $a_{\{k_l\}}$ in the basis $E_{\{k_l\}}$ (see Section C.1 for details). The components of any power H^k in the same basis are polynomials of $a_{\{k_l\}}$. Let us write the components of the vectors H^k, $k = 0, \ldots, 2^N - 1$ in the form of a $2^N \times 2^{2N}$ matrix T. The coordinates of any of the 2^N vectors H^k form one row of the matrix. Let us first select an arbitrary Hamiltonian H_1 of the form (C.7). Then the rank of the matrix T is 2^N since all of its rows are linear independent. Hence, T has a nonzero minor M_T of size 2^N. Let us now consider an arbitrary Hamiltonian H. We form the matrix T and compute exactly the same minor as for H_1, i.e., select the same columns that form M_T and compute the determinant of the square matrix, formed by those 2^N columns. We obtain a polynomial of $a_{\{k_l\}}$. We know that the minor is nonzero for one particular choice of the variables $a_{\{k_l\}}$. Since it is a polynomial, it follows that it is nonzero for almost any other choice. Thus, the rank of the matrix T is 2^N almost everywhere and hence the 2^N operators H^k are linear independent indeed.

We need to prove the converse statement now: almost all Hamiltonians have no more than 2^N fermionic zero modes. We will prove instead that there are no more than 2^N bosonic modes. This is enough since multiplying Hermitian bosonic zero modes by Γ establishes a one-to-one correspondence between bosonic and fermionic zero modes.

A zero mode F is a Hermitian operator that satisfies the equation $[H, F] = 0$. We consider F as a vector in L_{even} and introduce a linear operator $\tilde{H}$ from L_{even} to L_{even} such that $\tilde{H}F = i[H, F]$. Since zero modes form the kernel of $\tilde{H}$, our goal is to prove that dim ker$\tilde{H} \leq 2^N$ for almost all H.

As above, we first prove that inequality for a particular Hamiltonian

$$H_0 = U \sum_{k=1}^{N} 2^k \alpha_k, \tag{C.8}$$

where $U \neq 0$. An arbitrary zero mode is determined by its coefficients in the basis $E_{\{k_l\}}$. It will be convenient to change the notation for the basis vectors. This will help us better exploit the structure of H_0. We define the following operators: $Z^k_{0,1} = 1$, $Z^k_{0,-1} = \alpha_k$, $Z^k_{1,1} = \sqrt{i}\gamma_{2k-1}$, $Z^k_{1,-1} = \sqrt{i}\gamma_{2k}$, $z_0 = 1$, and $z_1 = \sqrt{i}\gamma_0$, where $k = 1, \ldots, N$. Any operator $E_{\{k_l\}}$ can be represented as a product $z_{s_0}\Pi_{k=1}^N Z^k_{p_k,s_k}$. We will denote such products as $e_{s_0,p_1,s_1,\ldots,p_N,s_N}$. Let us cut the set of integers $S = \{1, 2, \ldots, N\}$ into two nonintersecting sets S_1 and S_2 whose union is S. Consider the subspace L_{S_2} of L_{even}, spanned by the vectors $e_{s_0,p_1,s_1,\ldots,p_N,s_N}$ with $p_k = 0$ for all $k \in S_1$, $p_k = 1$ for all $k \in S_2$, and $s_0 = (\text{card } S_2) \text{mod } 2$, where card means the number of the elements in a set. Any such subspace is an invariant subspace of $\tilde{H}$. Thus, in order to find the kernel of $\tilde{H}$ it is sufficient to find the kernels of its restrictions to the above subspaces.

Let us first consider the subspace $L_\emptyset$ that corresponds to $S_2 = \emptyset$. This space of dimension 2^N is all in the kernel ker$\tilde{H}$. Thus, we need to prove that the restrictions of $\tilde{H}$ to all other subspaces L_{S_2} have trivial kernels.

Let us focus on one such subspace $\tilde{L} = L_{S_2}$, $S_2 \neq \emptyset$. It will be convenient to change the notation for the basis vectors in the subspace $\tilde{L}$ one more time. We define

$e_{s_0,p_1,s_1,\ldots,p_N,s_N} = (s_{k_1}, s_{k_2}, \ldots, s_{k_C})$, where C is the number of the elements of S_2 and $k_1 > k_2 > \cdots > k_C$ are the elements of S_2. Consider an arbitrary nonzero vector in $\tilde{L}$, $v = \sum a_{s_{k_1},\ldots,s_{k_C}}(s_{k_1}, \ldots, s_{k_C})$. Let $a_{r_1,\ldots,r_C}$ have the maximal absolute value $|m|$ among all the components of v. We will now compute the projection of $\tilde{H}v$ on the vector $(-r_1, r_2, r_3, \ldots, r_N)$ (the inner product was defined in Section C.1). We find that the absolute value of the projection is no less than $2|m||U|(2^{k_1} - \sum_{r=2}^{C} 2^{k_r}) > 0$. Hence, $\tilde{H}v \neq 0$. Since v is an arbitrary vector, we have established that the restriction of $\tilde{H}$ to $\tilde{L}$ has a trivial kernel. It follows that dim ker$\tilde{H} = 2^N$ and H_0 has exactly 2^N bosonic (and hence also fermionic) zero modes.

What about an arbitrary Hamiltonian? The number K of the bosonic (and fermionic) zero modes is determined by the rank of the linear operator $\tilde{H}$ in the space L_{even}: $K = 2^{2N} - \text{rank } \tilde{H}$. We want to prove that rank $\tilde{H} \geq 2^{2N} - 2^N$ for almost all Hamiltonians. The latter inequality has been established for H_0. Consider the matrix of the operator $\tilde{H}$, corresponding to $H = H_0$, in the basis $E_{\{k_l\}}$. It has a nonzero minor of the dimension $(2^{2N} - 2^N)$. The minor is a polynomial of the matrix elements of $\tilde{H}$. Those matrix elements are, in turn, linear combinations of the coordinates of H, if H is interpreted as a vector in L_{even} and expanded as a linear combination of $E_{\{k_l\}}$. Thus, the minor is a polynomial function of the components of H seen as a vector in L_{even}. That polynomial is nonzero at $H = H_0$. It follows that it is nonzero for almost all choices of the components of H, i.e., for almost all Hamiltonians. Thus, the rank of $\tilde{H}$ is almost always at least $2^{2N} - 2^N$. This finishes the proof of the statement of Section C.2.

C.3 Structure of zero modes.

In this section we derive Eq. (5.15). As discussed in Section 5.5, we are only interested in the limit of large N.

C.3.1 The idea of the argument

We start with the summary of our argument.

Zero modes are polynomials of γ_k's. Long decoherence times correspond to polynomials with large coefficients in front of the terms of low powers in γ_k and small coefficients in front of the terms of high powers in γ_k. We want to prove that for almost all Hamiltonians, all of their fermionic zero modes have decoherence times that scale as $1/N$ and satisfy Eq. (5.15).

In order to make the above statements precise, we introduce a measure on the set of all possible Hamiltonians of a system of $2N+1$ Majorana fermions. This gives a clear meaning to the phrase "almost all Hamiltonians". We also need to define what is meant by low and high powers. We introduce a constant $\epsilon < 1$. Low powers p satisfy

$$p < \epsilon N. \tag{C.9}$$

What is meant by long and short decoherence times also depends on the choice of ϵ: long decoherence times correspond to zero modes whose expressions are dominated by terms of power $< \epsilon N$. Thus, the choice of ϵ defines the set of all Hamiltonians H_{long} that possess at least one fermionic zero mode $F_{\text{long}}(H_{\text{long}})$ with a long decoherence time. We denote the measure of that set of Hamiltonians by σ (the measure of the set

of all Hamiltonians is normalized to 1). Our goal is to find the smallest ϵ such that σ remains finite in the limit of large N. The upper bound (5.15) on the decoherence time for an arbitrary Hamiltonian outside a set of zero measure can then be derived from the knowledge of ϵ.

As the first step of the argument, we introduce a family of measure-preserving unitary transformations U_k. They transform Hamiltonians into Hamiltonians and zero modes into zero modes. The total number N_U of the transformations in the family grows rapidly as a function of N.

Next, we consider all Hamiltonians $H_{\rm long}$ that possess at least one fermionic zero mode $F_{\rm long}(H_{\rm long})$ with a long decoherence time. We track the fate of the Hamiltonians from that set under the action of each unitary transformation U_k. Each pair $(H_{\rm long}, F_{\rm long})$ is transformed by U_k into a new Hamiltonian $H_k(H_{\rm long})$ and a fermionic zero mode $F_k(F_{\rm long})$ of the new Hamiltonian $H_k(H_{\rm long})$. In general, $F_k(F_{\rm long})$ may have arbitrary coefficients in front of high- and low-power terms.

At the third step, we sum over k the measures of the sets of the Hamiltonians of the form $H_k(H_{\rm long})$. At large N, the sum $\tilde{\sigma} = \sigma N_U \gg 1$. This means that those sets intersect and some Hamiltonians H can be represented as $H = H_k(H_{\rm long})$ at multiple choices of k and $H_{\rm long}$. For each of those choices, $F_k^H = F_k(F_{\rm long}(H_{\rm long}))$ is a fermionic zero mode of H. Not all of the modes F_k^H are linear independent. We use the structure of the operators U_k to derive the lower bound $\tilde{N}_F$ on the number of the linear independent zero modes F_k^H. It assumes the form $\tilde{N}_F = N_U/r$, where r is a function of N and ϵ, Eq. (C.9). According to Section C.2, $\tilde{N}_F \leq 2^N$. Hence, $r \geq 2^{-N} N_U$. This yields an inequality for ϵ whose solution leads to Eq. (5.15).

C.3.2 Measure in the space of Hamiltonians

According to Section C.1, every Hamiltonian H is determined by its coordinates $a_{\{k_l\}}$ in the basis $E_{\{k_l\}}$. We define a volume element in terms of those components and the inner product, introduced in Section C.1: $dV = f[(H,H)]\Pi_{\{k_l\}} da_{\{k_l\}}$, where $f(x)$ is an arbitrary function of the inner square of H. The only restriction is that the total volume of the space of the Hamiltonians must be finite: $\int dV = 1$.

We will not prove that relevant sets are measurable or integrals exist. Such proofs can be deduced from a physically sensible assumption that zero modes depend continuously on the Hamiltonian for almost all Hamiltonians.

C.3.3 Unitary transformations

Consider the operators

$$U_{\{k_l\}} = \frac{1 + iA_{\{k_l\}}}{\sqrt{2}} = \frac{1}{\sqrt{2}}(1 + i^{M/2+1}\Pi_{l=1}^{M}\gamma_{k_l}), \tag{C.10}$$

where $M = N$ for even N, $M = N+1$ for odd N, and $\{k_l\}$ is a shorthand for the set of the indices $k_1 < k_2 < \cdots < k_M$. All such operators are unitary. The total number of different operators U is

$$N_U = C_{2N+1}^{M} \approx \frac{2^{2N+1}}{\sqrt{\pi N}}. \tag{C.11}$$

The action of $U_{\{k_l\}}$ on a Hamiltonian H and its fermionic zero mode Γ_α is defined by $H \to H' = UHU^\dagger$, $\Gamma_\alpha \to \Gamma'_\alpha = U\Gamma_\alpha U^\dagger$. Clearly, Γ'_α is a fermionic zero mode of H'. It is also clear that the action of $U_{\{k_l\}}$ preserves the measure, Subsection C.3.2.

We wish to understand the action of the operators (C.10) on fermionic zero modes. Each fermionic zero mode can be represented as a linear combination of the vectors $O_{\{k_l\}}$, Eq. (C.4). To simplify notations we will use Greek indices with a bar to denote sets of the indices $\{k_l\}$. Thus, we may write $O_{\bar{\alpha}}$ instead of $O_{k_1,\ldots,k_{2n+1}}$ and represent zero modes as $\Gamma_i = \sum_{\bar{\alpha}} a_{\bar{\alpha}} O_{\bar{\alpha}}$. Let us first consider the action of $U_{\bar{\beta}} = (1 + iA_{\bar{\beta}})/\sqrt{2}$ on $O_{\bar{\alpha}}$. There are two possibilities.

1) The index sets $\bar{\alpha}$ and $\bar{\beta}$ have an even number of indices in common. In such a case, $U_{\bar{\beta}}$ and $O_{\bar{\alpha}}$ commute so that $U_{\bar{\beta}} O_{\bar{\alpha}} U_{\bar{\beta}}^{\dagger} = O_{\bar{\alpha}}$.

2) The index sets $\bar{\alpha}$ and $\bar{\beta}$ have an odd number of indices in common. Then

$$U_{\bar{\beta}} O_{\bar{\alpha}} U_{\bar{\beta}}^{\dagger} = iA_{\bar{\beta}} O_{\bar{\alpha}} = \pm O_{\bar{\alpha}'}, \tag{C.12}$$

where $\bar{\alpha}' = \bar{\alpha}'(\bar{\alpha}, \bar{\beta}) \neq \bar{\alpha}$. Note also that $U_{\bar{\beta}} O_{\bar{\alpha}'(\bar{\alpha},\bar{\beta})} U_{\bar{\beta}}^{\dagger} = \mp O_{\bar{\alpha}}$.

Thus, there are two types of operators $O_{\bar{\alpha}}$ for each $U_{\bar{\beta}}$: 1) some operators $O_{\bar{\alpha}}$ are fixed points of the action of $U_{\bar{\beta}}$ and 2) the rest consists of the pairs of operators $O_{\bar{\alpha}}, O_{\bar{\alpha}'}$ that transform into each other by the action of $U_{\bar{\beta}}$.

Let us fix a number $\epsilon \ll 1$. Consider a fermionic zero mode

$$\Gamma_i = \sum_{\bar{\alpha}} a_{\bar{\alpha}} O_{\bar{\alpha}} \tag{C.13}$$

of some Hamiltonian H. We introduce the notation Γ_i^{ϵ} for the sum of all monomials of the degrees less than ϵN in the above expansion of Γ_i:

$$\Gamma_i^{\epsilon} = \sum_{\bar{\alpha} \text{ contains fewer than } \epsilon N \text{ indices}} a_{\bar{\alpha}} O_{\bar{\alpha}}. \tag{C.14}$$

The action of $U_{\bar{\beta}}$ transforms Γ_i^{ϵ} into the sum $\Gamma_i^{\epsilon,0}+\Gamma_i^{\epsilon,U_{\bar{\beta}}}$, where $\Gamma_i^{\epsilon,0}$ includes terms of degrees less than ϵN in γ_k's and $\Gamma_i^{\epsilon,U_{\bar{\beta}}}$ combines monomials of degrees between $M-\epsilon N$ and $M+\epsilon N-2$. We define $\Gamma_i^{\mathrm{rest},U_{\bar{\beta}}}$ according to the equation $U_{\bar{\beta}}\Gamma_i U_{\bar{\beta}}^{\dagger}=\Gamma_i^{\epsilon,U_{\bar{\beta}}}+\Gamma_i^{\mathrm{rest},U_{\bar{\beta}}}$, and expand $\Gamma_i^{\epsilon,U_{\bar{\beta}}}=\sum b_{\bar{\gamma}}O_{\bar{\gamma}}$ and $\Gamma_i^{\mathrm{rest},U_{\bar{\beta}}}=\sum c_{\bar{\gamma}}O_{\bar{\gamma}}$. It follows from the way how $U_{\bar{\beta}}$ acts on the operators $O_{\bar{\alpha}}$, that $b_{\bar{\gamma}}$ and $c_{\bar{\gamma}}$ cannot be simultaneously nonzero for any $\bar{\gamma}$. This statement will be important below. We will refer to it as **Proposition C.3.3**.

$\Gamma_i^{\epsilon,U_{\bar{\beta}}}$ depends on $U_{\bar{\beta}}$ in a complicated way. It will be thus convenient for us to switch from the discussion of the action of an individual unitary operator $U_{\bar{\beta}}$ on a zero mode Γ_i to a discussion of an average action of the whole set of the unitary operators (C.10) on a given zero mode. Note first that

$$(\Gamma_i^{\epsilon,U_{\bar{\beta}}},\Gamma_i^{\epsilon,U_{\bar{\beta}}})=\sum_{\substack{\bar{\alpha}\text{ has an odd number of common indices with }\bar{\beta}\\ \bar{\alpha}\text{ contains fewer than }\epsilon N\text{ indices}}} a_{\bar{\alpha}}^2, \tag{C.15}$$

where $a_{\bar{\alpha}}$ are defined in Eq. (C.13). Simple combinatorics shows that for each index set $\bar{\alpha}$ with fewer than ϵN indices there are approximately $N_U/2$ operators $U_{\bar{\beta}}$ such that the index sets $\bar{\alpha}$ and $\bar{\beta}$ have an odd number of indices in common. We use that fact and Eq. (C.15) to obtain that

$$\sum_{\bar{\beta}}(\Gamma_i^{\epsilon,U_{\bar{\beta}}},\Gamma_i^{\epsilon,U_{\bar{\beta}}})>cN_U(\Gamma_i^{\epsilon},\Gamma_i^{\epsilon}), \tag{C.16}$$

where the summation runs over all operators $U_{\bar{\beta}}$ and the constant $c\approx 1/2$. Upper and lower bounds on c can be easily derived from combinatorics but will not be needed below.

C.3.4 Counting zero modes

The Majorana fermion condition (5.5) implies $(O, O) = 1$. Thus, we may assume that all zero modes are normalized: $(\Gamma_i, \Gamma_i) = 1$.

Let us estimate the decoherence time for a qbit, built using a fermionic zero mode Γ_i. We will do it in terms of Γ_i^ϵ, introduced in the previous subsection. From the normalization condition $(\Gamma_i, \Gamma_i) = 1$ one finds: $(\Gamma_i - \Gamma_i^\epsilon, \Gamma_i - \Gamma_i^\epsilon) = 1 - (\Gamma_i^\epsilon, \Gamma_i^\epsilon)$. Combining this expression with Eq. (5.13) and the definition of Γ_i^ϵ, one finds the decoherence time

$$\tau < \frac{1}{2\epsilon N A[1 - (\Gamma_i^\epsilon, \Gamma_i^\epsilon)]}. \tag{C.17}$$

Thus, in the search for a long decoherence time, we need to focus on the zero modes with large $(\Gamma_i^\epsilon, \Gamma_i^\epsilon)$.

At the same time, we are not interested in special cases, corresponding to a zero-measure set of Hamiltonians. Below we fix a positive constant $f < 1$ and consider the Hamiltonians H such that each of them has at least one fermionic zero mode Γ_H, satisfying

$$(\Gamma_H^\epsilon, \Gamma_H^\epsilon) > f. \tag{C.18}$$

We assume that ϵ and f are chosen so that the measure $\sigma(S_f)$ of the set S_f of all such Hamiltonians remains nonzero in the limit of large N: $\sigma(S_f) > \mu > 0$, where μ does not depend on N. For each Hamiltonian H in S_f we select exactly one fermionic zero mode Γ_H, satisfying Eq. (C.18).

Note that $(\Gamma_H^{\epsilon,U_{\bar\beta}}, \Gamma_H^{\epsilon,U_{\bar\beta}}) \leq (\Gamma_H^\epsilon, \Gamma_H^\epsilon) \leq (\Gamma_H, \Gamma_H) = 1$. It follows then from

Eqs. (C.16,C.18) that for each Γ_H, Eq. (C.18), there are more than

$$K_U = fcN_U/2 \tag{C.19}$$

operators $U_{\bar{\beta}}$ such that

$$(\Gamma_H^{\epsilon,U_{\bar{\beta}}}, \Gamma_H^{\epsilon,U_{\bar{\beta}}}) > cf/2. \tag{C.20}$$

We will denote as S_H the set of all such operators $U_{\bar{\beta}}$ for a given Γ_H, $H \in S_f$. We will also define the sets $S_{U_{\bar{\beta}}}$ made of all such Hamiltonians H that $U_{\bar{\beta}} \in S_H$. Each $S_{U_{\bar{\beta}}}$ is a subset of S_f.

Consider now the action of $U_{\bar{\beta}}$ on the Hamiltonians in the set $S_{U_{\bar{\beta}}}$. Each Hamiltonian $H \in S_{U_{\bar{\beta}}}$ is transformed into a new Hamiltonian $H^{U_{\bar{\beta}}}$. Each $U_{\bar{\beta}}$ transforms $S_{U_{\bar{\beta}}}$ into a set $S^U_{U_{\bar{\beta}}}$ of the same measure,

$$\sigma(S^U_{U_{\bar{\beta}}}) = \sigma(S_{U_{\bar{\beta}}}). \tag{C.21}$$

Below we will evaluate the sum of the measures (C.21) in several ways. The sum of the measures $\Omega = \sum_{\bar{\beta}} \sigma(S_{U_{\bar{\beta}}})$ can be represented as

$$\Omega = \sum_{\bar{\beta}} \sigma(S_{U_{\bar{\beta}}}) = \int dV N(S_H), \tag{C.22}$$

where $\int dV$ means integration over all Hamiltonians with the measure, defined in Subsection C.3.2, and $N(S_H)$ denotes the number of the elements in the set S_H for $H \in S_f$, $N(S_H) = 0$ for H that are not in S_f. The discussion around Eq. (C.19) shows that all nonzero $N(S_H)$ exceed K_U. Hence,

$$\Omega > K_U \sigma(S_f) > K_U \mu. \tag{C.23}$$

On the other hand, Eq. (C.21) implies that

$$\Omega = \sum_{\bar{\beta}} \sigma(S^U_{U_{\bar{\beta}}}). \tag{C.24}$$

Let us introduce a new piece of notations. For each Hamiltonian $\tilde{H}$, consider all such pairs (H,$U_{\bar{\beta}}$) that $H \in S_f$, $\tilde{H} = U_{\bar{\beta}} H U^\dagger_{\bar{\beta}}$ and $U_{\bar{\beta}} \in S_H$. We will denote the set of such pairs as $\tilde{S}_{\tilde{H}}$ and their number as $\tilde{N}(\tilde{H})$. Note that different pairs (H,$U_{\bar{\beta}}$) in $\tilde{S}_{\tilde{H}}$ contain different operators $U_{\bar{\beta}}$. We can now rewrite Eq. (C.24) as

$$\Omega = \int dV \tilde{N}(H). \tag{C.25}$$

Recall that the total measure of the whole space of Hamiltonians is $\int 1 dV = 1$. Hence, a comparison of Eq. (C.25) with (C.23) shows that

$$\tilde{N}(H) > K_U \mu \tag{C.26}$$

for the Hamiltonians H from some set of a nonzero measure.

According to Section C.2, a generic Hamiltonian H_0 in that set has exactly 2^N linear independent fermionic zero modes. On the other hand, for each pair $(H, U_{\bar{\beta}}) \in \tilde{S}_{H_0}$ there is a fermionic zero mode Γ_H such that: 1) it satisfies Eq. (C.18) and 2)

$$\Gamma_0^{\bar{\beta}} = U_{\bar{\beta}} \Gamma_H U^\dagger_{\bar{\beta}} \tag{C.27}$$

is a zero mode of H_0. The number of the zero modes $\Gamma_0^{\bar{\beta}}$ with different sets of indices $\bar{\beta}$ is $\tilde{N}(H_0)$. At the same time, it is easy to see that $\tilde{N}(H_0) > K_U \mu > 2^N$ at large N. Thus, if all $\tilde{N}(H_0)$ modes $\Gamma_0^{\bar{\beta}}$ were distinct and linear independent we would arrive at a contradiction. In what follows we count the linear independent modes among

$\Gamma_0^{\bar{\beta}}$ and use the limit of 2^N on their number to estimate ϵ.

Our estimate relies on a geometric lemma and a combinatorial inequality, proven in the next two subsections.

C.3.5 Geometric lemma

Consider n unit vectors $v_1, \ldots, v_n$ and another set of n mutually orthogonal unit vectors $e_1, \ldots, e_n$ in a D-dimensional Euclidean space E. Let $(v_k, e_k)^2 > g$ for each k. Then the dimension d of the linear space V, spanned by the n vectors v_k, is greater than gn.

Proof. The projection $P_V(e_k)$ of the vector e_k onto the space V cannot be shorter than the absolute value of the inner product of e_k with an arbitrary unit vector in V. Hence, $P_V^2(e_k) \geq (v_k, e_k)^2 = g$. Since the unit vectors e_k, $k = 1, \ldots, n$ are mutually orthogonal, we can consider them as a part of the orthonormal basis $e_1, \ldots, e_n, e_{n+1}, \ldots, e_D$ in the space E. Clearly, $S = \sum_{i=1}^{D} P_V^2(e_i) \geq \sum_{i=1}^{n} P_V^2(e_i) > gn$. Let $w_1, \ldots, w_d$ be an orthonormal basis in V. Then $S = \sum_{i,j}(e_i, w_j)^2 = \sum_{j=1}^{d}(w_j, w_j) = d$. It follows that $d > gn$.

C.3.6 Combinatorial inequality

Consider two sets $\bar{\alpha}$ and $\bar{\beta}$ of M indices $k_1^\alpha < k_2^\alpha < \cdots < k_M^\alpha$ and M indices $k_1^\beta < k_2^\beta < \cdots < k_M^\beta$, assuming values between 0 to $2N$. The constant M was defined in the beginning of Subsection C.3.3. Let us define the *overlap* $o(\bar{\alpha}, \bar{\beta})$ of $\bar{\alpha}$ and $\bar{\beta}$ as the number of the common indices in the sets $\{k_1^\alpha, k_2^\alpha, \ldots, k_M^\alpha\}$ and

$\{k_1^\beta, k_2^\beta, \ldots, k_M^\beta\}$. For a given $\bar{\alpha}$, we wish to estimate the number R of the sets of indices $\bar{\beta}$ whose overlap with $\bar{\alpha}$ exceeds $(M - \epsilon N)$.

Consider an arbitrary subset $[\bar{\alpha}]_{\rm short}$ of $(M - \epsilon N)$ indices in $\bar{\alpha}$. Let us count all sets $\bar{\gamma}$ which contain the same subset $[\bar{\alpha}]_{\rm short}$. Next, let us add the resulting numbers for every choice of $[\bar{\alpha}]_{\rm short}$. This way we will count every $\bar{\gamma}$ with $o(\bar{\alpha}, \bar{\gamma}) > (M - \epsilon N)$ at least once. Thus, we will get an upper estimate for R. One can choose $[\bar{\alpha}]_{\rm short}$ in $C_M^{M-\epsilon N}$ ways. There are $C_{2N+1-M+\epsilon N}^{\epsilon N}$ ways to complement $[\bar{\alpha}]_{\rm short}$ by ϵN additional indices to make a set of M different indices. Thus, we obtain the inequality $R < C_M^{M-\epsilon N} C_{2N+1-M+\epsilon N}^{\epsilon N}$. Using the inequality

$$\frac{(2N+1-M+\epsilon N)!}{(M-\epsilon N)!} < (2N+1-M+\epsilon N)^{2N+1-2M+2\epsilon N}$$

and the Stirling formula, we estimate

$$R < \frac{C}{\epsilon N} \left(\frac{[1+\epsilon]e}{\epsilon} \right)^{2\epsilon N}, \tag{C.28}$$

where the constant C does not depend on N and ϵ.

C.3.7 Linear independent zero modes

We now come back to the end of Subsection C.3.4 and determine the number of linear independent zero modes among the modes $\Gamma_0^{\bar{\beta}}$ of the Hamiltonian H_0. Recall that Eq. (C.27) establishes a correspondence between the modes $\Gamma_0^{\bar{\beta}}$ and the zero modes Γ_H of the Hamiltonians H such that $H_0 = U_{\bar{\beta}} H U_{\bar{\beta}}^\dagger$, $(H, U_{\bar{\beta}}) \in \tilde{S}_{H_0}$.

We now observe that the operators $\Gamma_H^{\epsilon, U_{\bar{\beta}}}$ satisfy Eq. (C.20). Let us introduce the set S_e of the unit vectors $e_{\bar{\beta}} = \Gamma_H^{\epsilon, U_{\bar{\beta}}} / \sqrt{(\Gamma_H^{\epsilon, U_{\bar{\beta}}}, \Gamma_H^{\epsilon, U_{\bar{\beta}}})}$ in the space $L_{\rm odd}$. The number

$N(S_e)$ of the vectors in S_e satisfies Eq. (C.26), i.e.,

$$N(S_e) > K_U \mu = fc\mu N_U/2. \tag{C.29}$$

Note that $N(S_e)$ counts different index sets $\bar{\beta}$ and it may happen that some $e_{\bar{\beta}} = e_{\bar{\gamma}}$ at $\bar{\beta} \neq \bar{\gamma}$. Eq. (C.20) can be rewritten as

$$(e_{\bar{\beta}}, \Gamma_H^{\epsilon, U_{\bar{\beta}}})^2 > cf/2. \tag{C.30}$$

Proposition C.3.3 implies now that

$$(e_{\bar{\beta}}, \Gamma_0^{\bar{\beta}})^2 > cf/2. \tag{C.31}$$

At this point our tactics becomes obvious: In order to find the number of linear independent modes $\Gamma_0^{\bar{\beta}}$, we need to use geometric lemma C.3.5 with $\Gamma_0^{\bar{\beta}}$ in place of v_k and $e_{\bar{\beta}}$ in place of e_k. However, a difficulty emerges: In general, the unit vectors $e_{\bar{\beta}}$ are not mutually orthogonal. That is where the combinatorial inequality (C.28) is going to help.

Any vector $e_{\bar{\beta}}$ is a linear combination of some operators of the form $O_t^{\epsilon,\bar{\beta}} = U_{\bar{\beta}} O_t^{\epsilon} U_{\bar{\beta}}^{\dagger}$, where the operators O_t^{ϵ} satisfy two conditions:

1) $O_t^{\epsilon,\bar{\beta}} \neq O_t^{\epsilon}$;

2) O_t^{ϵ} are the vectors $O_{\{k_l\}}$, Section C.1, with fewer than ϵN indices.

We can be sure that $(e_{\bar{\beta}}, e_{\bar{\gamma}}) = 0$, if there is no overlap between the sets of all operators $O_t^{\epsilon,\bar{\beta}}$ and all operators $O_t^{\epsilon,\bar{\gamma}}$. Using Eq. (C.12) one can show that this is

guaranteed to occur, if $o(\bar{\beta}, \bar{\gamma}) \leq M - \epsilon N$, where the overlap function o is defined in Subsection C.3.6. We now select a vector $e_{\bar{\beta}_1}$. There are no more than R, Eq. (C.28), operators $e_{\bar{\gamma}}$ in S_e such that $o(\bar{\beta}_1, \bar{\gamma}) > M - \epsilon N$, $\bar{\gamma} \neq \bar{\beta}_1$. Remove all such vectors $e_{\bar{\gamma}}$ from S_e. All remaining vectors $e_{\bar{\alpha}} \in S_e$, $\bar{\alpha} \neq \bar{\beta}_1$ are orthogonal to $e_{\bar{\beta}_1}$. We next select an arbitrary vector $e_{\bar{\beta}_2} \neq e_{\bar{\beta}_1}$. By removing no more than R additional vectors from S_e we guarantee that all remaining vectors are orthogonal to $e_{\bar{\beta}_2}$. We then select an arbitrary remaining vector $e_{\bar{\beta}_3} \neq e_{\bar{\beta}_{1,2}}$ and continue in the same spirit until only selected vectors $e_{\bar{\beta}_k}$ remain in S_e. Clearly, $e_{\bar{\beta}_k}$ form an orthonormal basis. Since we started with at least $K_U \mu$ elements in S_e, we end with at least $K_U \mu / R$ orthogonal vectors $e_{\bar{\beta}_k}$.

Finally, we use geometric lemma C.3.5 and Eq. (C.31) to estimate the number $\tilde{N}_F$ of linear independent zero modes among the operators $\Gamma_0^{\bar{\beta}}$. $\Gamma_0^{\bar{\beta}_k}$ play the role of the vectors v_k in the lemma and $e_{\bar{\beta}_k}$ play the role of the vectors e_k. There may be additional linear independent modes $\Gamma_0^{\bar{\beta}}$ with $\bar{\beta} \neq \bar{\beta}_1, \ldots, \bar{\beta}_k$. H_0 may also have zero modes that do not assume the form $\Gamma_0^{\bar{\beta}}$. Thus, the total number of linear independent modes $N_F \geq \tilde{N}_F$. We find

$$N_F > \frac{cfK_U\mu}{2R} = \frac{(cf)^2\mu}{4}\frac{N_U}{R}, \tag{C.32}$$

where $4R/[\mu(cf)^2]$ plays the role of r from Subsection C.3.1.

C.3.8 The lowest decoherence rate

Only one step is left: we will use Eq. (C.32) to estimate ϵ. Combining Eqs. (C.11,C.28,C.32) and using the fact that $N_F = 2^N$, one finds

$$2^N > 2^{2N} \frac{(cf)^2 \mu \epsilon \sqrt{N}}{2C\sqrt{\pi}} \left(\frac{\epsilon}{[1+\epsilon]e} \right)^{2\epsilon N}. \tag{C.33}$$

In the limit of large N, Eq. (C.33) reduces to $\ln 2 < 2\epsilon[1 + \ln \frac{1+\epsilon}{\epsilon}]$. The solution is $\epsilon > 0.103$. In other words, for any $\epsilon < 0.103$ and for almost all Hamiltonians H, all fermionic zero modes Γ_H have vanishing $(\Gamma_H^\epsilon, \Gamma_H^\epsilon)$. We now substitute $\epsilon = 0.1$ into Eq. (C.17) and obtain Eq. (5.15). Finally, we must mention that some of the modes Γ_H do not satisfy the Majorana fermion condition $\Gamma_H^2 = 1$, Section 5.3, and hence Eq. (5.15) is meaningless for such modes.

C.4 Bosonic degrees of freedom in contact with weakly interacting fermions

In this section we investigate the effect of bosonic degrees of freedom on the dephasing time (5.13). We address only the case of weakly interacting fermions below, i.e., we assume that the Hamiltonian is quadratic in Majorana operators. We also assume that the number $2N + 1$ of the fermions is large. No assumptions are made about the dimension D_b of the Hilbert space of bosons (certainly, $D_b > 1$).

In the absence of Bose degrees of freedom, any quadratic Hamiltonian has an integral of motion, linear in Majorana operators. We show below that this is no longer the case in the presence of bosons. According to Eq. (5.13) this means that

the interaction with Bose degrees of freedom shortens the dephasing time.

We demonstrate this by working with a particular Hamiltonian:

$$H = i\hat{A}\sum_{n=0}^{N-1}\gamma_{2n}\gamma_{2n+1} + i\hat{B}\sum_{n=1}^{N}\gamma_{2n-1}\gamma_{2n}, \tag{C.34}$$

where $\hat{A}$ and $\hat{B}$ are Hermitian $D_b \times D_b$ matrices acting in the Hilbert space of the bosons. We select the basis in which $\hat{B}$ is diagonal and assume that its eigenvalues b_k, $k = 1, \ldots, D_b$ are nondegenerate. We also assume that all matrix elements A_{ij} of the operator $\hat{A}$ are nonzero in that basis.

Does a linear zero mode $\Gamma_L = \sum \hat{C}_k\gamma_k$ exist? Here $\hat{C}_k$ are operators in the Hilbert space of bosons. In order to answer the question we compute the commutator $[H, \Gamma_L]$. It must be zero for Γ_L to be an integral of motion. The commutator contains one- and three-fermion contributions. In particular, for each $k > 3$, the commutator contains contributions $X_1 = i\gamma_1\gamma_2\gamma_k[\hat{B}, \hat{C}_k]$ and $X_2 = i\gamma_0\gamma_1\gamma_k[\hat{A}, \hat{C}_k]$. For each $k < 2N - 3$, there are contributions $X_3 = i\gamma_k\gamma_{2N-1}\gamma_{2N}[\hat{B}, \hat{C}_k]$ and $X_4 = i\gamma_k\gamma_{2N-2}\gamma_{2N-1}[\hat{A}, \hat{C}_k]$. Each of those contributions $X_i = 0$. Hence, $[\hat{B}, C_k] = [\hat{A}, C_k] = 0$. This is only possible, if each $\hat{C}_k$ reduces to a c -number: $\hat{C}_k = c_k\delta_{ij}$. Thus, $\Gamma_L = \sum c_k\gamma_k$ and

$$[H, \Gamma_L] = 2i\hat{A}\sum_{n=0}^{N-1}(c_{2n+1}\gamma_{2n} - c_{2n}\gamma_{2n+1}) + 2i\hat{B}\sum_{n=0}^{N-1}(c_{2n+2}\gamma_{2n+1} - 2c_{2n+1}\gamma_{2n+2}) = 0. \tag{C.35}$$

This means that $\hat{A}c_{2n+1} = \hat{B}c_{2n-1}$ and $\hat{A}c_{2n} = \hat{B}c_{2n+2}$ and hence all $c_k = 0$.

We find that no zero mode, linear in Majoranas, exists for the Hamiltonian (C.34). It may exist at other choices of the Hamiltonian. Still, a general conclusion about the relaxation time being $\tau = (2N + 1)\tau_\Gamma$ no longer holds in the presence of bosons.

Bibliography

[1] R. E. Prange and S. M. Girvin, editors. *The Quantum Hall Effect*. Springer-Verlag, New York, 1987.

[2] K. v. Klitzing, G. Dorda, and M. Pepper. New method for high-accuracy determination of the fine-structure constant based on quantized Hall resistance. *Phys. Rev. Lett.*, 45:494, 1980.

[3] D. C. Tsui, H. L. Stormer, and A. C. Gossard. Two-dimensional magneto-transport in the extreme quantum limit. *Phys. Rev. Lett.*, 48:1559, 1982.

[4] B. Jeckelmann and B. Jeanneret. The quantum Hall effect as an electrical resistance standard. *Rep. Prog. Phys.*, 64:1603, 2001.

[5] X.-G. Wen. *Quantum Field Theory of Many-Body Systems: From the Origin of Sound to an Origin of Light and Electrons*. Oxford University Press, 2004.

[6] F. Wilczek. Quantum mechanics of fractional-spin particles. *Phys. Rev. Lett.*, 49:957, 1982.

[7] A. Yu. Kitaev. Fault-tolerant quantum computation by anyons. *Ann. Phys.*, 303:2, 2003.

[8] C. Nayak, S. H. Simon, A. Stern, M. Freedman, and S. Das Sarma. Non-Abelian anyons and topological quantum computation. *Rev. Mod. Phys.*, 80:1083, 2008.

[9] R. L. Willett, J. P. Eisenstein, H. L. Stormer, D. C. Tsui, A. C. Gossard, and J. H. English. Observation of an even-denominator quantum number in the fractional quantum Hall effect. *Phys. Rev. Lett.*, 59:1776, 1987.

[10] G. Moore and N. Read. Nonabelions in the fractional quantum Hall effect. *Nucl. Phys. B*, 360:362, 1991.

[11] B. I. Halperin. Theory of the quantized Hall conductance. *Helv. Phys. Acta.*, 56:75, 1983.

[12] X.-G. Wen and A. Zee. Classification of Abelian quantum Hall states and matrix formulation of topological fluids. *Phys. Rev. B*, 46:2290, 1992.

[13] M. Dolev, M. Heiblum, V. Umansky, A. Stern, and D. Mahalu. Observation of a quarter of an electron charge at the $\nu = 5/2$ quantum Hall state. *Nature (London)*, 452:829, 2008.

[14] R. L. Willett, L. N. Pfeiffer, and K. W. West. Measurement of filling factor 5/2 quasiparticle interference with observation of charge $e/4$ and $e/2$ period oscillations. *Proc. Natl. Acad. Sci. U.S.A.*, 106:8853, 2009.

[15] R. L. Willett, L. N. Pfeiffer, and K. W. West. Alternation and interchange of $e/4$ and $e/2$ period interference oscillations consistent with filling factor 5/2 non-Abelian quasiparticles. *Phys. Rev. B*, 82:205301, 2010.

[16] A. Bid, N. Ofek, H. Inoue, M. Heiblum, C. L. Kane, V. Umansky, and D. Mahalu. Observation of neutral modes in the fractional quantum Hall regime. *Nature (London)*, 466:585, 2010.

[17] M. Stern, P. Plochocka, V. Umansky, D. K. Maude, M. Potemski, and I. Bar-Joseph. Optical probing of the spin polarization of the $\nu = 5/2$ quantum Hall state. *Phys. Rev. Lett.*, 105:096801, 2010.

[18] T. D. Rhone, J. Yan, Y. Gallais, A. Pinczuk, L. Pfeiffer, and K. West. Rapid collapse of spin waves in nonuniform phases of the second Landau level. *Phys. Rev. Lett.*, 106:196805, 2011.

[19] L. Tiemann, G. Gamez, N. Kumada, and K. Muraki. Unraveling the spin polarization of the $\nu = 5/2$ fractional quantum Hall state. *Science*, 335:828, 2012.

[20] M. Stern, B. A. Piot, Y. Vardi, V. Umansky, P. Plochocka, D. K. Maude, and I. Bar-Joseph. NMR probing of the spin polarization of the $\nu = 5/2$ quantum Hall state. *Phys. Rev. Lett.*, 108:066810, 2012.

[21] W. E. Chickering, J. P. Eisenstein, L. N. Pfeiffer, and K. W. West. Thermoelectric response of fractional quantized Hall and reentrant insulating states in the $N = 1$ Landau level. *Phys. Rev. B*, 87:075302, 2013.

[22] S. An, P. Jiang, H. Choi, W. Kang, S. H. Simon, L. N. Pfeiffer, K. W. West, and K. W. Baldwin. Braiding of Abelian and non-Abelian anyons in the fractional quantum Hall effect. arXiv:1112.3400, 2011.

[23] I. P. Radu, J. B. Miller, C. M. Marcus, M. A. Kastner, L. N. Pfeiffer, and K. W. West. Quasi-particle properties from tunneling in the $\nu = 5/2$ fractional quantum Hall state. *Science*, 320:899, 2008.

[24] X. Lin, C. Dillard, M. A. Kastner, L. N. Pfeiffer, and K. W. West. Measurements of quasiparticle tunneling in the $\nu = 5/2$ fractional quantum Hall state. *Phys. Rev. B*, 85:165321, 2012.

[25] D. A. Ivanov. Non-Abelian statistics of half-quantum vortices in p-wave superconductors. *Phys. Rev. Lett.*, 86:268, 2001.

[26] H. L. Stormer, D. C. Tsui, and A. C. Gossard. The fractional quantum Hall effect. *Rev. Mod. Phys.*, 71:S298, 1999.

[27] N. W. Ashcroft and N. D. Mermin. *Solid State Physics*. Thomson Learning, 1976.

[28] A. H. MacDonald. Introduction to the physics of the quantum Hall regime. arXiv:cond-mat/9410047, 1994.

[29] S. M. Girvin. The quantum Hall effect: Novel excitations and broken symmetries. arXiv:cond-mat/9907002, 1999.

[30] F. D. M. Haldane. Fractional quantization of the Hall effect: A hierarchy of incompressible quantum fluid states. *Phys. Rev. Lett.*, 51:605, 1983.

[31] R. B. Laughlin. Anomalous quantum Hall effect: An incompressible quantum fluid with fractionally charged excitations. *Phys. Rev. Lett.*, 50:1395, 1983.

[32] B. I. Halperin. Statistics of quasiparticles and the hierarchy of fractional quantized Hall states. *Phys. Rev. Lett.*, 52:1583, 1984.

[33] N. Read. Excitation structure of the hierarchy scheme in the fractional quantum Hall effect. *Phys. Rev. Lett.*, 65:1502, 1990.

[34] B. Blok and X. G. Wen. Structure of the microscopic theory of the hierarchical fractional quantum Hall effect. *Phys. Rev. B*, 43:8337, 1991.

[35] J. K. Jain. Composite-fermion approach for the fractional quantum Hall effect. *Phys. Rev. Lett.*, 63:199, 1989.

[36] J. K. Jain. Incompressible quantum Hall states. *Phys. Rev. B*, 40:8079(R), 1989.

[37] J. K. Jain. Theory of the fractional quantum Hall effect. *Phys. Rev. B*, 41:7653, 1990.

[38] J. K. Jain. Hierarchy of states in the fractional quantum Hall effect. *Phys. Rev. B*, 45:1255, 1992.

[39] J. K. Jain. A note contrasting two microscopic theories of the fractional quantum Hall effect. arXiv:1403.5415, 2014.

[40] X.-G. Wen. Chiral Luttinger liquid and the edge excitations in the fractional quantum Hall states. *Phys. Rev. B*, 41:12838, 1990.

[41] F. D. M. Haldane. 'Luttinger liquid theory' of one-dimensional quantum fluids. I. Properties of the Luttinger model and their extension to the general 1D interacting spinless Fermi gas. *J. Phys. C: Solid State Phys.*, 14:2585, 1981.

[42] J. von Delft and H. Schoeller. Bosonization for beginners - refermionization for experts. *Ann. Phys. (Leipzig)*, 7:225, 1998.

[43] D. Senechal. An introduction to bosonization. arXiv:cond-mat/9908262, 1999.

[44] M. Levin, B. I. Halperin, and B. Rosenow. Particle-hole symmetry and the Pfaffian state. *Phys. Rev. Lett.*, 99:236806, 2007.

[45] S.-S. Lee, S. Ryu, C. Nayak, and M. P. A. Fisher. Particle-hole symmetry and the $\nu = 5/2$ quantum Hall state. *Phys. Rev. Lett.*, 99:236807, 2007.

[46] C. de C. Chamon and X. G. Wen. Sharp and smooth boundaries of quantum Hall liquids. *Phys. Rev. B*, 49:8227, 1994.

[47] J. Rammer and H. Smith. Quantum field-theoretical methods in transport theory of metals. *Rev. Mod. Phys.*, 58:323, 1986.

[48] X.-G. Wen. Edge transport properties of the fractional quantum Hall states and weak-impurity scattering of a one-dimensional charge-density wave. *Phys. Rev. B*, 44:5708, 1991.

[49] X.-G. Wen. Non-Abelian statistics in the fractional quantum Hall states. *Phys. Rev. Lett.*, 66:802, 1991.

[50] P. Bonderson and J. K. Slingerland. Fractional quantum Hall hierarchy and the second Landau level. *Phys. Rev. B*, 78:125323, 2008.

[51] M. Greiter, X.-G. Wen, and F. Wilczek. Paired Hall states. *Nucl. Phys. B*, 374:567, 1992.

[52] B. J. Overbosch and X.-G. Wen. Phase transitions on the edge of the $\nu = 5/2$ Pfaffian and anti-Pfaffian quantum Hall state. arXiv:0804.2087, 2008.

[53] A. Stern. Non-Abelian states of matter. *Nature (London)*, 464:187, 2010.

[54] E. Fradkin, C. Nayak, A. Tsvelik, and F. Wilczek. A Chern-Simons effective field theory for the Pfaffian quantum Hall state. *Nucl. Phys. B*, 516:704, 1998.

[55] S. Das Sarma, M. Freedman, and C. Nayak. Topologically protected qubits from a possible non-Abelian fractional quantum Hall state. *Phys. Rev. Lett.*, 94:166802, 2005.

[56] A. J. Leggett. Class note on the $\nu = 5/2$ fractional quantum Hall effect.

[57] C. Nayaka and F. Wilczek. $2n$-quasihole states realize 2^{n-1}-dimensional spinor braiding statistics in paired quantum Hall states. *Nucl. Phys. B*, 479:529, 1996.

[58] A. Y. Kitaev. Unpaired Majorana fermions in quantum wires. *Phys.-Usp.*, 44:131, 2001.

[59] N. Read and D. Green. Paired states of fermions in two dimensions with breaking of parity and time-reversal symmetries and the fractional quantum Hall effect. *Phys. Rev. B*, 61:10267, 2000.

[60] L. Fu and C. L. Kane. Superconducting proximity effect and Majorana fermions at the surface of a topological insulator. *Phys. Rev. Lett.*, 100:096407, 2008.

[61] Y. Ji, Y. Chung, D. Sprinzak, M. Heiblum, D. Mahalu, and H. Shtrikman. An electronic Mach–Zehnder interferometer. *Nature (London)*, 422:415, 2003.

[62] C. Caroli, P. G. de Gennes, and J. Matricon. Bound Fermion states on a vortex line in a type II superconductor. *Phys. Lett.*, 9:307, 1964.

[63] N. B. Kopnin and M. M. Salomaa. Mutual friction in superfluid He3: Effects of bound states in the vortex core. *Phys. Rev. B*, 44:9667, 1991.

[64] G. Goldstein and C. Chamon. Decay rates for topological memories encoded with Majorana fermions. *Phys. Rev. B*, 84:205109, 2011.

[65] J. C. Budich, S. Walter, and B. Trauzettel. Failure of protection of Majorana based qubits against decoherence. *Phys. Rev. B*, 85:121405(R), 2012.

[66] M. S. Scheurer and A. Shnirman. Nonadiabatic processes in Majorana qubit systems. *Phys. Rev. B*, 88:064515, 2013.

[67] F. Konschelle and F. Hassler. Effects of nonequilibrium noise on a quantum memory encoded in Majorana zero modes. *Phys. Rev. B*, 88:075431, 2013.

[68] M. J. Schmidt, D. Rainis, and D. Loss. Decoherence of Majorana qubits by noisy gates. *Phys. Rev. B*, 86:085414, 2012.

[69] B. van Heck, F. Hassler, A. R. Akhmerov, and C. W. J. Beenakker. Coulomb stability of the 4π-periodic Josephson effect of Majorana fermions. *Phys. Rev. B*, 84:180502(R), 2011.

[70] L. Fu and C. L. Kane. Josephson current and noise at a superconductor/quantum-spin-Hall-insulator/superconductor junction. *Phys. Rev. B*, 79:161408(R), 2009.

[71] F. Hassler A. R. Akhmerov and C. W. J. Beenakker. The top-transmon: a hybrid superconducting qubit for parity-protected quantum computation. *New J. Phys.*, 13:095004, 2011.

[72] P. J. de Visser, J. J. A. Baselmans, P. Diener, S. J. C. Yates, A. Endo, and T. M. Klapwijk. Number fluctuations of sparse quasiparticles in a superconductor. *Phys. Rev. Lett.*, 106:167004, 2011.

[73] J. Aumentado, M. W. Keller, J. M. Martinis, and M. H. Devoret. Nonequilibrium quasiparticles and $2e$ periodicity in single-Cooper-pair transistors. *Phys. Rev. Lett.*, 92:066802, 2004.

[74] A. J. Ferguson, N. A. Court, F. E. Hudson, and R. G. Clark. Microsecond resolution of quasiparticle tunneling in the single-Cooper-pair transistor. *Phys. Rev. Lett.*, 97(106603), 2006.

[75] M. D. Shaw, R. M. Lutchyn, P. Delsing, and P. M. Echternach. Kinetics of nonequilibrium quasiparticle tunneling in superconducting charge qubits. *Phys. Rev. B*, 78:024503, 2008.

[76] M. Zgirski, L. Bretheau, Q. Le Masne, H. Pothier, D. Esteve, and C. Urbina. Evidence for long-lived quasiparticles trapped in superconducting point contacts. *Phys. Rev. Lett.*, 106:257003, 2011.

[77] D. Rainis and D. Loss. Majorana qubit decoherence by quasiparticle poisoning. *Phys. Rev. B*, 85:174533, 2012.

[78] L. Sun, L. DiCarlo, M. D. Reed, G. Catelani, L. S. Bishop, D. I. Schuster, B. R. Johnson, G. A. Yang, L. Frunzio, L. I. Glazman, M. H. Devoret, and R. J. Schoelkopf. Measurements of quasiparticle tunneling dynamics in a band-gap-engineered transmon qubit. *Phys. Rev. Lett.*, 108:230509, 2012.

[79] A. Stern and B. I. Halperin. Proposed experiments to probe the non-Abelian $\nu = 5/2$ quantum Hall state. *Phys. Rev. Lett.*, 96:016802, 2006.

[80] P. Bonderson, A. Kitaev, and K. Shtengel. Detecting non-Abelian statistics in the $\nu = 5/2$ fractional quantum Hall state. *Phys. Rev. Lett.*, 96:016803, 2006.

[81] D. E. Feldman and A. Kitaev. Detecting non-Abelian statistics with an electronic Mach-Zehnder interferometer. *Phys. Rev. Lett.*, 97:186803, 2006.

[82] C.-Y. Hou and C. Chamon. "Wormhole" geometry for entrapping topologically protected qubits in non-Abelian quantum Hall states and probing them with voltage and noise measurements. *Phys. Rev. Lett.*, 97:146802, 2006.

[83] E. Grosfeld, S. H. Simon, and A. Stern. Switching noise as a probe of statistics in the fractional quantum Hall effect. *Phys. Rev. Lett.*, 96:226803, 2006.

[84] B. Rosenow and S. H. Simon. Telegraph noise and the Fabry-Perot quantum Hall interferometer. *Phys. Rev. B*, 85:201302(R), 2012.

[85] D. E. Feldman and F. Li. Charge-statistics separation and probing non-Abelian states. *Phys. Rev. B*, 78:161304(R), 2008.

[86] G. Viola, S. Das, E. Grosfeld, and A. Stern. Thermoelectric probe for neutral edge modes in the fractional quantum Hall regime. *Phys. Rev. Lett.*, 109:146801, 2012.

[87] B. J. Overbosch and C. Chamon. Long tunneling contact as a probe of fractional quantum Hall neutral edge modes. *Phys. Rev. B*, 80:035319, 2009.

[88] N. R. Cooper and A. Stern. Observable bulk signatures of non-Abelian quantum Hall states. *Phys. Rev. Lett.*, 102:176807, 2009.

[89] A. Seidel and K. Yang. Momentum-resolved tunneling into the Pfaffian and anti-Pfaffian edges. *Phys. Rev. B*, 80:241309(R), 2009.

[90] C. Wang and D. E. Feldman. Transport in line junctions of $\nu = 5/2$ quantum Hall liquids. *Phys. Rev. B*, 81:035318, 2010.

[91] K. Yang and B. I. Halperin. Thermopower as a possible probe of non-Abelian quasiparticle statistics in fractional quantum Hall liquids. *Phys. Rev. B*, 79:115317, 2009.

[92] T. Giamarchi. *Quantum Physics in One Dimension*. Clarendon Press, Oxford, 2004.

[93] E. Papa and A. H. MacDonald. Interactions suppress quasiparticle tunneling at Hall bar constrictions. *Phys. Rev. Lett.*, 93:126801, 2004.

[94] E. Papa and A. H. MacDonald. Edge state tunneling in a split Hall bar model. *Phys. Rev. B*, 72:045324, 2005.

[95] M. Levin and A. Stern. Fractional topological insulators. *Phys. Rev. Lett.*, 103:196803, 2009.

[96] T.-L. Ho. Broken symmetry of two-component $\nu = 1/2$ quantum Hall states. *Phys. Rev. Lett.*, 75:1186, 1995.

[97] M. P. A. Fisher and L. I. Glazman. Transport in a one-dimensional Luttinger liquid. arXiv:cond-mat/9610037, 1996.

[98] C. Dillard and X. Lin. Private communications.

[99] D. B. Chklovskii, B. I. Shklovskii, and L. I. Glazman. Electrostatics of edge channels. *Phys. Rev. B*, 46:4026, 1992.

[100] W. Bishara, P. Bonderson, C. Nayak, K. Shtengel, and J. K. Slingerland. Interferometric signature of non-Abelian anyons. *Phys. Rev. B*, 80:155303, 2009.

[101] A. Stern, B. Rosenow, R. Ilan, and B. I. Halperin. Interference, Coulomb blockade, and the identification of non-Abelian quantum Hall states. *Phys. Rev. B*, 82:085321, 2010.

[102] C. Wang and D. E. Feldman. Identification of 331 quantum Hall states with Mach-Zehnder interferometry. *Phys. Rev. B*, 82:165314, 2010.

[103] A. Braggio, D. Ferraro, M. Carrega, N. Magnoli, and M. Sassetti. Environmental induced renormalization effects in quantum Hall edge states due to $1/f$ noise and dissipation. *New J. Phys.*, 14:093032, 2012.

[104] C. Altimiras, H. le Sueur, U. Gennser, A. Anthore, A. Cavanna, D. Mailly, and F. Pierre. Chargeless heat transport in the fractional quantum Hall regime. *Phys. Rev. Lett.*, 109:026803, 2012.

[105] J. Biddle, M. R. Peterson, and S. Das Sarma. Variational Monte Carlo study of spin-polarization stability of fractional quantum Hall states against realistic effects in half-filled Landau levels. *Phys. Rev. B*, 87:235134, 2013.

[106] J. K. Jain. The 5/2 enigma in a spin? *Physics (APS)*, 3:71, 2010.

[107] K. T. Law, D. E. Feldman, and Y. Gefen. Electronic Mach-Zehnder interferometer as a tool to probe fractional statistics. *Phys. Rev. B*, 74:045319, 2006.

[108] D. E. Feldman, Y. Gefen, A. Kitaev, K. T. Law, and A. Stern. Shot noise in an anyonic Mach-Zehnder interferometer. *Phys. Rev. B*, 76:085333, 2007.

[109] V. V. Ponomarenko and D. V. Averin. Mach-Zehnder interferometer in the fractional quantum Hall regime. *Phys. Rev. Lett.*, 99:066803, 2007.

[110] V. V. Ponomarenko and D. V. Averin. Braiding of anyonic quasiparticles in charge transfer statistics of a symmetric fractional edge-state Mach-Zehnder interferometer. *Phys. Rev. B*, 82:205411, 2010.

[111] K. T. Law. Probing non-Abelian statistics in $\nu = 12/5$ quantum Hall state. *Phys. Rev. B*, 77:205310, 2008.

[112] G. Campagnano, O. Zilberberg, I. V. Gornyi, D. E. Feldman, A. C. Potter, and Y. Gefen. Hanbury Brown–Twiss interference of anyons. *Phys. Rev. Lett.*, 109:106802, 2012.

[113] C. Wang and D. E. Feldman. Fluctuation-dissipation theorem for chiral systems in nonequilibrium steady states. *Phys. Rev. B*, 84:235315, 2011.

[114] C. Wang and D. E. Feldman. Chirality, causality, and fluctuation-dissipation theorems in nonequilibrium steady states. *Phys. Rev. Lett.*, 110:030602, 2013.

[115] A. M. Chang. Chiral Luttinger liquids at the fractional quantum Hall edge. *Rev. Mod. Phys.*, 75:1449, 2003.

[116] R. H. Morf. Transition from quantum Hall to compressible states in the second Landau level: New light on the $\nu = 5/2$ enigma. *Phys. Rev. Lett.*, 80:1505, 1998.

[117] E. H. Rezayi and F. D. M. Haldane. Incompressible paired Hall state, stripe order, and the composite fermion liquid phase in half-filled Landau levels. *Phys. Rev. Lett.*, 84:4685, 2000.

[118] X. Wan, K. Yang, and E. H. Rezayi. Edge excitations and non-Abelian statistics in the Moore-Read state: A numerical study in the presence of Coulomb interaction and edge confinement. *Phys. Rev. Lett.*, 97:256804, 2006.

[119] X. Wan, Z.-X. Hu, E. H. Rezayi, and K. Yang. Fractional quantum Hall effect at $\nu = 5/2$: Ground states, non-Abelian quasiholes, and edge modes in a microscopic model. *Phys. Rev. B*, 77:165316, 2008.

[120] R. H. Morf, N. d'Ambrumenil, and S. Das Sarma. Excitation gaps in fractional quantum Hall states: An exact diagonalization study. *Phys. Rev. B*, 66:075408, 2002.

[121] R. Morf and N. d'Ambrumenil. Disorder in fractional quantum Hall states and the gap at $\nu = 5/2$. *Phys. Rev. B*, 68:113309, 2003.

[122] A. E. Feiguin, E. Rezayi, C. Nayak, and S. Das Sarma. Density matrix renormalization group study of incompressible fractional quantum Hall states. *Phys. Rev. Lett.*, 100:166803, 2008.

[123] M. Storni, R. H. Morf, and S. Das Sarma. Fractional quantum Hall state at $\nu = 5/2$ and the Moore-Read Pfaffian. *Phys. Rev. Lett.*, 104:076803, 2010.

[124] I. Dimov, B. I. Halperin, and C. Nayak. Spin order in paired quantum Hall states. *Phys. Rev. Lett.*, 100:126804, 2008.

[125] A. E. Feiguin, E. Rezayi, K. Yang, C. Nayak, and S. Das Sarma. Spin polarization of the $\nu = 5/2$ quantum Hall state. *Phys. Rev. B*, 79:115322, 2009.

[126] A. Wojs and J. J. Quinn. Landau level mixing in the $\nu = 5/2$ fractional quantum Hall state. *Phys. Rev. B*, 74:235319, 2006.

[127] A. Wojs, C. Toke, and J. K. Jain. Landau-level mixing and the emergence of Pfaffian excitations for the 5/2 fractional quantum Hall effect. *Phys. Rev. Lett.*, 105:096802, 2010.

[128] E. H. Rezayi and S. H. Simon. Breaking of particle-hole symmetry by Landau level mixing in the $\nu = 5/2$ quantized Hall state. arXiv:0912.0109, 2009.

[129] M. R. Peterson and C. Nayak. More realistic Hamiltonians for the fractional quantum Hall regime in GaAs and graphene. *Phys. Rev. B*, 87:245129, 2013.

[130] N. d'Ambrumenil, B. I. Halperin, and R. H. Morf. Model for dissipative conductance in fractional quantum Hall states. *Phys. Rev. Lett.*, 106:126804, 2011.

[131] Yu. A. Bychkov and E. I. Rashba. Properties of a 2D electron gas with lifted spectral degeneracy. *JETP Lett.*, 39:78, 1984.

[132] S. M. Dikman and S. V. Iordanskii. Spin relaxation of two-dimensional electrons with an odd Landau-level filling factor in a strong magnetic field. *JETP*, 83:128, 1996.

[133] S. M. Girvin. Particle-hole symmetry in the anomalous quantum Hall effect. *Phys. Rev. B*, 29:6012(R), 1984.

[134] S. H. Simon, E. H. Rezayi, and N. R. Cooper. Pseudopotentials for multiparticle interactions in the quantum Hall regime. *Phys. Rev. B*, 75:195306, 2007.

[135] W. Bishara and C. Nayak. Effect of Landau level mixing on the effective interaction between electrons in the fractional quantum Hall regime. *Phys. Rev. B*, 80:121302(R), 2009.

[136] C. L. Kane, M. P. A. Fisher, and J. Polchinski. Randomness at the edge: Theory of quantum Hall transport at filling $\nu = 2/3$. *Phys. Rev. Lett.*, 72:4129, 1994.

[137] T. Giamarchi and H. J. Schulz. Anderson localization and interactions in one-dimensional metals. *Phys. Rev. B*, 37:325, 1988.

[138] C. L. Kane and M. P. A. Fisher. Quantized thermal transport in the fractional quantum Hall effect. *Phys. Rev. B*, 55:15832, 1997.

[139] V. Venkatachalam, A. Yacoby, L. Pfeiffer, and K. West. Local charge of the $\nu = 5/2$ fractional quantum Hall state. *Nature (London)*, 469:185, 2011.

[140] E. Bocquillon, V. Freulon, J-.M Berroir, P. Degiovanni, B. Placais, A. Cavanna, Y. Jin, and G. Feve. Separation of neutral and charge modes in one-dimensional chiral edge channels. *Nature Communications*, 4:1839, 2013.

[141] N. Kumada, H. Kamata, and T. Fujisawa. Edge magnetoplasmon transport in gated and ungated quantum Hall systems. *Phys. Rev. B*, 84:045314, 2011.

[142] C. W. J. Beenakker. Edge channels for the fractional quantum Hall effect. *Phys. Rev. Lett.*, 64:216, 1990.

[143] N. Byers and C. N. Yang. Theoretical considerations concerning quantized magnetic flux in superconducting cylinders. *Phys. Rev. Lett.*, 7:46, 1961.

[144] J. P. Eisenstein, R. Willett, H. L. Störmer, D. C. Tsui, A. C. Gossard, and J. H. English. Collapse of the even-denominator fractional quantum Hall effect in tilted fields. *Phys. Rev. Lett.*, 61:997, 1988.

[145] M. H. Freedman, M. J. Larsen, and Z. Wang. A modular functor which is universal for quantum computation. *Commun. Math. Phys.*, 227:605, 2002.

[146] M. H. Freedman, M. J. Larsen, and Z. Wang. The two-eigenvalue problem and density of Jones representation of braid groups. *Commun. Math. Phys.*, 228:177, 2002.

[147] A. R. Akhmerov. Topological quantum computation away from the ground state with Majorana fermions. *Phys. Rev. B*, 82:020509(R), 2010.

[148] G. Goldstein and C. Chamon. Exact zero modes in closed systems of interacting fermions. *Phys. Rev. B*, 86:115122, 2012.

[149] J. Lee and F. Wilczek. Algebra of Majorana doubling. *Phys. Rev. Lett.*, 111:226402, 2013.

[150] D. M. Basko, I. L. Aleiner, and B. L. Altshuler. Metal-insulator transition in a weakly interacting many-electron system with localized single-particle states. *Ann. Phys.*, 321:1126, 2006.

[151] D. A. Huse, R. Nandkishore, V. Oganesyan, A. Pal, and S. L. Sondhi. Localization-protected quantum order. *Phys. Rev. B*, 88:014206, 2013.

[152] B. Bauer and C. Nayak. Area laws in a many-body localized state and its implications for topological order. *J. Stat. Mech.*, page P09005, 2013.

[153] J. D. Sau, R. M. Lutchyn, S. Tewari, and S. Das Sarma. Generic new platform for topological quantum computation using semiconductor heterostructures. *Phys. Rev. Lett.*, 104:040502, 2010.

[154] S. Tewari, T. D. Stanescu, J. D. Sau, and S. Das Sarma. Topological minigap in quasi-one-dimensional spin-orbit-coupled semiconductor Majorana wires. *Phys. Rev. B*, 86:024504, 2012.

[155] L. D. Landau, E. M. Lifshitz, and L. P. Pitaevskii. *Electrodynamics of Continuous Media*. Butterworth-Heinenann, Oxford, 1993.